THIN GLASS
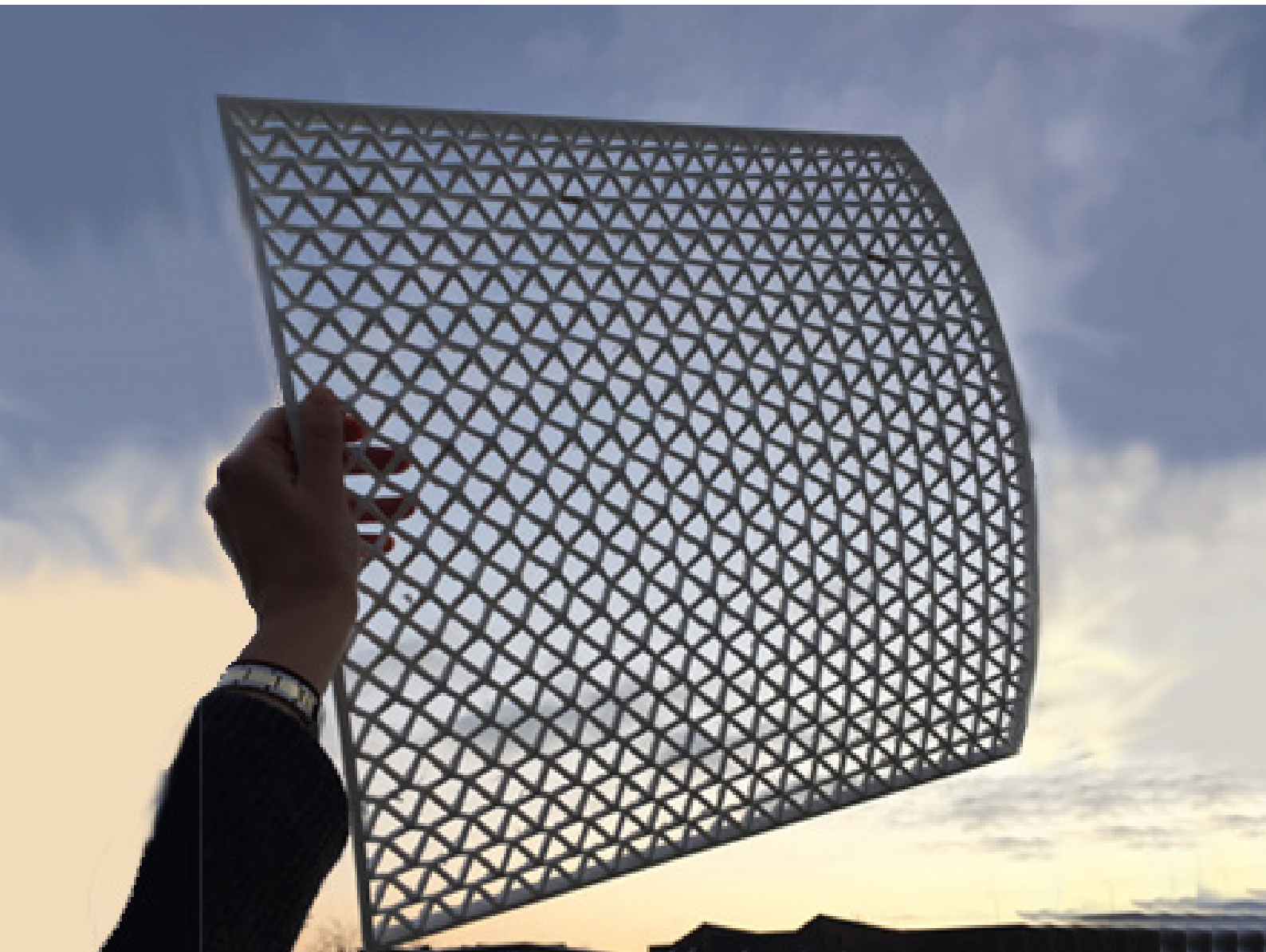# COLD BENT
SANDWICH PANEL

Marina Guidi

Delft University of Technology
February 2019

THIN GLASS
COLD BENT
SANDWICH PANEL

In partial fulfillment of the requirements
for the degree of:

Master of Science in Building Engineering
Faculty of Civil Engineering
at Delft University of Technology

Candidate:

Marina Guidi
Student number: 4634284
MSc Building Engineering
Specialization: Structural Design

Committee members:

Prof. Ir. Rob Nijsse	TU Delft
Dr. Ir. Christian Louter	TU Delft
Ir. Lennert van der Linden	TU Delft
Ir. Peter van de Rotten	Octatube

PREFACE

This graduation project represents the end of my study journey in Delft. I am grateful for this experience, for this city for having hosted me, and for the University, for what it taught to me. I would like to express my gratitude to all those people who provided me with the possibility to complete this graduation project.

Firstly, I would like to thank my graduation committee. Rob Nijsse, the chairman of the committee, who introduced me to the world of structural glass through his presentations at conferences and who helped me to transfer this interest into knowledge during the thesis period. Christian Louter, who presented me the possibility to investigate thin glass in its possibilities and introduced me to every person I needed to talk with during the project. Lennert van der Linden, who was present every time I needed help and could always find a positive feedback, which gave me the strength to continue and stay positive. A big thanks also to Peter van de Rotten, my daily supervisor at Octatube, who guided me throughout every step of this research, adding a nice joke for every bad news coming.

Secondly, I would like to express my gratitude to Octatube, the company who hosted me during the whole graduation experience. Thanks for the amazing atmosphere that can be breathed in this company which helped to make those days more pleasant and homey. In particular, I would like to thank Youri Baidjoe, for his patience and his time taken to introduce me to FE Models, Michele Akilo, Joey Janssen and all the constructer's department for all their precious advice.

Also, I would like to thank AGC for the glass panels they kindly provided. Thanks to MTB3D and 3Delft for their printing suggestions and their excellent work. I would also like to express my appreciation to Fred Veer, who found the time to help me with the testing in the laboratory. I am grateful to the people who helped me to manufacture the mock-up, Charbel and David.

Furthermore, I would like to thank my friends who made my stay in Delft more enjoyable: Matteo and Giovanni. I want to thank my boyfriend, Lodovico, who supported me every day from the beginning to the end of this project. Thanks also to my housemates, Brian, Gabriele and Vittorio, who were always there for a talk on the sofa.

Last, but not least, I would like to thank my friends from home, which were able to support me despite the distance: Giuditta and Sofia thanks for the encouraging talks. Ludovica, with whom I could fully share my graduation experience and Costanza, who always gave me the right suggestion at the right moment. A big thanks to my family: my parents, mamma e papà, and my brother Giovanni for all the support and for permitting this experience in the Netherlands to be real. Grazie.

Marina, Delft 18/02/19

SUMMARY

In the 21st century, thin glass has been used as a screen protector for electronic devices and smartphones. During the last 10 years, several studies have been carried out to introduce the thin glass in the building industry. The advantages of this material are light weight, high strength and high flexibility. On the other hand, thin glass, due to its low thickness, has a limited bending stiffness. Therefore, it is challenging to apply this innovative material in the building field. Within this research, the stiffness of thin glass is increased by the realization of a thin glass cold bent sandwich panel.

The proposed sandwich panel is realized by using thin glass faces and a 3D printed polymeric core. Due to the high flexibility of the glass, the material can be easily bent and glued to the core. The curved core hold the cold bent glass in shape without the use of any frame. This results in a cold bent sandwich panel.

In order to realize the core of the sandwich panel, two different pattern has been investigated and compared. The first one is a pyramidal spaceframe, manufactured with FDM technique. This core topology is characterized by a high strength and stiffness related to a low density pattern. The second core type is a closed square cells pattern, realized by laser cutting technique which has a higher shear stiffness but also a higher relative density.

The two sandwich panels are reproduced and studied with numerical models by the use of Finite Element Software. The aim of this study is to investigate the structural behaviour of the sandwich panels. From the numerical results, information regarding the failure methods of the sandwich panel is obtained. The connections between the glass faces and the core of the sandwich structure revealed to be the most critical part. The panel is expected to have its first failure in the glue connection, then the stiffness of the panel will decrease due to the absence of the sandwich behaviour, finally the glass pane will fail.

To validate the numerical results, laboratory tests have to be carried out. Before performing the tests, the sandwich panels is manufactured. First of all, the bottom pane of the sandwich is cold bent on a wooden mould. Then, the glass and the core are glued together and the glue is cured through the use of UV light machine. Subsequentely, the core itself is used as a mould to cold bend the top glass pane and the gluing porcess is repeted. Finally, the panel is ready to be tested.

The manufactured panels have been tested with simply supported boundary conditions and loaded by a point load. The experimental results are in line with the numerical results. Also in the tests the first failure appeares in the glue connection between the core and the glass faces. Moreover, the pyramidal spaceframe pattern shows a stiffer behaviour compared to the closed cell pattern. The closed cells pattern did not behave as expected, due to the chosen manufacturing conditions related to the laser cutting technique. In detail,the joints within the ribs of the core behaved as hinged connection instead of fixed connections. Therefore, the pyramidal spaceframe pattern has been chosen for the final design.

Lastly, a final design has been carried out in order to demonstrate the suitability of the reserached cold bent sandwich panel in the building industry. A panel of 1200mm x 3000mm has been realized by the use of 0,5 mm Falcon glass ply and an 11 mm, 3D printed interlayer, realized by PETG. The sandwich panel is assumed to be applied to the Netherlands Architecture Institute (NAI) building in Rotterdam. The composite panel is supported on two edges and loaded by self-weight and wind load.

The design of the curved sandwich panel revealed to be a feasible façade panel proposal. The feasibility is defined in terms of a structural façade element, which fulfil the limits of safety and comfort. The curved sandwich panel, proposed in the final design, results to be 280 times stiffer compared to a curved two layered thin glass laminated panel.

Furthermore, it was demonstrated that the proposed sandwich panel could guarantee a weight reduction of more than 80% in comparison to the glass used nowadays in building façades. This characteristic not only facilitates the assemblage of the façade, but also can bring to the usage of a lighter support structure. This can bring advantages both in terms of cost of the total structure and energy required to assemble the building.
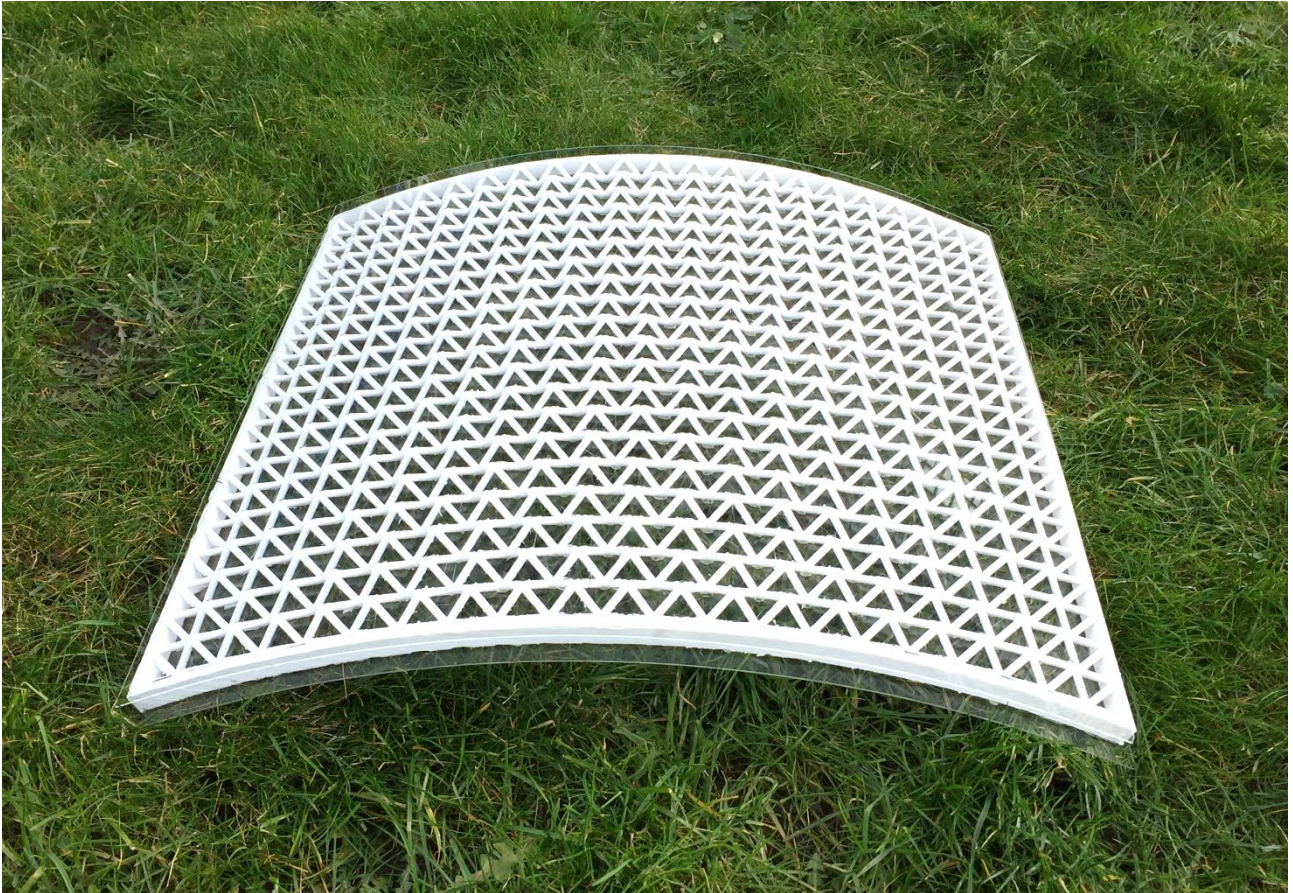
Cold bent sandwich panel – Thin glass faces and 3D printed polymeric core

Table of Contents

List of Symbols

Symbols

A	Area of the glass panel	m^2
B	Panel width	mm
b	Panel strip	mm
E_c	Core Young's modulus	MPa
E_g	Glass Young's modulus	MPa
F	Transverse load	N
G_c	Core Shear modulus	MPa
G_g	Glass Shear modulus	MPa
H	Total Height sandwich panel	mm
h	Core height	mm
l	Panel length	mm
N	Normal Force	N
ν	Poisson ratio	–
q	Distributed transverse load	kN/m^2
R	Radius of curvature	mm
ρ	Density	kg/m^3
σ	Normal stress	MPa
t	Glass thickness	mm
τ	Shear stress	MPa
V	Shear force	N
w	Deflection	mm
w_{lim}	Deflection limit	mm

Abbreviations

ABS	Acrylonitrile Butadiene Styrene
AGC	Asahi Glass Co.
AM	Additive Manufacturing
CS	Compressive Stress
CT	Chemically Tempered
DOL	Depth of Layer
FDM	Fused Deposition Modelling
FEA	Finite Element Analysis
FEM	Finite Element Model
FTG	Fully-Tempered Glass
HSG	Heat Strengthened Glass
IGU	Insulating Glass Unit
LG	Leoflex glass
PA	Polyamide
PE	Polyethylene
PC	Polycarbonate

PET   Polyethylene Terephthalate
PLA   Polylactis Acid
PMMA Polymethylmethacrylate
PVB   Polyvinyl Butyral
SLA   Stereolithography
SLS   Selective Laser Sintering
SLS   Serviceability Limit State
SLS   Soda Lime Silica
TO   Topology Optimization
TPU   Thermoplastic Polyurethane
TS   Tensile Stress
ULS   Ultimate Limit State
UV   Ultraviolet
VGU   Vacuum glazing unit

INTRODUCTION

1. Introduction

The use of thin glass has become popular in the 21st century within the electronic field. Many electronic devices, such as smartphones and tablet, use thin glass as a screen protector. Although this function may seem curious for a brittle material as it is glass, thin glass shows a high scratch resistance and high strength. Since 2010, the chemical composition of thin glass has been investigated by Gomez (2011) and the possibility of using thin glass as a building material has been proposed first by Lambert & O'Callaghan (2013) and later by Hundervad (2014). Hundervad has noticed that the tendency in architecture of making increasingly bigger glass panes, brought the panels to become considerably heavier. As they became heavier, the necessity to thicken the panes and to laminate them was needed for structural purposes and safety reasons. Glass panes have been produced increasingly thicker to satisfy the requirements. This tendency brought to the necessity of having heavier supporting structures, which means more use of supporting material since more mechanical capacity is needed. Hundervad underlined the fact that we should investigate a manner to "save material rather than using more of it" (Hundevad, 2014). Therefore, the technology of thin glass, already existent in the electronic field, was proposed and investigated to be used in the building industry.

Thin glass can be classified as an innovative material, if considered to be used for the building environment. It is certain that aluminosilicate thin glass, compared to currently used soda lime glass, offers two main advantages:

1. Weight reduction
since a thinner glass is used

2. Less energy required for production
because less raw materials are used

A summary of the characteristics of thin glass is summarized below. Once the material has been chemically strengthened, aluminosilicate thin glass shows the following characteristics (Hundevad, 2014):

- Lightweight structure: the dead load will considerably decrease.
- High strength: since the chemical procedure will enlarge design stresses up to 10 times stronger than thermally tempered glass.
- High flexibility: the combination of thin glass and a high strength allows large deformations without breakage.

The high flexibility of the glass, combined to the thinnest of the material, brings thin glass to exhibit large deflections, due to a poor bending stiffness. In order to use thin glass as a structural material, the stiffness has to be increased, to reduce the deflection of the structure, and thus, to assure comfort. Different strategies to improve the bending stiffness of thin glass have been proposed by Hundervad, Lennert and O'Callaghan, and have been summarized by Simoen (2016) as it is shown in the figure below.
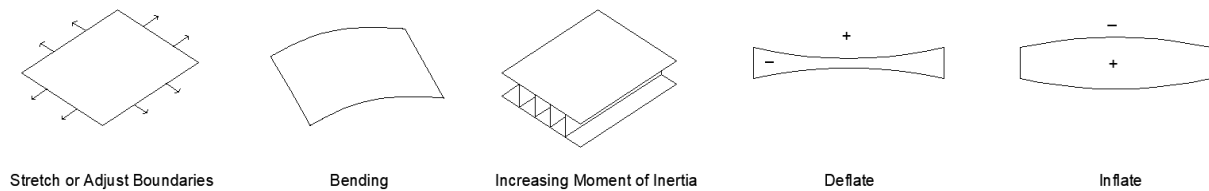
Figure 1.1 Stiffening method available

Nowadays, much attention is given at curved building envelopes. For this reason, it seems reasonable to investigate a thin glass curved panel. Moreover, in order to increase the stiffness of the thin glass, a sandwich panel is realized, which increases the second moment of inertia of the structure. The purpose of this study is to research the increase in stiffness of a thin glass cold bent sandwich panel.
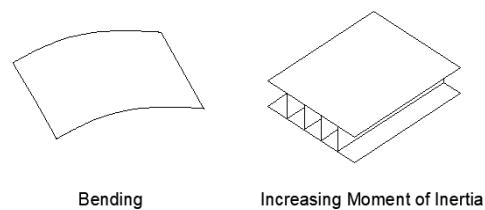

Figure 1.2 Stiffening method investigated in this research

1.1   State of the art

In the last years, the literature available on thin glass has been deeply expanded. The possibility to increase the stiffness of thin glass by laminating the panel, proposed by Lambert and O'Callaghan (2013), has been further investigated by Akilo (2018) and Neeskens (2018). In their research, chemically strengthened thin glass has been laminated with a 3D printed polymeric material.

The project, carried out by Akilo (2018), investigates how to stiffener thin glass by the usage of sandwich structures. The utilization of two innovative techniques have been combined: thin glass to be used in the building industry and Additive Manufacturing, better known as 3D printing. The result of the research shows a panel which is 125 times stiffer compared to two thin glass panes laminated together. The appearance of the sandwich panel is shown in the following figures.
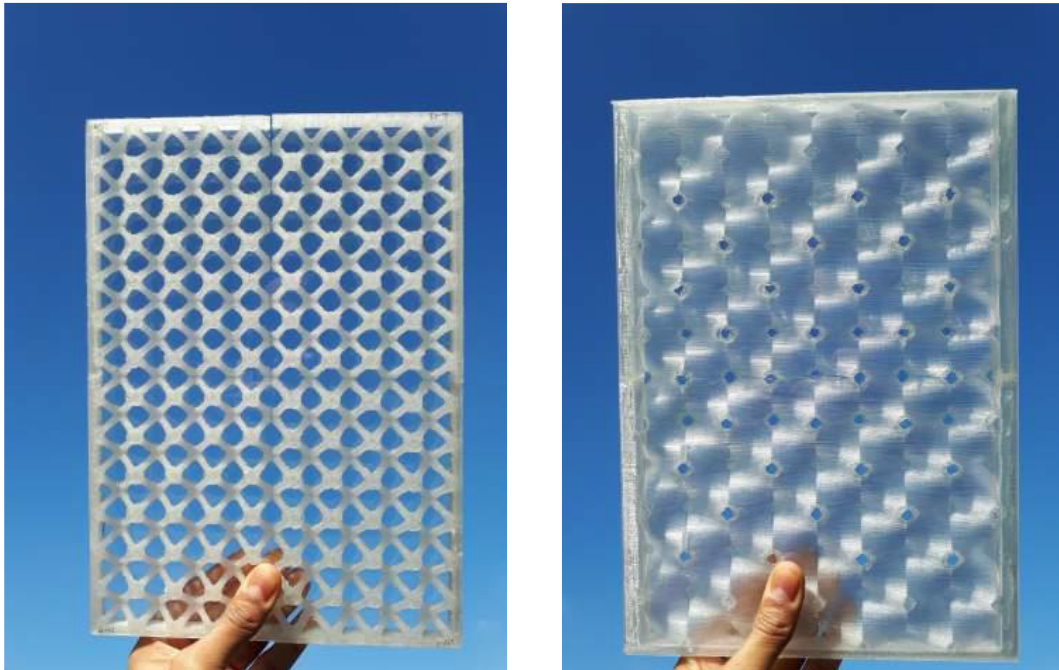
Figure 1.3 Composite panel with Thin Glass faces and 3D printed polymeric core (Akilo, 2018)

Moreover, Neeskens (2018) has investigated new patterns for the core of the sandwich panel. After having analysed different types of structures, the use of a Voronoi pattern has been chosen as a final design. The core of the structure has been optimized according to different boundary conditions. Three different panel proposals are shown in Figure 1.4.

This research demonstrates how versatile this panel is. The applicability of this panel can be highly required by architects who want to design their own core pattern. Moreover, the pattern can be optimized depending on the function, the loading conditions and many other parameters.
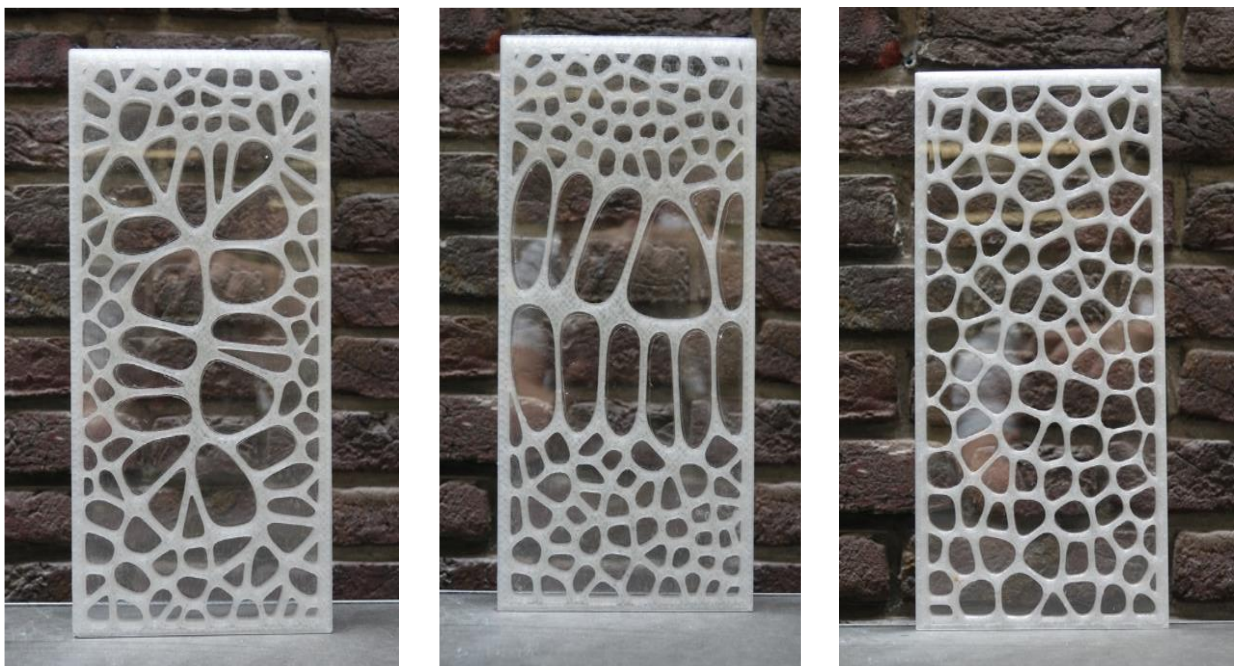

Figure 1.4 Thin Glass composite panel - Voronoi structure (Neeskens, 2018)

According to the research of Lambert & O'Callaghan (2013), further investigation for the utilization of chemically strengthened glass in cold form surfaces and tensile membrane structure would be of great interest. Researches on the suggested strategies to increase the bending stiffness of thin glass have been carried out in the last years, enlarging the available literature on this topic.

The option of cold bending the glass has been investigated by Carlyn Simoen and Rafael Ribeiro Silveira, both from TU Delft University. Simoen (Simoen, 2016) investigated the feasibility of a second skin facade made by cold bent thin glass panels. The material has been deeply researched and then the design of a cylindrically bent panel has been realized. The outcome of her research is shown in Figure 1.5.
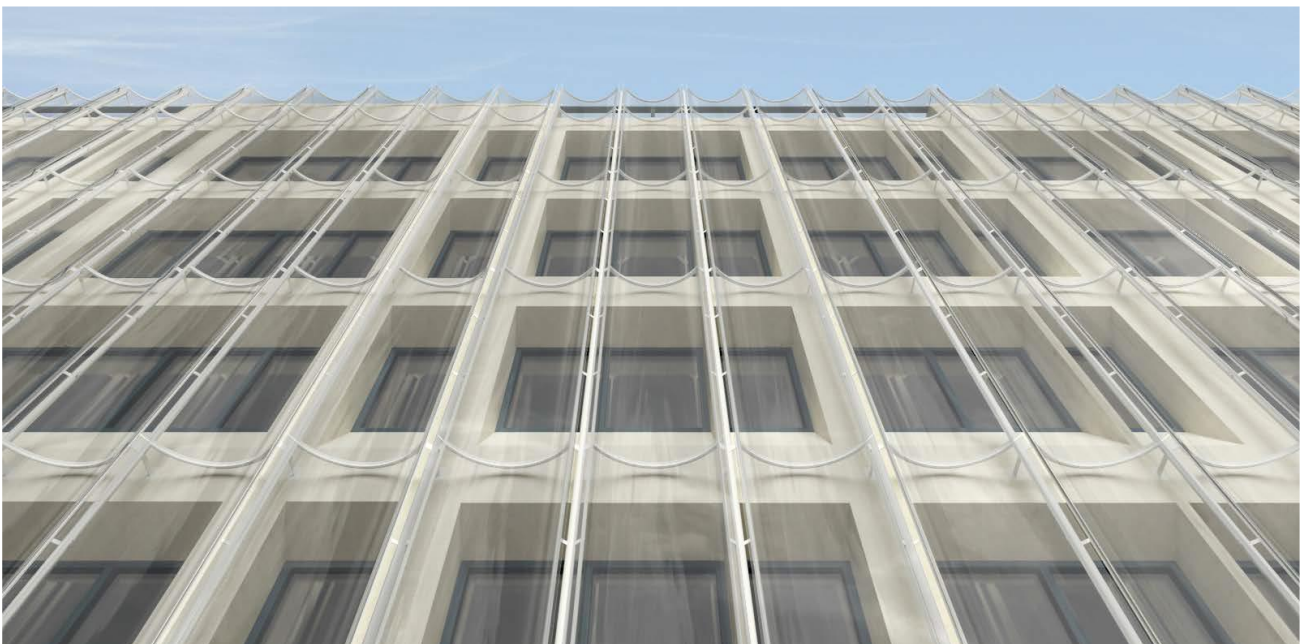

Figure 1.5 Cold Bent Thin Glass for a second skin façade (Simoen, 2016)

As further research, Silveira (Silveira, 2016) investigated the possibility of realizing an adaptive second skin façade, by taking advantage of the flexibility of thin glass. The design proposes a movable facade panel, realized by adaptive supports. Those supports are created by a rail system frame on the edge of the panel. This solution enables the glass to curve and to change its shape according to different external conditions.

Figure 1.6 Adaptive thin Glass façade (Silveira, 2016)

The work of Topcu (Topcu, 2017) further explores the adaptive thin glass façade concept and focus on the possibilities to create a water and airtightness façade in closed conditions (Louter, et al., 2018). After having investigated different design possibilities, the author proposes an adaptive thin glass façade with magnetic sealing at the edges.

Figure 1.7 Adaptive thin glass facade - water and airtight boundary conditions (Topcu, 2017)

During the last year, this concept has been further developed by the research of Miri (Miri, 2018) and the research of Zha (Zha, 2018). Miri has integrated the use of Shape Memory Alloy (SMA) in the windows configuration. By the use of SMA, the glass will be pulled or bent to reach the desired shape in accordance with boundary conditions, since the SMA will shorten when heated. At the same time, Zha has introduced soft pneumatic actuators as a boundary element. The concept is to bend thin glass though inflations of the pneumatic.

Moreover, Schlösser (Schlösser, 2018) has investigated the post-breakage behaviour of cold bent laminated thin glass panels. All the researches, which has been named above, are realized with a single ply of glass. If thin glass is proposed as an alternative to soda-lime glass in the building industry, safety has to be treated accordingly. The need for laminate thin glass panel becomes of prime importance. The study of Schlösser has enlarged the knowledge on the post-breakage behaviour of curved thin glass laminated panels (Figure 1.8).
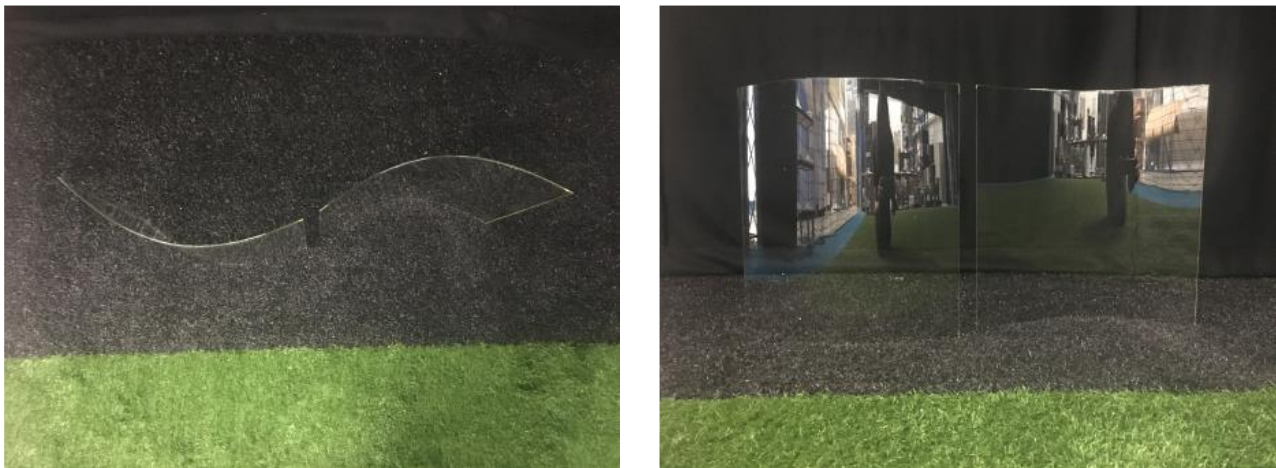

Figure 1.8 Thin Glass as Cold Bent Laminated Panels (Schlösser, 2018)

1.2   Problem Statement

The flexibility of thin glass can be seen as an advantage, because it allows creating curved shapes with cold bending technique easily. On the other hand, it can also be seen as a limitation for this product to be used in building applications. If this flexibility is not adequately controlled, the glass will exhibit large deflections. The deflection does not have to exceed the limit value of the Serviceability Limit States (SLS), given by the normative. Deflection of thin glass could bring to noise production and technical problems in long term applications. Moreover, large deflections could induce fear perception by users.

1.3 Research Objective

The purpose of this research is to broaden the knowledge of thin glass and its structural behaviour, to propose this material to be used as a façade panel in the building industry. The objective of the project is to design, prototype and testing the realization of a curved sandwich panel, composed of cold bent thin glass faces, kept in shape by the core of the sandwich structure. The purpose of the curved panel is to be used in freeform curved building facades, fulfilling the limitations imposed by the existing normative.

Main Research Question

To what extent can thin glass be stiffened by the realization of a cold bent sandwich panel – made by thin glass faces 0,5mm and a polymeric core – to be used in the building industry as a façade element?

Sub-questions

The first sub-question is related to the material, glass. It will be addressed in Chapter 2, and answered in Paragraph 2.6:

- *What are the characteristics of chemically strengthened aluminosilicate glass, compared to the commonly used soda lime silica glass?*
- *To what extent can thin glass be cold bent?*

Later, the theory of sandwich structure will be introduced in Chapter 3 and the related sub-questions will be answered in Paragraph 3.6.

- *To what extent will a sandwich structure increase the stiffness of the panel?*
- *Which technique is the most appropriate for realizing the core?*

Then, Additive Manufacturing technique is introduced in Chapter 4 and the following sub-questions will be answered in Paragraph 4.5:

- *What is Additive Manufacturing (AM)?*
- *Which techniques of AM are currently available?*
- *Which core material is the most appropriate for the analysed problem?*

From Chapter 5, the Preliminary design will be introduced. In Paragraph 5.3, the cold bending procedure of thin glass will be illustrated, and the following sub-questions will be answered.

- *How can the cold bending process be modelled in FEM?*

Moreover, in Paragraph 5.5 the numerical calculation of the design proposed will be illustrated and the following sub-question about Finite Element Software will be addressed.

- *Which differences between the software Femap and Karamba can be underlined after the analysis of the models?*

Finally, the manufacturing and testing of the panel will be presented and the last sub-question is answered in Paragraph 7.4:

- *Which test set up can be used to test this cold bent sandwich panel?*

1.4   Hypothesis

Based on the previous consideration about the research investigation topic and the proposal approach which will be used, a hypothesis is developed. It has to be verified that if the two proposed approaches are combined – cold bending the glass and making a sandwich panel – the arch-shaped panel will stay in shape by itself, without the need of a frame. The hypothesis is that cold bent glass will be kept in shape by the core of the sandwich structure, resulting in the realization of a free-standing arch (Figure 1.9). This characteristic could simplify the assemblage of the façade, since the panel is already in shape. This hypothesis will be considered during the development of the research and it will be addressed in the conclusions of the report.
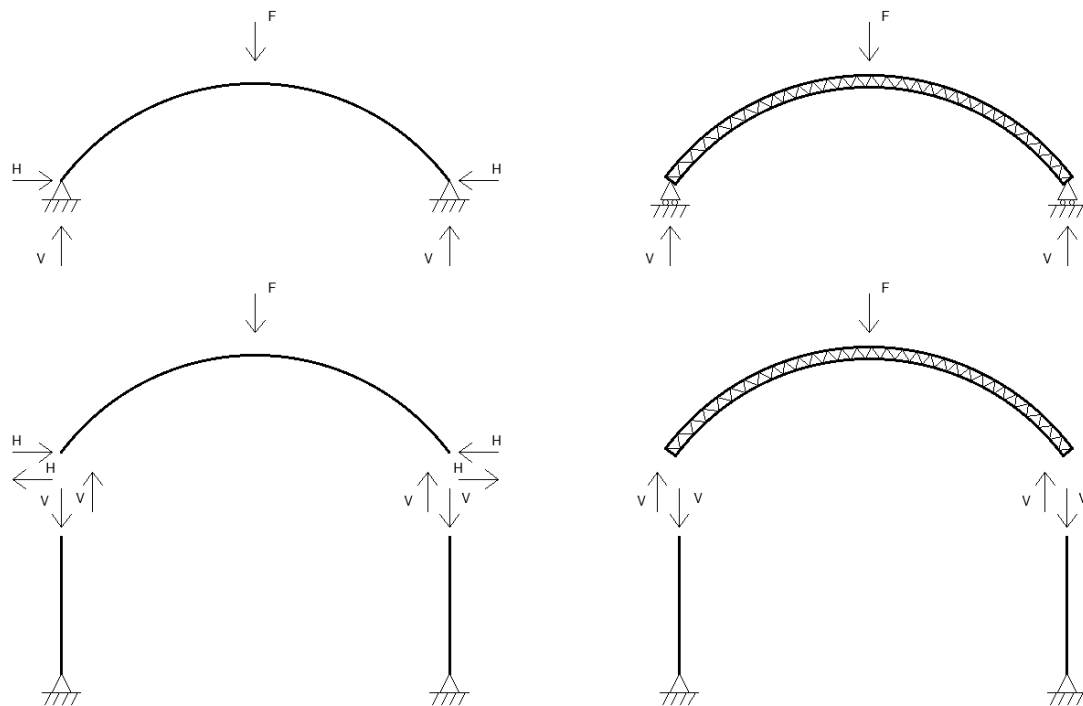

Figure 1.9 Arch with a frame (left) - Freestanding arch (right)

1.5 Methodology

This research can be classified as a *Practical Investigation* of a new technology: a curved sandwich panel realized by thin glass faces and a polymeric core. This research will involve laboratory testing and it will follow an experimental approach. Experimental data will be analysed to draw conclusions. The methodology used in each part of the thesis is explained below:

Part I – Literature Review

In the first part of the graduation, a literature review will be performed to determine the properties of glass and particularly, thin glass. Furthermore, the structural behaviour of sandwich panels will be analysed. The available techniques and materials to realize the core will be researched. Then, the technique available to optimize the core will also be addressed.

Later, the first sub-questions will be answered and the starting points for the preliminary design will be delineated. The type of glass, thickness and dimensions will be set and the material and the technique to realize the core will be defined.

Part II – Preliminary Design

Starting from the conclusions of the literature review, the material and the dimensions of the sandwich panel will be defined. Then, the loading and boundary condition will be illustrated. The sandwich panel will be designed by the use of Rhino + Grasshopper and then studied in this preliminary design by the plug-in Karamba, a parametric structural engineering tool to perform structural calculations. Since Grasshopper is a parametric programme, it enables to quickly change the design accordingly with the result obtained. Simplified analytical calculations will also be made to check numerical calculations. Moreover, when a preferred design will be reached, the model will also be tested by Femap, a Finite Element Program developed by Siemens to ensure the correctness of the numerical results.

Part III – Manufacturing and Laboratory Testing

This phase will be performed in the laboratory. The preliminary design, carried out in the previous stage, will now be manufactured, assembled and tested. The thin glass panel will be cold bent by the use of a wooden mould. Subsequently, experimental testing will be performed. Having considered the possible failure modes in the design phase gives the opportunity to predict how the panel is expected to fail. The assumption made according to the numerical models can now be verified with experimental results. The comparison of the results given by the numerical calculations and the experimental testing will be performed, analysed and commented.

Part IV – Final Design

The information gained from the numerical and experimental results will be used to create a final design of the cold bent sandwich panel. Finally, all the data will be evaluated together to draw conclusions and recommendations for further researches.

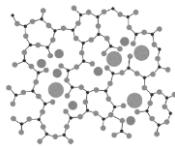The schematization of the methodology used in this graduation project is summarized in Figure 1.10.
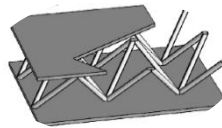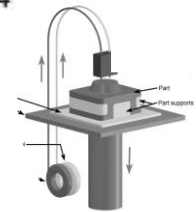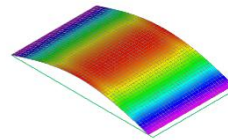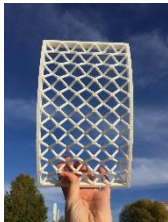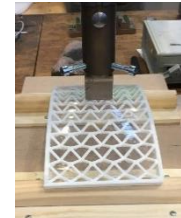
Figure 1.10 Methodology Schematization

LITERATURE REVIEW

2. Glass – the material

2.1   Introduction

In this chapter, the main features of glass are introduced. The chemical and physical properties of the material will be investigated. Then, the processing and post-processing techniques available nowadays will be illustrated. Finally, an overview of the material, which includes both glass and thin glass, will be presented. The following research sub-question will be answered:

- *What are the characteristics of chemically strengthened aluminosilicate glass, compared to the commonly used soda lime silica glass?*

2.2   Material Properties

2.2.1   Chemical properties

Glass is a non-crystalline amorphous solid. Although at nano-level there can be recognized some regular elements, there is no systematic repetition of this structure and thus no crystallinity, as can be seen in Figure 2.1. This lack of a crystalline structure does not allow any dislocations; therefore neither any plasticity in the material. Glass can only deform elastically, or it immediately breaks (Veer, 2007).
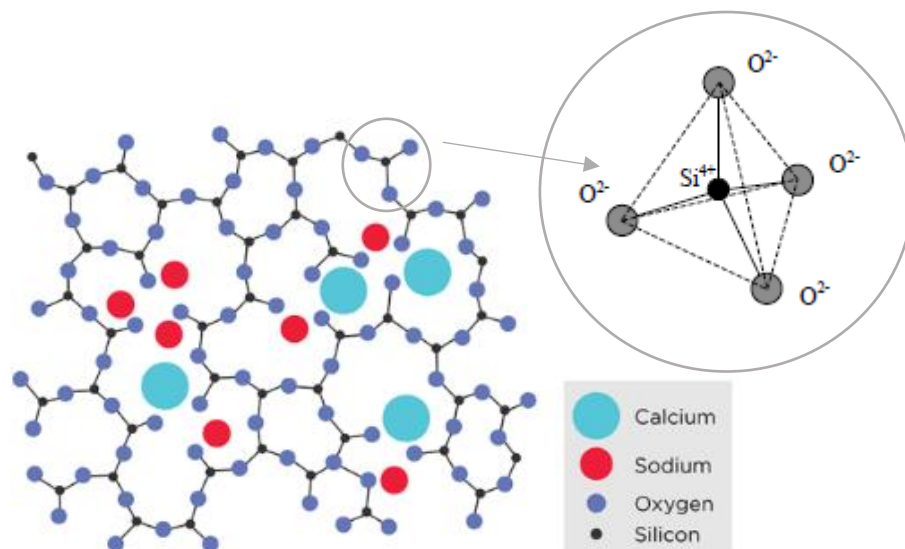
Figure 2.1 Atomic structure of Soda Lime Silica Glass

Silica (SiO_2) is a common fundamental constituent of glass. The content of silica can be used to classify different categories of glass. The chemical differences between soda lime silica glass, borosilicate glass and aluminosilicate glass are summarized in Table 2.1 (Schittich, Staib, Balkow, Schuler, & Sobek, 2007 and Louter, 2017). As shown in the table, borosilicate glass contains approximately 7 – 15% of boron-oxide, which is not present in soda lime silica glass. Since the coefficient of thermal expansion is lower, borosilicate glass has a higher thermal fatigue resistance. For this reason, it is used for special purposes, for instance when fire protection is required. This glass also has high resistance to alkaline solutions and acids (Schittich, Staib, Balkow, Schuler, & Sobek, 2007). Soda lime silica glass is generally used in

the building industry, due to the lower cost of production. Whereas borosilicate glass is adopted when particular characteristics are required. On the other hand, in aluminosilicate glass, an increased amount of alumina (Al_2O_3) can be noticed. This characteristic gives to aluminosilicate glass a higher melting point, in fact, it is used for fire-resistant glazing applications (Schittich, Staib, Balkow, Schuler, & Sobek, 2007). Aluminosilicate glass is similar to borosilicate glass, but it has greater chemical durability.

		Soda Lime Silica Glass	Borosilicate Glass	Aluminosilicate Glass
Silica Sand	SiO_2	69 – 74 %	70 – 87 %	58 – 62 %
Lime	CaO	5 – 12 %	-	5 – 8 %
Soda	Na_2O	12 – 16 %	0 – 8 %	0 – 1 %
Boron-Oxide	B_2O_3	-	7 – 15 %	0 – 5 %
Magnesia	MgO	0 – 6 %	-	4 – 7 %
Alumina	Al_2O_3	0 – 3 %	1 – 8 %	14 – 18 %
Others	-	0 – 5 %	0 – 8 %	0 – 6 %

Table 2.1 Soda Lime Silica Glass, Borosilicate Glass and Aluminosilicate Glass – Compositions

(Schittich, Staib, Balkow, Schuler, & Sobek, 2007)

Different material properties give different characteristics to the final product, which can be used in accordance with the specific demand. General characteristics and possible applications of soda lime silica glass, borosilicate glass and aluminosilicate glass are summarized in Table 2.2.

	Primary Components	Thermal Shock Resistance	Chemical Resistance	Applications
Soda-Lime Silica Glass	SiO_2 Na_2O CaO	Low	Average	Food and beverage containers
				Windows
				Lamp envelopes
Borosilicate Glass	SiO_2 B_2O_3	Average – High	High	Industrial equipment
				Exterior lighting
				Laboratory and kitchen glassware
Aluminosilicate Glass	SiO_2 Al_2O_3	High	High	Cookware
				Glass ceramics
				Resistors for electronic circuity

Table 2.2 Soda Lime Silica Glass, Borosilicate Glass and Aluminosilicate Glass – Properties and Applications

2.2.2   Physical Properties

Glass shows a linear elastic behaviour with a brittle fracture. This can be seen in the stress and strain relationship diagram in Figure 2.2. This figure shows a qualitative comparison of the physical properties of glass, compared with the one of steel and wood. Those two building material shows a plastic range in their behaviour, while no yielding capacity is shown in glass. Glass breaks suddenly and without any warning, for this reason, safety measures have to be taken in order to use glass as a building material (Paragraph 2.4).
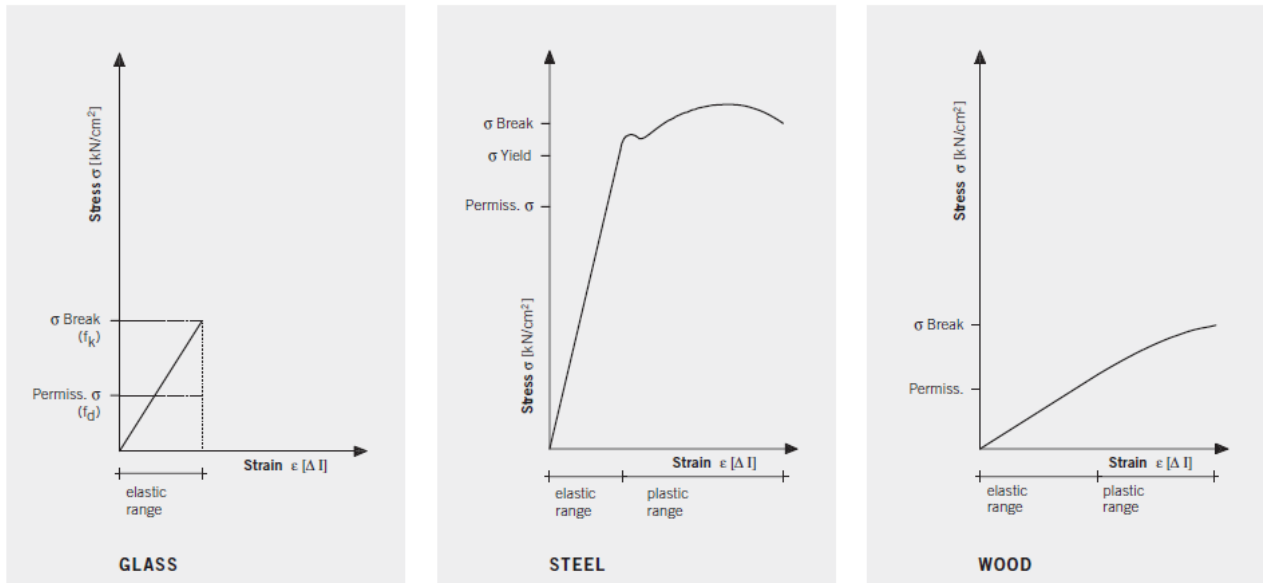

Figure 2.2 Physical Properties of Glass, Steel and Wood (Wurm, 2007)

The binding energy of the SiO_4 tetrahedron gives to glass a high strength in the material, which is up to 8 000 MPa in the literature (Wurm, 2007). However, the tensile strength achievable in practice is not even close to this value, it is less than 1%, because the presence of flaws on the glass surface can create the material to crack, due to the brittle nature of glass. The strength of glass depends on the degree of damage of the surface, taking into account scratches and flaws. Tensile stresses at these notch sites lead the stress concentrations in the crack root, which cause the propagation of the crack. Therefore, the tensile or bending strength of glass reflects the surface quality and it is not a constant value.
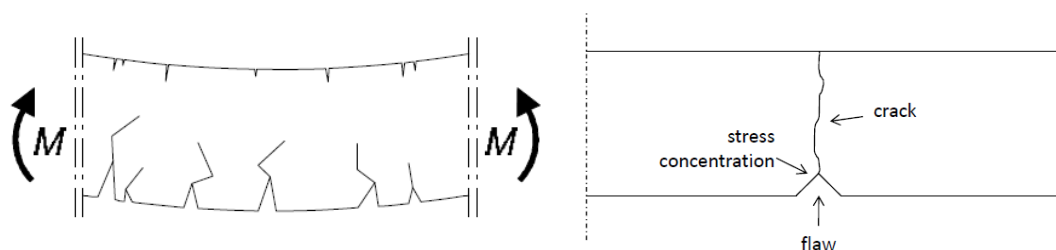

Figure 2.3 Flaws in the glass surface act as stress concentrators (Louter, 2017)

An overview of the main properties of Soda Lime Glass, compared to Aluminosilicate Glass, in particular, Falcon Glass and Leoflex Glass from AGC, is shown in Table 2.3.

			Soda Lime Silica	Aluminosilicate	
				Falcon Glass	Leoflex Glass
Mechanical					
Density	ρ	kg/m^3	2 500	2 480	2 480
Young's Modulus	E	MPa	70 000	73 000	74 000
Shear Modulus	G	MPa	30 000	30 000	30 000
Poisson Ratio	ν	-	0,22	0,22	0,23
Bending strength	$f_{b,k}$	MPa	45	45	45
Bending strength after prestressing	$f_{b,k}$	MPa	HS: 70 FT: 120 CT: 150	- - CT: 314	- - CT: 260
Knoop Hardness	$HK_{0,1/2}$	MPa	439 before CT -	450 before CT 546 after CT	- 706 after CT
Thermal					
Transition Temp	T_g	°C	530	575	604
Thermal Expansion	α_T	10^{-6} °C^{-1}	85E^{-7}	91E^{-7}	98E^{-7}
Thermal Conduct	λ	W/m°C	0,96	0,95	-
Light Transmission	LT	%	90	91	91
General					
Max Panel Size	A	mm x mm	3210 x 18000	3210 x 1600	2070 x 1650
Thickness Range	t	mm	2 – 19	0,5 – 2,1	0,55 – 2

Table 2.3 Properties of Soda Lime Glass compared to Aluminosilicate Glass (Falcon Glass and Leoflex Glass)

2.3   Production Process

In this paragraph, the production processes available to realize glass will be presented. First of all, the floating process, which is the most common production technique used nowadays, will be explained. Later on, newer production processes, known as the down-drown process and the overflow fusion process, will be described. Those last processes are used to fabricate thin glass in particular.

2.3.1   Floating Technique

The process used to produce glass sheets is called Float Glass Process (Figure 2.4) and it was invented and patented in 1959 by the British manufacturer, Alastair Pilkington, reason why this process is also known as Pilkington process.

The first step consists in collecting the required raw materials and mixing them together. Then, the mixing is melt in a furnace at a temperature of approximately 1400 – 1600 °C. Once the glass is completely melted, the temperature is stabilized around 1200°C. The melted glass floats on top of a bath of molten tin. This part of the process assures the flatness of the outer product. The speed of the roller dictates the thickness of the glass: the higher the speed, the thinner the glass. Later, the sheet of glass is slowly cooled to prevent the arising of stresses. As the last step, the glass is inspected and then cut according to the required dimensions. Standard sheet dimensions are 6m x 3,21m, while the nominal thickness realized with this process are 2, 3, 4, 5, 6, 8, 10, 12, 15, 19 (and 25) mm. Oversized sheets can be realized in required and exceptional cases, if the equipment available is able to realize the required dimensions.
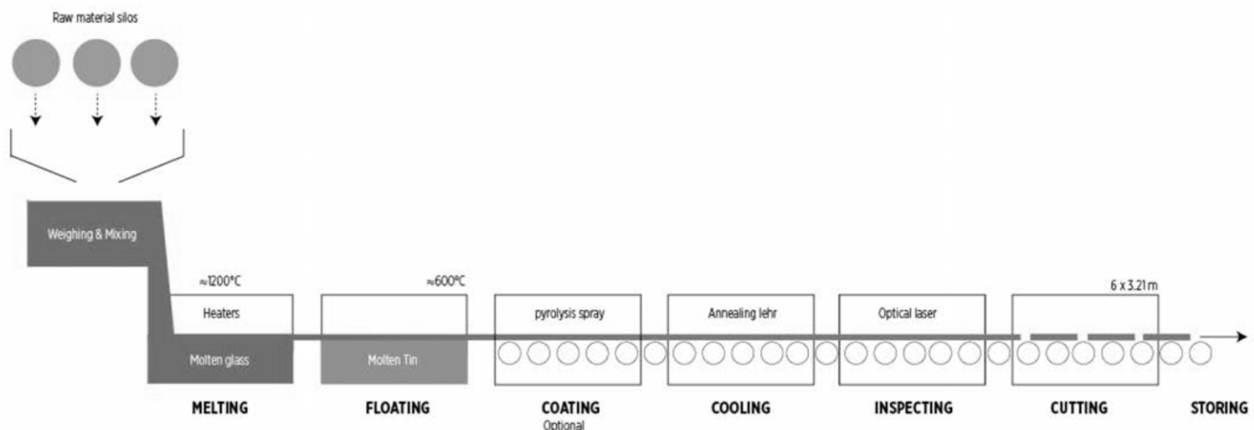

Figure 2.4 Float Glass production process (Tangram Technology, s.d. 2009, edited by Simoen, 2016)

2.3.2   Production Process for Thin Glass

In order to realize thinner glass, an adapted process of the common Float Glass production process can be utilized. However, thin glass can be better realized by two other processes: the Overflown fusion process and the Down-drawn process (Figure 2.5). Those methods are vertical drowing production processes. They both have the advantage of generating the sheet of glass without being touched by molten tin. Therefore, both side of the glass has the same properties, and no flaw is generated.

The Overflow fusion method (Figure 2.3, right image) consists in pouring the molten glass from a V-shaped tank. When the tank is full, molten glass "overflows" from both sides and fuses at the bottom of the V-shaped tank. After a cooling phase, the glass is cut into specific sizes.

The Down-drawn process (Figure 2.3, left image) is actually inspired by ancient techniques for making glass. It is similar to the Overflow fusion method, but the tank has a thin hole at the bottom, from which molten glass can flow. The molten glass is cooled to ambient temperature by annealing furnaces. After this controlled cooling process, the glass is cut into specific sizes.
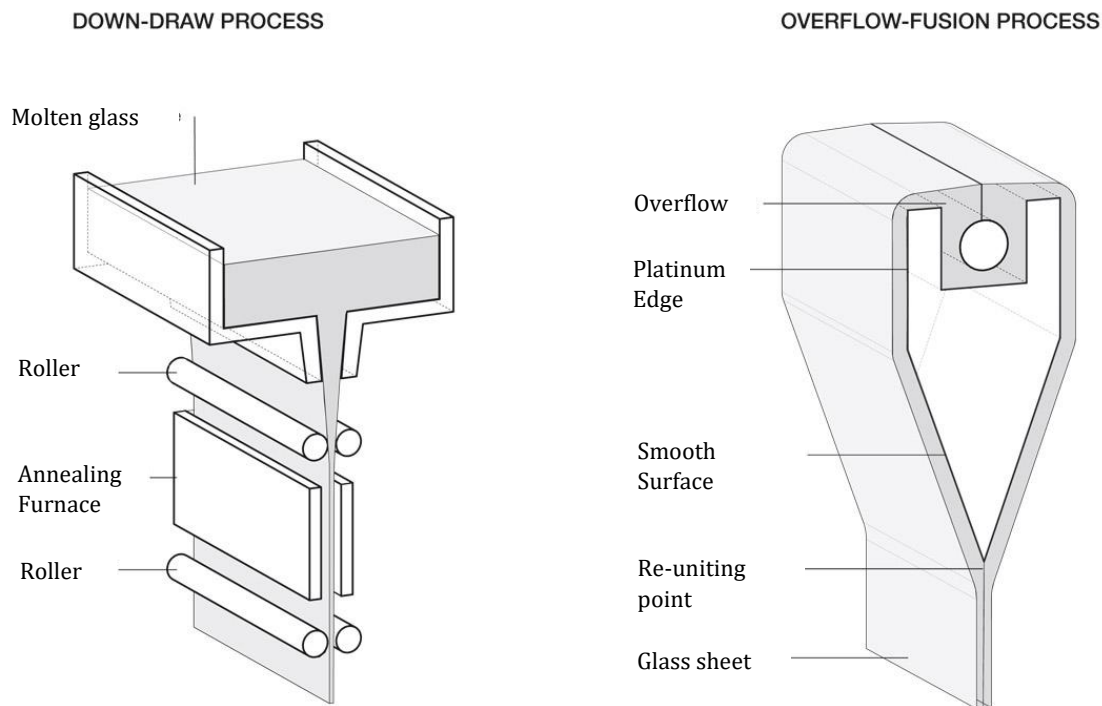

Figure 2.5 Thin glass production processes – Down-Drawn Process (left) and Overflow Process (right)
(Albus & Robanus, 2014)

2.4   Post Processing

Once the glass has been produced, some post-processing operations are needed to meet requirements for performance, safety, shape and appearance. To avoid unexpected breakages, post-processing measurements are taken in respect of specific regulations. First of all, the glass has to be cut, according to design dimensions. Then, the edges can be left as cut or chamfered, or they can be treated as preferred: ground, polished, round or facetted (Louter, Material Characteristics, Production, Processing & Products, 2017). If a hole is needed in the glass, drilling has to be realized before any surface treatment, like coating, is done. Moreover, specific treatment to strengthen the glass can be performed: thermal or chemical treatment can be realized.

2.4.1   Thermal and Chemical Treatment

Thermal Treatment

Thermal treatment is a typical process of prestressing, according to EN 12150, in which the glass is moved forward on rollers into the heating zone and is heat up above the transition point. After this phase, the glass is blown with air. During the phase of cooling to ambient temperature, the glass is

permanently moved forwards and backwards on rollers in the furnace. The thinner the glass, the greater the so-called roller waves occur (Neugebauer & Waller-Novak, 2018).

Thermally treated glass can be distinguished in: thermally toughened, heat-strengthened and heat-soaked thermally toughened safety glass (Schittich, Staib, Balkow, Schuler, & Sobek, 2007).

Thermally toughened glass: The flat glass pane is heated to its transformation point (min 640°C). Once the entire glass has reached this temperature, the material is cooled down. The surface cools faster than the core of the glass. This creates additional compressive stresses in the surfaces, which make the glass stronger.

Heat-strengthened glass: The production of Heat Strengthened Glass is similar to the one of thermally strengthened glass, since the glass is heated and cooled with air. However, the cooling phase is done more slowly, resulting in lower stresses at the surface, but better breakage behaviour.

Heat-soaked thermally toughened safety glass: Toughened glass is heated for a specific period at moderately high temperatures to reduce the possibilities of spontaneous fracture in service. Heat soaking is recommended where roof applications are required.

The principle of glass tempering consists in prestressing the glass, as it is shown in Figure 2.6. A layer of compressive stress on the surface of the glass can make the glass stronger and more resistant to existing flaws and imperfections.
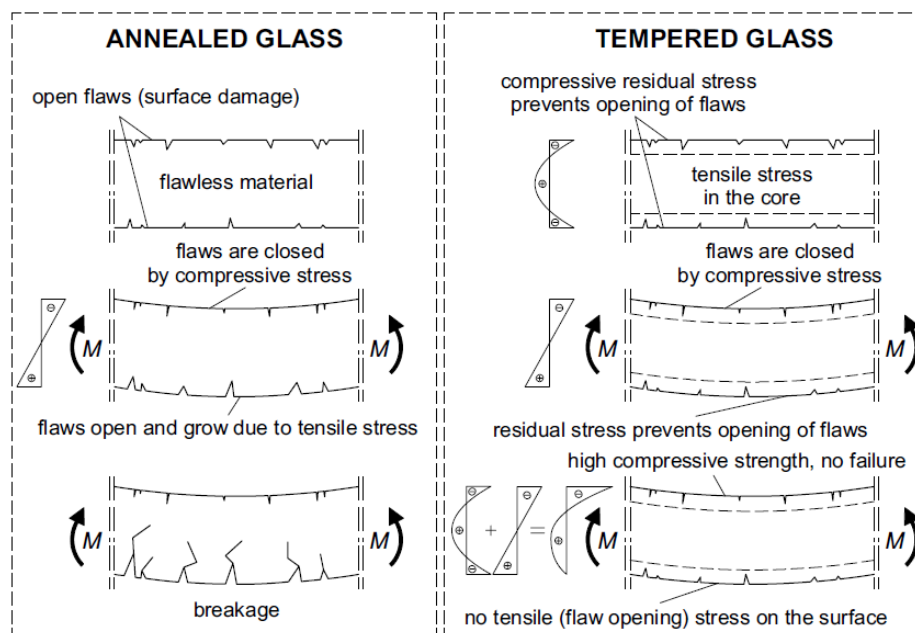

Figure 2.6 Principle of glass tempering (Louter, 2017)

The fractural pattern of glass depends on the amounts of energy stored in the glass. For this reason, the post breakage pattern is different, because it is related to the energy released by the panel. As a general rule of thumb, the more energy the glass contains, the smaller the particles are that results in breakage (Hundevad, 2014). The fractural patter of annealed, heat strengthened and fully tempered glass is shown in the following picture.
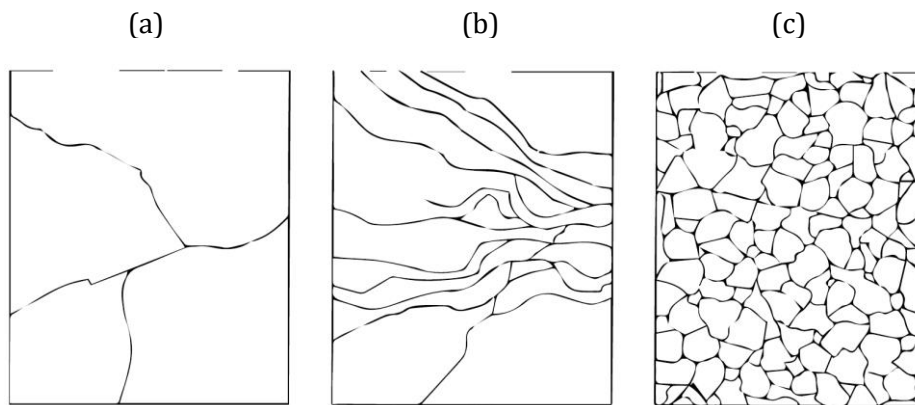
Figure 2.7 Fracture pattern - (a) Annealed, (b) Heat strengthened and (c) Fully tempered glass

(Schittich, Staib, Balkow, Schuler, & Sobek, 2007)

Chemical Treatment

The chemical treatment is the one generally used for thin glass, and for this reason, it will be explained more in detail. Chemical tempering is a post-process procedure in which the glass is submerged in a salt bath. The bath contains potassium salt (typically potassium nitrate). During this time, exchanging of ions will occur: the sodium ions in the glass will be replaced by potassium ions, which are larger (Figure 2.8). When large diameter K+ replace the space of smaller Na+, the larger ions are squeezed into a smaller space. Since the volume of the glass has to remain constant, the ions are compressed to fit the space. This squeezing force is better named as compressive stress. This procedure will generate a uniform layer of Compressive Stress on the outside layer, as it is shown in Figure 2.9 (Materials., September 2007).
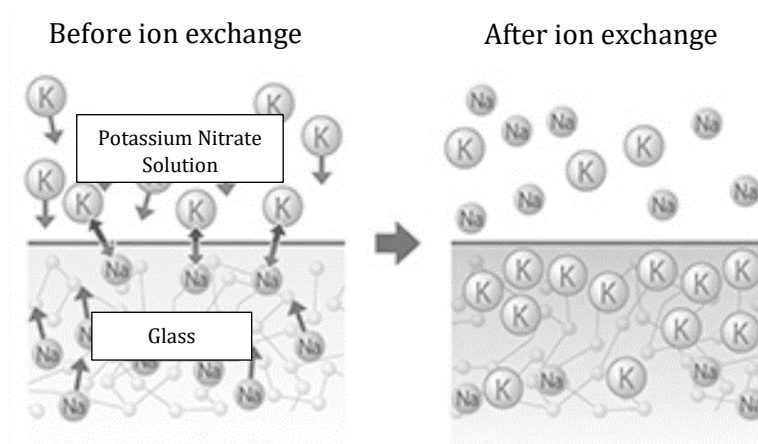
The ion exchange mechanism of glass strengthening

Figure 2.8 Chemical Strengthening Ion Exchange (http://www.neg.co.jp/en/product/dp/dinorex, s.d.)
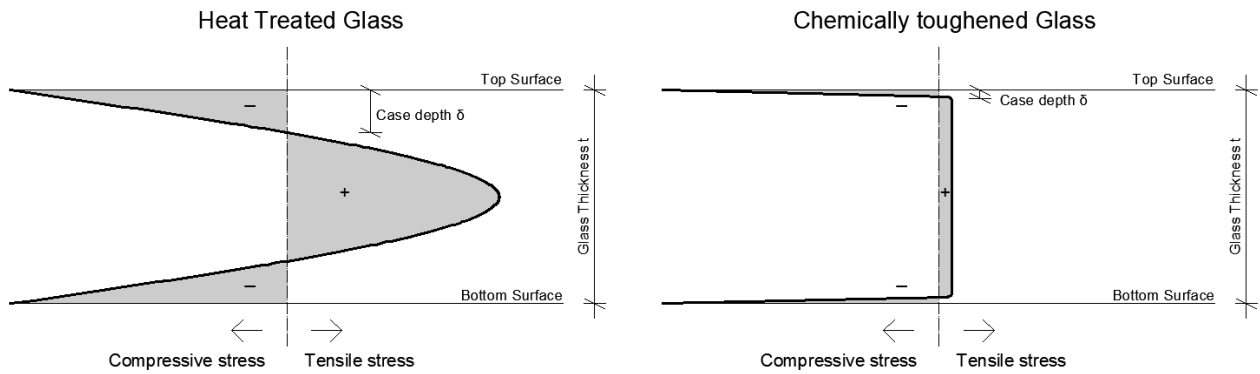
Figure 2.9 Comparison of stresses introduced by Heat treated glass (left) and chemically toughened glass (right)

The degree of chemical tempering is measured by the magnitude of Compressive Stresses (CS) and the depth of the compressive stress layer, also called Depth of Layer (DOL). The process depends on the time the glass is left in the bath, the temperature of the salt bath and the composition of the salt bath. Generally, at a higher temperature the DOL will be deeper, thanks to a higher value of ion exchanging; while the CS will be lower, due to the relaxation of stresses at a higher temperature.

The effect of the chemically strengthened glass has been compared between Aluminosilicate glass and Soda Lime glass, in the research of Gomez (Gomez, S. et al., 2011). As it has been explained above, the exchange of smaller sodium ions with bigger potassium ones, creates a compressive layer in the glass surface producing compressive stress (CS). On the other hand, just below the compressive stress, a volume under tensile stress (TS) will equalize the situation. As time and temperature increase, DOL increases, while CS decreases. The interesting fact is that comparing to Soda Lime Glass, Gorilla Glass, a particular Aluminosilicate type of glass, is not only able to reach a deeper DOL, but also maintaining higher CS. Those facts underline the potentialities of using a chemical treatment on this type of glass. The results of the experiments (Gomez, S. et al., 2011) are shown in the picture below:
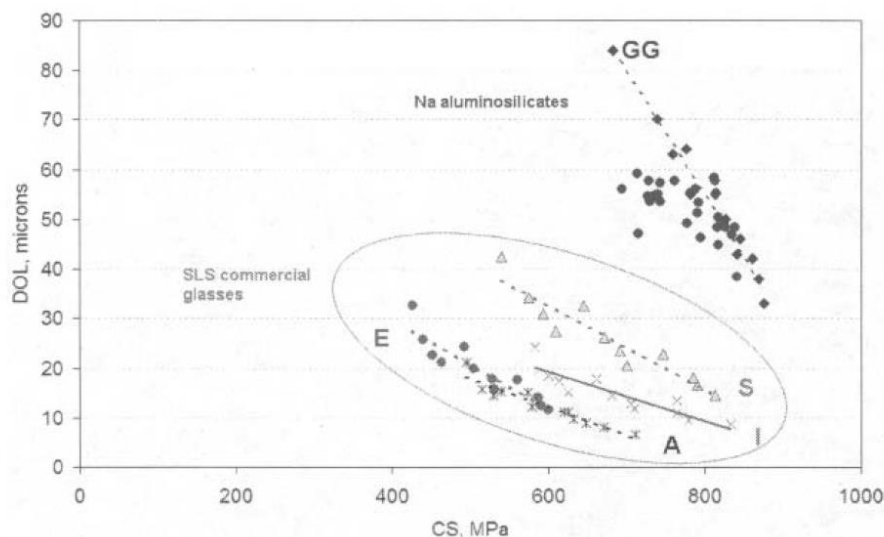

Figure 2.10 DOL vs CS for a set of commercial Soda Lime Glass (SLS) and Gorilla Glass (GG) (Gomez, et al., 2011)

Another feasible alternative of Gorilla Glass is offered by AGC Group. Similar results can be achieved with Falcon glass, a new type of Aluminosilicate thin glass, suitable for chemical toughening and produced by very high quality, cost-efficient float process. The comparison between Soda-Lime Glass, Falcon and Aluminosilicate Glass is shown in Figure 2.11. The specific performances of Falcon glass are summarized in Appendix A.
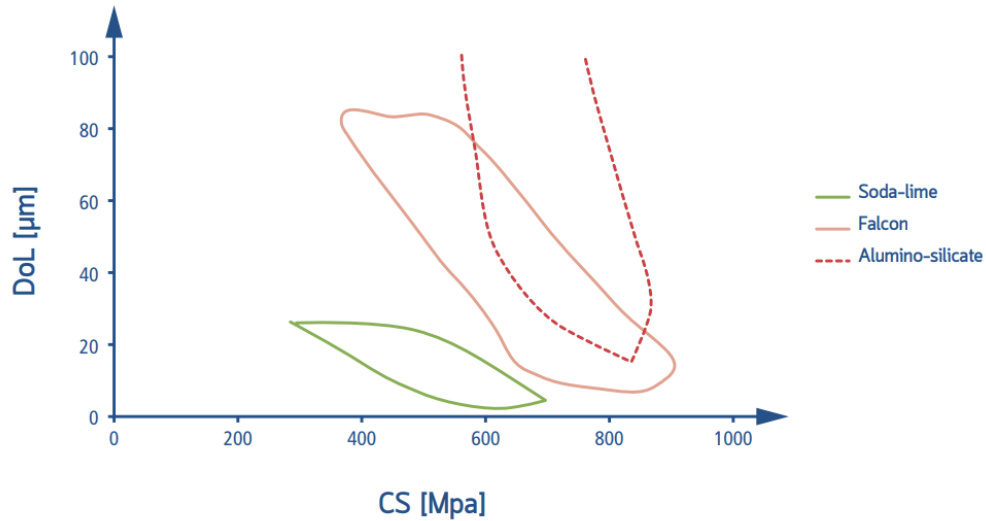

Figure 2.11 Performance achievable with chemical tempering (AGC Group, 2016)

2.4.2   Laminated Glass

Laminated glass consists of two or more layers of glass bonded together with an intermediate layer. The lamination process is usually obtained by treating glass to heat (140°C) and pressure (up to 14bar) and takes place in autoclaves. Lamination does not avoid brittle glass behaviour, however, laminated glass is a type of safety glass that holds together when shattered (Schipper, 2015). In the event of breakage, the glass is held in place by the interlayer, typically polyvinyl butyral (PVB). The interlayer keeps the broken glass bonded to the other ply of glass, preventing the panel from falling apart. Laminated glass is typically used when there is a possibility of human impact or when the glass could fall is shattered.

Layering
(Panes + PVB foil)

Compressing

Autoclave
(Heat + Pressure)
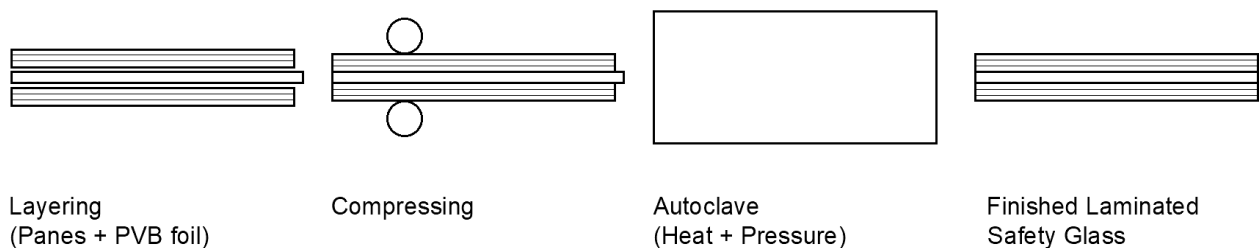
Finished Laminated
Safety Glass

Figure 2.12 Lamination process with Autoclave (Schittich, Staib, Balkow, Schuler, & Sobek, 2007)

Laminated glass without safety features can be used for sound insulation. The interlayer can be made from casting resins as well as other organic or inorganic compounds (Schittich, Staib, Balkow, Schuler, & Sobek, 2007).

2.4.3   Curved Glass

Curved glass can be produced in case a not flat surface is required. There are two ways of bending the glass, the first is hot bending, while the second is cold bending.

Hot Bending

Hot bending can be realized by means of gravity or by pushing the glass into a mould at a temperature of about 640°C. The first technique is also known as "sag bending", where the glass, once heated, will deform under its own weight, and it will assume the shape of the supporting mould. The second process consists in putting a glass pane into a top and bottom mould with the desired shape, it also allows to realize double curved shapes. Moreover, a smaller bending radius, which means bigger curvature, can be reached with this second technique. Both hot bending processes are shown in Figure 2.13. Curved panes can be allowed to curve down normally, or they can be subsequently prestressed. Due to their shape, curved panes are less flexible than flat ones and so are less able to deform under load.

Figure 2.13 Hot Bending - Sag bending technique (left) and Autoclave (right) - (Louter, Material Characteristics, Production, Processing & Products, 2017)

Cold Bending

Cold bending is a process that uses the linear elastic deformation behaviour of glass. Since cold bending is a linear elastic process, the glass has to be mechanically fixed once it has reached the desired shape. Permanent tensile stresses are induced in the glass due to cold bending, which is why usually a stronger glass is used (thermally or chemically strengthened). When single curvature is considered, the thickness of the glass is decisive for the tensile bending stress and the possible bending radii. The minimum bending radius R_{min} depends on the thickness of the glass and the strength of the glass.

$$\kappa_u = \frac{1}{R_{min}} = \frac{M_u}{EI} = \frac{\sigma/W}{EI} = \frac{\sigma}{E \cdot \frac{h}{2}}$$

Then, the minimum bending radius can be written as:

$$R_{min} = \frac{E\,h}{2\,\sigma}$$

Where σ is the glass bending strength, E is the Young's Modulus, which is around 70 GPa for glass, and h/2 is the distance of the outer fiber from the neutral axis, considered at midway in this case (Figure 2.14).
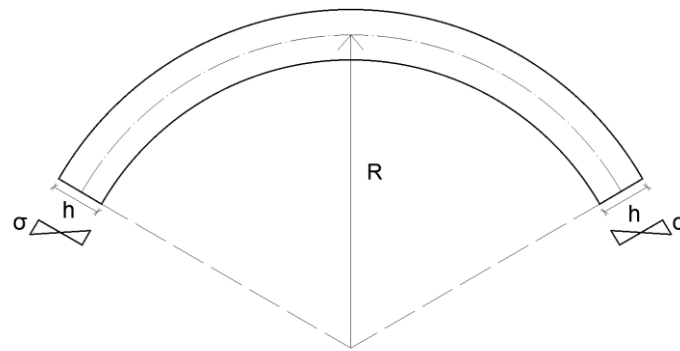
Figure 2.14 Relation between bending radius R and glass bending strength σ

Cold bending has copious advantages. First of all – as it can be deduced from the name – it does not require a heating process, and thus, it is less expensive to realize. The glass sheet is fabricated as a flat panel, and then it is curved in situ. Moreover, cold bending does not introduce optical distortions, so the final product assures an optical and technical quality. The negative side of the process is that the material and shape properties limit the range of adequate double curved shell geometries that can be realized. Since cold bending of glass is an elastic, reversible procedure, the applied deformation has to be fixed either by fastening to a supporting substructure or by "conserving" the curved shape by laminating the curved glass panes with a shear-stiff interlayer (Fildhuth & Knippers, 2011).

Double curvature shapes could also be of interest with the usage of glass, due to the load bearing behaviour for glass applications. The load bearing behaviour is via membrane forces. In particular anticlastic geometries results in small, uniform bending moments and high membrane forces. Those can be distinguished into circular in-plane tensile forces along the pane periphery, and compression about the center (Fildhuth & Knippers, 2011). Limitations of glass are the low tensile stress resistance and the possible dimensions of laminated glass elements, which bring the glass shell design a challenge.

An experimental study has been carried out by Thiermo Fildhuth and Jan Knippers (Fildhuth & Knippers, 2011). The behaviour of double curved cold bent glass laminated shell is investigated to be used as a roof or façade panels. The analysis has been made for three basic shell shape of 10m x 10m, and then some parameters have been varied to observe the different trends. Joint stiffness, load cases, minimum radii of the shell, and support conditions were the parameters used in the study. From the results (Fildhuth & Knippers, 2011), it can be seen that the façade panel has better behaviour compared to the roof glass panels. Moreover, shell shapes allow sufficient structural stiffness and membrane behaviour, which permit high transparent, attractive shell for architectural applications. According to Fildhuth and Knippers, the realization of double curved cold bent glass panel is a possible process for facade applications. Many examples have been already researches. The focus point of the research is now to find the correct interlayer to keep the curved glass in shape without the use of a frame or supporting structures.

2.5   Thin Glass – potential applications

Thin glass has become popular in the 21st century, with electronic devices. It is a common material to be used as screen protector of many smartphones. Since 2010, the possibility of using thin glass as a building material has been investigated.

After having explained the characteristics of thin glass, from its chemical composition to the way it is produced, the structural benefit of thin glass are listed by Hundevad (Hundevad, 2014):

- Lightweight structure – the dead load will considerably decrease.
- High strength – since the chemical procedure will enlarge design stresses up to 10 times stronger than thermally tempered glass.
- High deformation – the combination of thin glass and a high strength allows large deformations without breakage.
- Cold for bending – easily to perform due to the flexibility of the glass sheet.

Hundevad suggests not to continue in the prevailing trend of making the glass thicker to enlarge the design strength, which would be useless with the new technology of thin glass. However, the design approach needs to be adjusted accordingly. The author believes that the characteristics of high deformation and high strength should be combined to form a curved structure. "Applying a curvature to a flat panel results in an increase in stiffness where the forces inside the glass change from being bending forces to in-plane forces" (Hundevad, 2014).

Lastly, energy considerations are underlined in the final paragraph of the paper (Hundevad, 2014). The lightweight of the structure leads to less material to be fabricated, which leads to energy savings. A rough calculation estimates that chemically toughened glass could reduce overall energy consumption up to 20% compared to that of conventionally heat tempered soda lime glass, by enormous savings in CO_2 emissions for the future. On the other hands, it needs to be underlined that the emissions due to the chemically strengthened process are still unknown. For this reason, an average between the reduction from the less material used and the addition of chemically strengthened process, cannot be drawn yet.

Other interesting researches on thin glass have been performed by Lambert and O'Callaghan. The paper presents the properties of Gorilla Glass™ (Code 2318), a type of glass developed by Corning®, chemically strengthened and its potential applications. The Fusion glass fabrication process has been developed by Corning in 1964 (Lambert & O'Callaghan, 2013). The process has been explained in the previous chapter (Paragraph 2.3.2 Production Process for Thin Glass). This process grants to have a very thin sheet of glass as a final product. After having being submerged in a salt bath, the thin sheet of glass, chemically strengthened by ion exchange, will also reach a high strength. According to Lambert and O'Callaghan, Gorilla Glass has a significant architectural potential.

The most significant part of the paper is the Potential Applications chapter, in which the authors underline possible research fields. Due to the limited bending stiffness offered by the thin glass in its flat form, three approaches are proposed to improve the stiffness of the glass:

1. Laminate the glass to a core structure
2. Cold bend the glass
3. Treat the material as a fabric glass

The paper deeply analysed the first option, by carrying out tests on a laminated flat plate composed by code 2318 and other types of glass, such as annealed soda lime glass, heat strengthened soda lime glass, fully tempered soda lime glass or even with polymeric materials such as polycarbonate, polymethylmethacrylate and thermoplastic polyurethane. According to the paper, by laminating the code 2318 with other types of glass, the result is something very similar to the laminated glasses, already present on the market, but with a higher failure resistance. Thus, this product could be a valid alternative to laminated heat strengthened safety glass or security glazing and for those reasons is deeply investigated in the paper. Testing is performed to compare the behaviour of a two plies heat strengthened laminated panel, with a three plies laminated panel: chemically strengthened glass in the outer ply and soda lime glass in the core. The first panel exhibits a brittle failure mechanism, while the chemically strengthened laminated panel can be associated to a ductile failure mechanism. This behaviour is confirmed by laboratory tests as shown in the following figure.
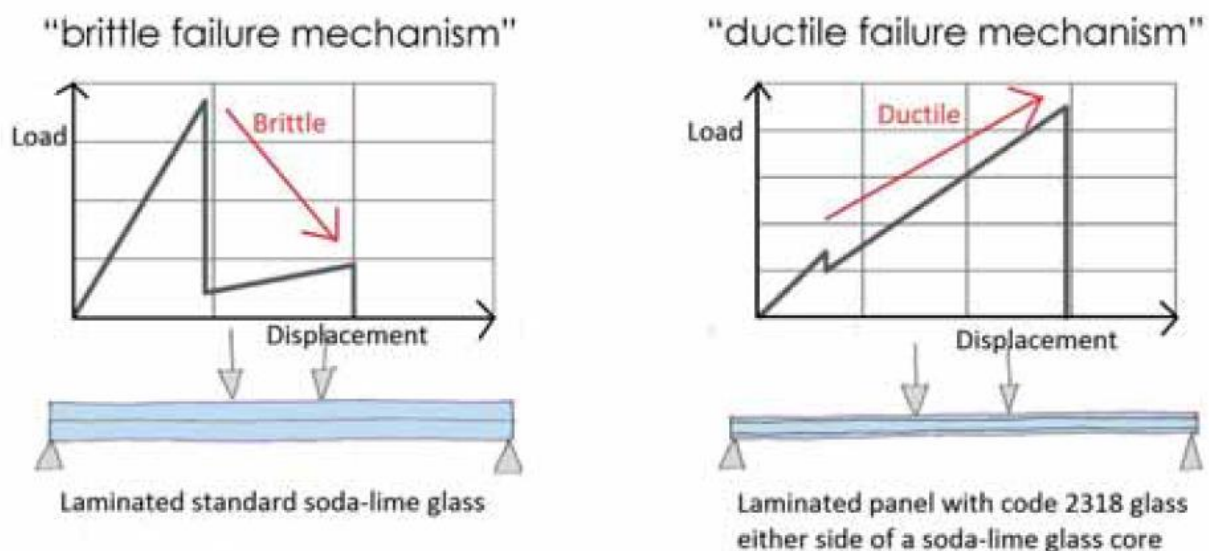

Figure 2.15 Comparison between laminated standard soda-lime glass and laminated panel with code 2318 glass and soda-lime glass (Lambert & O'Callaghan, 2013)

The same approach has been investigated by Michele Akilo and Tim Neeskens. Their research have been illustrated in the Introduction, Paragraph 0, Figure 1.3 and Figure 1.4.

According to Lambert and O'Callaghan (Lambert & O'Callaghan, 2013), further investigation for the utilization of chemically strengthened glass in cold form surfaces and tensile membrane structure would be of great interest. In Paragraph 1.1, the available researches on the suggested strategies have been illustrated.

2.6   Conclusion

After having discussed the characteristics of glass, the first sub-question can now be answered:

What are the characteristics of chemically strengthened aluminosilicate glass, compared to the commonly used soda lime silica glass?

The first difference is shown in the chemical composition of aluminosilicate glass, where a lower percentage of silica sand is replaced by a higher amount of alumina (Table 2.1). This aspect provides to aluminosilicate glass a higher melting point. In fact, it is used for fire-resistant glazing applications. The density and the strength of the two materials are about the same. However, the strength of aluminosilicate glass can be increased more effectively by the chemically strengthened procedure. In fact, alkali aluminosilicate glasses are more prone to chemically strengthened treatments compared to soda lime silica glasses, since high alkali content facilitates the glass for ion exchange and a thicker compression layer is created. For this reason, aluminosilicate glass has been chosen to be used in this research. With the usage of aluminosilicate glass, a lower thickness and high strength glass can be obtained, as a result of the chemically strengthened procedure. The same characteristics in strength could not be achieved with the use of a ply of soda lime silica glass of the same thickness.

To what extent can thin glass be cold bent?

Theoretically, if a single curvature wants to be reached, the minimum bending radius R_{min} depends on the thickness of the glass and the strength of the glass. As it has been demonstrated in paragraph 2.3.3, the minimum bending radius can be written as:

$$R_{min} = \frac{E\,t}{2\,\sigma}$$

Where σ is the glass bending strength, which has been defined 260 MPa for Leoflex glass (Appendix A), E is the Young's Modulus of Leoflex glass, which is 74 GPa, and t/2 is the distance from the outer fiber to the neutral axis, considered at midway in this case. Therefore, the minimum bending radius that can be obtained with thin glass, 0,55mm Leoflex Glass is 78,3mm. The same calculations can be performed with the properties of Falcon Glass.

Cold bending is a process that uses the linear elastic deformation behaviour of glass. Since cold bending is a linear elastic process, the glass has to be mechanically fixed once it has reached the desired shape. Permanent tensile stresses are induced in the glass due to cold bending, which is why usually a stronger glass is used (thermally or chemically strengthened). When single curvature is considered, the thickness of the glass is decisive for the tensile bending stress and the possible bending radii.

3. Sandwich Structures

3.1   Introduction

In this chapter, the theory of sandwich structures will be explained. Initially, sandwich structures will be briefly discussed through a historical background. Then, the sandwich theory will be summarized. After having explained the advantages of sandwich structures, the following sub-questions will be answered:

- *To what extent will a sandwich structure increase the stiffness of the panel?*
- *Which technique is the most appropriate for realizing the core?*

3.2   Historical Background

A sandwich panel consists of two thin, stiff, strong sheets made by a dense material which are bonded with a thick layer of low density material, named core (Allen, 1969). The roles of the core are mainly two: it has to keep apart the faces at the designed distance and it must not allow the faces to slide. These requirements can be translated into having a rigid and robust element, which is able to transfer shear from one skin to the other (Hexcel Composites, 2000). The separation of the skins by the core increases the moment of inertia of the panel with little increase in weight, producing and efficient structure for resisting bending and buckling loads (Petras, 1998). An example of a sandwich panel is shown in the following figure.
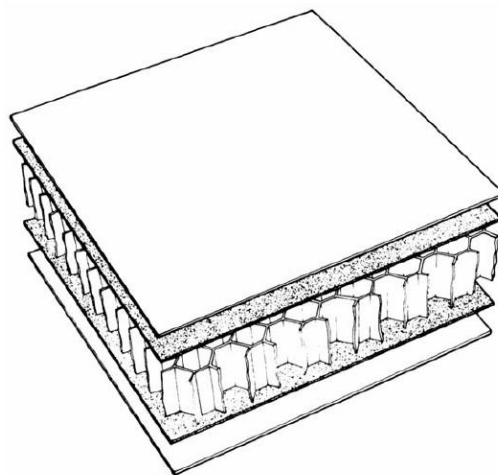

Figure 3.1 Sandwich Structure with Honeycomb Core (Petras, 1998)

The behaviour of a sandwich structure can be compared to the one of an I-beam. The web of an I-beam resists the shear forces, while the flanges resist the bending moment experienced by the beam. Similarly, the core of a sandwich structure carries the shear forces while the faces resist the bending moment. An increase of the thickness of the sandwich structure brings to the increasing of the stiffness of the panel. An indication of how much the stiffness is increased by the use of a sandwich structure, is given in the following table. Table 3.1 shows the results of the research on sandwich panels obtained by HexWeb (Hexcel Composites, 2000).
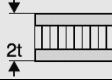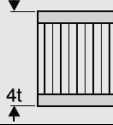
	Solid Material	Core Thickness t	Core Thickness 3t
Stiffness	1,0	7,0	37,0
Flexural Strenght	1,0	3,5	9,2
Weight	1,0	1,03	1,06

Table 3.1 Relative Stiffness and Weight of Sandwich Panels compared to Solid Panels (Hexcel Composites, 2000)

Sandwich structures are popular in high performance applications where the weight must be kept to a minimum, for example aeronautical structures, high speed marine craft and racing cars (Petras, 1998). The concept of a sandwich structure was already present in nature. Nature discovered and evolved low density cellular material soon after life began on earth. Figure 3.2 shows how well nature exploits these clever design practices to create structures that can support high bending loads at a minimal weight (Wadley Research Group, 2014).
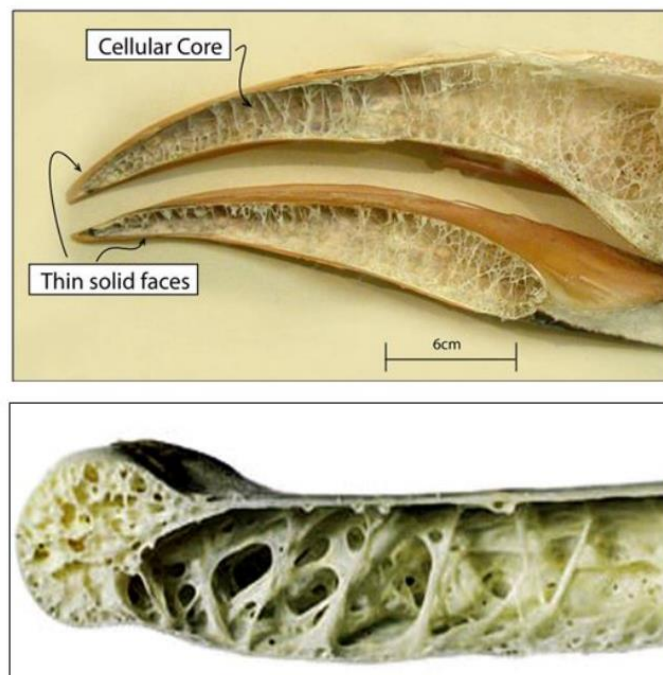

Figure 3.2 Cross sections of (top) the break of a Hornbill and (bottom) an avian wing bone

Engineers imitated the nature in its type of structures. One of the first industry which starts using sandwich structures was the aerospace industry. The first honeycomb structure was designed for the Mosquito airplane, during the Second World War. The purpose of this structure was to find a light weight but strength resistance structure, combined to seek structural efficiency.

Figure 3.3 Mosquito aircraft (left), sandwich structure of an airplane wing (right)

3.3   Sandwich Theory

In order to investigate the theory of sandwich structures, let's consider a cantilever beam with a punctual load applied at the end. The applied load creates a bending moment which is maximum at the fixed end, and a shear force along the length of the beam. Tension will occur at the upper face of the sandwich, while compression in the lower face, as it is shown in Figure 3.4. In order to reach this global behaviour, it is essential that the adhesive layer is strong enough not to delaminate and to ensure structural integrity. The function of the core is to transfer shear between the faces of the composite panel and to make it work as a homogenous structure (Hexcel Composites, 2000).
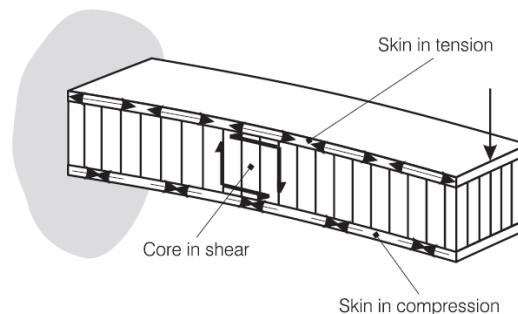

Figure 3.4 Sandwich Beam behaviour under loading (Hexcel Composites, 2000)

The deflection of a sandwich panel is made up from bending and shear components. The total deflection of the beam is a sum of the bending deflection and the shear deflection, as it is shown in Figure 3.5. The bending deflection depends on the Young's Modulus (E) of the skin material, while the shear deflection depends on the Shear Modulus (G) of the core.
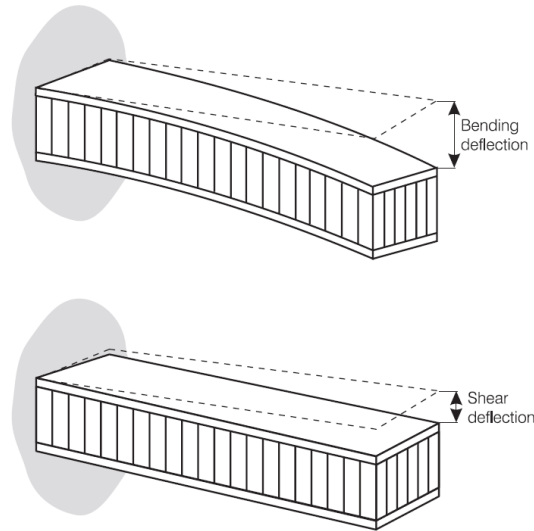
Figure 3.5 Bending and Shear Deflection of a Sandwich Panel (Hexcel Composites, 2000)

3.3.1   Failure Modes

In order to design a sandwich structure correctly, it is essential to know where the structure could fail. Designers must ensure that all potential failure modes are considered in their analysis. A summary of the key failure modes of sandwich structures are shown in the following list (Hexcel Composites, 2000):

1.   Strength

The stresses induced in the panel must not exceed the yield limit state of the material, both in the skin and in the core material. Moreover, the adhesive used between the skin and the core must be capable of transferring the shear stresses.
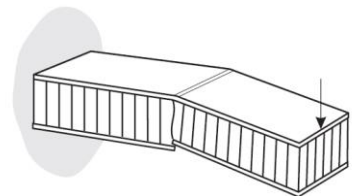
2.   Stiffness

The sandwich structure has to have enough bending and shear stiffness to deflect too much according to limitations imposed by the codes.
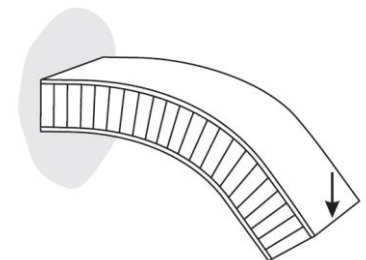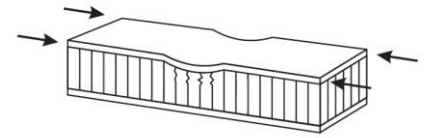

3.   Panel buckling

The thickness of the sandwich panel has to be designed in order to prevent the panel to buckle under compression load. The shear modulus must be high enough to prevent buckling on the global scale of the panel.
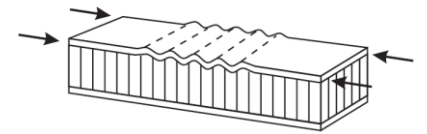
4. Skin wrinkling

Failure occurs in one skin due to face yielding when the axial stress reaches the in-plane strength of the face material. The compressive modulus of the skin has to be big enough to prevent skin wrinkling failure.
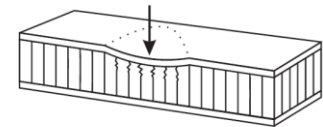
5. Intra cell buckling

The core cell size must be small enough to prevent intra cell buckling.

6. Local compression

The core compressive strength must be adequate to resist local loads on the panel surface.

3.3.2   Design Guidelines

Hexcel Composites (Hexcel Composites, 2000) gives some key steps that need to be followed in order to design a sandwich structure correctly.

1. Define loading conditions
2. Define support conditions
3. Define physical/space constraints (e.g. deflection limit/thickness limit/weight limit/safety factor)
4. Preliminary calculations
   4.1 Assume face material, thickness and panel thickness
   4.2 Ignore the core material at this stage
   4.3 Calculate stiffness
   4.4 Calculate deflection (ignoring shear deflection)
   4.5 Calculate facing skin stress
   4.6 Calculate core shear stress
5. Optimize design
6. Detailed calculations
   6.1 Strength
   6.2 Deflection
   6.3 Facing skin stress
   6.4 Core shear stress
   6.5 Panel buckling
   6.6 Intra-cell buckling
   6.7 Local compression

3.4   Core Topologies

This section gives an overview of the most common core topologies, typically found in literature and adopted in many engineering fields. The first distinction, which is usually done, is between homogeneous and non-homogeneous cores: the first ones are generally high-density foams, while the second ones can be divided into other three categories: bi-directional support, uni-directional support and punctual support cores (Wadley, 2006). Homogeneous cores will not be taken into consideration in this research, because the purpose of the proposed sandwich panel, which has thin glass as a face material, is to find a solution where the sunlight can pass through the panel.

3.4.1   Bi-directional support

Bi-directional support cores are the well-known honeycomb cores. Honeycombs have closed cell pores and are well suited for thermal protection, while also providing load support. The most common closed shape cores are shown in Figure 3.6, where the well-known honeycomb is shown in Figure 3.6 (a), then, if the angle between the cells is 90°, the pattern is called square honeycomb (b). Moreover, if the angle is 60°, the pattern is composed of triangular elements (c).
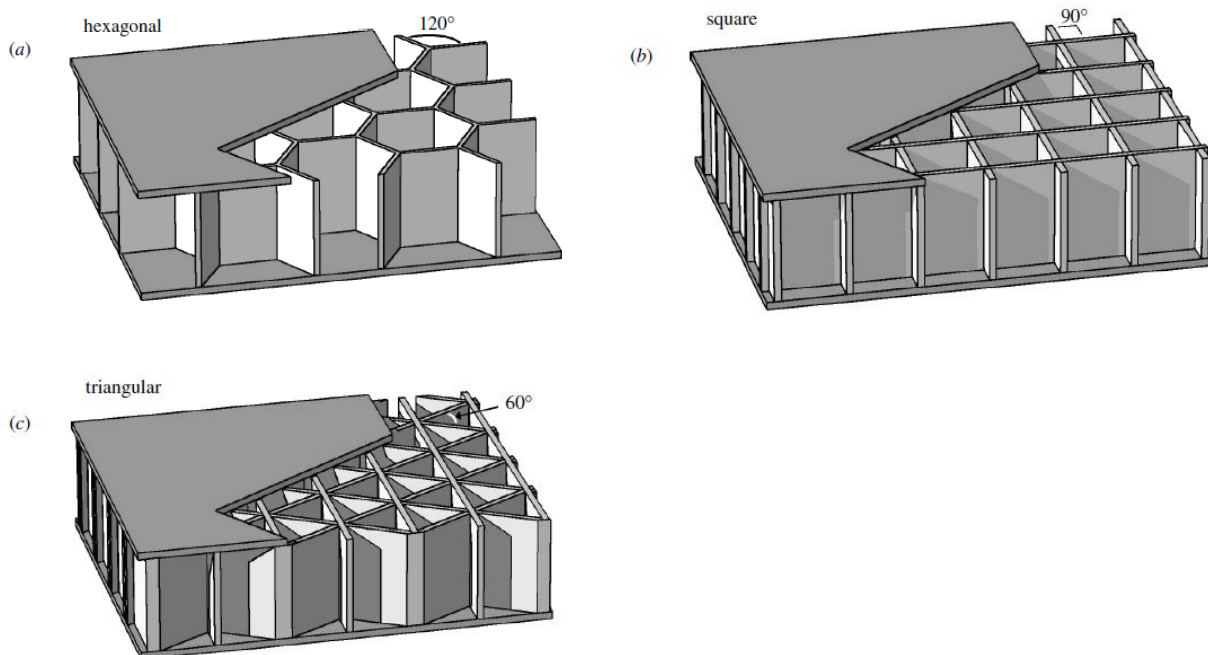

Figure 3.6 Bi-directional Structure - (a) honeycomb, (b) square, (c) triangular (Wadley, 2006)

3.4.2   Uni-directional support

Uni-directional corrugated core structures are highly anisotropic, but enables cross flow heat exchange because their pores are continuous in one direction. For this reason, those structures are highly utilized in building structures. The most common corrugated cores are shown in Figure 3.7, which includes triangular, diamond topology and a steeper web truss corrugation with a flat top that is widely used in buildings and for marine applications, and thus, it is called Navtruss.
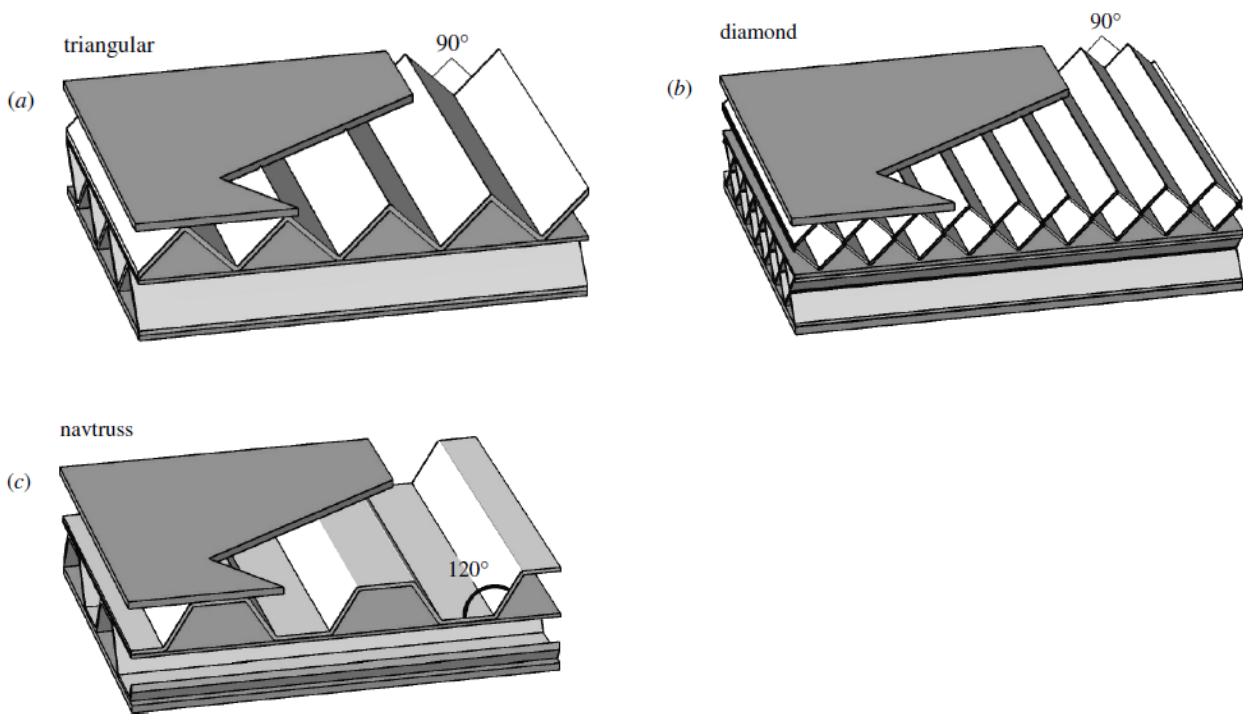
Figure 3.7 Uni-directional Structure - (a) triangular, (b) diamond, (c) navtruss (Wadley, 2006)

3.4.3   Punctual Support

More recent topology designs have led to truss structures with an open cell structure. This topology provides supports for high stresses while also enable cross flow heat exchange in two directions. The most common patterns are shown in Figure 3.8. The three dimensional kagome pattern is the one who provides the highest strength per relative density (Vitalis, 2017). However, it has to be underlined that the geometry of the kagome patter would introduce more challenges during manufacturing, for the gluing phase. According to the same research (Vitalis, 2017), the pyramidal lattice structures is the second pattern which provides a relatively high strength and stiffness for a low relative density.
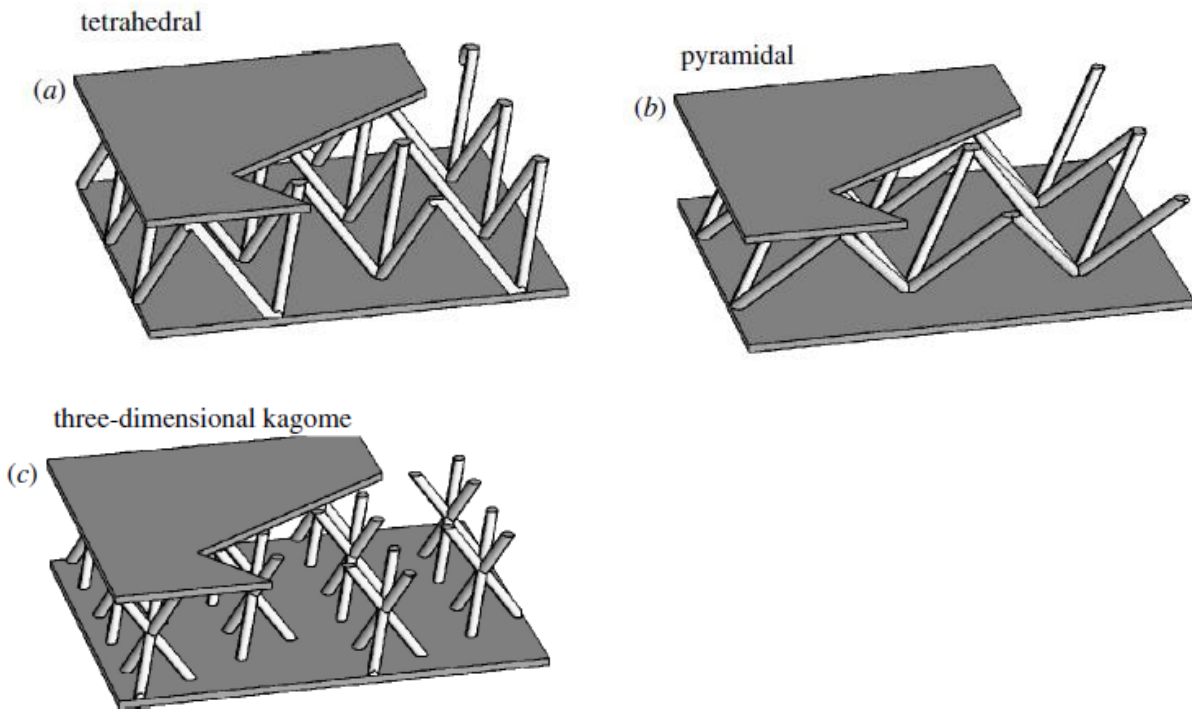
Figure 3.8 Punctual Structure - (a) tetrahedral, (b) pyramidal, (c) three-dimensional kagome (Wadley, 2006)

3.5   Comparison of Core Topologies

In order to decide which pattern will be further investigated in this research, a more in depth analysis of the previously proposed core topologies will be performed. The parameters defined for this specific research have been set to:

- Shear stiffness provided by the core pattern
- Possibility to realize a curved shaped panel

Punctual Support Core

The first pattern that has been deeper analysed is the punctual support core. In Figure 3.9 (right) an analogy within the above mentioned open cell structures core (Figure 3.8) and a space frame can be seen. A space frame is a spatial configuration composed by members in tension or compression which are connected to each other by nodes which work as hinges. Double layer grids take advantages from the two spanning structural system which distribute the load more efficiently compared to single layer grids. This concept can be easily understood by Figure 3.9.
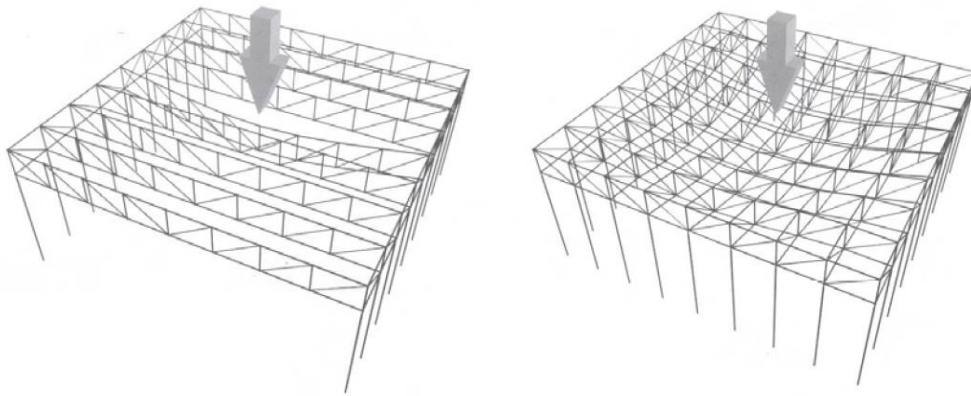
Figure 3.9 Deflection of a system of individual trusses (left), Deflection of a system of intersecting trusses (right)

(Coenders, 2008)

A spaceframe is made by the same unit cell repeated in two main directions, as well as the realization of a tetrahedral or pyramidal lattice core. Both topologies have geometrical freedom in their structures that make them suitable for many applications in which a stiff and light weight structure are needed.

One of the main advantages of the space frame is that it is structurally efficient, because it generally consists of triangles, which are form stable elements. Moreover, by the use of a space frame structure, free form design can be easily realized. A single curvature shape, which is the desired configuration for the panel, could be simply achieved by a space frame.

The reason why a punctual support core was chosen to be investigated more in detail is because these patterns are those with the lowest relative density. In between the punctual support patters, the pyramidal unit was chosen since it could provide the best compromise in term of strength and stiffness added to the panel and simplicity in panel production, according to the research of Vitalis (2017).

Bi-directional Support Core

Shear stiffness is one of the main characteristic needed in the core. For this reason, honeycomb cores are taken into account. For flat panels subjected to bending, honeycomb cores show the best result in stiffness behaviour (Evans, 2001). For curved panels and shells, the preferences differ because the loading on the core is biaxial. A more significant benefit derives from isotropic topologies. It has been decided to choose the square cell pattern as a second core proposal. This choice has been made in order to compare a punctual support structure with a bi-directional support structure. This second core proposal has a higher relative density of the core, but it should also add more stiffness to the core. Moreover, the closed cell pattern has been chosen because there are no diagonal elements in the structure. Since the faces of the sandwich panel will be made by glass, the light can pass directly from one face to the other without obstructions.

Topology Optimization

Another possibility is to realize a freeform geometry with the use of Topology Optimization (TO). This technique combines mechanics, mathematical programming and seeks an optimal structure depending on the boundary conditions and the loading conditions that have been set by the user. TO takes off all

the parts of material which are not necessary to carry the load. In this way, an optimized free form structure is reached. An example is shown in Figure 3.10. The end product will have the same structural carrying properties, but the weight of the structure will be highly reduced. A more in-depth explanation of this technique can be found in Appendix B – Structural Optimization.
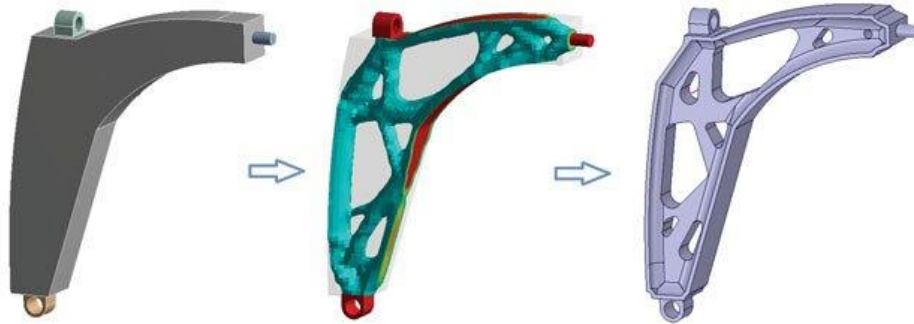

Figure 3.10 Example of Topology Optimization (ANSYS, 2018)

3.6   Conclusion

After having explained the theory of sandwich structures, and the core topologies that were considered in this research, the related sub-questions can now be answered.

To what extent will a sandwich structure increase the stiffness of the panel?

According to the theory of sandwich structure, by using a sandwich panel of double the height of a solid panel, the stiffness of the sandwich panel is increased by a factor of 7, as it has been shown in Table 3.1 (Hexcel Composites, 2000). In practice, in the last paragraph of Chapter 9, the stiffness of the designed sandwich panel is underlined. The sandwich panel, which has a height of 12mm, revealed to be 279,7 times stiffer than a panel made by two layered glass plies, respectively 0,5mm + 0,5mm. It has to be underlined that particular attention has to be given to the connection between the core and the glass faces of the sandwich panel.

Which technique is the most appropriate for realizing the core?

Topology Optimization was the initial preferred method in order to realize a freeform core, designed specifically for the studied sandwich panel. However, after some time constraints due to the computer capacity, programme licences and other practical problems, the two other proposed pattern cores have been started to be designed. The investigated core topologies were a space frame pattern realized by pyramidal unit elements and a close core realized by square cells. The spaceframe has been chosen due to the high strength and low density pattern. While, the square honeycomb has been selected due to high shear stiffness in the core, which is one of the parameters needed in the core of the sandwich panel.

4. Additive Manufacturing

4.1   Introduction

In this chapter, the theory of Additive Manufacturing (AM) will be explained. Firstly, a comparison of all the available AM techniques will be performed. Then, the theory of the chosen AM will be described. Finally, after having explained the advantages and disadvantages of AM, the following sub-questions will be answered:

- *What is Additive Manufacturing (AM)?*
- *Which techniques of AM are currently available?*
- *Which core material is the most appropriate for the analysed problem?*

4.2   General Process of AM

Additive Manufacturing (AM) is the proper name of what it is commonly known as 3D Printing. The term recalls the basic principle of these technologies, which fabricate an object using an additive approach. The technology can fabricate, from a three-dimensional Computer Aided Design (3D CAD), a tangible solid realized by adding material in layers. All commercialized AM machines use a layer-based approach. What can differ, from one technique to another, lies in the materials that can be used and how the layers are created and bonded to each other. Those differences determine the accuracy of the final product and the mechanical properties. Depending on the technology and the machines components, the process chain consists of six steps (Yang, Hsu, Baughman, Godfrey, & Medina, 2017):

1. Generation of CAD model;
2. Conversion of CAD into AM machine acceptable format;
3. CAD model preparation;
4. Machine setup;
5. Part removal;
6. Post-processing.

Step 1: Generation of CAD model
The starting point if any object wants to be developed is to conceptualize an idea and a function of the product. The project description has to be designed in a software model that describes the full geometry of the object that is intended to be 3D printed. It is essential that the geometry is made by a continuous solid, which not comprehend gaps between two surfaces. Otherwise, errors will be detected by the AM Machine.

Step 2: Conversion of CAD into AM machine acceptable format
Once the CAD model has been correctly designed, the file has to be exported to STL file format. This format is the one that can be read by the printing machine. STL file describes the external object's geometry with a polygonal mesh. It also divides the model into slices, in order to create the layers that will be subsequently printed. The file has to be sent to the AM Machine. Some general adjustment may be needed in the model.

Step 3: CAD model preparation

Generally, scale, position and orientation of the model have to be checked. Moreover, the support generation, if applicable, will be create in this phase. A slicer program is used to divide the models into layers in the desired build direction.

Step 4: Machine Set up

The machine has to be correctly set up in its building parameters. Each parameter can depend on the type of process that is being used. Parameters generally consist of material constraints, energy source, layer thickness, printing speed, etc. Then the machine can start building the parts.

Step 5: Part removal

Once the AM Machine has finished, the objects can be removed from the AM Machine. This operation has to be carried with extremely careful. The parts have to be separated from the build platform. The supports, if present, have to be taken off. Finally the product has to be cleaned.

Step 6: Post-processing

The post-processing consists of a manual phase in which additional procedure is taken in accordance with the product's application. This may involve abrasive finishing, like polishing and sand papering or application of coatings.

Finally, the product is ready to be used in its intended application. It is important to underline that the object may not behave according to standard material specifications. In most of the cases, the properties are anisotropic. Rapid cooling results in different micro-structures than those from conventional manufacturing. For the moment, the most common materials used for Additive Manufacturing are plastics. The technology was first developed as a method to realize in a fast manner a prototype of a design. This is the reason why Additive Manufacturing (AM) was known as Rapid Prototyping (RP). With the development of the technique, the product starts to be stronger and more accurate, until it could be used as a part of the final product itself and not just a prototype. Moreover, the research starts to widen in using other material. Nowadays, Additive Manufacturing with metals is also possible, and even glass is being investigated to be printed.

Advantages of AM in general:
- Nowadays a great range of materials can be utilized;
- Freedom of shape;
- Time saving/Speed advantage;
- Reduction in process steps;
- Not needed to design the part according to how it is manufactured. Design the part to perform a particular function. It is possible to focus more on the intended application.

4.3   Available AM techniques

The techniques of AM currently available are Stereolithography (SLA), Selective Laser Sintering (SLS), Fused Deposition Modelling (FDM), 3D printing and Inkjet Printing. A comparison of the main characteristics of these techniques can be found in Table 4.1. The parameters, which have been taken into considerations, are: Accuracy, End Surface of the product, Building Speed, if the Support Material is needed to print the part and the Maximum Printing Size available for each technique.

	Accuracy	End Surface	Building Speed	Support Material	Max Part Size (mm)
SLA	++	++	+	Needed	1500 x 750 x 500
SLS	++	+	+	Not Needed	550 x 550 x 760
FDM	+	+	-	Needed	915 x 610 x 915
3D Printing	+	+	++	Not Needed	1500 x 750 x 700
Inkjet Printing	++	++	-	Needed	304 x 152 x 152

Table 4.1 Comparison between Additive Manufacturing techniques

Since all the parameters can have a different weight in the evaluation of which is the preferred technique, these have been defined for this specific research. Considering the fact that a curved part will have to be printed, technologies in which support material is not needed are preferred. For this reason, SLS and 3D printing will be considered. Moreover, since the accuracy of the final part can make a huge difference in the gluing and assembling phase of the panel, Selective Laser Sintering is the preferred technique and it will be deeper described in the next paragraph.

Selective Laser Sintering (SLS)

Selective Laser Sintering (SLS) is based on photopolymerization. It uses a moving laser beam to delineate and selectively sinter a polymer. The primary building material has to be a powdered polymer. In fact, the term "sintering" means to melt powders below the actual melting temperature (Strauss, 2013). After one powder layer is sintered, additional powder is deposited on top of the solidified layer, and the process can start again to create the next layer. One of the biggest advantages of SLS is that, even if hangouts or undercuts are present, support material is not necessary because the not-sintered powder will act as a support during the process. Recent improvements in accuracy and resolution have been achieved with this technique, as can be seen in Figure 4.2. Moreover, a broad range of materials can be used, which also include metals and ceramics. As a drawback of this technique, the parts that can be generated with SLS have limited dimensions, dictated by the dimension of the building chamber.
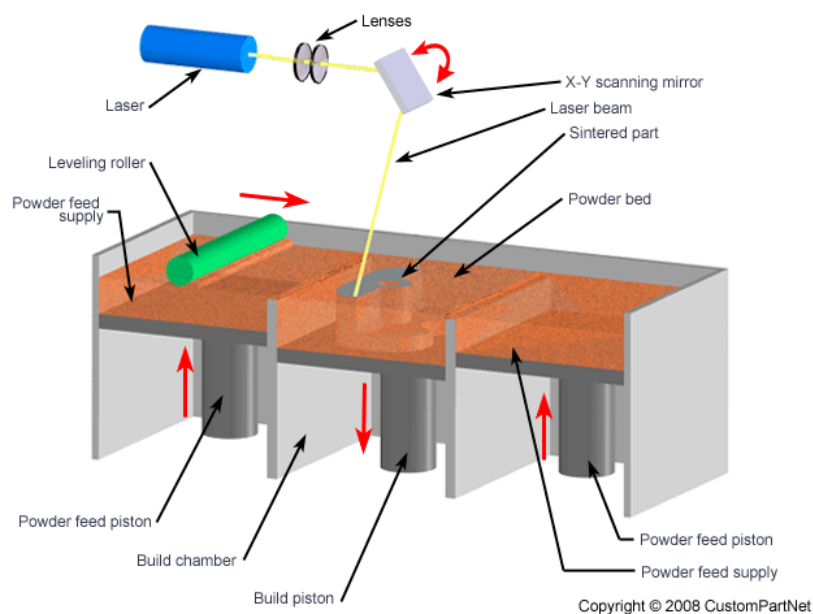

Figure 4.1 Selective Laser Sintering (SLS) Process (CustomPartNet, 2008)

Figure 4.2 Selective Laser Sintering (SLS) Product

SLS Advantages: Building speed;
                     Recent improvements in accuracy and resolution;
                     Parts possess high strength and stiffness;
                     No supports material needed for hangouts and undercuts;
                     A wide range of materials (including nylon, glass-filled nylon, SOMOS (rubber-
                     like), Truform (investment casting), and metal composite).

SLS Disadvantages: SLS printed parts have a porous surface. It can be improved with an infiltration
                     with other materials;
                     Limited dimensions for printing parts.

Max part size: 550 x 550 x 760 mm.

Considerations

Initially, SLS was the preferred technique. After having realized the market availabilities, it has been faced the economical aspect that was not taken into account in the initial evaluation. Seeing that, in order to realize a part with the same size, SLS technique can have triple the price of FDM technique, the latter technique has been reconsidered. FDM is described in detail in the next paragraph. Nevertheless, SLS technique is highly recommended to be investigated in future researches, if the usage of this technology will become more affordable.

Fused Deposition Modelling (FDM)

Nowadays, Fused Deposition Modelling (FDM) is the most commonly used technique in Additive Manufacturing (CustomPartNet, 2008). In this process, a melting nozzle is used to extrude a plastic or wax material. The extruder (melting nozzle) works at a temperature just above the material's melting point so that it can flow smoothly through the nozzle. To ensure that the layers bond one to each other, the entire process chamber is heated and maintained at a certain temperature. This technique first makes the contour lines, and then fill up the interior of the part with a certain percentage of material

settled in advance (infill parameter). Generally the material section is not entirely filled, in order to reduce material consumption, the cost and time. If the part has a structural application, the infill parameter has to be carefully checked and the percentage of infill must be increased. Once one layer has been built, the building platform lowers, and the extrusion nozzle deposits another layer on the top of it. The layer thickness and the vertical accuracy is determined by the extruder diameter. A larger nozzle diameter will ensure the material to flow easily, and thus rapidly, but it will result in lower accuracy of the finished product. If hangouts are present, a supporting structure is needed. The supports can be generated by a secondary nozzle, which is filled with a specific material. Later, the support material can be removed either mechanically or in a solvent bath.
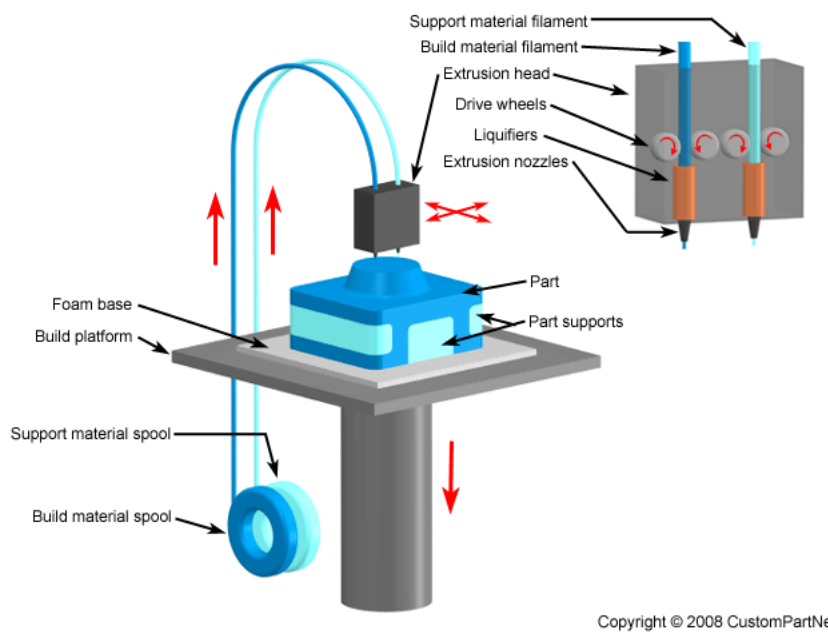
Figure 4.3 Fused Deposition Modelling (FDM) Process (CustomPartNet, 2008)

Figure 4.4 Fused Deposition Modelling (FDM) Product

FDM Advantages: A wide range of materials are available (ABS, Nylon PA, PC, PE, PET, and investment casting wax);

Parts made using FDM are among the strongest for any polymer-based additive manufacturing process.

FDM Disadvantages: Building speed is relatively slow.

Max part size: 915 x 610 x 915 mm

4.4   Materials and Properties

Nowadays, a wide range of material can be used in AM. Manufacturers continuously develop new material for specific applications. Materials available for AM can be divided into three main categories: plastic, metals and other materials (ceramics, wax, gypsum…). In this research, plastic will be taken into considerations.

Plastics that have always been used for AM were Polylactis Acid (PLA) and Acrylonitrile Butadiene Styrene (ABS). PLA has the problem that is not easy to glue, while ABS is UV sensitive. Depending on the applications of the 3D printed product, different requirements were requested. Nowadays, it is also possible to print Polyethylene Terephthalate (PETG), Nylon PA, Thermoplastic Polyurethane (TPU) and Polycarbonate (PC). PETG is becoming more popular in the 3D filament field, because it does not produce bad chemical odours and it is totally recyclable. PETG filament is originally colourless and crystal clear. However, when heated up, the material changes its transparency. PC offers a higher strength but at the same time it is difficult to print due to the high temperature required for the bed of the printing chamber. For this reason, there are not many manufacturers available to print this material. The characteristics of the analysed materials are summarized in the following table:

	Properties			
	Yield Strength (MPa)	Tensile Strength (MPa)	Elongation (%)	Thermal Expansion Coefficient
PLA	2800-3400	47-70	2-3,5	126-145
ABS	1400-2200	30-50	-	108-234
PETG	2400-3000	55-75	-	115-119
Nylon PA	1700-2000	29-31	8-15	176-184
PC	3100-3900	63-72	-	120-125

Table 4.2 Comparison of material properties available for AM

According to the research of Lazzaroni (2018), PC should not be taken into considerations due to printing impossibilities. The research of van Driel (2018), who tested 3D printed PETG under tension tests and three point bending tests, showed that the values of strength shown in the table above for PETG decreases once the material is 3D printed, reaching a Yield Strength of about 600 MPa and a maximum tensile strength of 55 MPa. The positive previous experiences with PETG, by Akilo (2018), Neeskens (2018) confirmed the quality of the material to be printed with FDM technique. For this reason, PETG has been chosen to be utilized in this research.

4.5   Conclusion

After having illustrated the characteristics of the available AM techniques on the market, the related sub-questions can now be answered.

What is Additive Manufacturing (AM)?

Additive Manufacturing (AM) is the proper name of what it is commonly known as 3D Printing. This technology can fabricate, from a three-dimensional Computer Aided Design (3D CAD), a tangible solid realized by adding material in layers. The techniques can be distinguished by the material used, the initial condition of the material (liquid or powder) and how the layers are created and bonded to each other. Those differences determine the accuracy of the final product and the mechanical properties.

Which techniques of AM are currently available?

The techniques of AM currently available are Stereolithography, Selective Laser Sintering, Fused Deposition Modelling, 3D printing and Inkjet Printing. A comparison of the main characteristics of each technique can be found in Table 4.1. SLS has been evaluated to be the most advisable technique to be used in the analysed study. With the use of SLS support material is not needed and the accuracy of the final product is relatively high. However, due to economic reasons, FDM has been used to realize in practice the core of the sandwich panel.

Which core material is the most appropriate for the analysed problem?

After having analysed the available materials to be used with FDM technique, PETG has been chosen as the most suitable material. PETG is becoming more popular in the 3D filament field, because it is relatively easy to print and it is totally recyclable. PETG filament is originally colourless and crystal clear, then, when heated up, the material changes its transparency and it becomes translucent. The strength of the material changes when the material is 3D printed. From an E modulus of about 2000 MPa, the 3D printed PETG has an E modulus of about 600 MPa on average (van Driel, 2018).

Part II

STRUCTURAL DESIGN

5. Preliminary Design

5.1   Introduction

In this chapter, the preliminary design of the sandwich panel will be discussed. First of all, the approach used will be explained in paragraph 5.2. Then, in paragraph 5.3, the cold bending procedure of thin glass will be illustrated and the following sub-questions will be answered:

- *How can the cold bending process be modelled in FEM?*

In paragraph 5.4, the starting points for the design of the sandwich panel will be illustrated. Finally, in paragraph 5.5 the numerical analysis of the sandwich panel will be carried and the following sub-question about Finite Element Models will be answered:

- *Which differences between the software Femap and Karamba can be underlined after the analysis of the models?*

5.2   Approach

The design phase is composed of three main parts:

1. Cold bending of thin glass
2. Sandwich panel
3. Numerical calculations

In order to calculate the structural behaviour of the cold bent sandwich panel, firstly the prestressing due to the cold bending of thin glass is evaluated and then, the behaviour of the sandwich panel is considered. The core geometries were chosen after the research carried out in Chapter 3 of the literature review. In Paragraph 5.3 the starting point of the numerical calculations is summarized. Finally, the numerical analysis of the sandwich panels are performed both in Karamba3D version 1.2.2 and Femap version 11.3.1 and are explained in paragraph 5.5. Karamba3D – also known as Karamba – is a parametric structural engineering tool, which provides structural analysis for beam and shell elements. Karamba is a plug in of Grasshopper, which is a plug in of Rhinoceros 5.0 (Rhino3D). Femap v11.3.1 is an engineering analysis program, developed by Siemens, that is used to build finite element models of complex engineering problems.

The schematization of the described approach is shown in Figure 5.1.
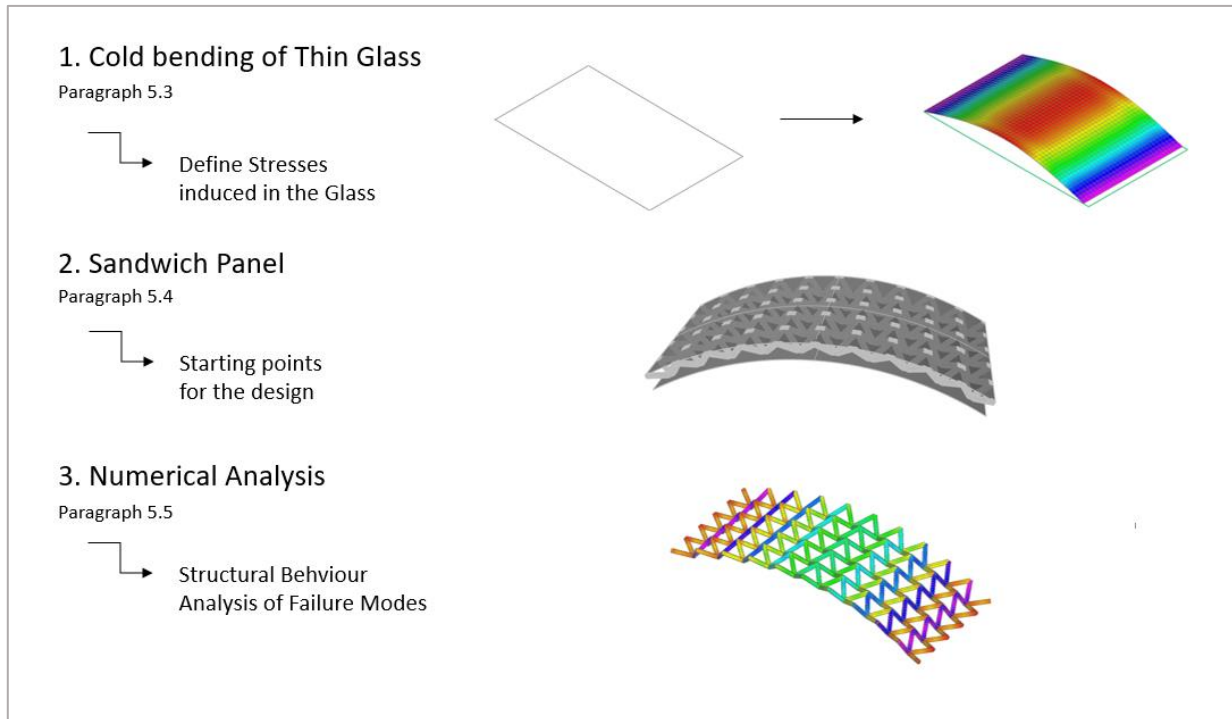
Figure 5.1 Design Approach

5.3   Cold Bending of Thin Glass

In order to choose the dimensions of the sandwich panel and initial evaluation has been performed. The glass, that has been decided to be used from the literature research evaluation, is the Falcon Glass provided by AGC. Since one of the main goals of this research project is to cold bend the glass, the choice was driven to the thinnest option possible. After the analysis of the stresses introduced in the glass due to cold bending (Appendix C.1), the choice of the thinnest glass will be confirmed. AGC provides Falcon glass with dimensions up to 1245mm x 3210mm and Leoflex Glass 0,55mm up to 2070mm x 1650mm.

In order to investigate the cold bending procedure, different situations were examined. First of all, the shape that is wanted to be reached with cold bending has to be defined, and this shape is related to the force applied to the panel. Each loading condition is linked to a certain shape, as it is shown in Figure 5.2: circular, sinusoidal, parabolic and catenary.

The most popular shape used in cold bending is the circular shape. This shape can be described as a part of a circle, therefore it has a constant curvature. The total stresses caused by cold bending a flat panel to a circular shape are lower compared to the other shapes shown in Figure 5.2. The stresses increase for the catenary and the parabolic shape, and they are the highest for the sinusoidal shaped cold bending (Schlösser, 2018). This is because the constant curvature better distributes the stresses along the curve. On the other hand, shear stresses at the edges are maximal for the constant curvature shape and the lowest for the sinusoidal shape (Galuppi & Royer-Carfagni, 2015).

Loading Conditions   Shape

Imposed Displacement   Circular (mould needed)

Point Load   Sinus

Uniformily distribuited   Parabolic

Gravity   Catenary
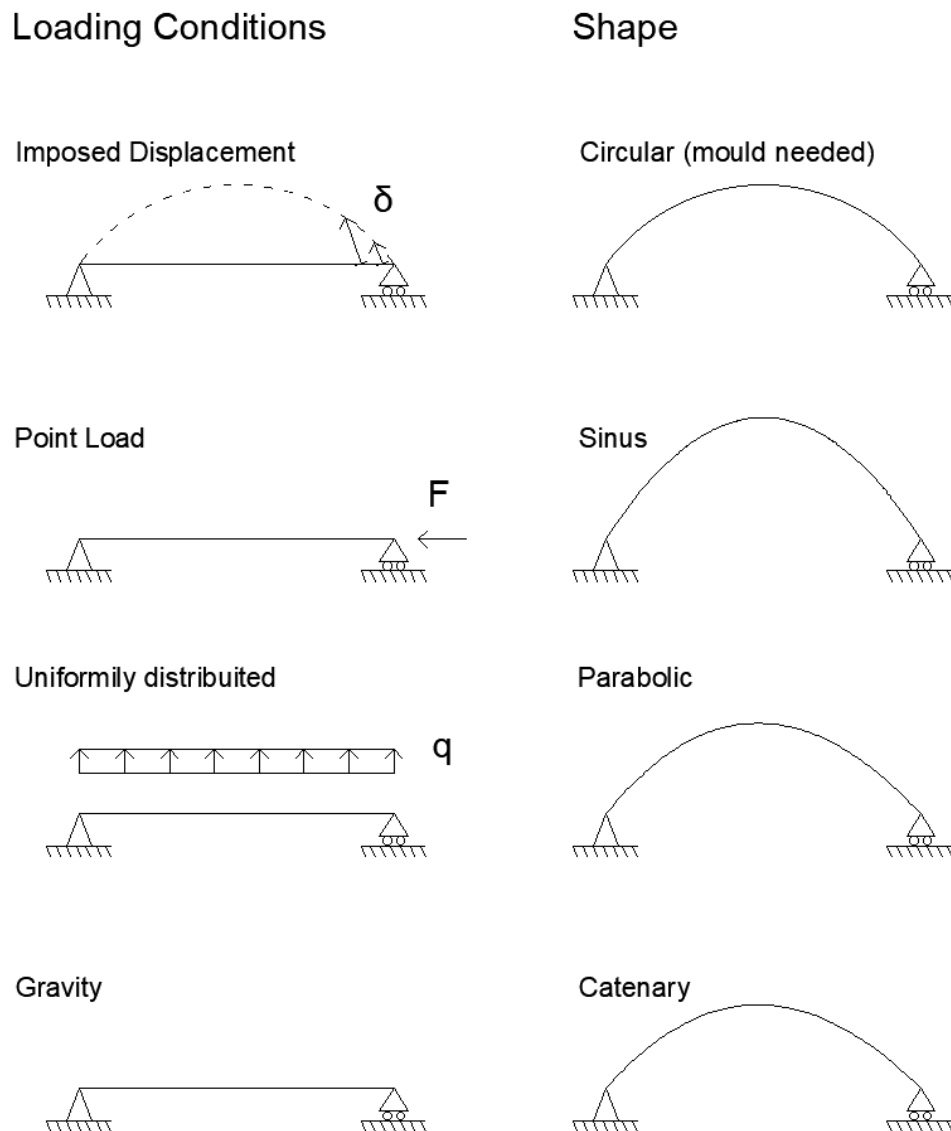
Figure 5.2 Cold bending possible shapes

Finite Element Models (FEM) are created for the above illustrated shapes: circular shape, sinusoidal shape and parabolic shape have been taken into account. In order not to induce just compression with a horizontal displacement or load, an initial eccentricity is given to the glass panel. This eccentricity is created by a pressure load perpendicular to the surface of magnitude 1×10^{-9} N/mm^2. This load will make the model to deflect just the little needed (order of magnitude of 1×10^{-3} mm) not to compromise the final result, but, at the same time, to make the glass bent in the desired direction. The thinness of the glass is crucial during the analysis of the glass panel. A Static Linear Analysis can only be performed under the hypothesis of small displacement, which means that the deformation of the element is expected to be less than half of the thickness of the analysed element. This condition is not verified in this case, because the thickness of the glass used is 0,5 mm. Therefore, Non Linear Static Analysis has been performed, because displacements were higher than the one allowed in order to fulfill the hypothesis of small displacement.

The analysis of the cold bent shapes is shown in Appendix C.1. Those specific analyses have been carried to evaluate the preferred shape, that it is wanted to be used in this research. The circular shape results to be the shape in which lower stresses are induced, as a confirmation of the research of Galuppi & Royer (Galuppi & Royer-Carfagni, 2015). For this reason, the circular shape has been decided to be further investigated in this project.

Since Falcon glass panels of dimensions of 250mm x 150mm were already available at the University, these dimensions will be used for the experimental testing. They have been investigated in the FE Models as well. From geometrical considerations, a height of 30 mm has been decided to be reached in the middle of the panel. This means a radius of curvature of 255mm. A displacement of 10 mm has been imposed in the horizontal direction. In the figure below the stresses induced in the glass panel are shown.
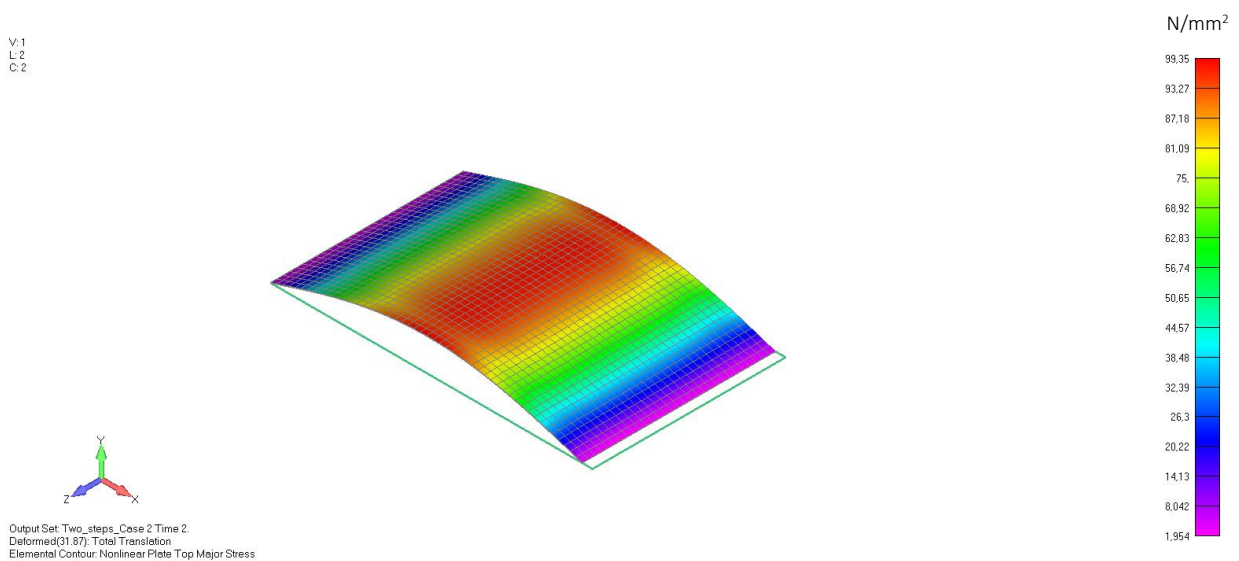
Figure 5.3 Top Plate Major Principal Stresses (Tension) = 99,35 N/mm^2
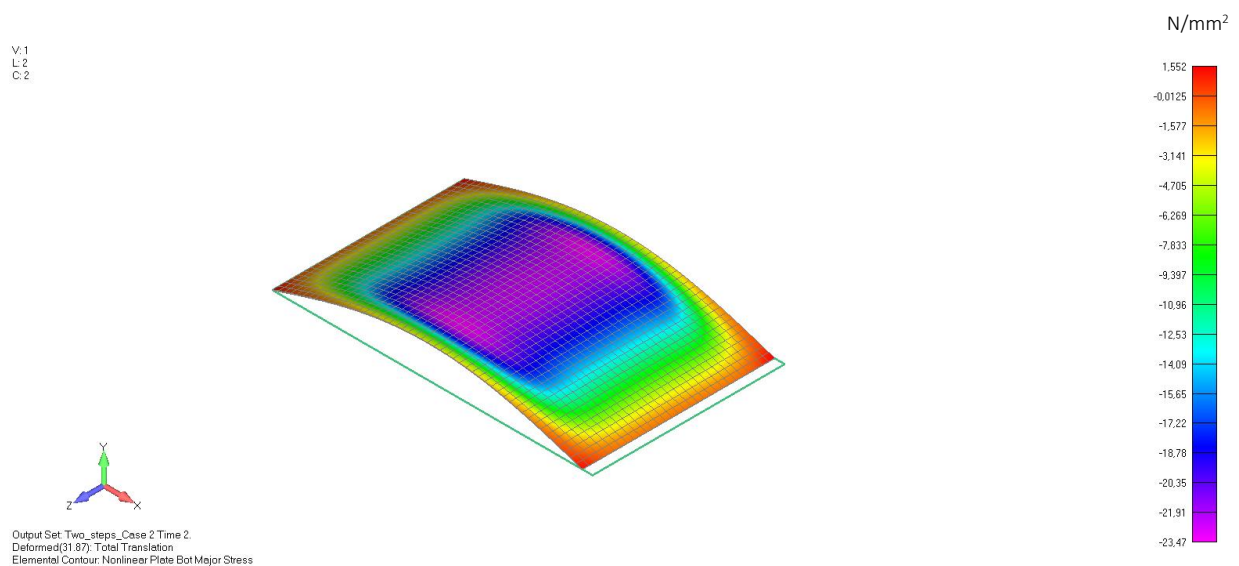
Figure 5.4 Bottom Plate Major Principal Stresses (Compression) = 23,47 N/mm^2

Results (cold bending)

From the first phase of the design, related to cold bending, the first sub-question can be addressed.

How can the cold bending process be modelled in FEM?

First of all, the shape that is wanted to be reached with cold bending has to be defined. Each loading condition is linked to a specific final shape, as it has been illustrated in Figure 5.2. Each situation has been modelled by FEM and it has been explained in Appendix C.1. The circular shape has been decided to be used in this research. This shape can be described as a part of a circle, therefore, it has a constant curvature. The total stresses caused by cold bending to a circular shape are lower compared to the ones introduced in other shapes (catenary, parabolic and sinusoidal). The final shape is obtained by imposing a defined displacement in each node of the panel. The horizontal displacement of the panel edge is calculated by geometrical consideration and then it is imposed at each node. The thinness of the glass is crucial during the analysis of the panel. Since thin glass does not fulfill the hypothesis of small displacement, Non-Linear Static Analysis has been performed.

5.4   Sandwich Design

In this paragraph, the design of the sandwich panel will be illustrated. First of all, the core topologies, which have been chosen to be investigated from the literature review, will be illustrated. Then, the starting points for the design of the sandwich panel will be explained and in Paragraph 5.5 the FEM of the panels will be performed and discussed.

5.4.1   Core Design

After the literature review study, two main patterns have been chosen to be further investigated in this research. The first one is a space frame pattern, composed by pyramidal elements, which will be called Truss Model from now on. This pattern has been chosen because it could guarantee a high strength and stiffness related to the density of the core. As a starting point it has been decided to use a square unit cell with an angle of 45° within the pyramidal elements of the truss, as it is shown in the figure below.
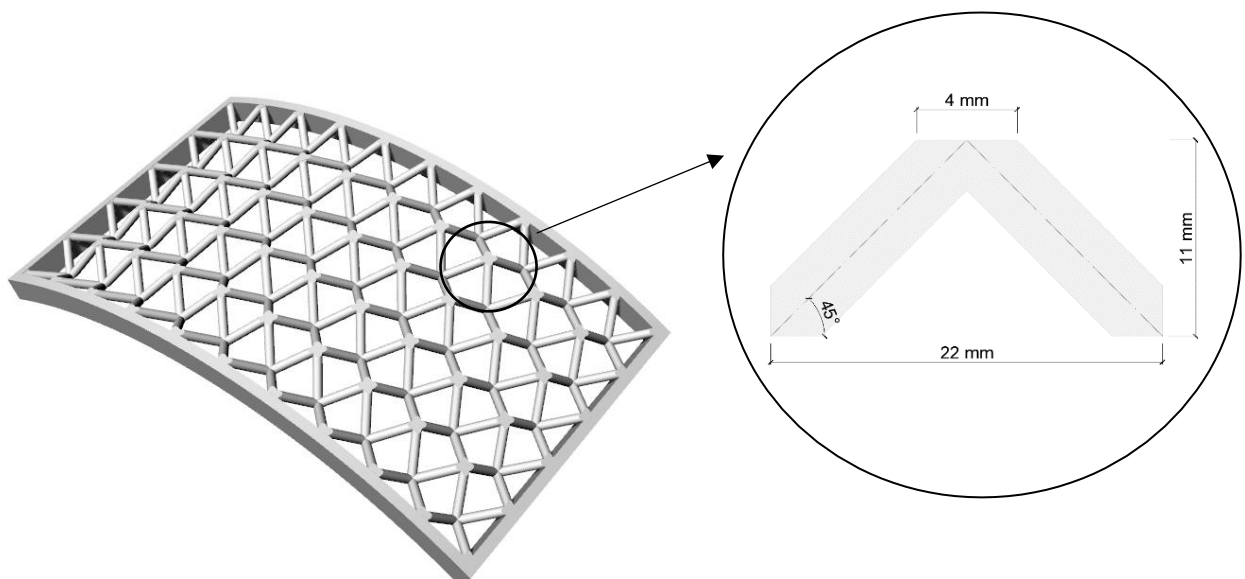
Figure 5.5 Truss Model Geometry

The second pattern, that has been decided to be investigated from the literature review, is a closed pattern, made by squared cell elements that are oriented orthogonally to the glass faces of the sandwich panel. This model will be called the Waffle Model, and it is shown in Figure 5.6. This pattern has been chosen due to the high shear stiffness related to this shape. Moreover, the core elements are all oriented orthogonally to the glass face. Therefore, light can pass directly from one face of the sandwich panel to the other, without encountering any visual obstruction.
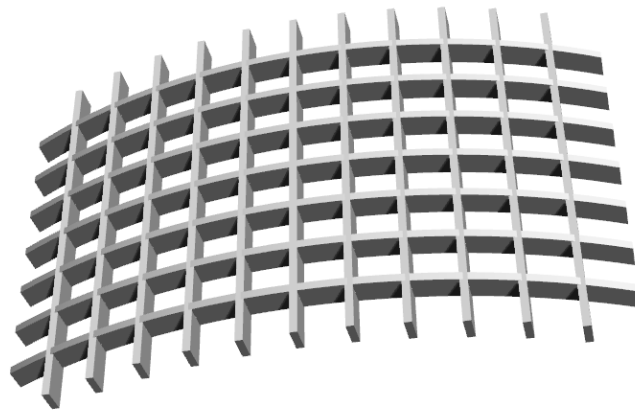
Figure 5.6 Waffle Model Geometry

Both models have been designed with Rhinoceros + Grasshopper, in order to be able to change the design more easily, e.g. inclination of pyramidal elements in the Truss Model or number of cell elements in the Waffle Model.

5.4.2   Starting Points

In order to make a first estimation of the height of the sandwich panel, previous studies on similar topic were taken into consideration. Iris van der Wijde (van der Weijde, 2016) used a thickness of 10 mm for her honeycomb core, Michele Akilo (Akilo, 2018) chose an height of 11 mm for the core of his truss sandwich panel, while Tim Neeskens (Neeskens, 2018) used 16 mm for his Voronoi pattern core, but his panel has to be used as a roof element. Considering the analogies with Michele Akilo thesis, the starting height of the core has been chosen as 11 mm.

- Panel dimensions (Appendix C.3): 250 mm x 150mm
- Panel dimensions (Paragraph 5.5): 500 mm x 500 mm
- Panel thickness: 0,5 + 11 + 0,5 = 12mm

Accordingly to the literature review studies, thin glass has a high strength but, due to its low thickness shows large deflections. For this reason it is important to keep in mind the deflection limit, while talking about SLS calculations. The deflection limit is given by NEN 2608:2011, and it is:

$$w_{lim} = \frac{L_{diag}}{65}$$

Moreover, when the ultimate stress of the material is discussed (ULS) the value of 314 MPa is considered for Falcon Glass. This value has been calculated according to EN16612.

$$f_{g,d} = \frac{k_{mod} \cdot k_{sp} \cdot f_{g;k}}{\gamma_{M;A}} + \frac{k_v \cdot (f_{b;k} - f_{g;k})}{\gamma_{M;v}}$$

Where:

$f_{g;k}$ is the characteristic value of the bending strength of Annealed Glass = 45 MPa
$f_{b;k}$ is the characteristic value of the bending strength of Falcon Glass = 400MPa (Appendix A)
k_{mod} is the factor for the load duration. Wind load, short duration = 0,74
k_{sp} is the factor for the glass surface profile. For float glass production = 1
k_v is the factor for strengthening of prestressed glass. Horizontal toughening = 1
$\gamma_{M;A}$ is the material partial factor for annealed glass = 1,8
$\gamma_{M;v}$ is the material partial factor for surface prestress glass = 1,2

Then, the designed value of strength for Falcon Glass can be defined as:

$$f_{g,d} = \frac{0,74 \cdot 1 \cdot 45}{1,8} + \frac{1 \cdot (400 - 45)}{1,2} = 314 \, MPa$$

5.5   Numerical Analysis

Before being able to realize an accurate Finite Element Model, some simple examples were carried, both analytically and numerically, in order to be able to make comparisons and to better understand how Karamba and Femap actually work. This section can be found in Appendix C.2.

5.5.1   Panel 250 mm x 150 mm

The first model that has been realized was the Truss Model on Karamba. The geometry, that has been previously realized on Rhino + Grasshopper, is now used to perform the FEA with Karamba and then with Femap.

The top and bottom curved surfaces have been meshed in Karamba. The surface has been divided into 2400 elements, by dividing the short edge into 40 elements and the long edge into 60 elements. By default, Karamba split the mesh from Quad elements into Triangular elements for making the calculations. It is still not possible to use Quad elements in Karamba. If in future the option of Quad Elements willl be available, is highly recommended to use it in order to have more accurate results.

Supports and load conditions are given differently, based on the case that will be examined. In general, pinned supports and roller supports have been taken into account. Different loading conditions were also taken into account: a surface load of 1kN/m² has been used to simulate the Wind Load and a Point Load of 50N has been used to compare the numerical model with the analytical model. Moreover, since the local point load on a node is unlikely to happen in reality, a more distributed point load has been taken into account. The load of 50 N has been spread into 9 nodes, to have more distributed stresses in the results and to avoid peak stresses. A line load has also been taken in considerations while comparing the models.

Falcon Glass has been used for experimental tests. Its characteristics have also been reproduced in the computer models. The top and bottom shells have a thickness of 0,5 mm and the properties of Falcon Glass has been attributed:

E_g = 73 000 N/mm²
G_g = 30 000 N/mm²
Specific Weight = 25 kN/m³

The beam element of the core has a circular hollow section with a radius of 2mm. The thickness of this hollow section is 1mm, since the 3D printed element has not a full cross section. The properties of PETG has been attributed to the core:

E_c = 2 000 N/mm²
G_c = 730 N/mm²
Specific Weight = 12,7 kN/m³

Since the realized panel will also have 3D printed side elements, as a frame of the core, those elements of 5 mm has been added to the computer model as well, in order to realize a schematization which is as similar as possible to the physical model. PETG side elements have been added.

The model can now be assembled on Karamba, and analysed. A Static linear analysis has been performed with the assumptions that the whole sandwich panel, which behaves like a monolithic element, will deflect following the theory of small displacement. The numerical analysis and results of the Truss Model can be found in Appendix C.3.

Later, the Waffle Model of dimensions 250mm x 150mm has also been analysed both in Karamba and Femap. The numerical calculations can be found in the second part of Appendix C.3.

5.5.2   Panel 500mm x 500mm

After having made a comparison between the two Finite Element Programmes in Appendix C.3, a panel with bigger dimensions is below described in details. A panel of dimensions 500 mm x 500 mm will be investigated both with Numerical and Experimental analyses.

In order to realize the numerical model, the same procedure as the one explained in Paragraph 5.2 was followed. Firstly, the thin glass has been cold bent to reach a radius of curvature of R=440mm. The cold bending procedure induces a maximum tensile stress of 64 MPa in the top layer of the glass and compressive stress of 14,4MPa in the bottom layer of glass.

After the glass has been cold bent, the sandwich panel has been investigated under external loading conditions. The panel has been simply supported on two edges and an external point load has been applied. The load case of a point load of 400 N is described in Appendix C.4. Below, a line load is examined.

In order to discuss the failure modes taken into consideration in literature, the Truss Model 500mm x 500mm has been analysed under a line load of 1kN, the model is simply supported along two edges. A three point bending test has been schematized in the numerical model. In this manner, the model can be easier checked by analytical calculations, as a simply supported beam with a point load in the center of the span (Figure 5.7).

Loading: Line Load of 1kN
Support conditions: left pinned, right roller support
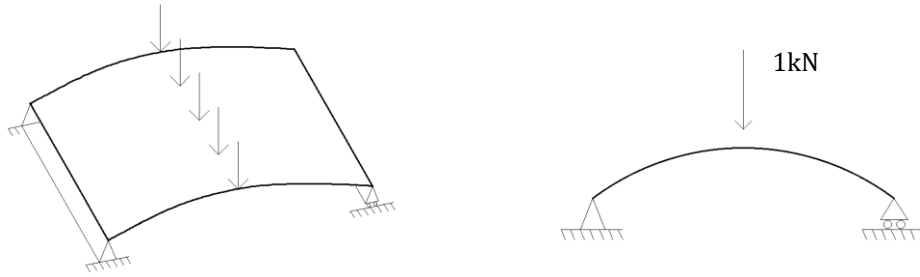
Figure 5.7 Mechanical Schematization

Analysis of Failure Modes

Strength in the face

The first failure mode mentioned in the literature review, Chapter 3, was the failure due to lack of strength in the faces of the sandwich panel, therefore in the glass. It is known that glass has a worse behaviour in tension, compared to the one in compression. The principal stresses of the glass are shown in the following figure.
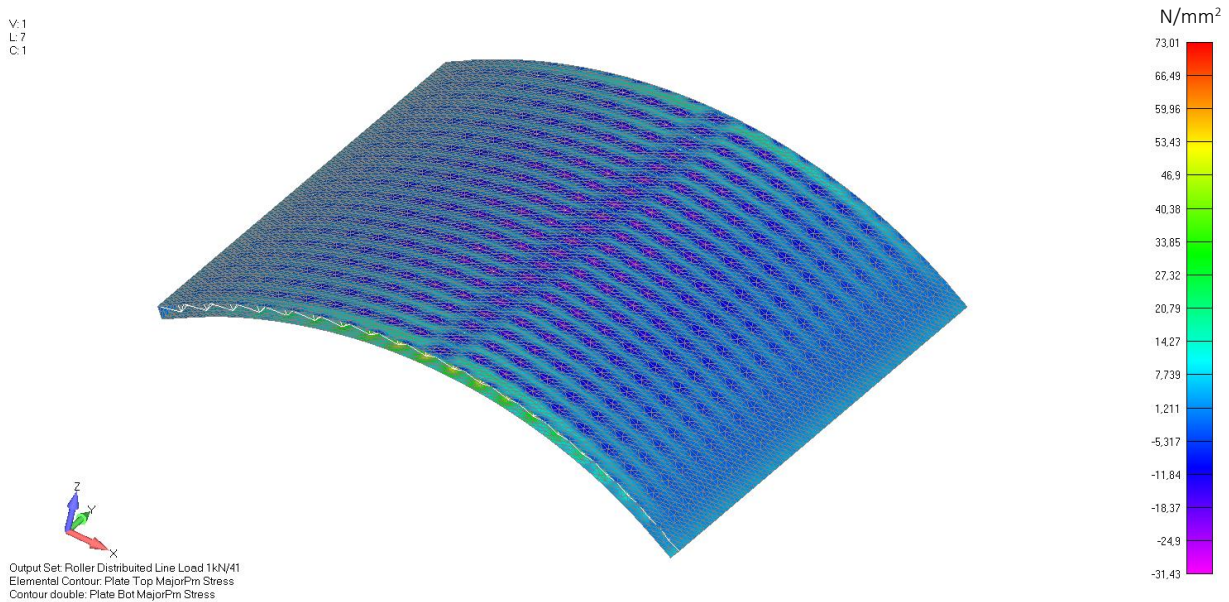
Figure 5.8 Major Principal Stress due to Line Load = 73,0 N/mm^2

In the worst case scenario, the maximum tension stress in the glass is at the center of the panel, where the line load is applied. The total stress is the sum of the stress caused by cold bending and the stress due to loading, in the bottom layer of the top ply of glass. The tension stress in this case is:

$$\sigma_{max} = -14{,}4 \ MPa + 73{,}0 \ MPa = 58{,}6 \ MPa$$

The maximum tensile stress allowed in Falcon Glass, chemically strengthened, is 314 MPa, as it has been previously calculated in Paragraph 5.2. Then, the unity check it is fulfilled:

$$\frac{\sigma_{max}}{\sigma_{lim}} = \frac{58{,}6 \ MPa}{314 \ MPa} = 0{,}19 \le 1$$

Panel stiffness

The second failure mode, which has been taken into consideration, is the one due to a lack of stiffness in the panel. Code limitation does not express limits on curved panels, for this reason the limit deflection of a flat panel according to NEN 2608:2011 will be taken into considerations.

$$w_{lim} = \frac{L_{diag}}{65} = \frac{\sqrt{500^2 + 500^2}}{65} = 10{,}88 \ mm$$
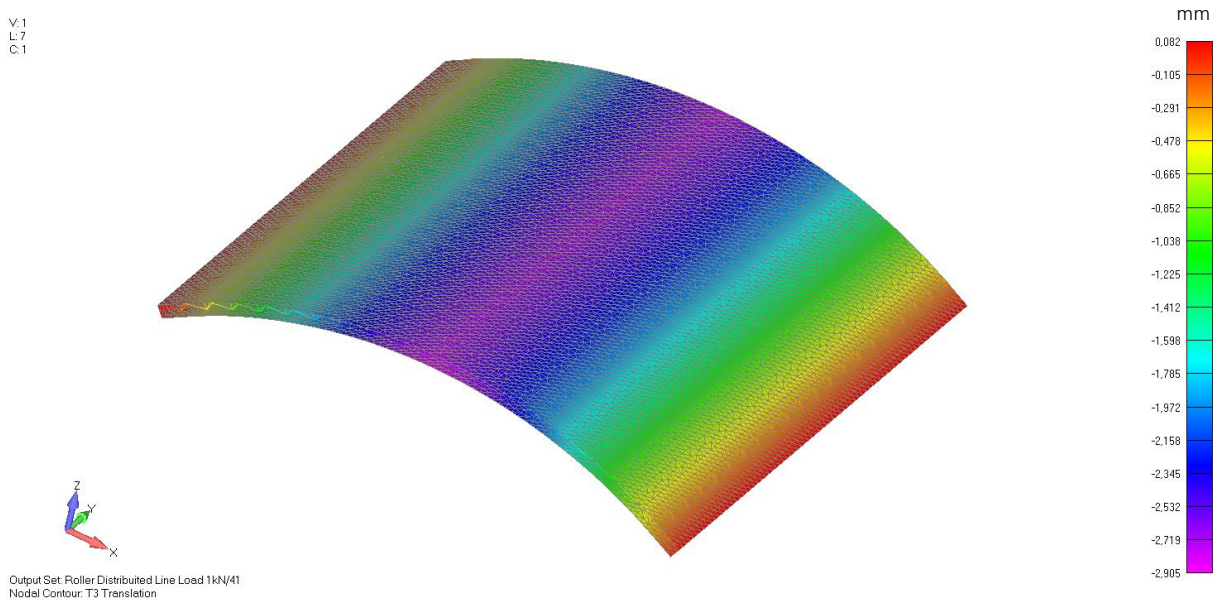
Figure 5.9 Maximum Deflection = 2,91 mm

The deflection of a simply supported sandwich panel under a line load is maximum at the center of the span and the value results to be 2,91 mm (Figure 5.9). Then, the Unity Check related to stiffness is:

$$\frac{w_{max}}{w_{lim}} = \frac{2{,}91 \ mm}{10{,}88 \ mm} = 0{,}27 \le 1$$

Shear in the core

Another important check regards the failure of the core due to shear. The maximum shear stress has to be lower than the allowable shear stress of the panel. The shear stress limit is given by the minimum value between the shear stress of the core and the shear stress of the glue.

$$\tau_{lim} = min \left\{ \tau_{PETG}; \tau_{glue} \right\}$$

The shear stiffness of the PETG is 12 MPa, while the shear stiffness of the glue, Delo Photobond 4494 between glass and plastic is 4 MPa. Appendix A can be consulted for the data sheet of the products. It is evident that the shear stress of the glue, 4 MPa, will be taken as the governing value.

Since the shear in the glue has to be checked. The local shear in the connection due to the loading condition has to be investigated. To calculate the maximum shear force in the adhesive, the mechanical schematization showed in the picture below has been used. The force in the glass (ΔN) is equal to the area of the glass multiplied by the delta sigma, ΔN = A_{glass} Δσ, where Δσ = σ_{left} − σ_{right}. Then, the shear stress in the connection (τ) is equal to the calculated force divided by the area of the glue, τ = ΔN / A_{glue}.
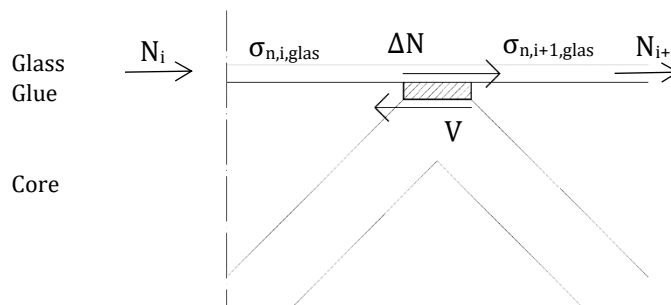
Figure 5.10 Mechanical schematization of the shear in the connection

Where:
$N_i = \sigma_{n,i} \cdot A_{glass}$
$\Delta N = N_i - N_{i+1}$
$\Delta N = V$
$\tau_{glue} = \dfrac{V}{A_{glue}}$

Therefore, the normal force in the glass needs to be calculated in order to derive the shear stress in the connection. The mechanical schematization of the analysed panel can be simplified as a simply supported beam, loaded in the center of the beam with a point load F=1kN, as it has been shown in Figure 5.7.

Therefore, the moment in the center of the beam can be calculated as M=Fl/4. While, the normal force in the glass has been calculated as the moment (M) divided by the distance between the two faces of glass (d), according to the schematization of Figure 5.11. The value of the normal force N, which is equal to N = M/d, results in a total normal force in the glass of N of 10 kN.
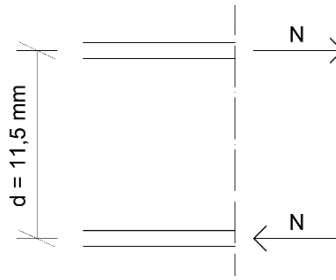
Figure 5.11 Normal Force in the glass

The Normal Force (N) at each connection has to be calculated by taking into account that every time there is a truss element, the force will be transferred both in the glass and in the truss, resulting in a decrease of force on the next connection point. This concept has been schematized in the next figure.
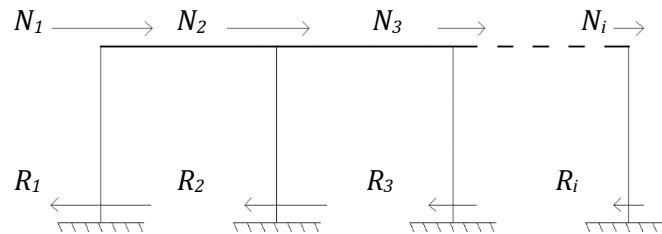
Figure 5.12 Decreasing of the Normal Force in the glass, due to the presence of the Truss Element

Where:
$N_2 = N_1 - R_1$
$N_3 = N_2 - R_2$
...
$N_i = N_{i-1} - R_{i-1}$
$R_i = \tau_i A_i$
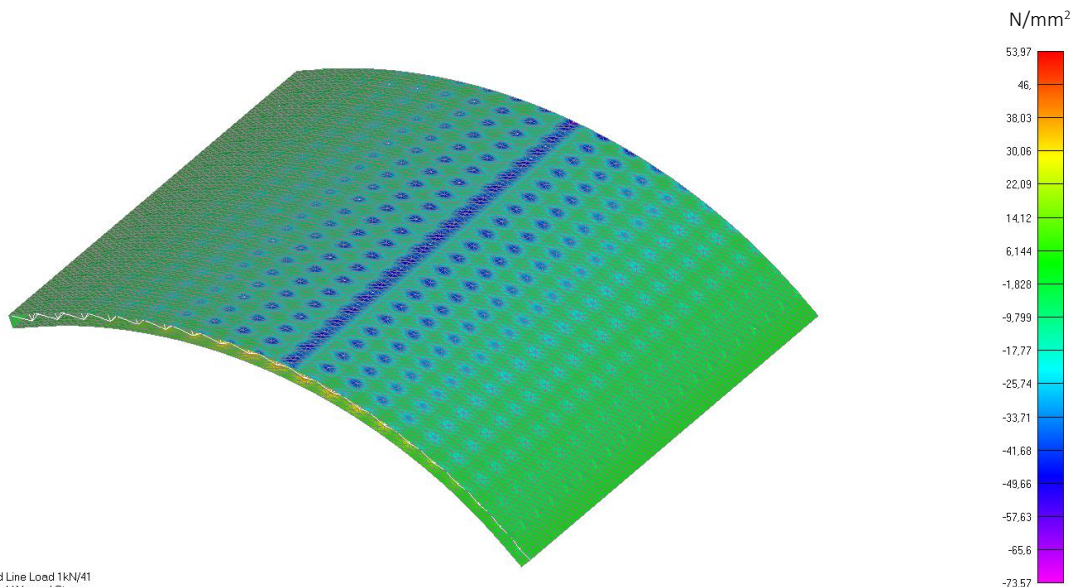
Figure 5.13 Plate Normal Stress

As can be seen from Figure 5.13, the normal force in the glass will decrease from the center of the panel until the edge. To simplify the calculation, it is taken as a hypothesis that the force N will decrease linearly along the length of the curved beam. The local stress in the glue will be maximum under the position of the force (center of the beam) and it will be zero at the support. The cross section taken into account is at a distance dx from the center of the beam. The load N at this point is half of the load F, due to the symmetry of the system, since half load will be transferred in the left part of the system and half load in the right part.
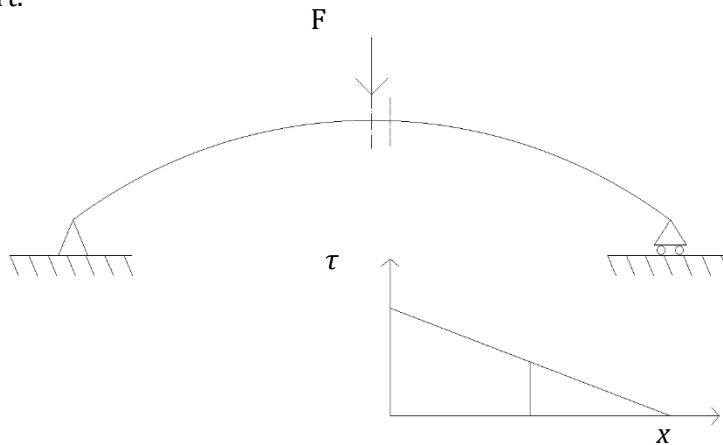
Figure 5.14 Shear stress in the contact areas

To calculate the value of shear stress in the glue, it is known that the average value will be at half of the span. At this point, the shear stress is calculated as:

$$\tau = \frac{5000 \ N}{21 \cdot 10 \cdot 12{,}57 \ mm^2} = 1{,}89 \ MPa$$

Where 12,57 mm² is the area of one truss surface of radius 2mm, 21 are the nodes present in the width of the panel and 10 are the truss element on half length of the panel. The maximum local shear stress is 1,89 MPa x 2 = 3,78 MPa, at the cross-section taken into account. The maximum value is still lower than the shear resistance of the glue, which is 4 MPa.

It has to be underlined that, by reproducing the inverse procedure, a maximum line load of 1,06 kN can be handled by the glue. With a higher load, the connection will fail due to high shear stresses.

To validate this approach, another method (Gere & Timoshenko , 1993) is used to verify the result.
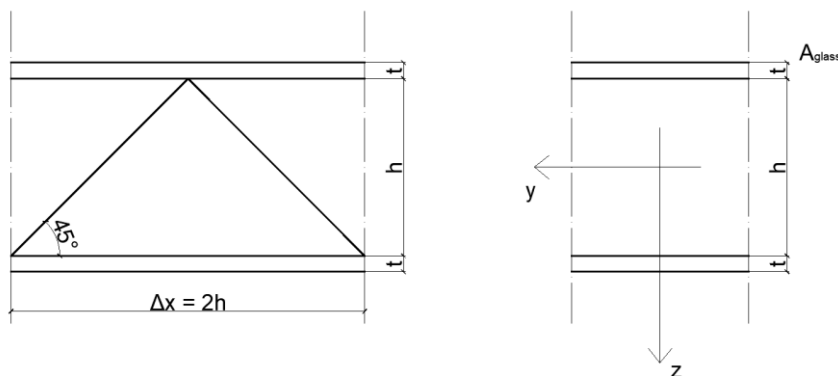
Figure 5.15 Sandwich cross section along the x and y direction

Considering a portion of the sandwich beam, composed by a unit of truss, as it is shown in the figure above, ΔN can be derived from the following formula (Gere & Timoshenko , 1993):

$$\Delta N = \frac{V \, S_y \, \Delta x}{I_y}$$

The panel can be simplified as a simply supported curved beam, therefore the shear force V is equal to F/2, considering an acting Force of 1kN, the shear force will be V = 500N.

The length taken into account Δx is = 2h = 22mm since the angle of the truss is 45°.

The first moment of area S_y is defined as $S_y = y \, A_{glass}$, thus, it resulted to be 60,5 mm³

The moment of Inertia I_y calculated for the portion of beam taken into account is $I_y = 2[(b \, t^3/12) + A \cdot z^2]$. Where b is equal to Δx = 22 mm, and z is half of d, the distance between the center of the two faces. The moment of Inertia I_y results to be equal to 665,96mm⁴. The Normal force in the glass can be now calculated:

$$\Delta N = \frac{500 \cdot 60,5 \cdot 22}{665,96} = 999,3 \, N$$

Therefore, the shear force in the connection results to be τ. Where 21 is the number of truss unit in one row.

$$\tau_{max} = \frac{999,3 \, N}{21 \cdot 12,57 \, mm^2} = 3,79 \, MPa$$

The stress result to be higher than the one calculated before, because this is considered to be the local stress in the middle of the beam. It is still less than the allowable shear strength of the glue, 4MPa. Therefore the Unity Check (U.C.) is fulfilled.

$$\frac{\tau_{max}}{\tau_{lim}} = \frac{3,79 \, MPa}{4 \, MPa} = 0,94 \le 1$$

Buckling of the truss element

A failure mode that has to be taken into consideration is the buckling of the truss element. This failure mode is particularly dangerous because it is not easy to evaluate how the post-breakage behaviour would be for this kind of structure. The critical load can be calculated with the formula of Eulero:

$$N_{cr} = \frac{\pi^2 EJ}{l_b^2}$$

Where J is the moment of inertia of the truss element, with a circular cross section, which is *J = πd⁴/64.* The diameter of the truss element is 4mm, thus the moment of inertia is 12,57mm. The buckling length takes into account the boundary condition of the truss element. For a fixed element, the buckling length is *lb=0,5l,* while for a pinned element, the buckling length is the same as the length of the element *lb=l.* In this case, the truss element is glued to the glass, and monolithically connected to the three other 3D printed elements which compose the pyramidal unit in the truss core. Since the situation cannot be considered as fixed support, but it will be in between the pinned and the fixed support, the worst case will be taken into account. Pinned support will be considered because it will give the most conservative

result, thus the buckling length of the truss element is equal to the element length, which is 19,8mm. The critical load can now be calculated as:

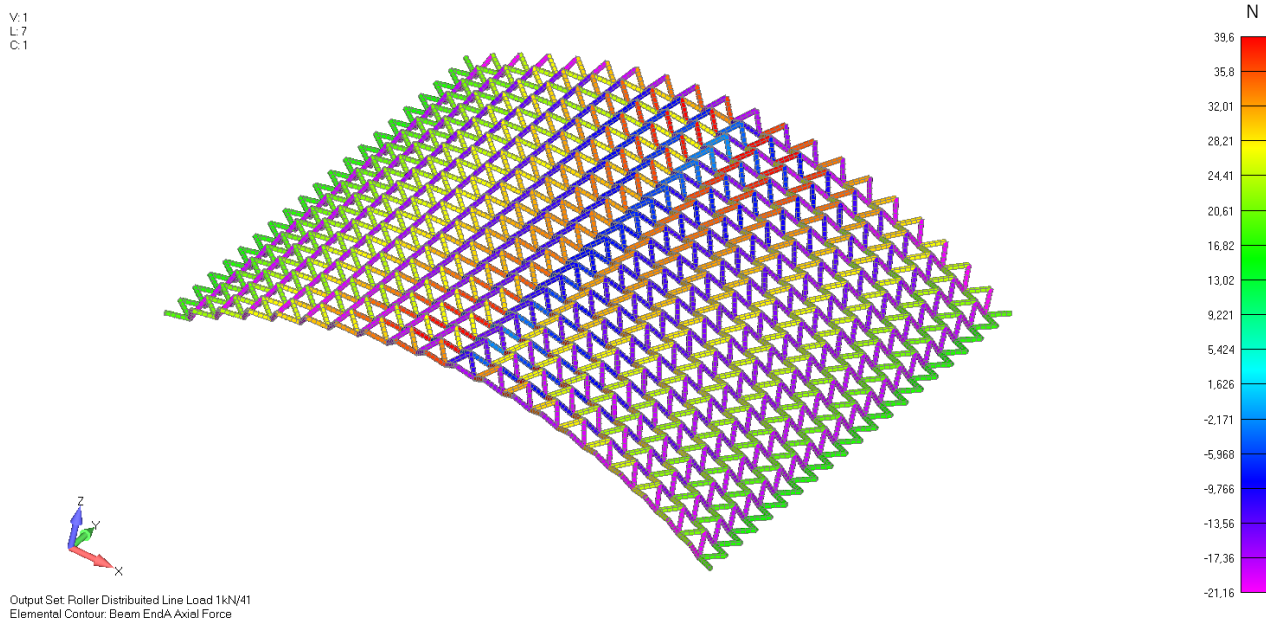$$N_{cr} = \frac{\pi^2 \cdot 2000 \cdot 12,57}{19,8^2} = 632,72\ N$$

Figure 5.16 Maximum Compressive Force in the Core = 21,16 N

The maximum compression force in the truss element has been calculated in Femap and it is equal to 21,16 N (Figure 5.16). From the Unity Check it can be seen that buckling is not likely to happen in the model.

$$\frac{N_{max}}{N_{cr}} = \frac{21,16\ N}{632,72\ N} = 0,03 \leq 1$$

The other failure modes named in the literature review has not be analysed in details. The skin wrinkling of the panel is not expected to happen due to the elevated value of the compressive strength of glass. The intra-cell buckling has not be investigated because the unit cell of the truss has been considered to be small enough to prevent this failure mode.

The most critical failure modes have been checked and the panel results to be safe. The deflection of the panel results to be small and the panel will break more likely due to shear in the adhesive connection between the core and the glass faces. Therefore, the first failure is expected to appear in the glue. Having lost the contact, the panel will no longer behave as a sandwich structure, and the stiffness of the panel is expected to decrease significantly. Then, the core is expected to fail as a second element. Last, the stiffest element, the glass, will probably fail.

Results (FE Models)

Thanks to the development of the numerical analyses, the next sub-question related to FE Models can now be answered:

Which differences between the software Femap and Karamba can be underlined after the analysis of the models?

All the analyses have been performed both in Femap and in Karamba. The goal of this analysis was to understand how trustful are the programmes, and how much was the deviation between one and another. In Table 5.1 and Table 5.2 in Appendix C.3, the result of the comparison between the two finite element programmes is illustrated. As can be seen from the tables, the two programmes showed comparable results. In order to reach this outcome, it was essential to have an identical mesh in both programmes. Since Karamba can just solve the analysis with Triangular Mesh Elements, the same elements have been used in Femap too. For future researches would also be advisable to check calculations accuracy with Quad4 or Quad8 node elements, when Karamba will offer this option. Another difference between the two programmes is that Karamba still does not provide the possibility to analyze solid elements, while Femap does. Certainly, the advantage of Karamba is the possibility to quickly vary the input of the analysis and see the output results in real time. The negative side of this programme is that the visualization of the results is not always intuitive. For instance, for shell elements just Principal Stresses can be displayed, while σ_{xx}, σ_{yy} and σ_{zz} stresses can be only seen as a value and not as a global qualitative visualization on the panel. Another critical check has to be done to the inputs, while Femap calculations give Fatal Error every time that some inputs are not correct, in Karamba if the data has a mistake the programme considers the closer correct input as a value, which is not always the one intended by the user. For this reason, before performing an analysis with Karamba, the manual of the programme has to be fully understood.

Part III

MANUFACTURING and TESTING

6. Manufacturing

The manufacturing process can be divided in different steps: first the glass have been ordered from AGC. Then the core has to be realized. And third, the two parts has to be assembled together.

6.1   Glass

As it has already been mentioned, the glass was provided by AGC. The thinnest glass available is Falcon glass 0,5 mm or Leoflex glass 0,55 mm. The first samples that have been realized where supposed to be made with glass of 250 mm x 150 mm x 0,5 mm. Since the glass availability delayed, the one of 300 mm x 150 mm x 0,5 mm has been used, even if the core had been already manufactured in a dimension of 250 mm x 150 mm.

6.2   Core

The core has been realized with different techniques: the core of the Truss Model has been realized with Additive Manufacturing FDM technique, while the core of the Waffle Model has been realized with Laser Cutting.

6.2.1   Additive Manufacturing (AM)

FDM technique turned out to be the most affordable choice, however it revealed not to be the easiest solution. As it has been said in the Literature Review chapter, FDM is a technique based on extrusion of material from a nozzle. The material is deposed in layers. This means that, in order to be able to deposit one layer, it must exist below a layer to lean on, and this was the main challenge of the curved shaped core.

The first idea was to rotate the model 90° around the y axis, as it is shown in the figure below. On the left we can see the model as it has been realized. On the right, it is illustrated the rotated model. In this manner, it was thought that the support material would no longer be necessary.

Figure 6.1 Truss model to be realized with FDM technique

However, this idea turned out not to be suffient. In fact, the frame now could be more easily printed, but the pyramidal truss elements resulted to be impossible to be printed without support material anyway. It has been decided to proceed with the use of support material, but, as the first printing experience has shown, the support material was actually stiffer that the truss itself, and by trying to remove it, the pyramidal elements broke, Figure 6.2
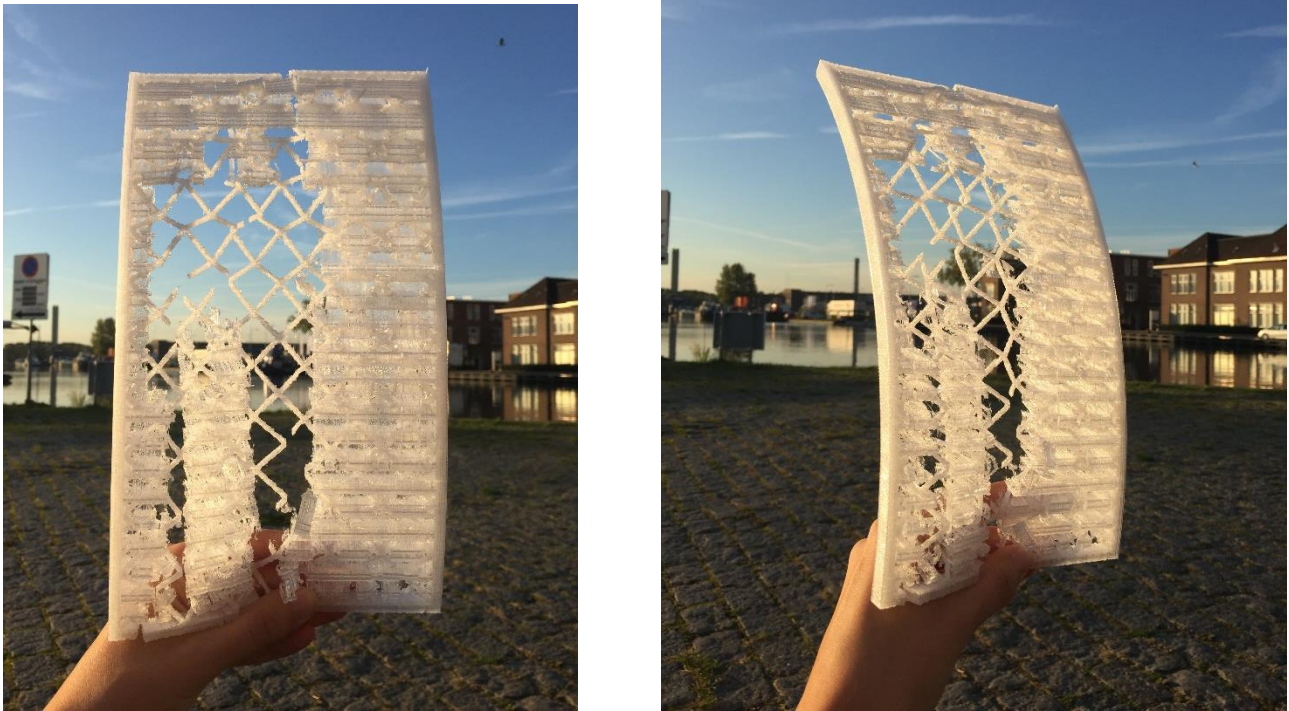
Figure 6.2 Broken truss core

This first trial was useful to understrand that the diameter of the pyramidal elements were actually too thin to be printed with FDM. So for further printing model, the diameter of the truss element has been increased from 2mm to 4mm.

The goal was to find a way to print this core without the use of support material. Since the core is realized by a single curvature, one idea was to split the model into many flat strips, and later glue it at the curved glass. The 3D printed strips are shown in the following figures.

Figure 6.3 Truss core divided into straight strips

Even by printing the core into flat strips, it turned out that support material were needed anyway. So it has been decided to go back to the original concept and print the curved truss core as it has been designed, and how it has been show in Figure 6.1 on the left. The print succeed with the following specifications: PLA white filament 200 microns and 0,4mm nozzle. The downside of this method was the huge amount of support material used on the bottom part of the model, shown in Figure 6.4. The final result, after the supporting material has been removed, can be seen in Figure 6.5 and in Figure 6.6.
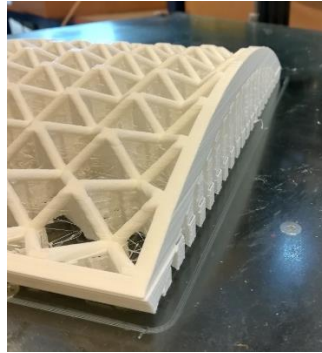
Figure 6.4 Curved truss core - Support material needed for FDM printing

Figure 6.5 Curved truss core – FDM printed - Second trial - Side view
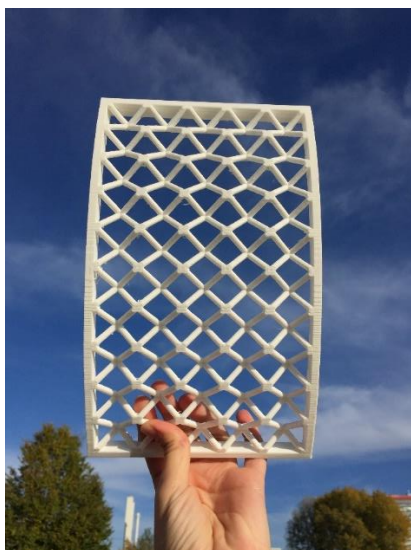
Figure 6.6 Curved truss core - FDM printed - Second trial - Perspective view

With the same specifications, also the Truss Model 500mm x 500mm has been realized. Since the quality of the printing was requested to be the same, the same filament size and nozzle dimensions have been used. The first time, the printing failed due to a shifting of the base of the 3D printing machine. The printing speed has been lowered down to achieve a successful printing. In order to print the model shown in Figure 6.7, 168 hours of printing were needed.
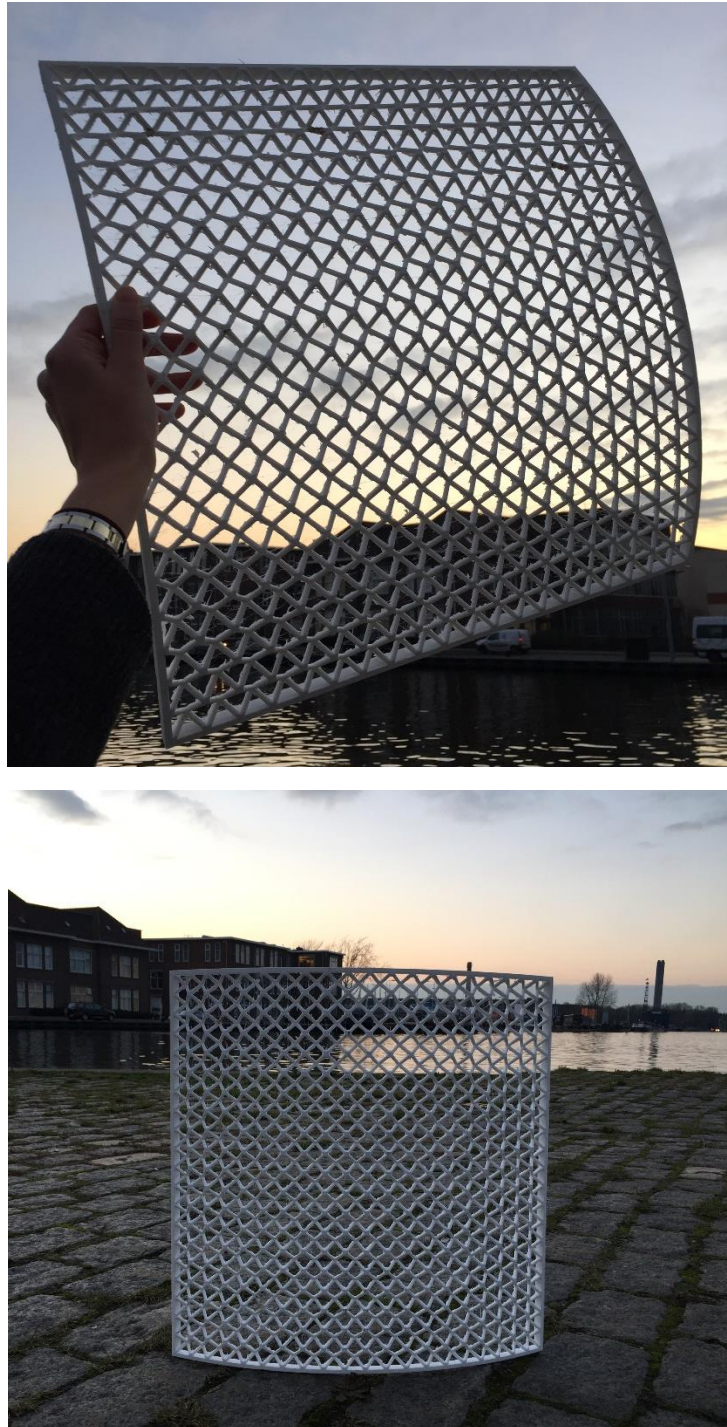
Figure 6.7 Truss Model 500mm x 500mm

6.2.2   Laser Cutting

The Waffle Model, instead, could not be printed by FDM, because the 90° elements could not be realized by this technique. For this reason another technique has been taken into account in this research. Laser cutting turned out to be an excellent solution. This technique revealed to be faster, cheaper and the final result was more transparent.

The material used is PMMA acrylic plastic of 3 mm thickness. The material is 100% recycled plastic. The Laser Cutting process will be illustated in the following images, Figure 6.8, Figure 6.9 and Figure 6.10:

Figure 6.8 Laser cutting pattern
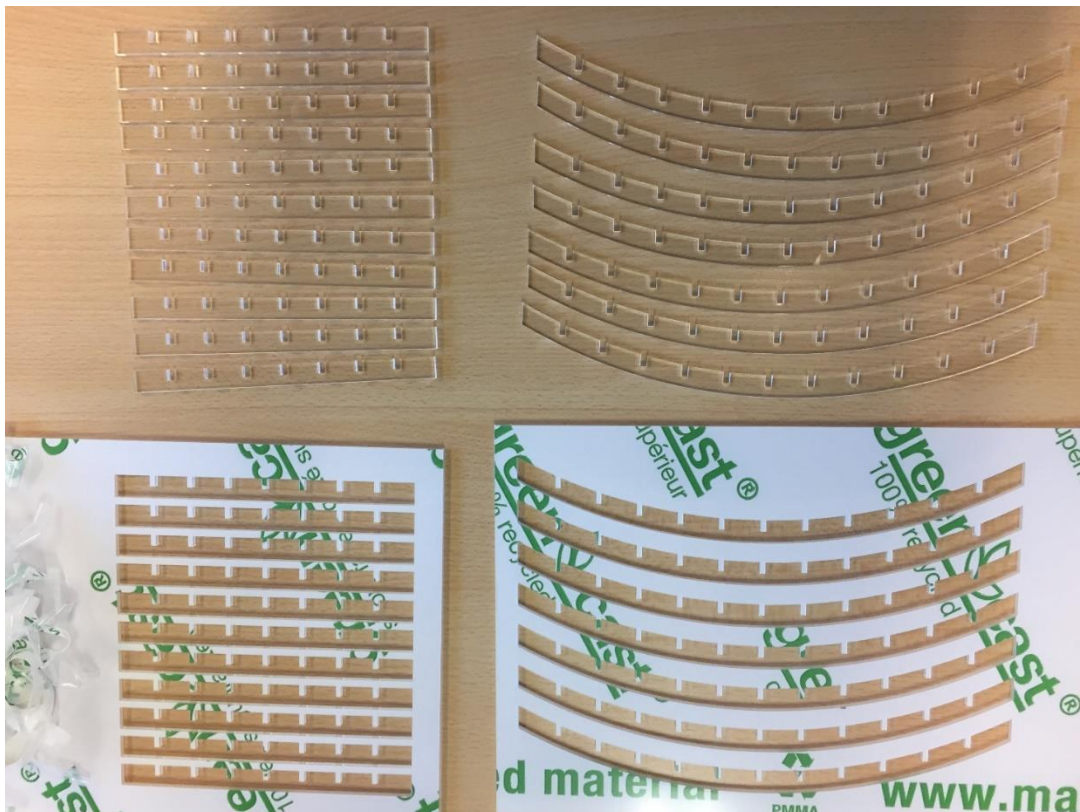
Figure 6.9 Laser cutting result
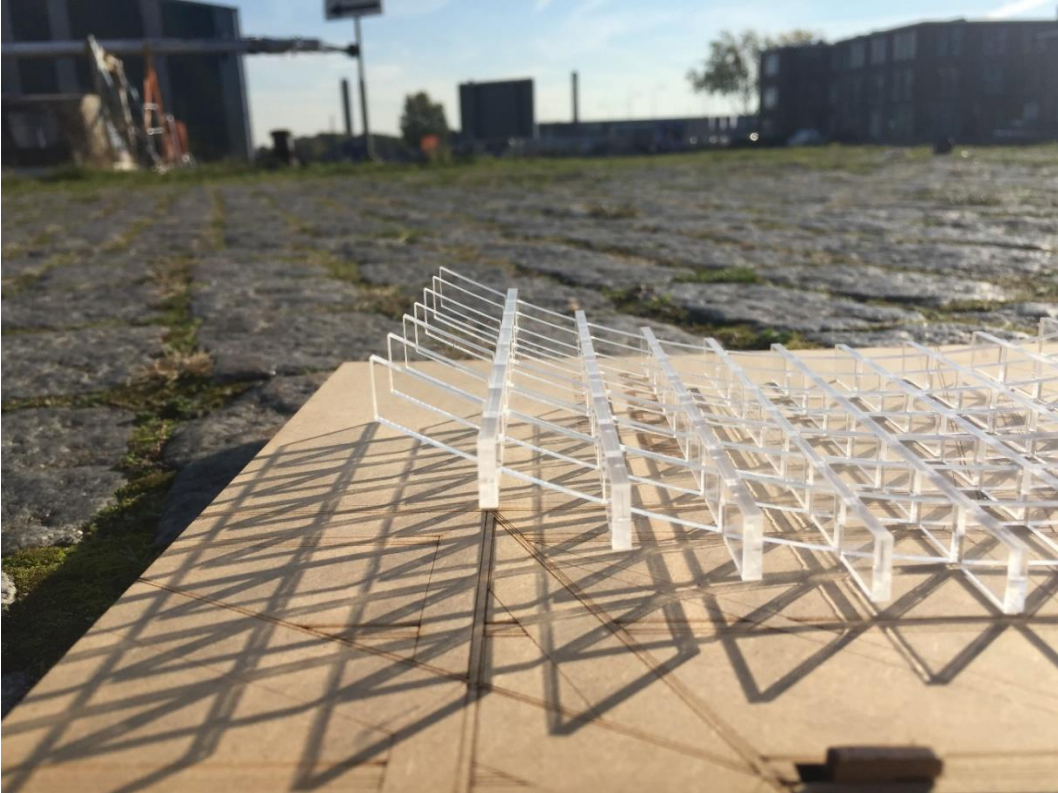
Figure 6.10 Laser cutting assembled pattern

6.3   Assembling

After having realized the core for all the models and after having received the glass sheets, the sandwich panel can be assembled. Delo Photobond Acrylic glue 4494 has been used, cured by UV light, Figure 6.11.

Figure 6.11 Delo Photobond 4494 acrylic glue cured with UV light

6.3.1   Waffle Model

The first model, that have been manufactured, was the waffle model, since the laser cutted core was faster to realize. First of all, the frame itself has to be glued. Then, the glass has been curved by using a clamp, Figure 6.12 and Figure 6.13. First the glass at the bottom, then the glass at the top, have been glued and cured with UV light. The final result of the assembled sandwich panel, Waffle Model, can be seen in Figure 6.14.
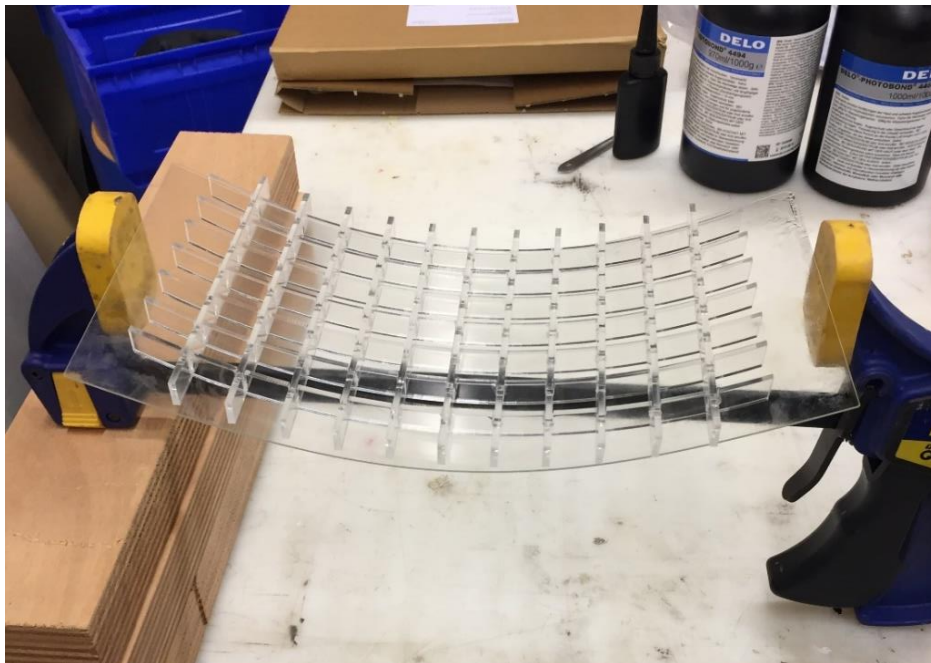
Figure 6.12 Cold Bending Procedure by the usage of a clamp
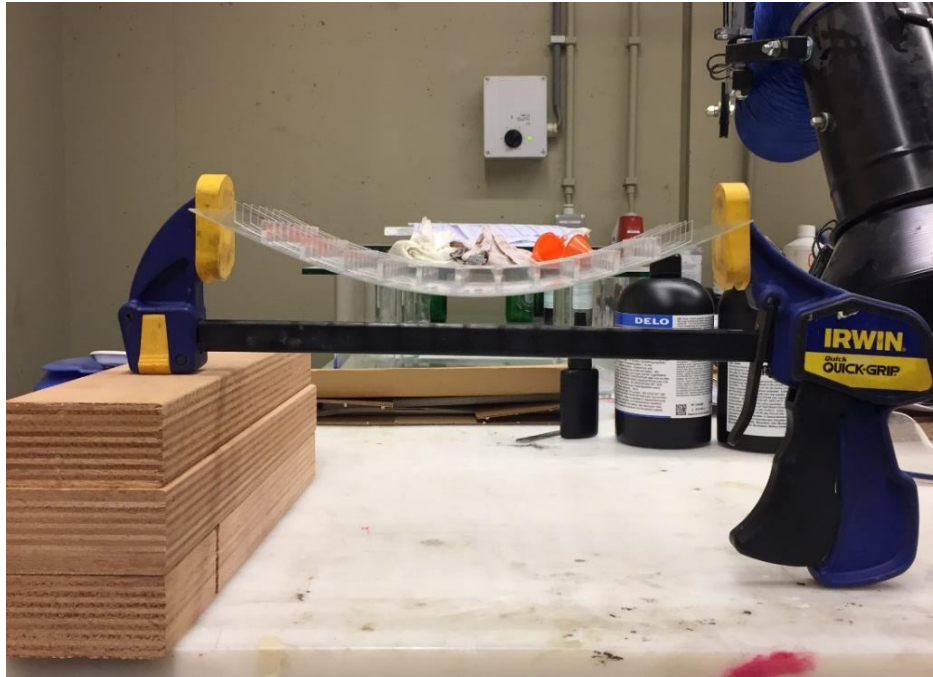
Figure 6.13 Cold Bending procedure - side view
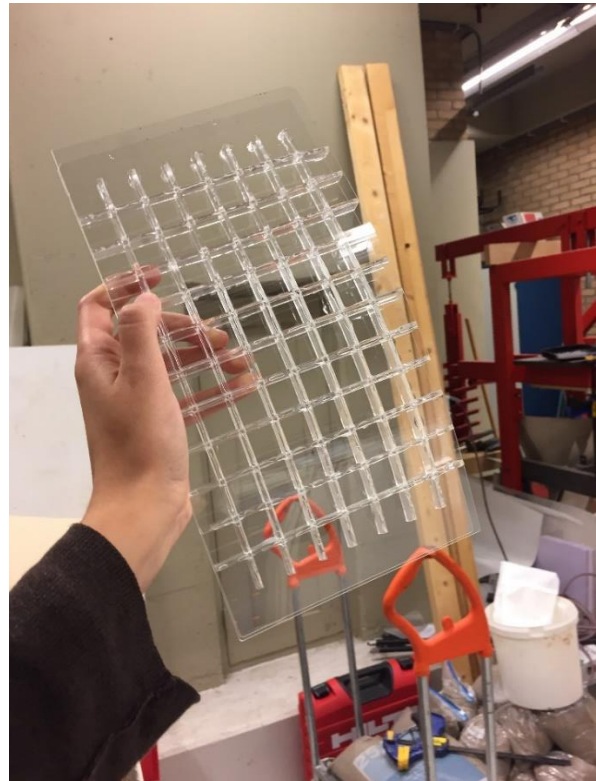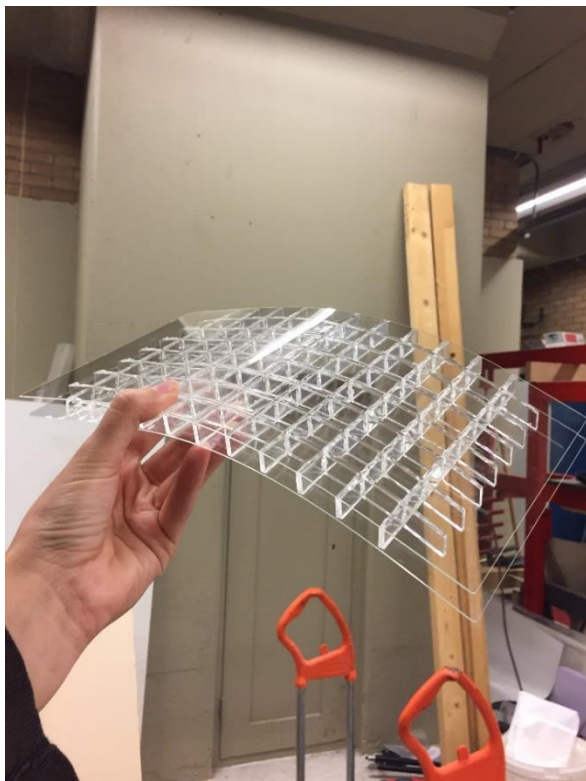
Figure 6.14 Final result - Waffle Model – Panel 2.1

6.3.2   Truss Model

Since the curvature realized by cold bending the glass with a clamp was not precise enough, in order to produce the second model, a laser cutted MDF mould has been realized. The mould has been designed with the exact final curvature, that the glass has to reach with cold bending, Figure 6.15.

Figure 6.15 Wooden Mould to cold bent the glass

A double sided adhesive tape has been used to attach the glass to the wooden mould. The tape is called Powerstrips by Tesa, it is a double sided tape that can be taken off, when it is not needed anymore, by pulling the end of the strip, which has been left not bonded to the glass and the wood. By tension, the strips will separate from the material without leaving any sign.

The glass has been stick to the mould with the double sided adhesive tape. Once curved to the correct shape, the core has been glued to the glass. Then, the acrylic glue has been cured with UV light. In order to glue the sencond glass ply, the core itself has been used as a mould for the cold bending procedure. Finally, the Powerstrips were taken off and the sandwich panel was realized. The whole procedure is shown in Figure 6.16 and the final result in Figure 6.17:
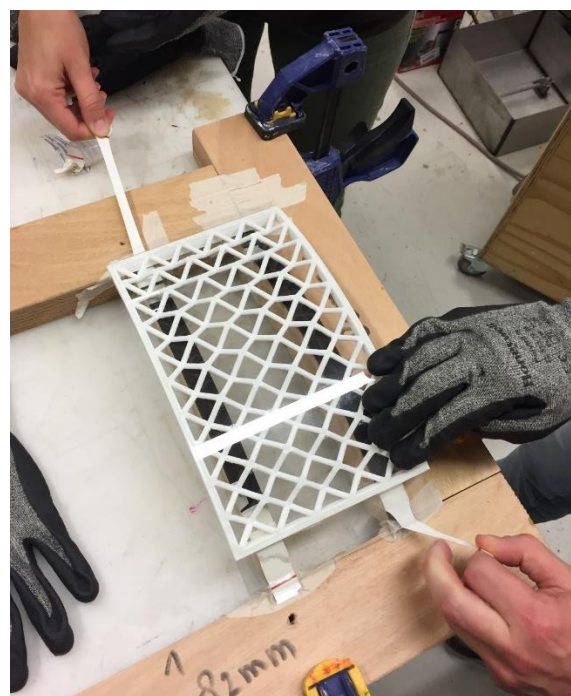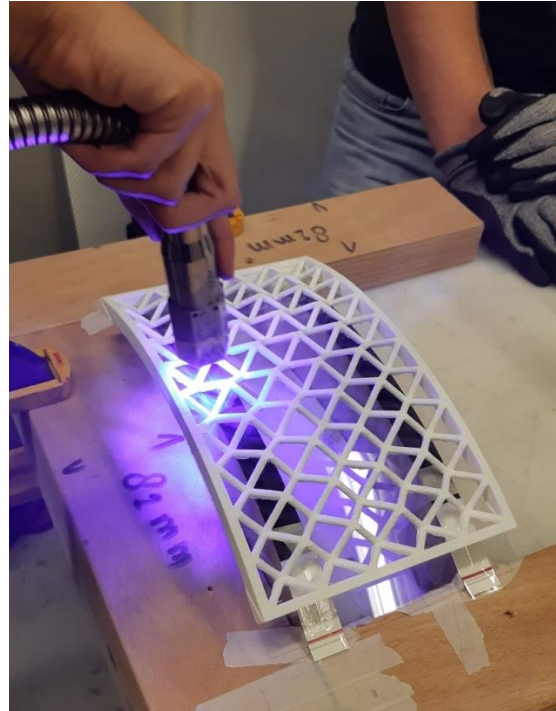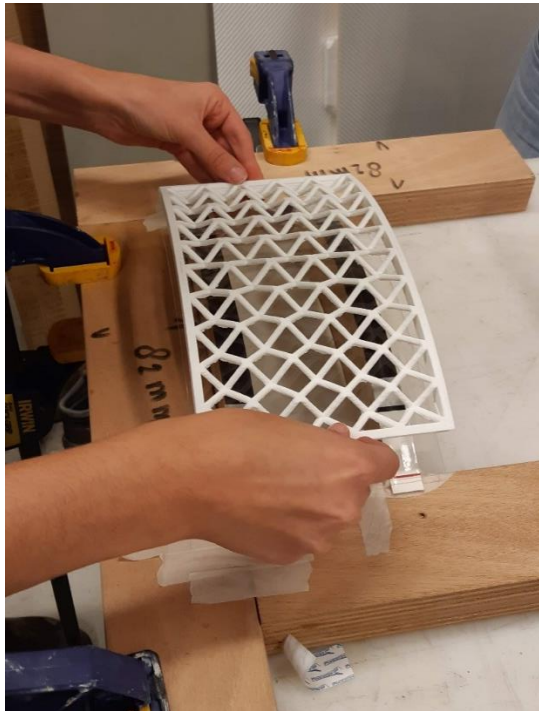
Figure 6.16 Truss Model - Manufacturing Process
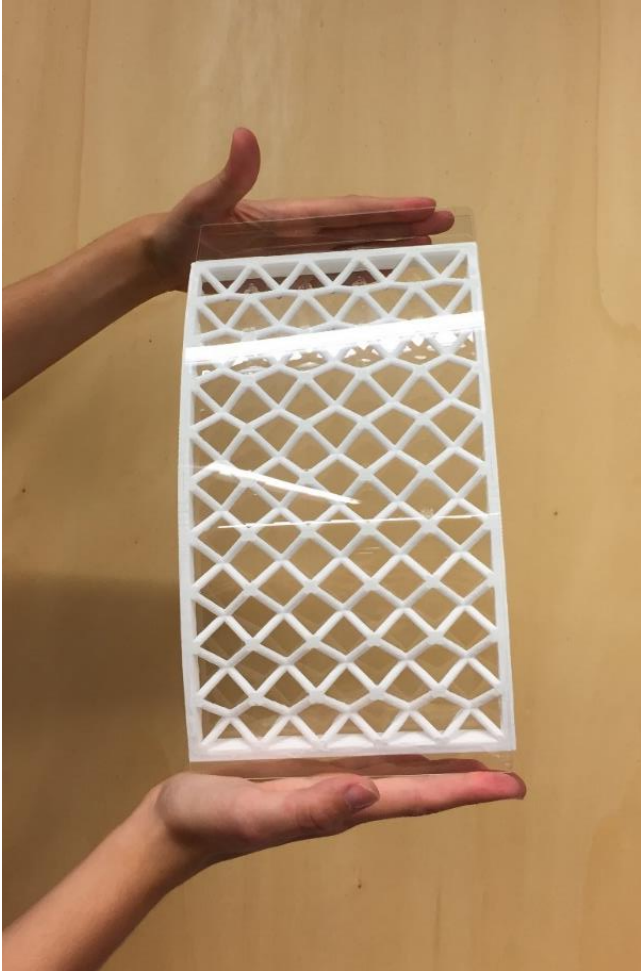
Figure 6.17 Truss Model - Final result – Panel 1.1 and 1.2

In the same manner, the Truss Model 500mm x 500mm has been manufactured. A wooden mould has been realized and the same procedure has been used. Unfortunately, even if the panel has been designed with a glass of thickness 0,5mm, a glass ply of 0,7mm was provided. Initially, it was thought that this difference would not be reflected in manufacturing problems. However, the difference of 40% in thickness cause many problems in the manufacturing procedure and thus, in the testing, as it will be explained in the next Chapter. A glass ply of dimensions 500mm x 500mm and thickness 0,5mm was expected to be very flexible and easier to bend compared to the smaller ply. On the contrary, the glass was quite stiff as can be seen from Figure 6.18. Since the set up revealed to be problematic, it was impossible to cure the glue properly. The best result that could be obtained is shown in Figure 6.19. The panel seemed to be glued properly, although, the day after, some parts of the edges were already detached.
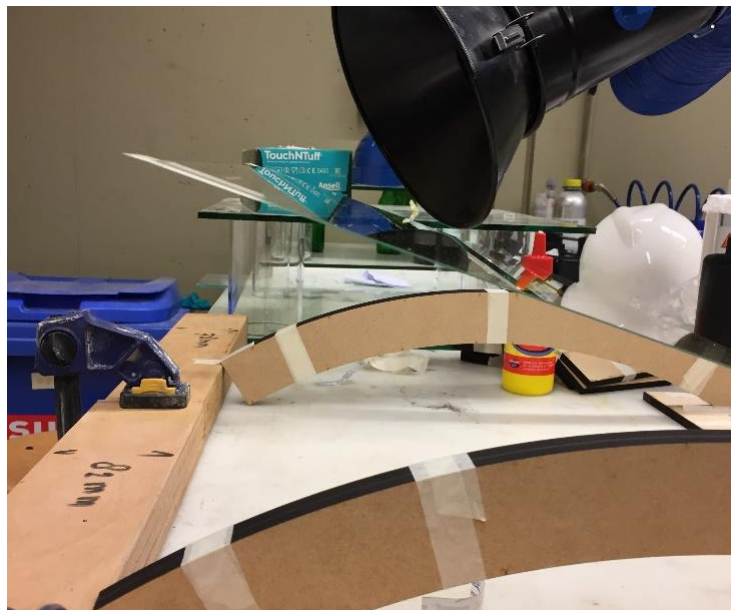
Figure 6.18 Truss Model 500mm x 500mm - Cold bending of the glass

Figure 6.19 Truss Model 500mm x 500mm - Final Result – Panel 3.1

7. Testing

7.1   Introduction

In this chapter the testing procedure is introduced. Firstly, the testing set up is illustrated and then the laboratory testing is shown. The following research sub-question will be answered:

- *Which test set up can be used to test the designed cold bent sandwich panel?*

7.2   Set up

In order to check the numerical models, testing has been performed. Since the panel is designed to be a façade panel, testing under a surface load would be ideal, because it would represents the wind action on the panel. However, it is challenging to realize in practice a uniformly distributed surface load on a curved panel. For this reason, the panel has been tested under a point load, which was easier to put in practice and it could bring to a more accurate result in the comparison between the numerical model and the experimental results. The set-up of the testing has been realized in order to have the support exactly at the same location of the end of the core. Since the glass panel is 50 mm longer, the glass will exceed the supports. The set up realized is reproduced in the following figure.
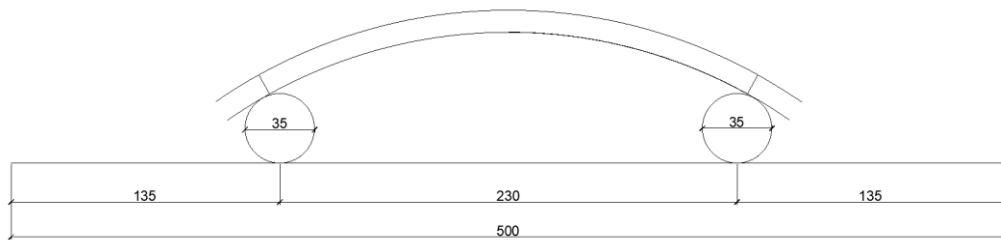
Figure 7.1 Point Load Test Set Up

The supports has been realized in wood, and the circular part has been nailed to the bottom plank. In order not to let the wood to roll under loading, two additional wooden pieces have been added at the side of the circular wood. The result is shown in Figure 7.2.
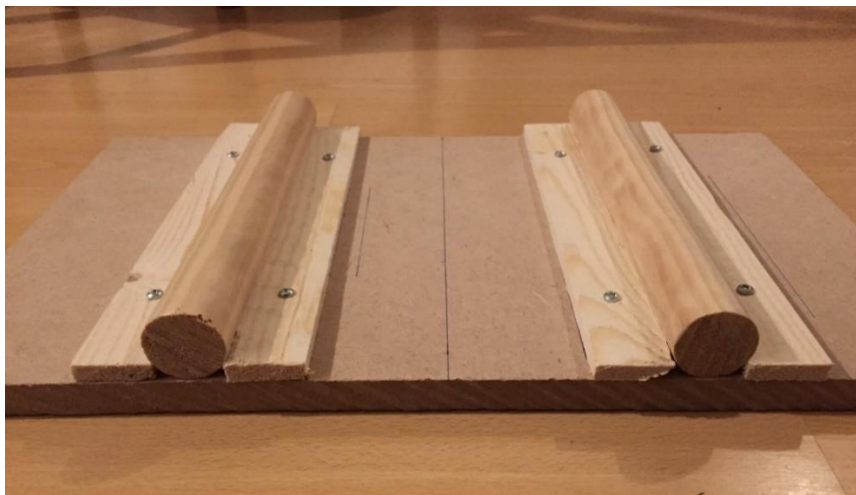
Figure 7.2 Wooden set up – simply supported boundary conditions

7.3   Laboratory testing

Panel 1.1 – Truss Model 250mm x 150mm

The Truss Model broke one week after it was assembled. The panel was laid on the table. In the moment the bottom pane touched the table surface, the top pane broke. From the fracture pattern (Figure 7.3), it can be seen that the panel broke due to prestressed stresses. The fracture lines goes horizontally from one edge of the panel to the other one, following the direction of the stresses due to the cold bending procedure. It is very difficult to predict exactly why the glass broke: maybe a scratch was present in the edge surface. In Figure 7.3, the starting point of the fracture is highlighted with a red circle. From this experience it was gathered that the edges of the glass has to be carefully treated because are the weak spots of the ply. To avoid dangerous situation, the core should be designed to be 1 millimetre larger than the glass, in order not to have the glass edges hanging out.

Figure 7.3 Panel 1.1 - Broken Top Layer of Glass

Panel 1.2 – Truss Model 250mm x 150mm

Since the first truss panel broke, an identical panel has been manufactured again. The core has been printed with the same specifications. Falcon Glass 0,5mm has been utilized to realize the sandwich panel. Once the sandwich panel was ready, it has been tested with the simply supported boundary conditions showed above and a point load of dimensions 40mm x 10mm, shown in Figure 7.4.
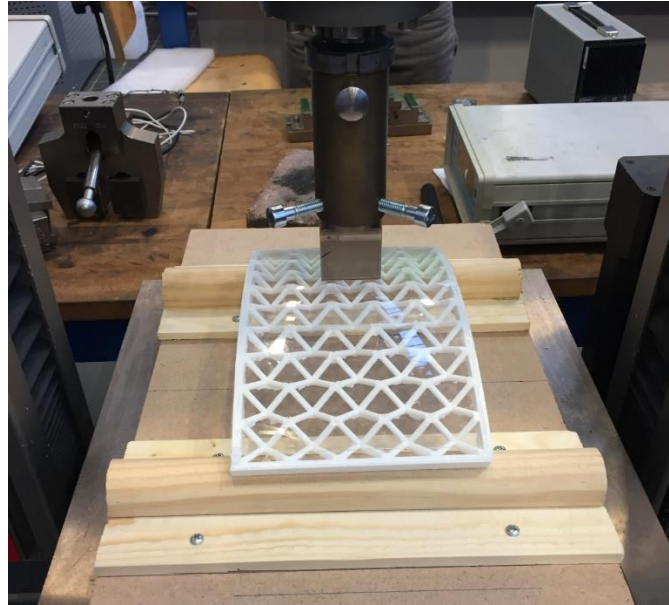
Figure 7.4 Panel 1.2 - Testing

Panel 1.3 Truss Model 250mm x 150mm – Core printed divided in strips

As it has been said in the manufacturing chapter, another Truss Model sandwich panel has been realized. The core was created by dividing the curved model into flat strips. The result was similar to the one realized by one 3D printed core. This second panel has been tested with the same support and loading conditions as Panel 1.2. During the testing, a safety plastic foil was used to cover the sandwich panel during the failure, as can be seen in Figure 7.5.

Figure 7.5 Panel 1.3 - Testing

Panel 2.1 Waffle Model 250mm x 150mm

The Waffle Model, which will be called Panel 2.1 in the following plot, has been tested under the same boundary conditions and loading conditions. The same testing machine has been used and the results will be explained in the next Chapter.
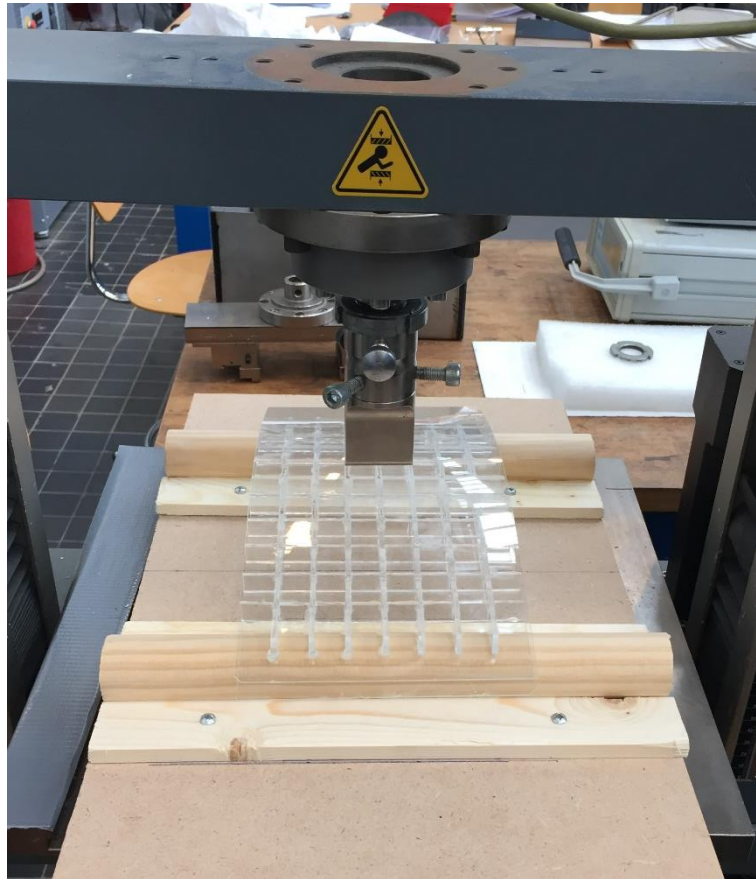
Figure 7.6 Panel 2.1 - Testing

Panel 3.1 Truss Model 500mm x 500mm

The Truss Model of bigger dimensions 500mm x 500mm, has been tested with another machine, due to the available dimensions. The boundary conditions have been realized with a wooden plank in the same manner as the one before. The point load has been realized with a cylinder with radius 150mm, as it is shown in Figure 7.7.
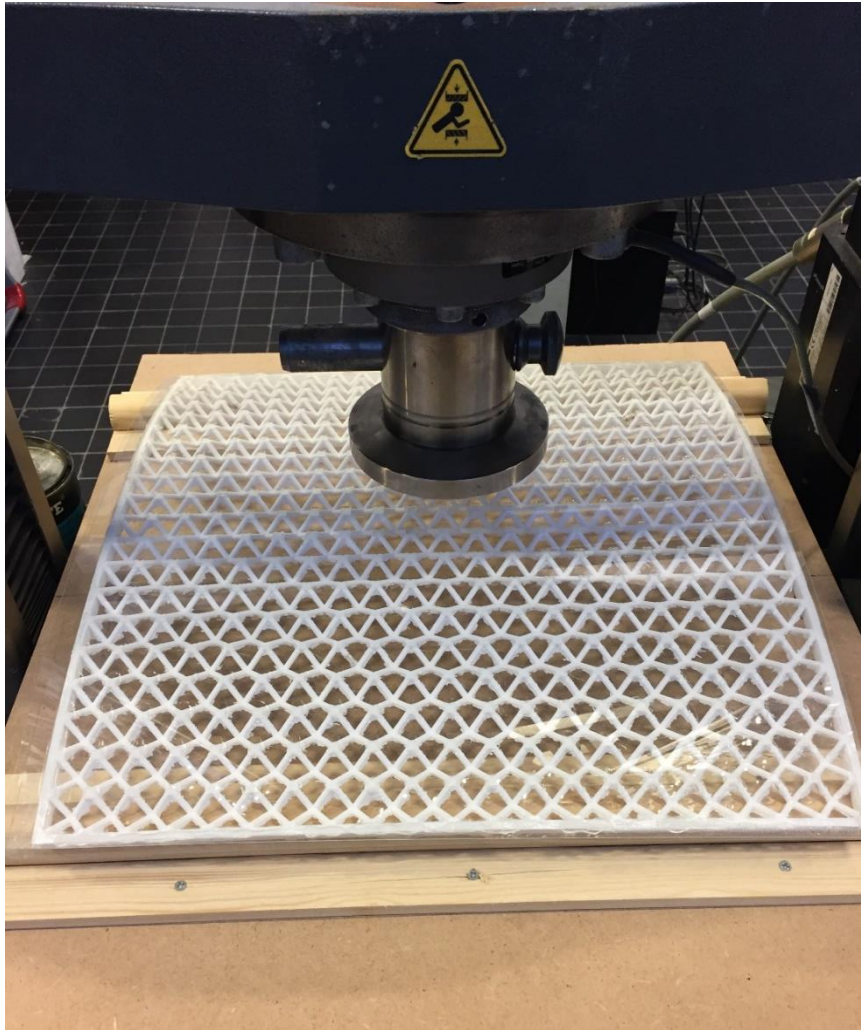
Figure 7.7 Panel 3.1 – Testing

7.4   Conclusion

Which test set up can be used to test the designed cold bent sandwich panel?

Since the panel is designed to be a façade panel, testing under a surface load would have been ideal, because it would have represented the wind action on the panel. However, it is challenging to realize in practice a uniformly distributed surface load on a curved panel. For this reason, the panel has been tested under a point load, which was easier to put in practice and it could bring to a more accurate result in the comparison between the numerical model and the experimental results. The set-up of the testing has been realized in order to have a simply supported panel. The boundary conditions have been realized with wooden elements and it is shown in Figure 7.1 and Figure 7.2.

8. Analysis of Results

In this chapter, the results obtained from experimental testing are illustrated. Every panel test is explained and commented individually. Moreover, these results are compared with the ones obtained from the numerical analysis. Similarities and differences are underlined to draw conclusions and new suggestion for further researches.

8.1   Panel 1.2

The Truss Model, realized with a unique 3D printed element core, was first tested. The point load was applied on the top of a pyramidal unit, as it is shown in Figure 8.1. The load was increased incrementally with a velocity of 2,5 mm/min from zero to a maximum load of 245,8N.

Specifications:
Boundary conditions: Simply supported
Load: Point Load on the top of a Pyramidal Element
Testing nozzle dimensions: 40mm x 10mm. Area of 400 mm^2
Testing velocity: 2,5 mm/min
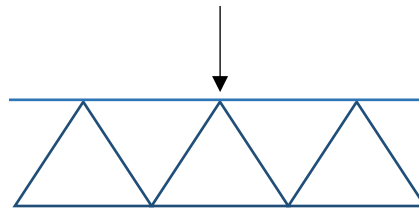
Figure 8.1 Point Load on Panel 1.2

In Figure 8.2, the comparison between the Numerical Model obtained with Femap and the Experimental Model, realized by testing, is shown. The stiffness of the sandwich panel results to be precisely detected by the FEA Model in the first phase of the experiment, which represents the elastic behaviour of the sandwich panel. In fact, the two curves overlap. Once the first glue failure occurs, the panel shows a decrease in stiffness. The overall trend of the sandwich panel illustrated a ductile behaviour which was introduced in the literature review with the study of Lambert and O'Callaghan (Lambert & O'Callaghan, 2013).

As can be seen in Figure 8.3, Panel 1.2 is characterised in the initial elastic phase by a stiff behaviour. The stiffness has been calculated to be equal to 74,18 N/mm. At Point 1 in the graph, the first local failure of the glue is highlighted. Once the load reaches a magnitude of 200 – 240N the glue continue detaching, until a maximum load of 245,8N, where the connections of the sandwich panel fail (Point 2). At Point 3 in the same Figure, the point in which the Bottom Glass pane broke is underlined. After that, the PLA core broke. As can be seen from the last part of the graph, the panel still has some loading capacity, due to the unbroken Top Glass Pane. However the test was stopped due to not valuable information for this specific research.
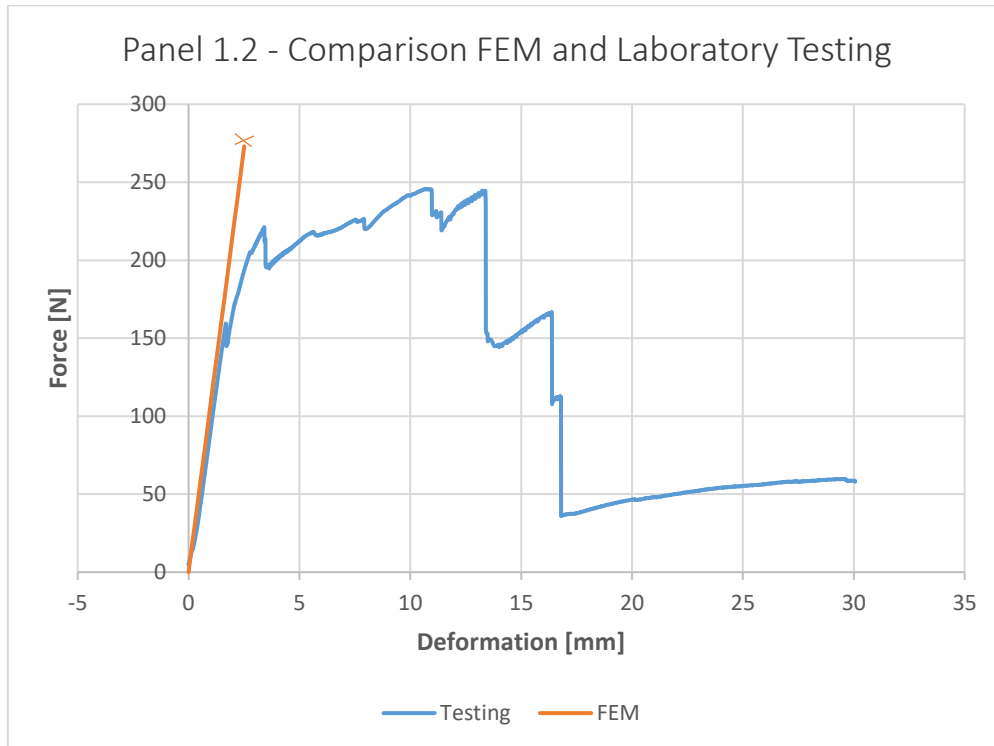
Figure 8.2 Panel 1.2 - Comparison between Numerical Models and Laboratory Testing
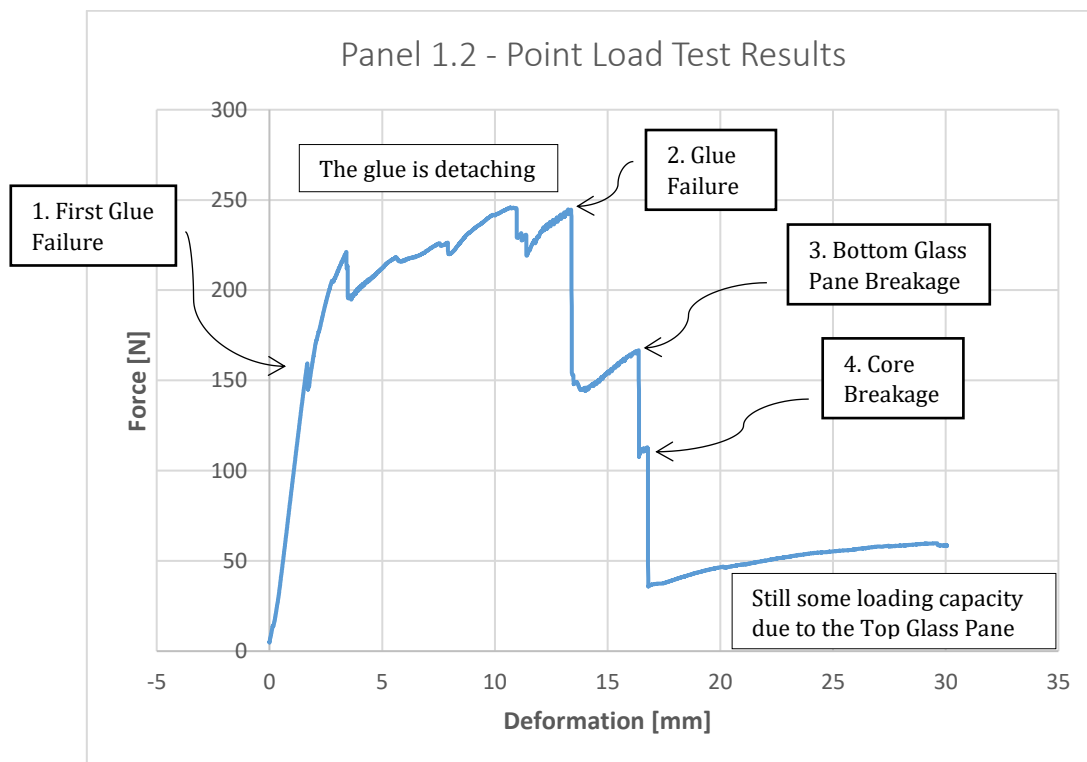

Figure 8.3 Panel 1.2 Test Results and Comments

Another important observation, given by experimental testing, is the way the glue fails. Adhesive failure occurs in the glue; sometimes the glue remains attached to the glass, other times to the PLA, even in two adjacent pyramidal elements (Figure 8.4). This experience demonstrates the fact that the glue does not bond properly the two materials. More comments will be drawn at the end of this chapter, after the analysis of all the tests.
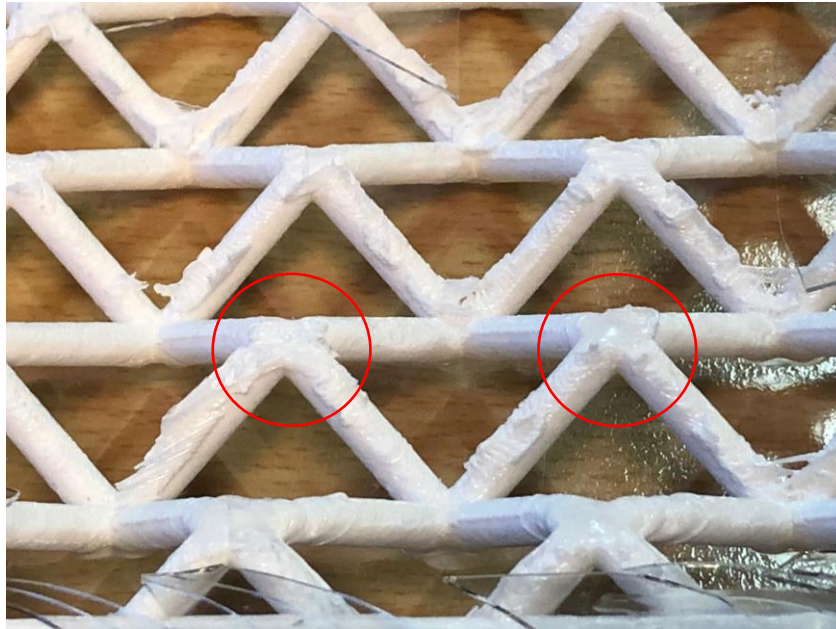
Figure 8.4 Adhesive Failure of the glue
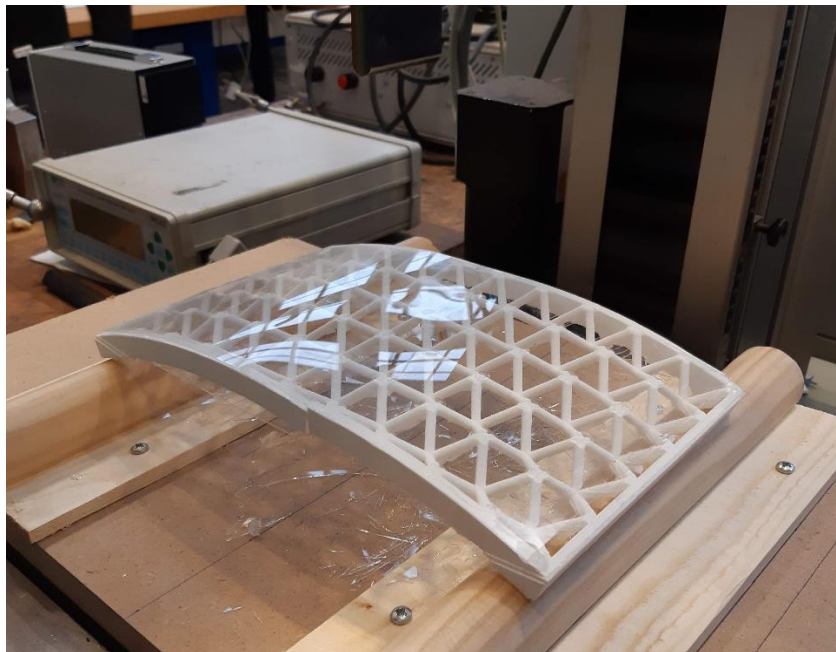
Figure 8.5 Panel 1.2 after testing - Top Glass Pane still intact

8.2   Panel 1.3

The Truss Model, with the core realized by 3D printed flat strip elements, was then tested. This time, due to different glass dimensions, the point load was applied on the glass, at the center of two pyramidal units, as it is shown in Figure 8.6. This difference was encountered because this panel was first designed when the glass 300mm x 150mm was available, and then manufactured when another dimension of glass was present, 250mm x 150mm. Therefore, it has to be reminded that different loading conditions are now present. The load was increased incrementally with a velocity of 10 mm/min from zero to a maximum load of 222,0 N.

Specifications:
Boundary conditions: Simply supported
Load: Point Load in between two Pyramidal Elements
Testing nozzle dimensions: 40mm x 10mm. Area of 400 mm²
Testing velocity: 10 mm/min
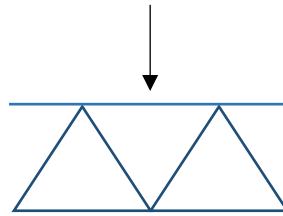
Figure 8.6 Point Load on Panel 1.3

In Figure 8.7, the comparison between the Numerical Model realized with Femap and the Experimental Model realized by testing is illustrated. The split core has been modelled with joint connections within every diagonal element. In practice, the stiffness of the panel results to be less than the one predicted by the model. This can be due to imprecision during the manufacturing of the core, since every strip has to be glued and put in position individually. From Figure 8.7, the overall trend of Panel 1.3 exhibits an elastic behaviour, since the first failure occurred in the glass. Besides, it can be noticed that the Numerical Model, with the same boundary and loading conditions, predicts the failure for a smaller load. This fact occurs due to the punctual load in the numerical model. The point load applied in the experimental testing is reproduced by a point load on adjacent nodes in the FEM. Even if the load has been distributed on nine nodes to avoid peak stresses, the punctual node on the glass cause higher stresses in the numerical model than the ones exhibited in the experimental testing.

As it can be seen from the following figures, the initial stiffness of the sandwich panel shows to be comparable to the one of Panel 1.2. During this test, the first element which is brought to failure is the top glass ply of the sandwich panel. This experience depends on the loading conditions of this test. Once the top glass failed, the whole sandwich panel exhibits a brittle behaviour (Figure 8.8 - Point 1). After this first failure, the panel is able to carry a lower load, thanks to the core and the bottom glass pane, which are still in place. When the load is increasing, the bottom pane and the split core are not able to carry the load anymore, therefore the bottom glass pane broke at Point 2.
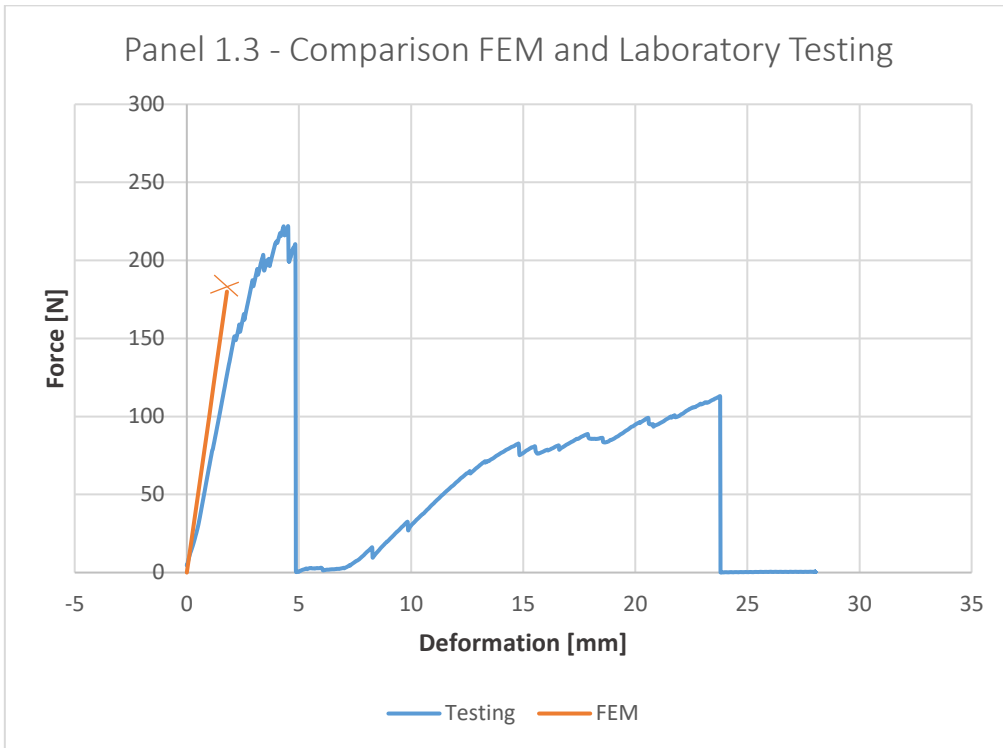
Figure 8.7 Panel 1.3 Comparison between Numerical Models and Laboratory Testing
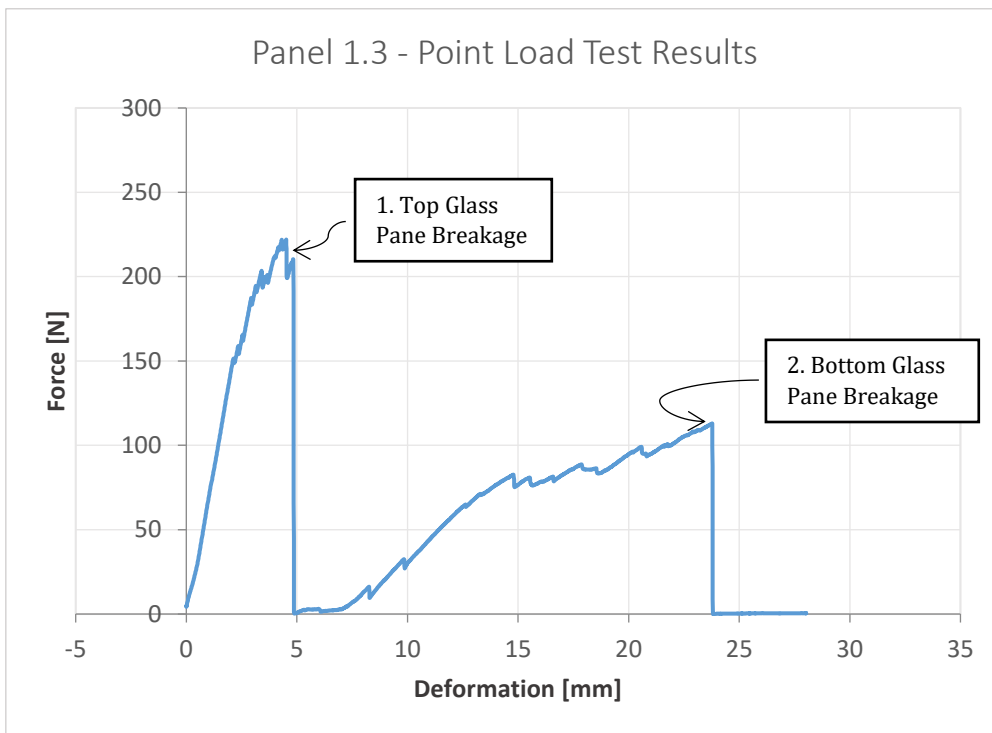

Figure 8.8 Panel 1.3 Test Results and Comments

From the comparison between Panel 1.2 and Panel 1.3 (Figure 8.9), it can be seen that the first specimen behaves stiffer than the second one, in fact the Force/Deformation plot is more inclined. Pane 1.2 handles a force of 245,8 N, while Panel 1.3 one of 222,0 N. It must be remembered that, the first panel has been loaded on the top of one pyramidal element, while the second panel at the center of two pyramidal units, so where no support where present. From Figure 8.10 the two panels after experimental tests are shown.
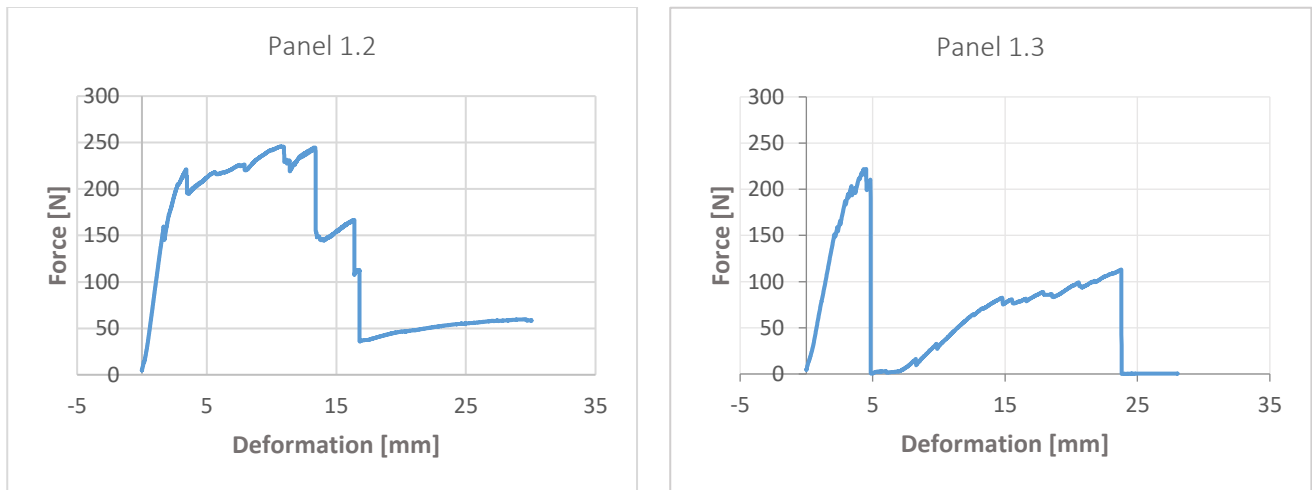
Figure 8.9 Comparison between Panel 1.2 and Panel 1.3

Figure 8.10 Panel 1.2 (right) and Panel 1.3 (left) after testing

8.3   Panel 2.1

The Waffle Model, realized with PMMA laser cut core, was then tested. The load was increased incrementally with a velocity of 10 mm/min from zero to a maximum load of 163,2N.

Specifications:
Boundary conditions: Simply supported
Load: Point Load
Testing nozzle dimensions: 40mm x 10mm. Area of 400 mm^2
Testing velocity: 10 mm/min

The Force Deformation plot of Panel 2.1 is illustrated in Figure 8.11. The first information, that can be noticed from this graph, is that Panel 2.1 can withstand just 163,2N, instead of 222,0 or 245,8N, evaluated in the previous testing. During the testing of the Waffle Model, the panel exhibits great flexibility, revealed by significant deflections. This deflection was present because the core was not able to maintain its designed shape. The gap, in which each laser cut element was embedded, was bigger than the thickness of the core ribs, and the connections result not to be fixed but they were able to rotate.

The testing was stopped because the panel was reaching a flat shape, such the deflection was deep Figure 8.12. Once the load has been removed, the sandwich panel returned back to the flat shape, which was the original shape of the manufactured glass. Since the core had no resistance anymore, the sandwich panel shape is driven by the glass, as can be seen in Figure 8.13.
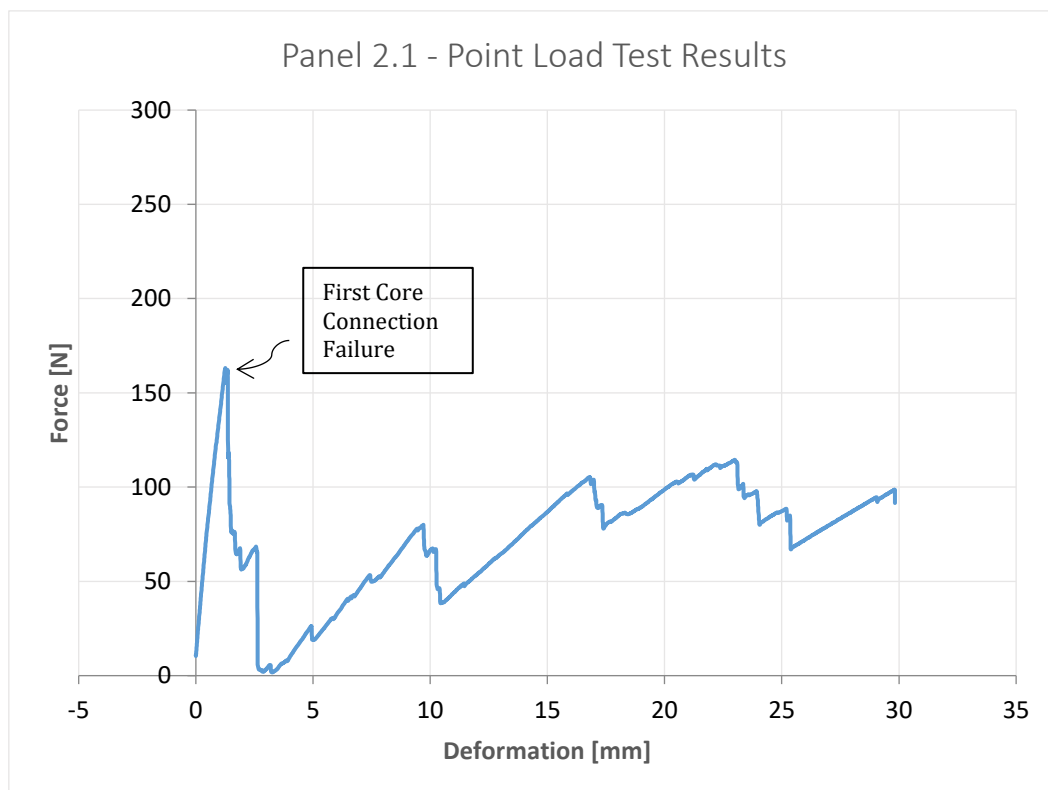
Figure 8.11 Panel 2.1 Test Results and Comments

The laser cutting technique revealed not to be ideal for the curved shaped core. Since laser cutting can be done just on a flat surface, the design has to be made by surfaces than later on would be assembled. However, the laser cutting nozzle has a tolerance of 0,2mm. The precision given by the laser cutting technique is not good enough to realize fixed connections in the core.

Figure 8.12 Deflection of Panel 2.1during Testing

Broken Core Connection

Figure 8.13 Panel 2.1 - Waffle Model - After Testing

8.4   Panel 3.1

The last panel, that has been tested, was the Truss Model 500mm x 500mm. As it has been explained in the last part of Chapter 6.3.2, during the manufacturing, there have been some problems which cause the glue not to adhere correctly. The main challenge was to keep the glass connected to the core, while curing the glue with UV light. Since the setup did not work correctly, some parts did not bond. As it is shown in the following picture, mainly in the bottom pane, some spots were already detached, even before start testing (Figure 8.14 left part).

Figure 8.14 The Glue was already detached before start testing
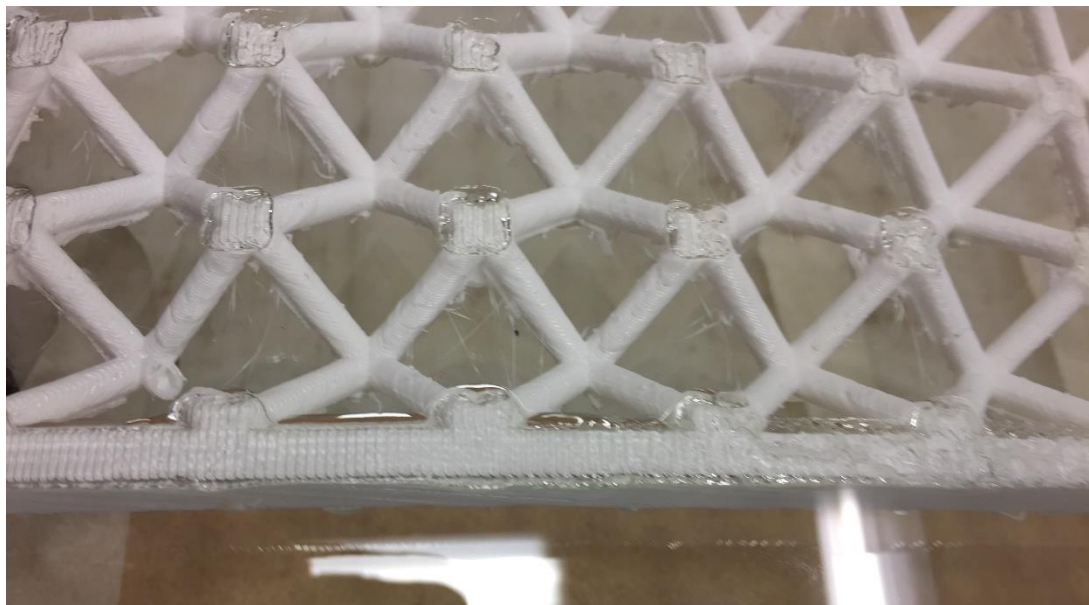
Figure 8.15 Glue added on the edge of the panel

Specifications:
Boundary conditions: Simply supported
Load: Point Load
Testing nozzle dimensions: Circle of 150mm = Area of 706,86 cm²
Testing velocity: 2,5 mm/min

Since the test was performed with a bigger machine, which has a lower accuracy in plotting the results, Figure 8.16 illustrates an area of results, instead of a line. Unfortunately, due to the problems having during manufacturing, the result given from this test is not of the expected quality. In any case, the analysis of the detected data has been performed. From the plot in Figure 8.16, it can be noticed that at a force of 183,3N, the glass panes are delaminated completely from the core (Figure 8.17); for this reason, the sandwich panel behaviour was not contributing anymore and the delaminated panel continued to deflect significantly (Figure 8.18). Since the sandwich behaviour was not acting anymore, and neither the curvature behaviour (the panel simply supported could largely deflect and it turned to be flat after a brief time), the test was stopped.
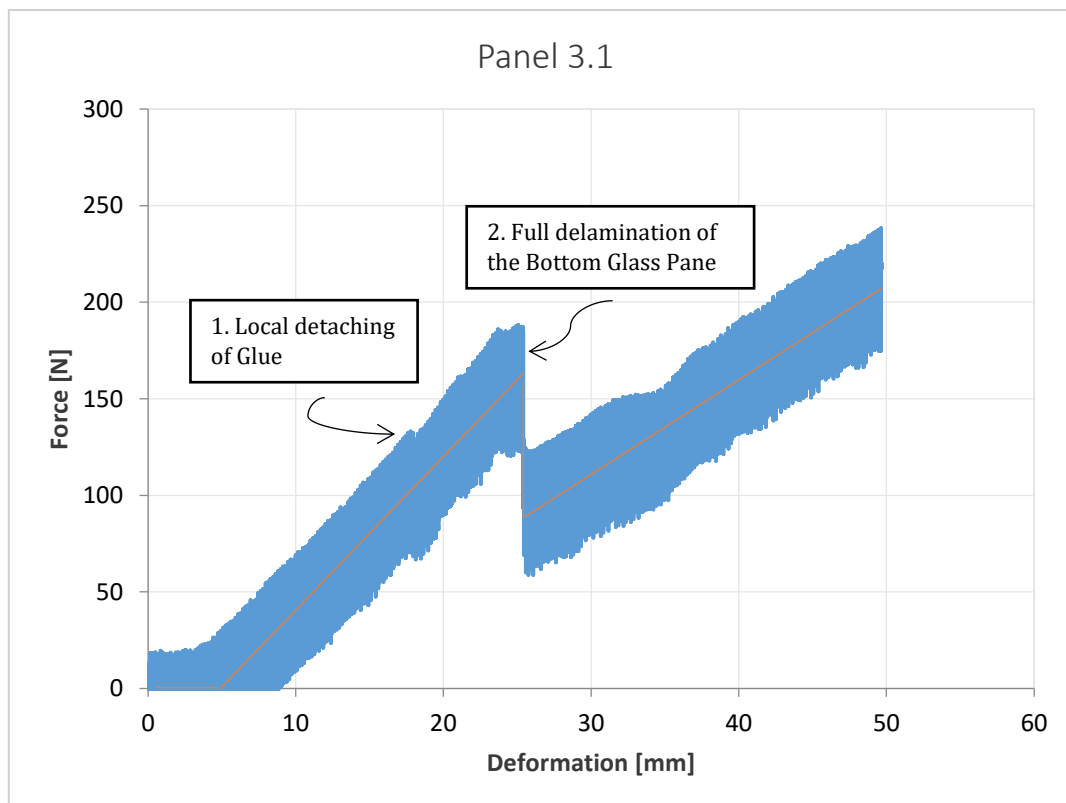
Figure 8.16 Panel 3.1 Test Results and Comments
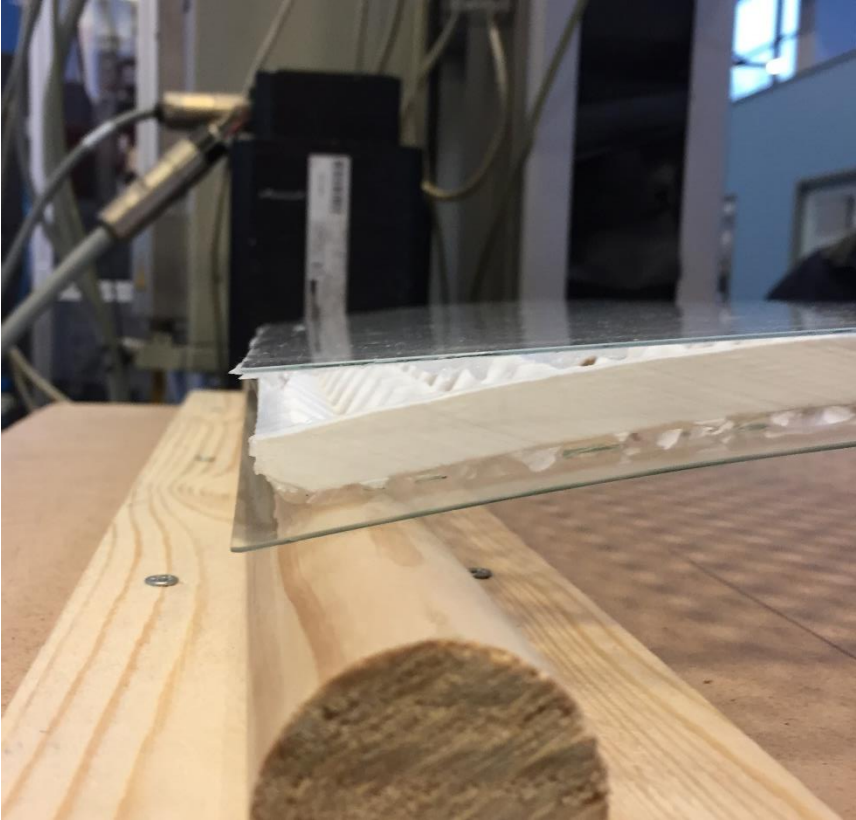
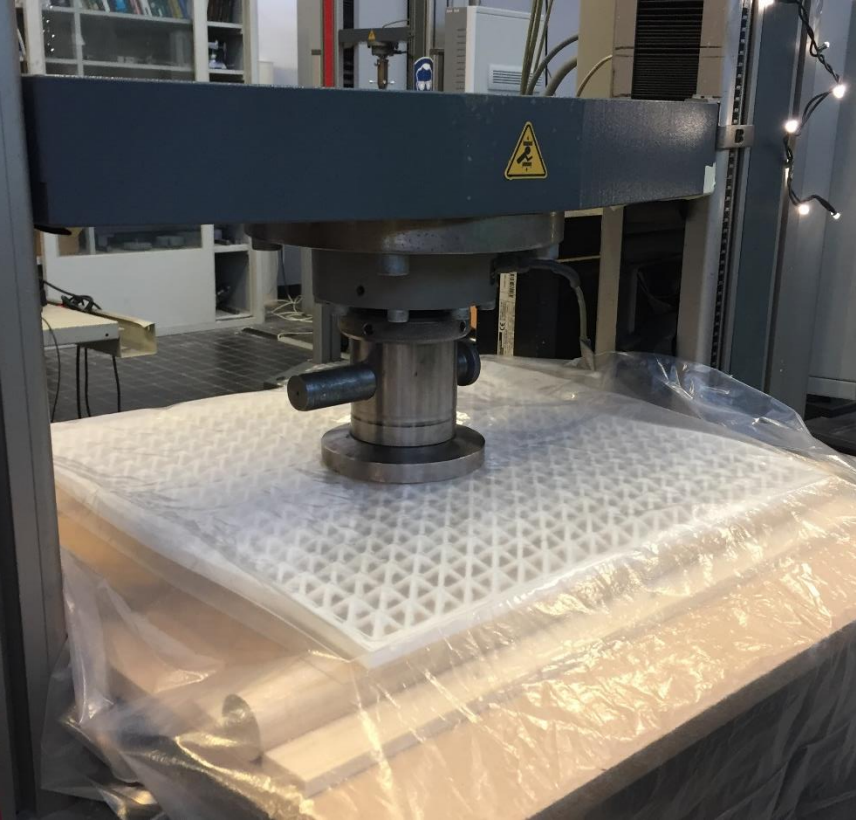Figure 8.17 Complete delamination of the sandwich panel

Figure 8.18 Significant deflection after delamination

From this experiment, it can be deduced that the glue was not strong enough to keep the glass and the PLA connected. Even before starting to load the panel, the glue was already off at the edges of the bottom ply. For sure, this condition has compromised the test. Therefore, it has been tried to understand the reasons of this delamination. Undoubtedly, the availability of materials had a large impact on the process. Moreover, the use of a thicker glass has influenced the situation. In the following analysis, the influence of the thickness of the glass has been studied. Once the sandwich panel is manufactured and the panel is loaded, the difference in thickness does not influence the amount of glue needed in the connection. However, the problem can arise during the cold bending procedure. In fact, the glue has to keep bonded a glass of 0,7mm, which has a higher stiffness, given by a greater thickness, which wants to go back to the flat condition. The tension in the connections due to cold bending of the Top Pane of Glass has been calculated by reproducing the cold bending procedure on the mould, Figure 8.19.
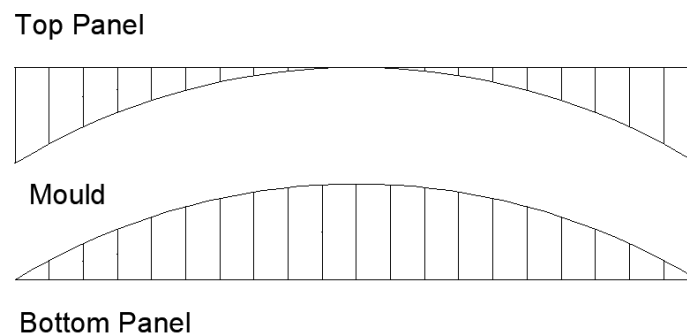

Figure 8.19 Cold Bending Procedure of Glass on the mould

A two-steps analysis has been performed to schematize the cold bending procedure of the Top Panel. The schematization is shown in the following figure: firstly the glass has been supported at the center, where it first touches the mould, and pushed down at the edges, Figure 8.20. Then, vertical supports have been added at each point, where the core pyramidal elements are present, the external load is taken off from the analysis, and the tension in the support is given by the reaction in each support point. The maximum reaction force is at the edge of the panel.
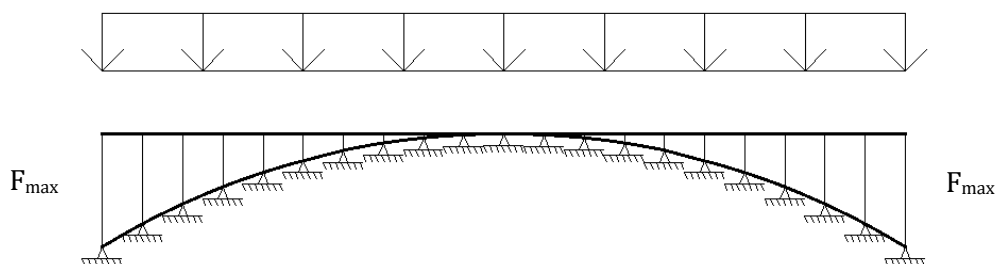

Figure 8.20 First step - curving the glass on the mould

This calculation has been done first with a glass of thickness 0,7mm, which is the one that has been utilized; and then with a glass of 0,5mm, which is the one that has been chosen in the design.

With a glass of thickness 0,7mm the maximum reaction force needed to keep the glass in the desired bent shape is F_{max} = 29,54N. This force, divided by the area of one pyramidal element, which is 12,57mm², gives a maximum tensile stress in the connection of 29,54/12,57=2,35 MPa. It has to be reminded that the strength of the utilized glue is 4 MPa, which means that more than half of the capacity of the glue is taken by the cold bending procedure. Moreover, since during the manufacturing phase, it was difficult to cure the glue correctly, it has to be said that it is possible that the glue did not have its full capacity, due to errors in the application.

On the other hand, with a glass of 0,5mm, the maximum force needed to keep the glass curved is 10,71N. If this force is now divided by the area of a pyramidal element, a tensile stress of 0,85MPa is obtained in the connection. It can be noticed that the use of a thicker cause the glue to deal with a stress of 2,35MPa instead of 0,85MPa. Moreover, a glass of 0,5mm is more flexible and thus it is easier to cold bend during manufacturing and the glue results easier to apply.

Another information, which can be gained from this experiment, is that the glue showed an adhesive failure. After failure, the glue remains attached just to the glass and not to the plastic PLA core. Since this problem has also been encountered in Panel 1.2, which was realized with 0,5mm Falcon Glass and did not have high stresses in the connections, Delo Photobond developers were contacted to have explanations on this behaviour. It has been suggested to change the type of glue, since the Delo Photobond 4494 behaves well in connecting glass to glass. On the other hand, when the glass has to be connected with plastic, Delo Photobond AD494 has better performance, with a shear strength Glass/PMMA of 9MPa instead of 4MPa (Appendix A). The use Delo Photobond AD494 is suggested for further researches.

Part IV

FINAL DESIGN

9. Final Design

In this research, an innovative structural element composed of thin glass and a polymeric core has been investigated. From the analysis chapter, the feasibility of this composite panel has been studied. The small scale Panel 1.2 behaves as it was predicted by numerical models. The bigger scale model (Panel 3.1) gave some challenges in the manufacturing phase. However, if the correct glue is chosen, it has been demonstrated that a proper behaviour can be obtained. The connection between the core and the glass faces revealed to be the weaker point of the structure, and for this reason they have to be addressed carefully. In this chapter, an application of the examined panel will be illustrated, where Falcon Glass 0,5mm is used and Delo Photobomb AD494 acrylic glue is used, to give more resistance to the connections.

9.1   Description of the building

The Netherlands Architecture Institute (NAI) is a cultural institute for architecture and urban development. It was established in Rotterdam in 1988, it was designed by Koolhaas. The NAI is a private organization, which manage the collection of archives on the history of Dutch architecture.

In 2011 the museum was decided to be refurbished (Figure 9.1). Octatube was involved in the engineering and the re-building of the new entrance area. Four main parts were modified: the new Bookshop, where a high glass façade connects the museum to the public part of the building. Underneath the concrete pergola, a completely redesigned glass façade was constructed. The entrance façade and the north façade are also renewed.

The idea for the final design is to propose the innovative studied panel for the façade on the left part of the building, where less transparency was required by the architect. The contrast between the glass parts and the hybrid part will clearly reveal the different effect of the transparency of a clear glass window and the hybrid thin glass panel.

Figure 9.1 Netherlands Architecture Institute (NAI)

9.2   Boundary Conditions and Load Definition

The final design consists of a façade made by the investigated curved thin glass sandwich panel. After the literature review and the preliminary calculations have been done, it has been decided to create a final panel with Falcon Glass 0,5mm, which is available up to 1245 mm x 3210 mm. For the sake of simplicity, it has been decided to use dimensions of 1200 mm x 3000 mm. This dimensions can easily be used to span from one floor to another, and represent the dimensions of a window. PETG transparent filament has been chosen as the material to realize the core of the sandwich structure.

The panel will be supported on the long side. This decision has been taken after the comparison made in the first paragraph of Chapter 5 has been performed. In fact, the deflection of a panel with 3 meters span and thickness 0,5mm, was too high. Moreover, by supporting the long side of a panel, the vertical layout of the panel will be transferred on the façade of the building, by giving a vertical layout to the building itself. Since the Truss Model has been already chosen as the best core pattern, because it showed a better behaviour by using less polymeric material, it has been decided to use the Truss Model also in the final design. The thickness of the final sandwich panel is 0,5mm + 11mm + 0,5mm, for a total thickness of 12mm.
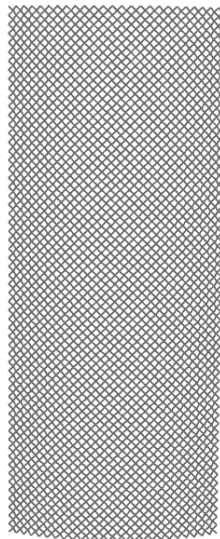
Figure 9.2 Panel geometry

Material Properties

FALCON GLASS

E_g = 73 000 N/mm²
G_g = 30 000 N/mm²
Specific Weight = 25 kN/m³

PETG

E_c = 2 000 N/mm²
G_c = 730 N/mm²
Specific Weight = 12,7 kN/m³

Boundary conditions

The panel is line supported on the long vertical edges as it is shown in the figure below.
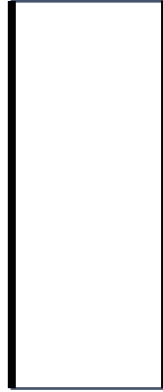

Figure 9.3 Boundary Conditions - line support on the edge

Load's definition

Self-weight

The dead load of the panel is automatically calculated by the FEM, once the materials with their specific weight are set. Falcon Glass *Specific Weight = 25 kN/m³* and PETG *Specific Weight = 12,7 kN/m³.*

Since the designed panel is a façade panel, the self-weight will act in the vertical direction, as an in-plane load. The Self-weight can be defined as:

$$q_{s-w} = 25\frac{kN}{m^3} \cdot 0,001m + 12,7\frac{kN}{m^3} \cdot 0,011m = 0,165\frac{kN}{m^2} = 0,165 \times 10^{-3}\frac{N}{mm^2}$$

Wind Load

The glass façade is designed to be built in Rotterdam, the Netherlands. The wind has been calculated according to the Dutch normative, NEN 1991-1-4. The calculations of wind loads can be found in Appendix E, the governing value is 0,582 ×10⁻³ N/mm² for wind pressure.

$$q_w = 0,582\frac{kN}{m^2} = 0,582 \times 10^{-3}\frac{N}{mm^2}$$

Load combinations

According to the codes, a glass façade must be safe in case a person will fall through the glass. The hypothesis of an internal balustrade is taken in order to assure the safety of the glass façade. By using the above explained loads, three different loading combinations have been checked. A safety factor of γ_p = 1,2 has been used for the permanent loads and γ_q = 1,5 for variable loads.

$LC1 = 1,5 \cdot q_w + 1,2 \cdot q_{s-w}$

$LC2 = 1,0 \cdot q_w + 1,0 \cdot q_{s-w}$

$LC3 = 1,35 \cdot q_{s-w}$

9.3   Structural Design

The same procedure used in the whole thesis is performed for the final design. First of all, a horizontal displacement of 50 mm is imposed at the edge of the panel to cause the desired cold bending shape. This procedure induces in the glass a maximum tensile stress in the top layer of the pane of σ = 20,91MPa and a compression stress in the bottom of the pane of σ = – 4,71MPa. The radius of curvature of the panel is 1,2 m, since this curvature is bigger than the one investigated in the research, the stress introduced is in the glass pane is lower than the previous ones. The stresses induced in the glass due to cold bending are shown in the figure below.
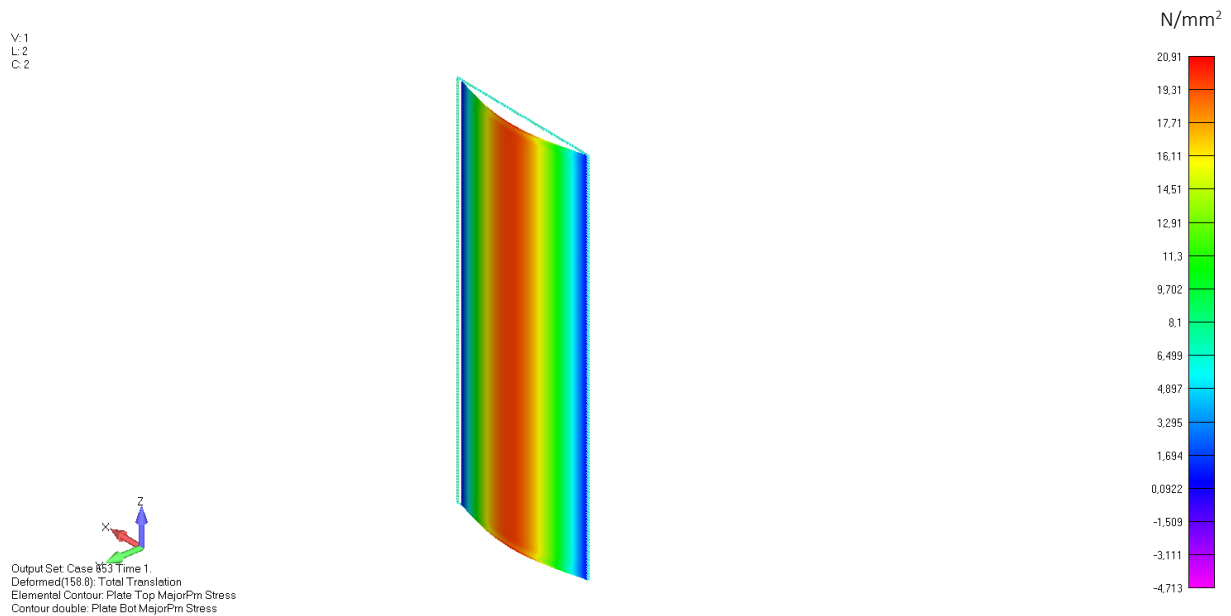
Figure 9.4 Principal Stresses in the glass due to cold bending

The most critical loading condition is here shown and it is given by LC1, where the maximum stress in the glass after loading is – 4,71MPa + 52,25 MPa = 47,54 MPa. Therefore, the unity check for the strength of the glass is fulfilled.
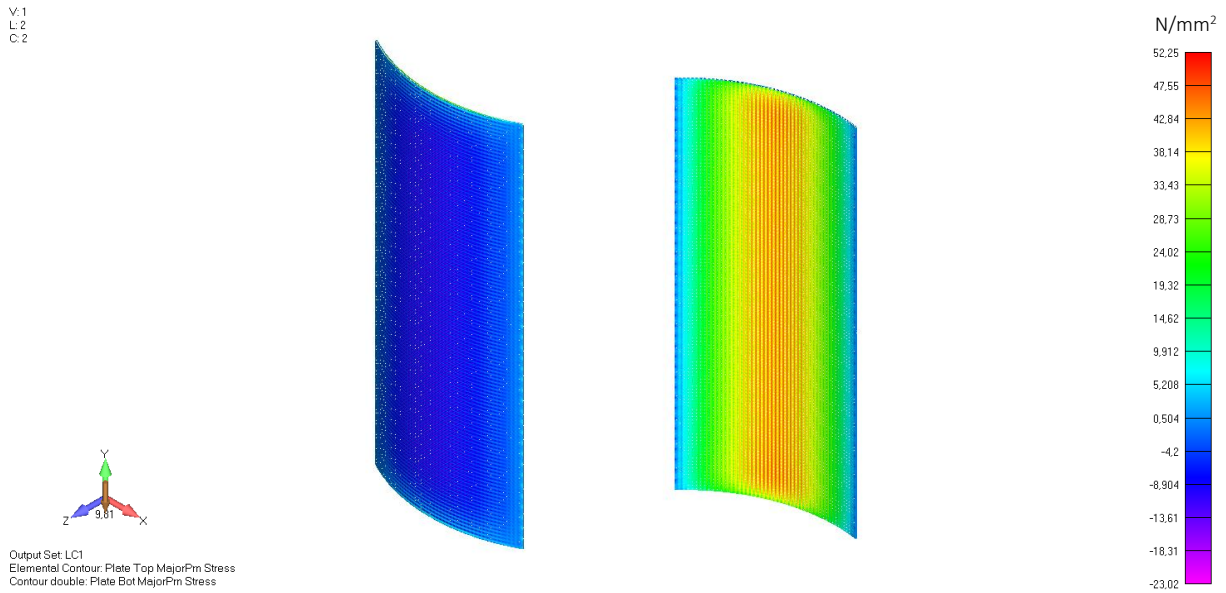
Figure 9.5 LC1 Plate Top Major Principal Stresses (Left) Plate Bottom Mayor Principal Stresses (right)

Wind suction is governing in the corner of the building. The value of wind suction has been calculated as – 0,874 ×10^{-3} N/mm^2. The stresses in case of wind suction have been checked. The maximum stress in the glass is +20,91 MPa + 63,42 MPa = 84,33 MPa.
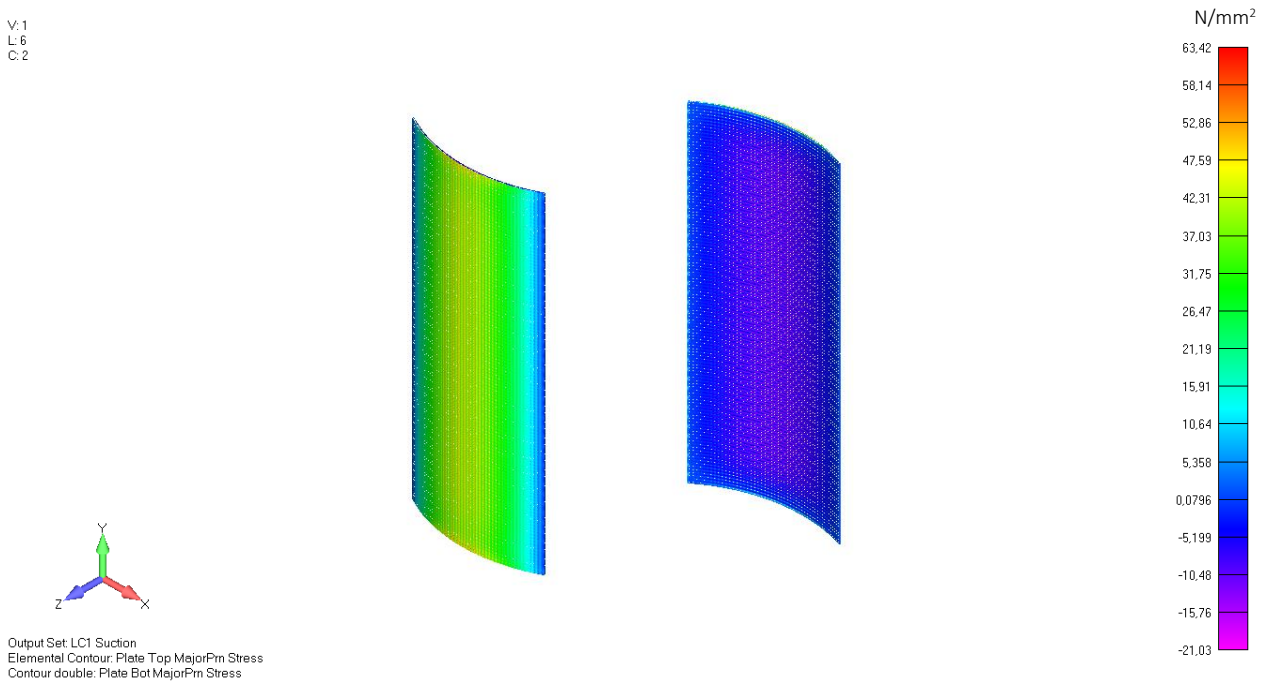
Figure 9.6 Wind Suction - Plate Top Major Principal Stresses (Left) Plate Bottom Mayor Principal Stresses (right)

The maximum displacement has to be check according to LC2. The deflection at the center of the panel results to be 10,5 mm (Figure 9.7). The panel is simply supported on the long edge. According to the normative, the deflection is limited to *49,7 mm* in the center:

$$L_{diag} = \sqrt{1200^2 + 3000^2} = 3231 \; mm$$

$$w_{lim,center} = \frac{L_{diag}}{65} = \frac{3231}{65} = 49,7 \; mm$$

Moreover, the maximum deflection allowed at the edge of the panel is L/100, where L is the unsupported edge.

$$w_{lim,edge} = \frac{L}{100} = \frac{1200 \; mm}{100} = 12 \; mm$$
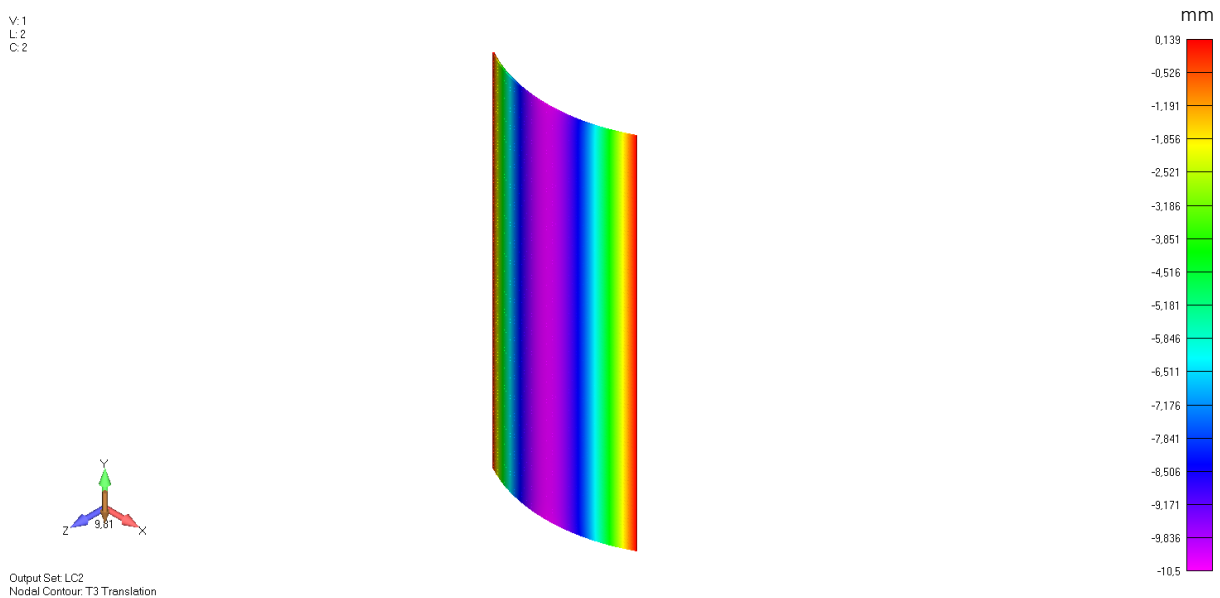
Figure 9.7 Maximum Displacement = 10,5 mm

The deflection of the sandwich panel results to be 10,5 mm. Therefore, the deflection limit has been met. The last thing that has to be checked is the strength in the connection. In this analysis Delo Photobond AD494 is proposed, therefore the shear strength of the glue is 9MPa. The maximum shear stress has been calculated according to the procedure shown at the end of Paragraph 5.5.2. In Appendix E the procedure is replied for the final design and the maximum shear stress value has been calculated to be 6,44 MPa. The value is lower than the shear resistance of the glue, which is 9 MPa. For this reason the Unity Check is fulfilled.

One of the most impressive characteristics of the panel is the total weight. The panel has dimensions of 3 m x 1,2 m and it is realized by two thin glass faces of 0,5 mm and a polymeric core of 11 mm. The total weight of the panel is 17,4 kg. It means that the panel has a weight of 4,8 kg/m², while a glass panel, normally used for façade nowadays, weights approximately 30 kg/m². The proposed hybrid panel can bring the singular façade panel to have a weight reduction of more than 80%. Moreover, 17,4 kg is a

weight that just one person on the construction site could hold! The lightness of the panel can simplify the assemblage of the façade enormously.

9.4   Connections

Another challenge presented by thin glass is the connection method within adjacent panels. Current existing bolted applications have not been investigated yet with the use of thin glass. The holes would develop high stresses in the thin glass with the risk of cracks. The convenience of the proposed hybrid sandwich panel is that the connections of adjacent panels can be realized by taking advantage from the 3D printed core. Since the core will be realized by 3D printing, the joint between two panels can be created with the printed PETG. Several possibilities can be realized, but this is not the primary aim of this research. One proposal is shown in the following figure.
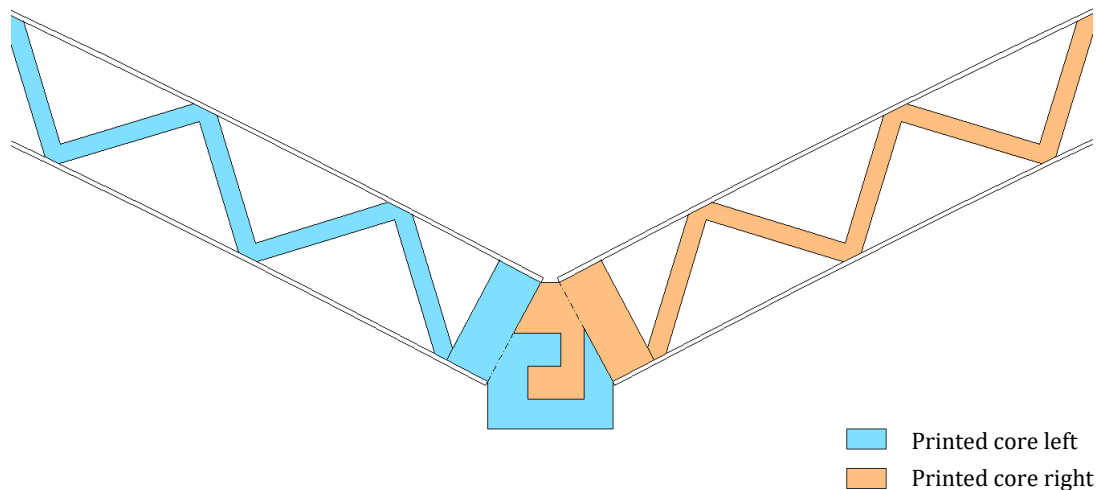
Figure 9.8 Joint between two adjacent panels

To connect the panels to the supporting structure, a steel structure is used. As it has been designed in the FE Models, the panel will be supported on the long edge. The supporting structure is realized by steel circular hollow section profiles. The panel is connected to the support structure by using an aluminium U profile and with bolt connections between the profile and the plastic core of the panel. Then, the U profile is welded to the support structure as it is shown in Figure 9.9.

Aluminium U Profile
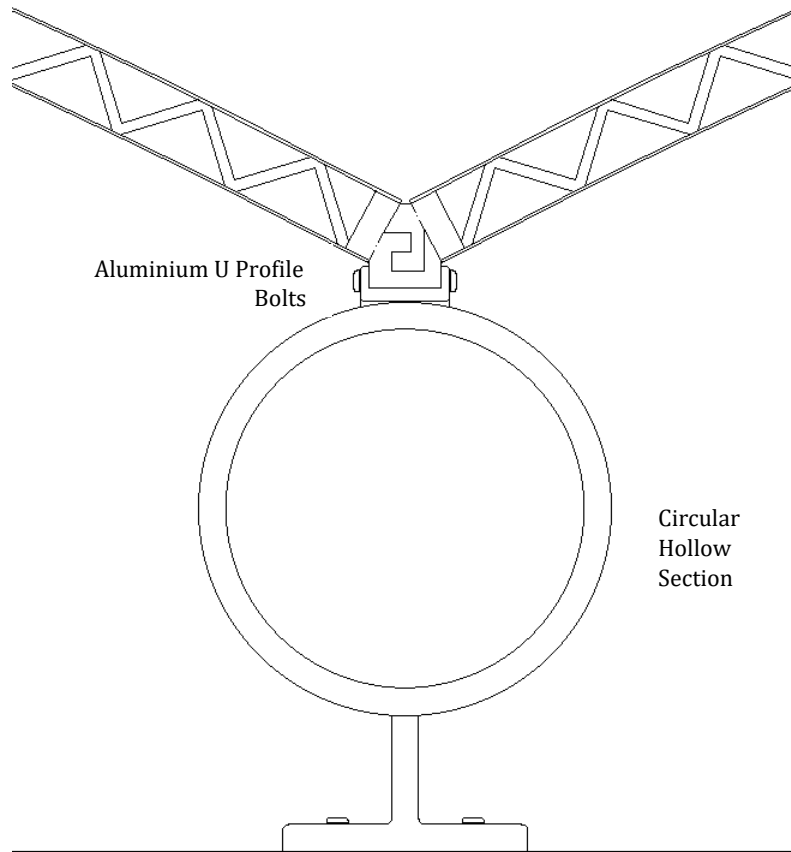Bolts

Circular
Hollow
Section

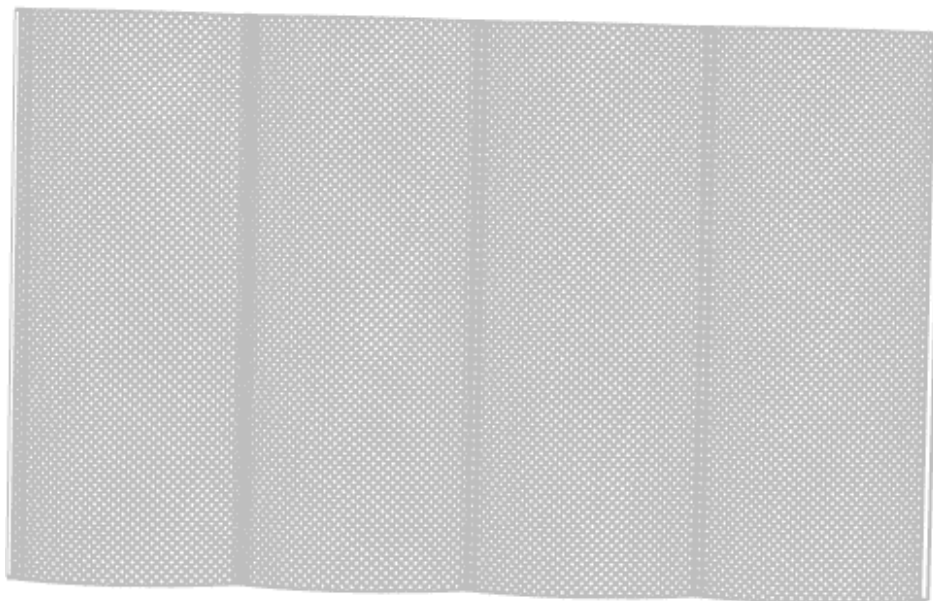Figure 9.9 Connection with the supporting structure

Figure 9.10 Visualization of the façade panels

9.5   Final results

To understand how much the stiffness of the panel is improved by the technique proposed, the following comparison has been taken. The deflection of the sandwich panel studied in this research has been compared with two curved glass panes laminated.
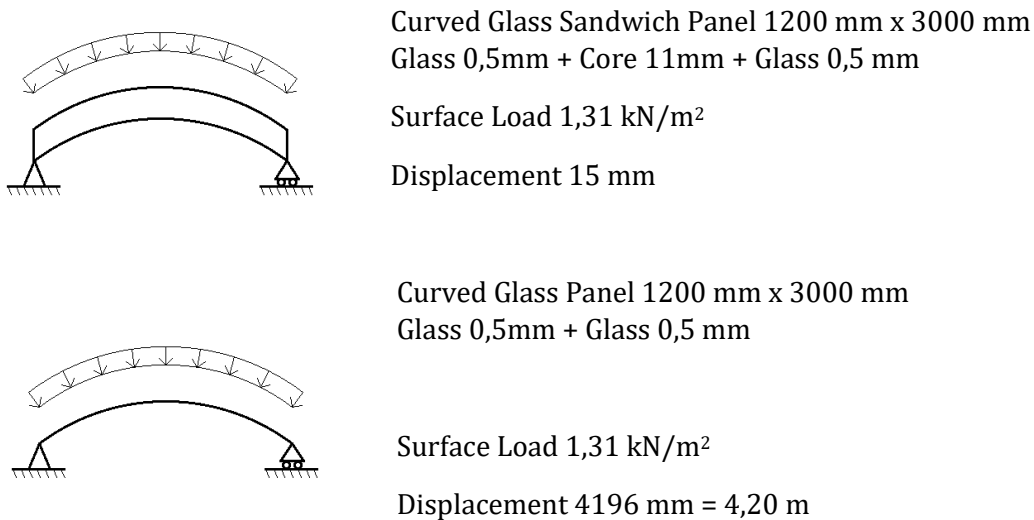
Curved Glass Sandwich Panel 1200 mm x 3000 mm
Glass 0,5mm + Core 11mm + Glass 0,5 mm

Surface Load 1,31 kN/m²

Displacement 15 mm

Curved Glass Panel 1200 mm x 3000 mm
Glass 0,5mm + Glass 0,5 mm

Surface Load 1,31 kN/m²

Displacement 4196 mm = 4,20 m

Figure 9.11 Stiffness of a curved sandwich panel compared to a two layers laminated panel

The studied sandwich panel revealed to be 280 times stiffer than a panel made by two layered glass plies. It has to be remembered that particular attention has to be given to the connection between the core and the glass face. If the connection is not strong enough, the two materials will be detached, and the panel will not act anymore as a sandwich panel. This could bring to really dangerous situations, since the effective stiffness of the panel will be 280 times less compared to the one designed.

CONCLUSIONS and RECOMMENDATIONS

10. Conclusions

The presented Master thesis report concerns the study of an innovative hybrid façade panel, realized by thin glass faces and a 3D printed polymeric core. The objective of this graduation project is to prove that the stiffness of thin glass can be increased in order to allow this new material to be used in the building industry. The proposed innovative façade panel is a thin glass cold bent sandwich panel.

Firstly, the conclusions are presented by following the structure of the report. Then, the main research question is answered. Finally, the hypothesis presented in the introduction chapter is commented and verified.

General Conclusions

In Chapter 2, the characteristics of aluminosilicate glass have been compared to the ones of soda lime glass. It has been explained that the density and the strength of the two materials have analogous values. However, the strength of aluminosilicate glass can be increased even more by the chemically strengthened procedure. In fact, alkali aluminosilicate glasses are more prone to chemically strengthened treatments compared to soda lime glasses, since high alkali content facilitates the glass for ion exchange and this results in the creation of a thicker compression layer.

Moreover, an investigation of the cold bending of thin glass is carried out. Theoretically, the minimum bending radius R_{min} (single curvature) depends on the thickness of the glass and the strength of the glass. As it has been demonstrated in paragraph 2.3.3, the minimum bending radius can be determinate as:

$$R_{min} = \frac{E\,t}{2\,\sigma}$$

Therefore, the minimum bending radius that can be obtained with thin glass, 0,55mm Leoflex Glass is 78,3mm. The cold bending procedure induces permanent tensile stresses in the glass; for this reason, usually a stronger glass is used (thermally or chemically strengthened). When single curvature is considered, the thickness of the glass is decisive for the tensile bending stress and the possible bending radii.

In Chapter 3, sandwich panel structures are presented. According to Hexcel Composites (2000), by using a sandwich panel of double the height of a solid panel, the stiffness of the sandwich panel is increased by a factor of 7 (Table 3.1). In the final design (see Paragraph 9.5) it is shown that by using a sandwich panel of 12 times the height of a solid panel, the stiffness is 280 times higher.

Furthermore, based on the literature review, two different patterns are selected: a space frame core pattern realized by pyramidal unit elements and a closed square cells pattern. The first pattern has been chosen because it is a well-known topology, which has a high strength and stiffness related to a low density. While the square cells pattern has been selected due to its higher shear stiffness, even if its relative density is larger.

A comparison of the main characteristics of each AM technique can be found in Chapter 4 (Table 4.1). SLS has been evaluated to be the most advisable technique to be used in the analysed study. With the use of SLS support material is not needed and the accuracy of the final product is relatively high. However, due to economic reasons, FDM has been used to realize in practice the core of the sandwich panel.

The cold bending procedure is described in Paragraph 5.3. The circular shape has been selected for the design of the panel because the total stresses are lower compared to the ones introduced in other shapes (catenary, parabolic and sinusoidal). To model the circular shape in the FEM analysis, a defined displacement in each node of the panel is imposed, then a Non Linear Analysis is performed.

During the manufacturing of the panels (Chapter 6), it has been found out that PETG revealed to give problems during production. When the support material in excess had to be removed, instead of separating from the final part, the material broke. For this reason PLA was suggested to be used by the 3D printing expert. Supports material was much easier to be taken off. However, PLA has proved to be not easy to glue. This caused more challenges in the manufacturing phase.

With the information achieved from numerical and experimental results, a final design is proposed. The final design shows a façade panel of dimensions 1200 mm x 3000 mm, with a total thickness of 12 mm, a weight of 17,4 kg, which exhibits a deflection of only 10,5 mm.

Main Research Question

To what extent can thin glass be stiffened by the realization of a cold bent sandwich panel – made by thin glass faces 0,5mm and a polymeric core – to be used in the building industry as a façade element?

The study reveals that the curved sandwich panel is a feasible façade panel proposal. Feasibility is defined in terms of a structural façade element, which fulfil the limits of safety (ULS) and comfort (SLS). One of the main characteristics for which the proposed panel was designed, was to increase the stiffness of thin glass. As a matter of fact, the curved sandwich panel proposed in the final design results to be 280 times stiffer, compared to a curved two layered thin glass panel.

It has to be underlined that particular attention has to be given to the connection between the core and the glass faces of the sandwich panel. If the connections are not designed correctly, the two materials will detach, and the panel will not behave anymore as a sandwich panel. In this case, the delaminated panel will not be able to withstand the design load.

Furthermore, it was discovered that the proposed sandwich panel could guarantee a weight reduction of more than 80% in comparison to the glass used nowadays in building façades. This characteristic not only facilitates the assemblage of the façade, but also can bring to the usage of a lighter support structure. This can achieve advantages both in terms of cost of the total structure and energy required to assemble the building.

Hypothesis

In the introduction chapter, a hypothesis was presented: the possibility of keeping the glass in shape by the use of the core of a sandwich structure, rather than with the use of a frame. The curved sandwich panel is demonstrated to be kept in the cold bent shape by the realization of a physical model of dimensions of 250mm x 150mm. The realization of a bigger panel, 500mm x 500mm, was more challenging. However, the production of a cold bent sandwich panel has been proved to be a feasible proposal even on a bigger scale, if the proper material is used, and the connections between the glass and the core are manufactured correctly.

The main advantage of the investigated structure lies in the forces transferred at the supports. A freestanding arch will induce in the supporting elements just compression forces and not shear forces.

In practical applications, this feature is translated into the possibility of using a more extensive number of materials as a supporting structure. The column elements could be realized with a broader range of material or they could be more slender than the ones nowadays designed. Moreover, the panel will be more easily applied in place, during the assemblage of the building, since the desired shape is already formed.

11. Recommendations

Since an innovative structural element has been investigated in this research, there are several possible future developments that can be addressed.

Thin Glass

First of all, since thin glass needs to be chemically strengthened, it is important to investigate the percentage of emissions of CO_2 due to the chemically strengthened process. It has been said that the use of thin glass could highly decrease the carbon footprint of the building industry, since less raw material would be used. However, in order to draw valid conclusions about the CO_2 reduction with the use of thin glass in the building industry, the contribution of the chemically strengthened process has to be added, and therefore, it is needed to be researched.

After the panels were manufactured, it has been faced the failure of one of the panels. It is arduous to predict exactly why the glass broke: probably a scratch was present in the edge surface. However, from this experience it has been learned that the edges of the glass must be carefully treated, because they are the weak spots of the glass ply. In the future, in order to avoid an unforeseen failure, it is suggested that the plastic core should be 1-2 millimetre larger than the glass ply, in order not to have glass edges which hang out.

It has to be underlined that the contribution due to the cold bending in the total stiffness of the panel has not been investigated. The boundary conditions used in this research were simply supported edges. It is recommended for further researches to investigate a curved sandwich panel supported by pinned connections. In this manner, an arch behaviour will be taken into consideration and it will stiffen the sandwich panel even more. The increase in stiffness due to the combination of the sandwich behaviour and the arch behaviour should be investigated.

Additive Manufacturing

If a curved shape core is designed, Selective Laser Sintering (SLS) was the preferred technique instead of Fused Deposition Modelling (FDM). When the material support, needed in FDM, is removed, it left parts with a low-quality surface. This fact was not only an aesthetic problem but also a gluing issue. With SLS, the support material is not needed and the quality of the surface is the same in all the printed parts. If in the future, SLS will become more affordable in the market, SLS technique is highly recommended to be investigated in further similar researches.

Another possibility to realize the 3D printed curved core of the sandwich structure is to print the core as a flat element with FDM, and then to curve it by warming it up. In order to curve the panel, a mould with the exact shape has to be realized. Then, the flat printed panel has to be heated up until 50-60°C and the panel will assume the shape of the mould. This approach will avoid the challenge of printing a curved shape with FDM technique. Moreover, the support material is not needed anymore.

Composite Behaviour

Further researches about the behaviour of the composite panel within thin glass and the adhesive connection with the core in case of high-temperature conditions should be performed. If the proposed hybrid panel is wanted to be used as a building façade, the panel must be proven to be safe according to the European and National building codes.

The utilized glue turned out not to have enough resistance to keep the bigger scaled panel curved in shape. By contacting Delo manufacturer, it has been suggested to use another type of glue, called Delo Photobond AD494, which has a better behaviour in gluing glass with plastic materials. It is suggested to investigate the connections within the core and the glass. Delo Photobond AD494 is recommended as a glue. It is essential to check if this glue can handle higher loading conditions and especially if it fails in a cohesive manner instead of adhesive failure, as it has happened in the presented research.

In order to avoid the glue to detach from the glass, a bigger area of contact within the core and the glass is suggested. If a larger area of contact is present, more glue can be applied and the connection is less prone to fail. A first suggestion of how to increase the area of contact without increasing excessively the density of the core is shown in the figure below.
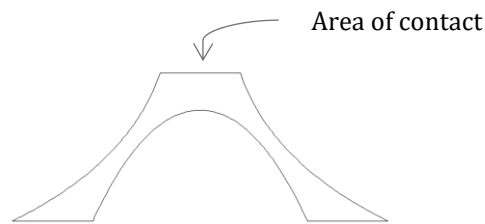
Figure 11.1 Core element - bigger area of contact

Core Optimization

Concerning the optimization of the sandwich panel, Topology Optimization is highly recommended to be further researched. This technique can offer a freeform pattern shape, designed specifically for the studied sandwich panel.

Finite Element Models

Since the weakest point of the sandwich panel turned out to be the connections between the core and the glass, it would be interesting to include the glue in the FEM Analysis. In this manner, a closer look into the behaviour of the glue could be gained. In order to model the glue in the FEM, it is suggested to move the core downwards of 1 or 2 mm, as it is shown in the figure below. Then, connect the core and the glass with a line element, which is associated with a truss element, therefore it can resist normal and shear forces.
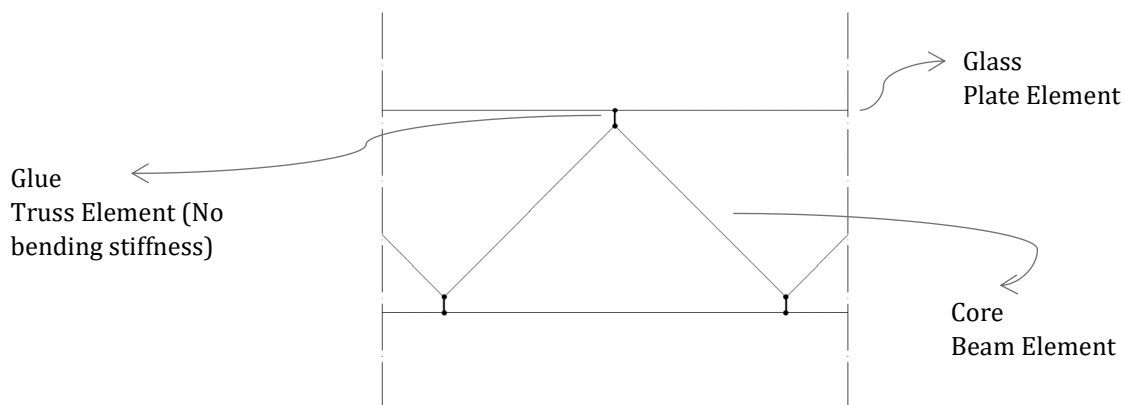
Figure 11.2 FE Model with glue connections

BIBLIOGRAPHY

Bibliography

Adriaenssens, S., Block, P., Veenendaal, D., & Williams, C. (2014). *Shell Structures for Architecture - Form Finding and Optimization.* Routledge.

Akilo, M. A. (2018). *Design and Analysis of a Composite Panel with Ultra-Thin Glass Faces and a 3D-Printed Polymeric Core.* Master Thesis, University of Bologna .

Albus, J., & Robanus, S. (2014). Glas in der Architektur: Neue Entwicklungen (1).

Allen, H. G. (1969). *Analysis and Design of Structural Sandwich Structures.* Pergamon Press.

ANSYS. (2018). *GENESIS Topology Optimization for ANSYS Mechanical (GTAM).*

Bendsoe, M. P., & Sigmund, O. (2003). *Topology Optimization: Theory, Methods and Applications.* Berlin: Springer.

Bijster, J., Noteboom, C., & Eekhout, M. (2016). Glass Entrance Van Gogh Museum Amsterdam. *Glass Structures & Engineering - Springer.*

Christensen, P. W., & Klarbring, A. (2009). *An Introduction to Structural Optimization* (Vol. Solid Mechanics and its Applications). Springer.

Coenders, J. (2008). *Structural Design, Special Structures reader.* Lecture notes CIE5251 - TU Delft University .

CustomPartNet. (2008).

EconCore. (n.d.). *http://www.econcore.com/en/products-applications/polycarbonate-panels.*

Evans, A. G. (2001). *Lightweight Materials and Structures.* Mrs Bulletin.

Fildhuth, T., & Knippers, J. (2011). *Double Curved Glass Shells from Cold Bent Glass Laminates.* Glass Performance Days 2011.

Galuppi, L., & Royer-Carfagni, G. (2015). Optimal cold bending of laminated glass. *International Journal of Solids and Structures.*

Gere, J. M., & Timoshenko , S. P. (1993). *Mechanics of Materials .* Chapman & Hall, Third SI Edition.

Gibson, I., Rosen, D., & Stucker, B. (2009). *Additive Manufacturing Technologies - 3D Printing, Rapid Prototyping, and Direct Digital Manufacturing .* Springer Publishing Company.

Gomez, S. et al. (2011). A look at the chemical strengthened process: alkali aluminosilicate glasses vs soda lime glass. 71st Glass Problem Conference.

Group, AGC. (2016). *FalconTM for chemical strengthening.*

Hexcel Composites. (2000). *HexWebTM Honeycomb Sandwich Design Technology.*

http://www.neg.co.jp/en/product/dp/dinorex. (n.d.).

Huang, X., & Xie, M. (2010). *Evolutionary Topology Optimization of Continuum Structures: Methods and Applications .* Wiley.

Hundevad, J. (2014). Super lightweight glass structures – a study . *GlassCon Global ,* 324-337 .

John, J. (n.d.). *https://www.pinterest.it/pin/496451558899447997/?lp=true*.

Lambert, H., & O'Callaghan, J. (2013). Ultra-thin High Strength Glass Research and Potential Applications. *Glass Performance Days 2013*.

Lazzaroni, L. (2018). *Structural Design and Experimental Validation of an Innovative Hybrid Lightweight Sandwich Glass Panel.* Master Thesis, University of Pisa.

Louter, C. (2017). *Material Characteristics, Production, Processing & Products.* Lecture notes, TU Delft University.

Louter, C. (2017). *Mechanical Connections - Adhesive Connections.* Lecture notes, TU Delft University.

Louter, C., Akilo, M., Miri, B., Neeskens, T., Ribeiro Silveira, R., Topcu, O., . . . O'Callaghan, J. (2018). Adaptive and Composite Thin Glass Concepts for Architectural Applications. *Heron*.

Materials., C. I. (September 2007). *Chemical Tempering Procedures Corning® Gorilla® Glass. .*

Miri, B. (2018). *Flexible Transparency With Smart Materials: A study on adaptive thin glass facade developed with Shape Memory Alloy.* Master Thesis, TU Delft University.

Neeskens, T. (2018). *Thin Glass Composites .* Master Thesis, TU Delft University.

Neugebauer, J., & Waller-Novak, M. (2018). *Let Thin Glass in the Facade Move - Thin Glass new possibilities for glass in the facade.*

Olason, A., & Tidman, D. (2010). *Methodology for Topology and Shape Optimization in the Design Process.* Master Thesis, Chalmers University of Technology.

Ottens, R. (2018). *High Strength Thin Glass as Stiff Structural Fabric.* Master Thesis, TU Delft University.

Petras, A. (1998). *Design of Sandwich Structures.* Doctor of Philosophy Dissertation, Cambridge University Engineering Department .

Prayudhi, B. (2016). *3F3D: Form Follows Foce with 3D printing.* Master Thesis, TU Delft University.

Preisinger, C. (2016). *Karamba User Manual for Version 1.2.2.*

Schipper, R. (2015). *Glass - The Material.* Lecture Notes CIE4215 - Facade Design Plus, TU Delft University.

Schittich, Staib, Balkow, Schuler, & Sobek. (2007). Glass as a building material. In *Glass Construction Manual.*

Schlösser, N. I. (2018). *Thin Glass as Cold Bent Laminated Panels in Architectural Applications.* Master Thesis, TU Delft University.

Silveira, R. R. (2016). *Flexible Transparency - A study on thin glass adaptive facade panels.* Master Thesis, TU Delft University.

Simoen, C. (2016). *Thin Glass - a study on the feasibility of thin chemical strengthened Aluminosilicate glass as a new material in the building industry.* TU Delft, Building Technology. Master Thesis, TU Delft University.

Strauss, H. (2013). *AM Envelope - The potential of Additive Manufacturing for facade construction.* Architecture and the Built Enviromnment.

Tangram Technology. (n.d.). Retrieved from http://www.tangram.co.uk.

Topcu, Ö. (2017). *Kinetic thin glass facade* . Master Thesis, TU Delft University.

Vakar, L., & Gaal, M. (2004). Cold Bendable, Laminated Glass - New Possibilities in Design. *Structural Engineerign International*.

van der Weijde, I. (2016). *Ultra Lightweight, Insulating Thin Glass Facade Panel* . Master Thesis, TU Delft University.

van Driel, T. C. (2018). *Onderzoek naar de materiaaleigenschappen van 3D-geprint PETG.* Bachelor Thesis, TU Delft University.

van Herwijnen, E., Staaks, D., & Eekhout, M. (2004). Cold Bent Glass Sheets in Facade Structures. *Structural Engineering International*.

Veer, F. (2007). *The strength of glass, a nontransparent value.* Heron.

Vitalis, D. (2017). *Glass Sandwich Panel.* Master Thesis, TU Delft.

Wadley Research Group. (2014). *Ultralight Cellular Materials.* University of Virginia.

Wadley, H. N. (2006). *Multifunctional periodic cellular metals.* The Royal Society.

Weber, F. (2009). Curved glass structures. *Glass Performance Days 2009*.

Wurm, J. (2007). *Glass Structures - Design and Construction of Self-Supporting Skins* . Birkhäuser.

Yang, L., Hsu, K., Baughman, B., Godfrey, D., & Medina, F. (2017). *Additive Manufacturing: the Technology.* Springer.

Zha, C. (2018). *Thin glass window embedded with soft pneumatic actuator.* Master Thesis, TU Delft University.

APPENDICES

Appendix A – Material Data Sheet

Thin Glass

AGC Falcon Glass Properties

Performance

Chemical strengthening properties	Compressive stress (@ 20µm DoL)	> 800 MPa
	Depth of Layer (in 8h)	> 40 µm
	Reinforcement (for 15µm defect)	> 500 MPa
	Warpage (in 0.7mm – 420°C/4h)	< 0.05%
Mechanical properties	Density	~ 2.48 g/cm³
	Young's Modulus*	~70 GPa
	Poisson's ratio*	~ 0.21
	Shear Modulus*	~ 30 GPa
	Knoop hardness HK$_{0.1,20}$	450 (before chemical tempering) – 546 (after chemical tempering)
Thermal properties	Softening point	~ 665 °C
	Tg	~ 575 °C
	Coefficient of thermal expansion	~ 9.10^{-6} (25-300°C)
	Thermal conductivity*	~ 1.19 W/(m.K)

* Computed values

Processing options

Safety	Toughening (chemical)
	Safe foil application
Cutting	Straight, circular or free shape
Shaping and edge finishing	Edge grinding, drilling, laser finish
	Bending (thermo-forming and cold-bending)
Special treatments	Anti-warping
	Silkscreen printing
	Acid etching (single or double)
	Anti-reflective coating
	Wet coating application (anti-fingerprint/hydrophobic coating)
	UV adhesive bonding

Availability

Thickness	Size
0.5 mm	Up to 1.245 x 3.21 m
0.7 mm	Up to 1.35 x 3.21 m
1.1 mm	Up to 1.48 x 3.21 m
2.1 mm	Up to 1.60 x 3.21 m

Other thicknesses and dimensions are available upon request.
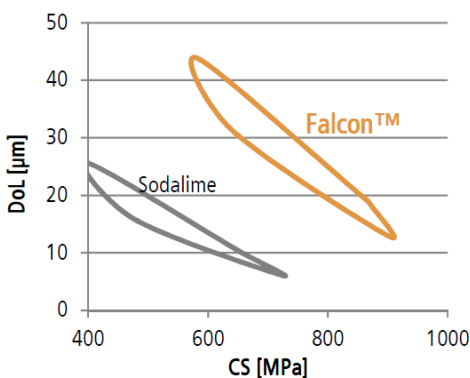
Mechanical properties

Density (g/cm³)	~2.48
Young Modulus (GPa)*	~73
Poisson's Ratio*	~0.22
Shear Modulus (GPa)*	~30

Chemical strengthening properties

Compressive stress	capable of >800MPa	(@ 20µm DoL)
Depth of Layer	capable of >40µm	(in 8h)
Reinforcement	capable of >600MPa	(for 15µm native defect)
Warpage	capable of <0.05%	(in 0.7mm – 420°C/4h)

* Computed values

Figure A. 1 AGC Falcon Glass Properties

AGC Leoflex Glass Properties

	Leoflex (0.85mm)	Thermally tempered (3.2mm)
MECHANICAL CHARACTERISTICS		
Strength / Marginal stress　短期許容応力 (MPa)	260	80
Young modulus　ヤング率 (GPa)	74	70
Poisson ratio　ポアッソン比	0.23	0.2
Density　密度 (g/cm³)	2.48	2.5
Vickers Hardness　ビッカース硬度	673	527
OPTICAL CHARACTERISTICS		
Energy Transmission　日射透過率 (%)	91.6	91.1
THERMAL CHARACTERISTICS		
Expansion coefficient　線膨脹係数 (10^{-6} 1/K)	9.8	9
Strain point　歪点 (℃)	556	500

** Values are not guaranteed.

(Thermal tempering : Conventional technique for PV module glass)

	Thermally tempered	Leoflex (Chemically tempered)	Leoflex features
Minimum thickness limit	3.2 mmt	0.55mmt	Light weight
Mechanical strength (Compressive Marginal stress)	80 MPa	260 MPa	Resistance to bending
Ion concentration at glass surface	Na^+ rich (Na_2O >10 wt.%)	less Na^+ (Na_2O < 3 wt.%) K^+ rich	Chemically stable

** Values are not guaranteed.

\<Image of thermally tempered glass\>

Heating up   Rapid cooling down
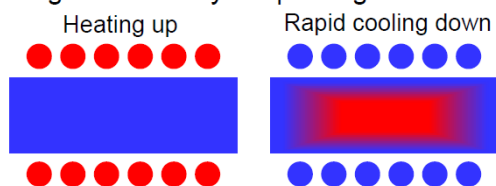
Rapid cooling glass after heating up beyond its softening point creates compressive stress at glass surface. There is no ion exchange at glass surface.

Figure A. 2 AGC Leoflex Glass Properties

Glue

Delo Photobond 4494 – Technical Properties

Technical data

Color cured in a layer thickness of approx. 0.1 mm	colorless clear
Density [g/cm³] at room temperature (approx. 23 ℃)	1.0
Viscosity [mPas] at 23 ℃, Brookfield spindle/rpm 4/5	20000
Minimal curing time [s] DELO Standard 23, UVA intensity: 60 mW/cm², DELOLUXcontrol	7
Minimal curing time [s] DELO Standard 23, LED 400nm, intensity: 200 mW/cm², DELOLUXcontrol	3
Compression shear strength glass/glass [MPa] DELO Standard 5 UVA intensity: 55 - 60 mW/cm², DELOLUXcontrol, irradiation time: 60 s	28
Compression shear strength glass/Al [MPa] DELO Standard 5 UVA intensity: 55 - 60 mW/cm², DELOLUXcontrol, irradiation time: 60 s	25
Compression shear strength glass/PC [MPa] DELO Standard 5 UVA intensity: 55 - 60 mW/cm², DELOLUXcontrol, irradiation time: 60 s	15
Compression shear strength glass/PMMA [MPa] DELO Standard 5 UVA intensity: 55 - 60 mW/cm², DELOLUXcontrol, irradiation time: 60 s	4
Compression shear strength PC/Al [MPa] DELO Standard 5 UVA intensity: 55 - 60 mW/cm², DELOLUXcontrol, irradiation time: 60 s	5
Compression shear strength PC/PC [MPa] DELO Standard 5 UVA intensity: 55 - 60 mW/cm², DELOLUXcontrol, irradiation time: 60 s	18
Compression shear strength PMMA/PMMA [MPa] DELO Standard 5 UVA intensity: 55 - 60 mW/cm², DELOLUXcontrol, irradiation time: 60 s	10
Tensile strength [MPa] according to DIN EN ISO 527	20
Shore hardness D according to DIN EN ISO 868	62
Decomposition temperature [℃] DELO Standard 36	180
Glass transition temperature [℃] rheometer	100
Coefficient of linear expansion [ppm/K] in a temperature range of +25 to +140 ℃	211
Shrinkage [vol. %] DELO Standard 13	9
Water absorption [weight %] according to DIN EN ISO 62, 24 h at room temperature (approx. 23 ℃)	1.3

Figure A. 3 Delo Photobond 4494 – Properties

Delo Photobond AD494 – Technical Properties

Technical data

Color cured in a layer thickness of approx. 0.1 mm	colorless clear
Density [g/cm³] at room temperature (approx. 23 ℃)	1.1
Viscosity [mPas] at 23 ℃, Brookfield rpm 7/5	50000
Minimal curing time [s] DELO Standard 23, UVA intensity: 60 mW/cm², DELOLUXcontrol	14
Minimal curing time [s] DELO Standard 23, LED intensity: 200 mW/cm², DELOLUXcontrol	9
Surface	tacky
Compression shear strength glass/glass [MPa] DELO Standard 5 UVA intensity: 55 - 60 mW/cm², DELOLUXcontrol, irradiation time: 60 s	13
Compression shear strength glass/Al [MPa] DELO Standard 5 UVA intensity: 55 - 60 mW/cm², DELOLUXcontrol, irradiation time: 60 s	12
Compression shear strength glass/VA [MPa] DELO Standard 5 UVA intensity: 55 - 60 mW/cm², DELOLUXcontrol, irradiation time: 60 s	13
Compression shear strength glass/PC [MPa] DELO Standard 5 UVA intensity: 55 - 60 mW/cm², DELOLUXcontrol, irradiation time: 60 s	13
Compression shear strength glass/PMMA [MPa] DELO Standard 5 UVA intensity: 55 - 60 mW/cm², DELOLUXcontrol, irradiation time: 60 s	9
Compression shear strength PC/ABS [MPa] DELO Standard 5 UVA intensity: 55 - 60 mW/cm², DELOLUXcontrol, irradiation time: 60 s	12
Compression shear strength PC/Al [MPa] DELO Standard 5 UVA intensity: 55 - 60 mW/cm², DELOLUXcontrol, irradiation time: 60 s	10

Figure A. 4 Delo Photobond AD494 – Properties

Appendix B – Structural Optimization

Structural Optimization is the subject of making an assemblage of materials sustain loads in the best way. However, to make any sense out of that objective the meaning of the term "best" needs to be specified (Christensen & Klarbring, 2009). The best structure could be the lightest one, another idea of "best" could be to make the structure as stiff as possible or make it insensitive to buckling. A structural optimization problem is formulated with a combination of those parameters as an objective function that should be maximised or minimised according to defined constrains.

A simple example of Topology Optimization is shown in Figure B. 1. The picture represents the optimization of a chair: the solid material of the chair on the left, is iteratively taken off, based on the load of the person sitting on it.
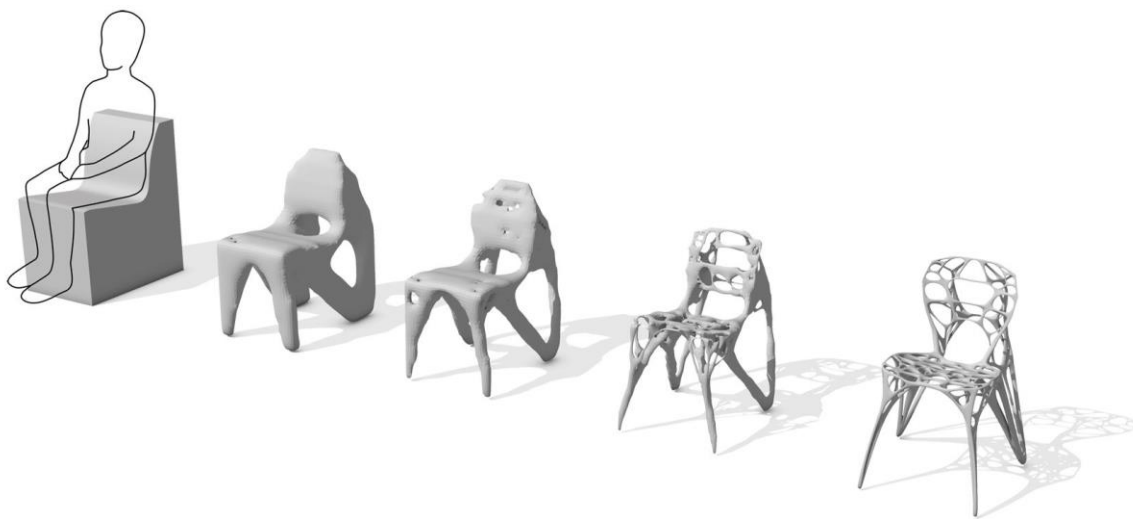
Figure B. 1 Topology Optimization of a chair (John, s.d.)

General Mathematical Form of a Structural Optimization Problem

A Structural Optimization problem has certain functions and variables which are always present (Christensen & Klarbring, 2009).

- *Objective function (f):* A function used to classify designs. Frequently *f* measures weight, displacement, stress, etc.

- *Design variable (x):* A function or vector that describes the design, and which can be changed during optimization. It may represent geometry or choice of material.

- *State variable (y):* For a given structure, i.e. for a given design x, y is a function or vector that represent the response of the structure. For a mechanical structure, response means displacement, stress, strain or force.

A general structural optimization problem can now be written as:

$$(\mathbb{SO}) \begin{cases} minimize \; f(x,y) \; with \; respect \; to \; x \; and \; y \\ subject \; to \begin{cases} behavioral \; constraints \; on \; y \\ design \; constraints \; on \; x \\ equilibrium \; constraints \end{cases} \end{cases}$$

A structural optimization problem can have several objective functions, and be defined a multi criteria optimization problem:

$$minimize \; (f_1(x,y), f_2(x,y), \dots, f_n(x,y))$$

Where n is the number of objective functions, and the constraints are the same as for ($\mathbb{SO}$). This is not a standard optimization problem, since all f_i in general are not minimized for the same *x* and *y.* Instead, the scope is to achieve the so-called *Pareto optimality:* a design is Pareto optimal if there does not exist any other design that satisfies all of the objectives better (Christensen & Klarbring, 2009).

Types of Structural Optimization

- Sizing Optimization

  In this type of optimization, the shape of the structure is known. The purpose is to achieve the optimal design by having as a design variables the size and the cross sectional dimensions.

- Shape Optimization

  As with sizing optimization, the topology (number of holes, beams size, etc.) of the structure is already known. In shape optimization, the distribution of the members is changed, while the boundaries and the connectivity of the structure are maintained the same.

- Topology Optimization

  The purpose of topology optimization, as well as sizing and shape optimization, is to find the optimum distribution of material. Despite the other two methods, the resulting shape or number of holes are not yet defined. The process begins by discretizing the geometry of the design domain, and takes off elements with a low influence in the object.
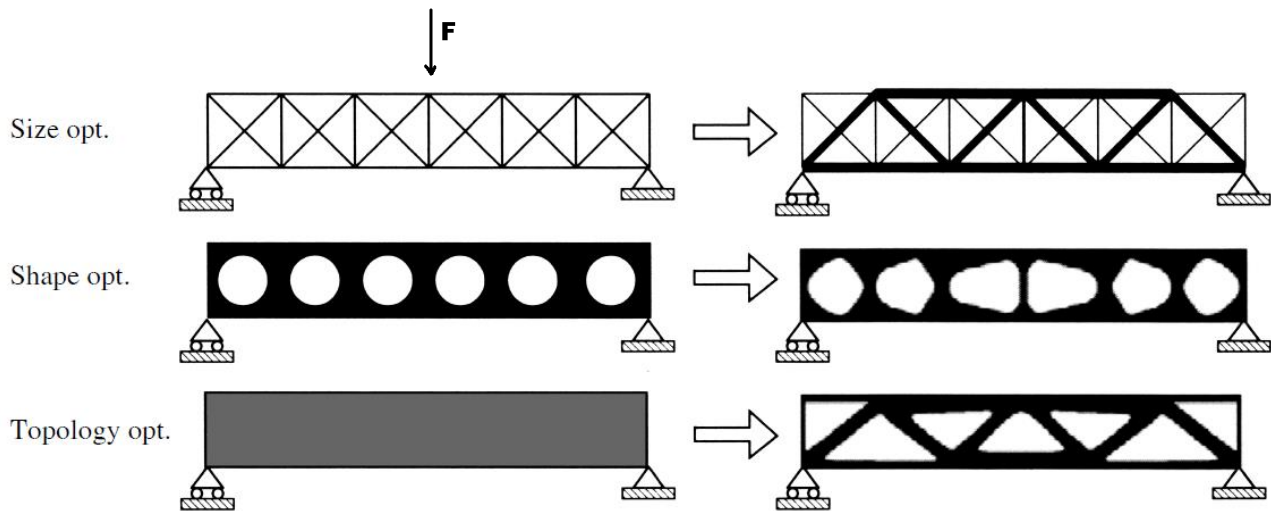
Figure B. 2 Size Optimization (a), Shape Optimization (b), Topology Optimization (c)

Method of Topology Optimization

Topology optimization is the most general form of Structural Optimization (Olason & Tidman, 2010). From a given domain, the purpose is to find the optimum distribution of material and voids. Finite Element Method (FEM) is used to discretized and solve the problem. The result is a so called 0-1 problem, in which the elements either exists or not.

There are several methods to carry out the Topology Optimization process, namely:

Solid Isotropic Microstructure with Penalization (SIMP) method
The SIMP method is based on the assumption that each element contains an isotropic material with variable density.

Evolutionary Structural Optimization (ESO) method
The ESO methods is based on the concept of iteratively remove less efficient material from a structure, by defining "inefficient" the portion of material with low value of stress (or strains).

Bi-directional Evolutionary Structural Optimization (BESO) method
The BESO method allows material to be removed and added simultaneously.

Homogenization method
The Homogenization method uses infinitely discretization of micro scale voids, forming a porous element which creates a linear elastic structure. If a portion of elements is made just of voids, the material is not placed.

Level set method
This method optimizes the structure by modifying the boundaries of the design domain. Material is removed and added in regions of low stress and high stress respectively. The method utilizes evolutionary process which can be characterized by the disappearance of holes which are initially positioned at the wrong places.

Topology Optimizations Softwares

- Millipede
- BESO3D -> Ameba
- Altair OptiStruct
- Solid Thinking Inspire

Limitations

In the last decades, the use of commercial optimization software has increased rapidly and has shown to be applicable to many different types of problems (Olason & Tidman, 2010). The purpose is that the designer and the structural engineer both are involved in the initial stage. Topology optimization is used to generate a good design concept. The limitations of this method have been underlined by Olason and Tidman in their dissertation (Olason & Tidman, 2010).

First of all, it is necessary to have a well-defined problem before performing the optimization. The loads and the boundary conditions need to be specified as precisely as possible. The optimal structure will probably violate requirements that are not specified, because the optimization will try to reduce the structure. Moreover, the result obtained from the topology optimization is far from a finished product. For this reason topology optimization should be seen as a tool in the design process that is useful to generate an efficient design in the early stages (Olason & Tidman, 2010).

Appendix C – Numerical Calculations

Appendix C.1 Cold bending

Finite Element Models for all the cold bending shapes illustrated in Figure 5.2 have been made and they will be illustrated in the following paragraph. Firstly, a comparison in thickness of the glass and edge supports (short edge or long edge) have been made. Later, when the supports and the thickness have been defined, the specific shape that will be investigate in this research is illustrated.

Parabolic Shape

Initially, to investigate the cold bending procedure, the biggest Falcon Glass plate dimensions available were taken into considerations: therefore, 1245 mm x 3210 mm. The first case, taken into account, is a line supported plate under a uniformily distribuited load, which will bring the glass to assume a parabolic shape. The glass panel has been investigated either supported on the long side of the panel and on the short side.

Summary
Plate Dimensions: 1245mm x 3210mm
Thickness: comparison between 1,1mm 0,7mm 0,5mm
Boundary conditions: Two side supported panel: comparison between Long side supported – Short side supported.

Perpendicular surface load q=0,01kN/m^2

Glass plate thickness = 1,1 mm
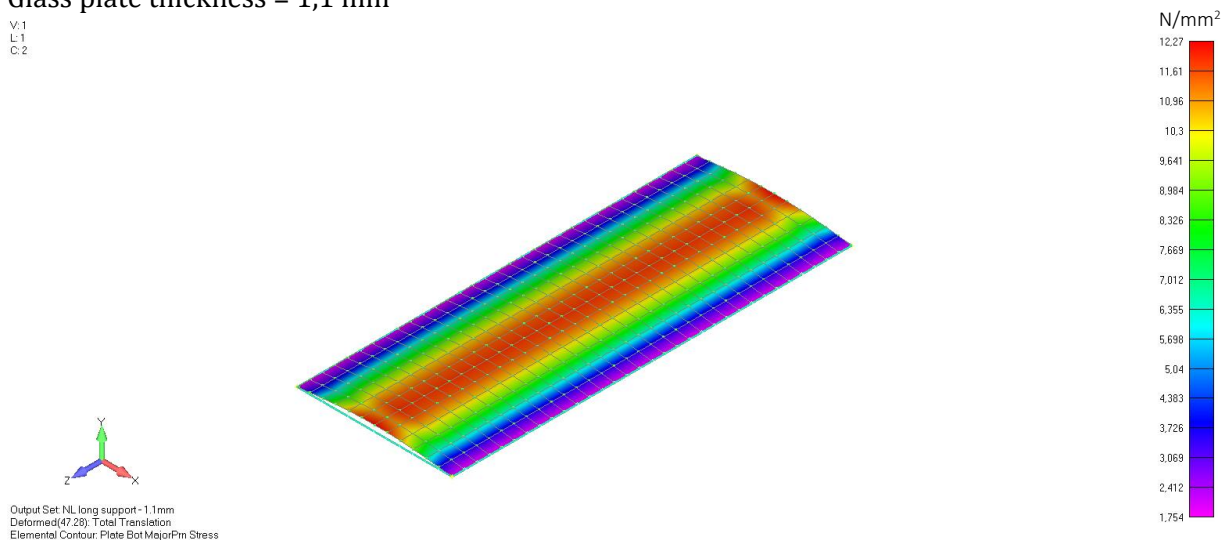
Figure C. 1 Plate thickness 1,1 mm – long side supported. Tensile stress = 12,27 N/mm2
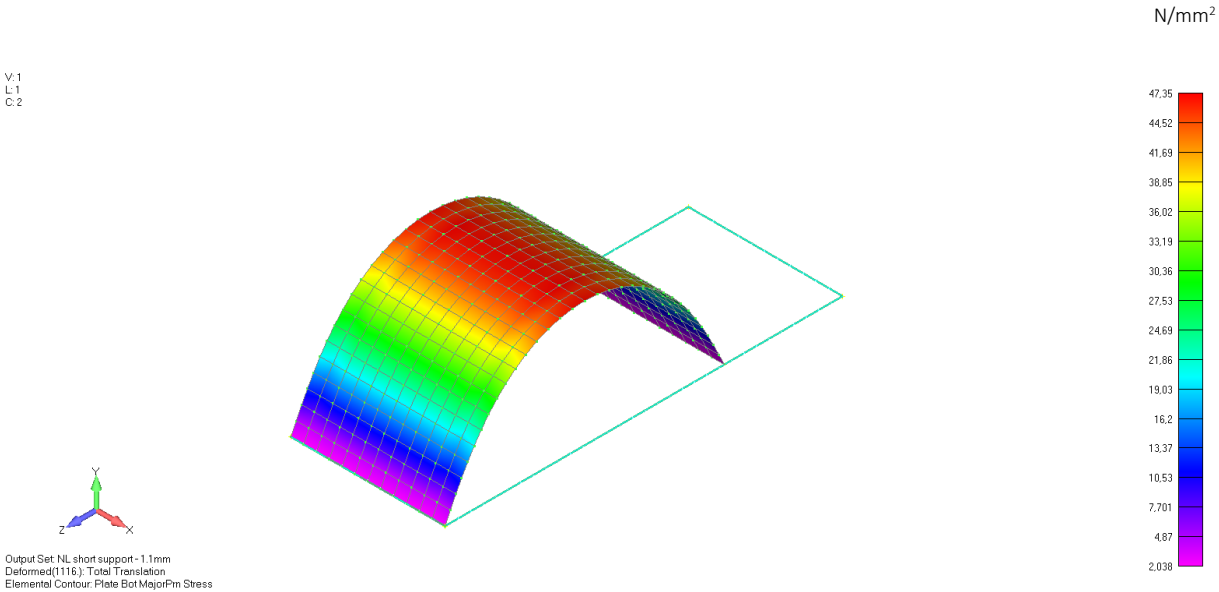
N/mm²

Figure C. 2 Plate thickness 1,1 mm – short side supported. Tensile stress = 47,35 N/mm2

Glass plate thickness = 0,7 mm
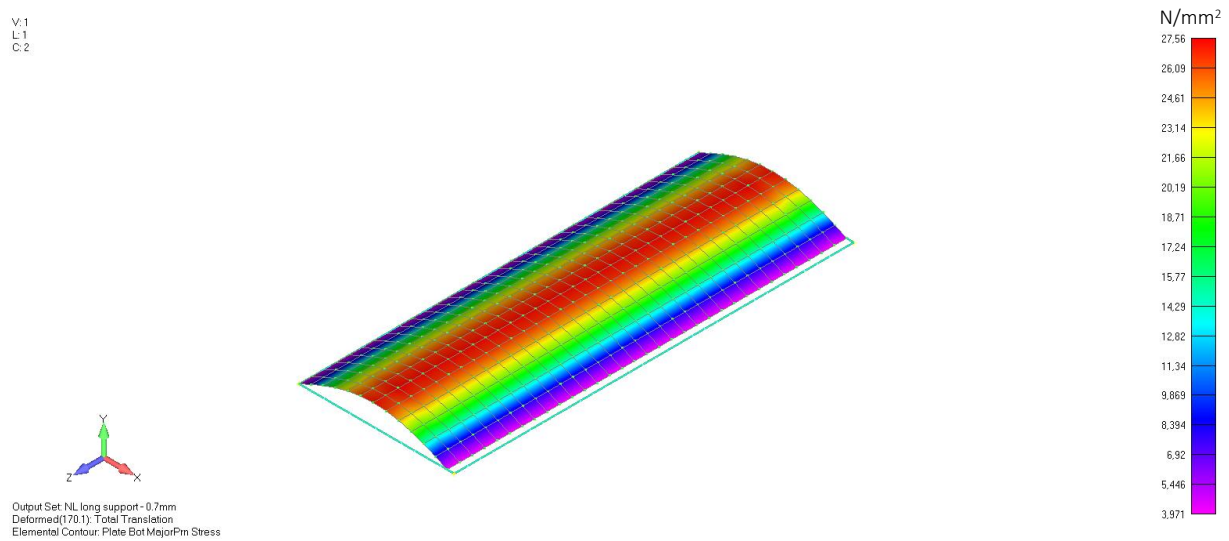
Figure C. 3Plate thickness 0,7 mm – long side supported. Tensile stress = 27,56 N/mm2
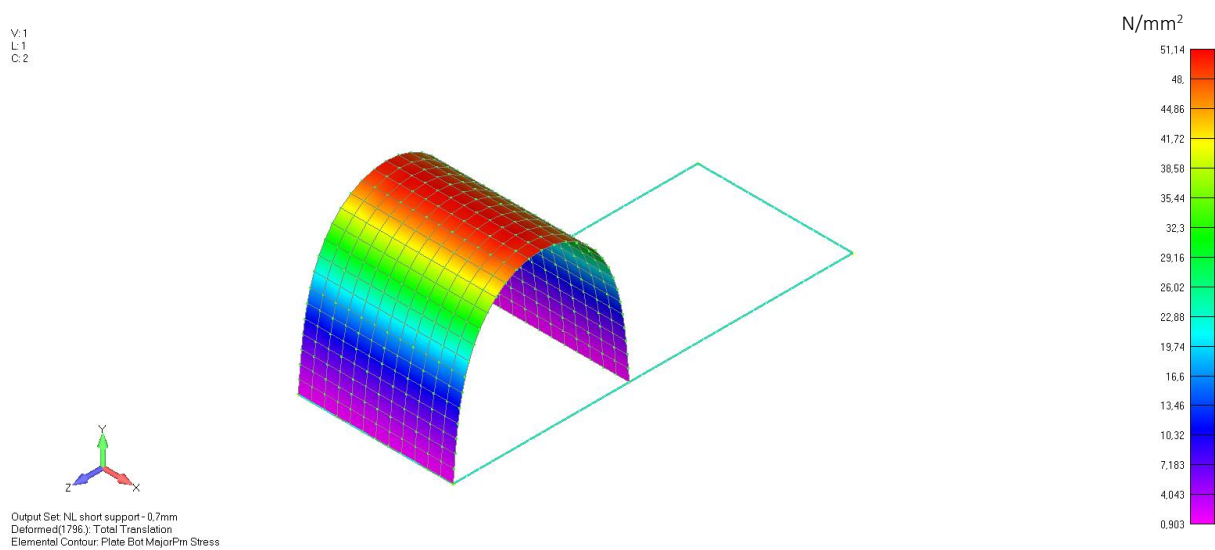
Figure C. 4Plate thickness 0,7 mm – short side supported. Tensile stress = 51,14 N/mm2

From this first examples it can be already seen that, with the same load applied, the panels supported on the short side will easily deflect. It is not a matter of strength, since tensile stresses are still low compared to the limit stresses that chemically strenghtened glass can reach (260 MPa for Leoflex glass). However, in terms of stiffness, the panel has lower deflection if it is supported on the long edges. Moreover, since the bent shape is one of the fist research goal of this project, it has been decided to investigate the thinnest glass available, 0,5 mm.

First conclusions
Panel supported on the long side edges

Glass plate thickness = 0,5 mm
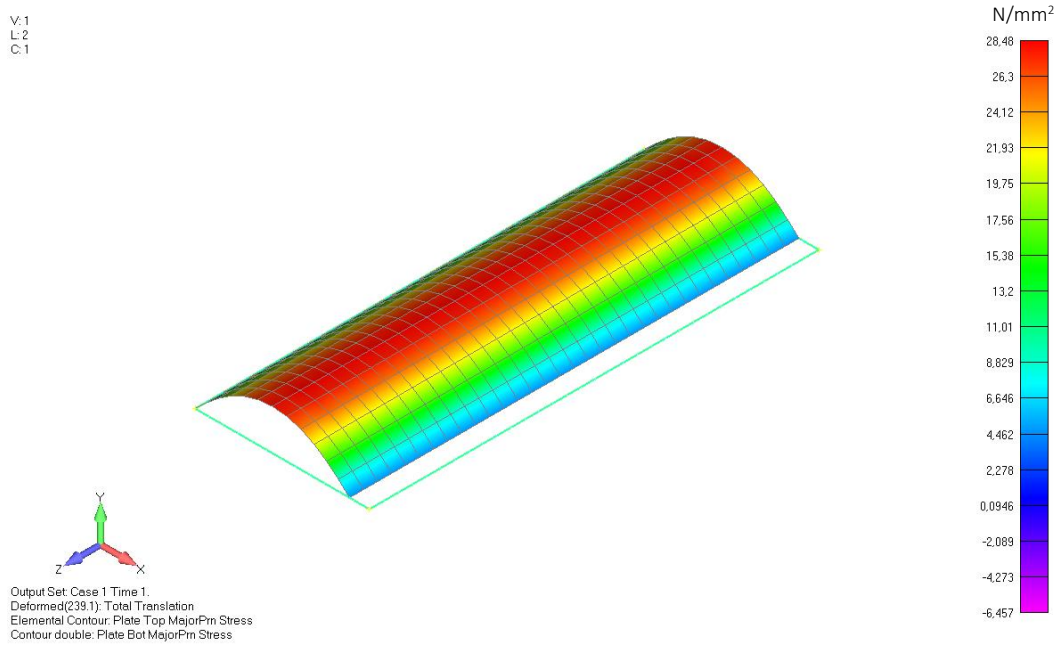
Figure C. 5 Plate thickness 0,5 mm – long side supported. Tensile stress = 28,48 N/mm2

Figure C. 6 Cold bending – Parabolic Shape

Circular Shape

The second shape taken into account is the circular shape, obtained by imposing a defined displacement in each node of the panel. The horizontal displacement of the panel's edge is calculated by geometrical consideration and, then, it is imposed at each node. An eccentricity is required in order to curve the glass instead of reaching just a compression state.

Imposed displacement x = 100 mm

Glass thickness 0,5 mm
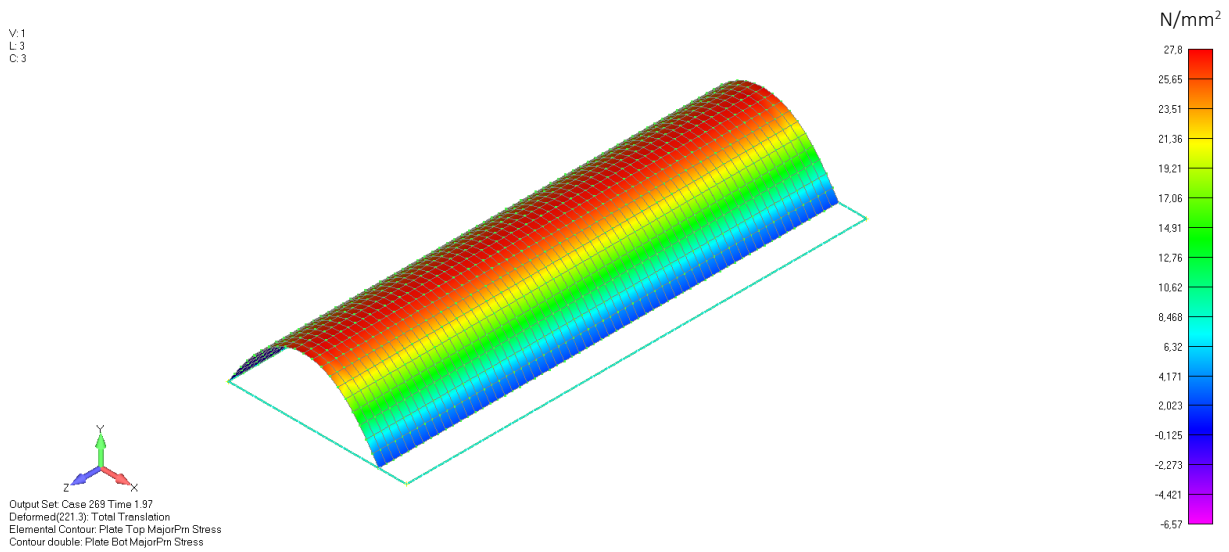
Figure C. 7 Plate thickness 0,5 mm – long side supported. Tensile stress = 27,8 N/mm2

Figure C. 8 Cold Bending – Circular Shape

Sinusoidal Shape

The third and last shape taken into consideration is the sinusoidal shape, reached by an applied horizontal force. Also in this case, an eccentricity is required in order to curve the glass instead of reaching just a compression state. A force F of 18 N has been divided by the number of nodes on the roller support, to cause a displacement around 100 mm, the same as the one in the previous case.

Horizontal force F = 18N

Glass thickness 0,5 mm
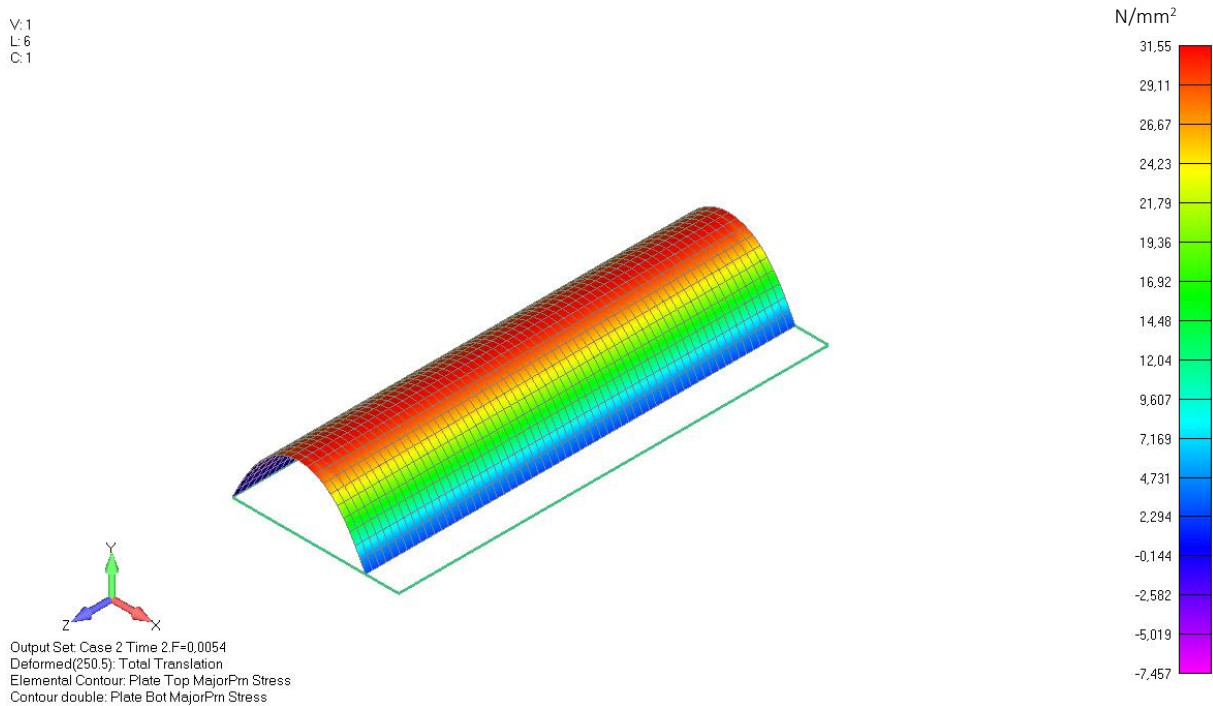
Figure C. 9 Plate thickness 0,5 mm – long side supported. Tensile stress = 31,55 N/mm2
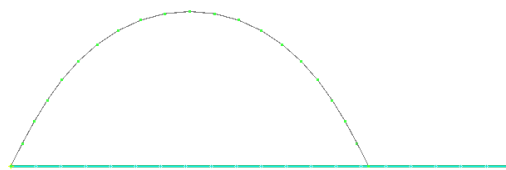
Figure C. 10 Cold Bending – Sinusoidal Shape

Those specific analyses have been carried to evaluate the preferred shape, that it is wanted to be used in this research. The circular shape results to be the shape in which lower stresses are induced, as a confirmation of the research of Galuppi & Royer (Galuppi & Royer-Carfagni, 2015). For this reason, the circular shape has been decided to be further investigated in this project.

Appendix C.2 Karamba and Femap Comparison

The approach used in this preliminary design phase is the following: first of all, to get acquainted with the program, a beam element has been calculated analytically and then with Karamba. The second step was to make a comparison between plate elements, which has been compared also with an equivalent model on Femap. The third step was to make a truss element, and finally, once the trust in the program has been gained, the final model – a sandwich panel with the Truss and the Waffle core – has been calculated in Karamba and Femap.

The approach used to better understand Karamba and Femap was to realize the following models:

- Beam
- Plate element
- Sandwich Beam – Truss elements
- Sandwich Panel

<u>Beam Model</u>

Fist, a simply supported glass beam, loaded with a point load *F=5kN* in the middle of the span *l=3m,* has been calcualted. The results of this simple example helped me to find out how to input correctly the parameters in Karamba, and, just as important, how to read the results available.
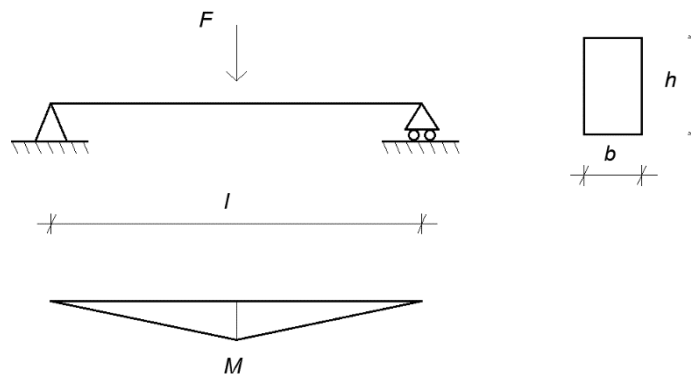
Figure C. 11 Simply supported glass beam (left) – Cross sectional dimensions (right)

Analytical Calculations:

The Moment *M* and the displacement *w* in the center of the beam can be easily calculated by use of the following formulas:

$$M = \frac{1}{4}Fl$$

$$w = \frac{1}{48} \cdot \frac{Fl^3}{EI}$$

Where:

F = 5000 N
l = 3000 mm
b = 150 mm
h = 300 mm
E = 73000 N/mm²
G = 30000 N/mm²
I = (150*300³)/12=337 500 000 mm⁴

$$M = \frac{1}{4} \cdot 5 \cdot 3 = 3{,}75 \; kNm$$

$$w = \frac{1}{48} \cdot \frac{5000 \cdot 3000^3}{73\,000 \cdot 337\,500\,000} = 0{,}114 \; mm$$

Numerical Calculations – Karamba:

One important annotation is that Karamba works with Meters and KiloNewton predominantly. So the Rhinoceros + Grasshopper model has to be converted in Meters before input the parameters in Karamba. This characteristic was easy to realize due to the simple model in examination.

From the geometrical description in Grasshopper, Karamba enables to convert Line Element to Beam Element and Mesh to Shell Element (Shell will be discussed in the next example). Thus, the line designed in Grasshopper has been converted to a Beam Element in Karamba. The start and end point of the line have been exploded and input in the position of the supports. Then, each degree of freedom (T_x, T_y, T_z, R_x, R_y, R_z) can be set as free or fixed. In this case, to reproduce a the pinned support on the left, translations T_x, T_y, T_z have been constained, while on the right T_y, T_z have been constrained to reproduce the roller. The Load of 5 kN is introduced as a Point Load at the center of the beam. It is important to split the beam line into two different lines, with a node in the center, to let the programme understand on which node the point load is applied.

The result can be seen in the picture below. A displacement of 0,117 mm and a Moment of 3,75 kNm is found by the programme.
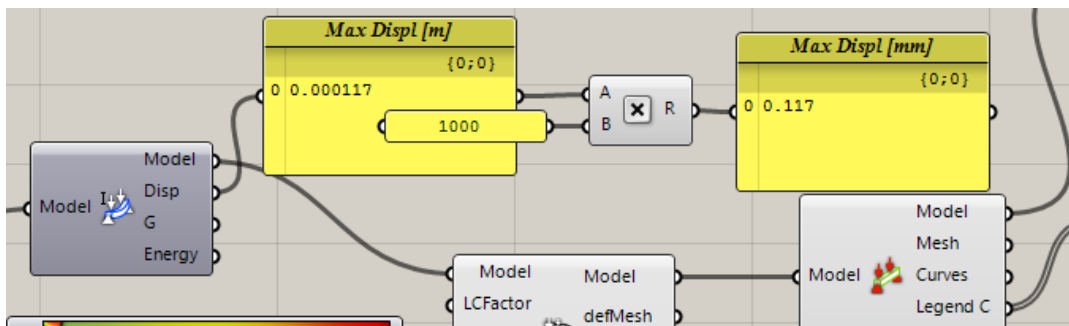
Figure C. 12 Beam Model - Karamba result - Displacement = 0,117 mm
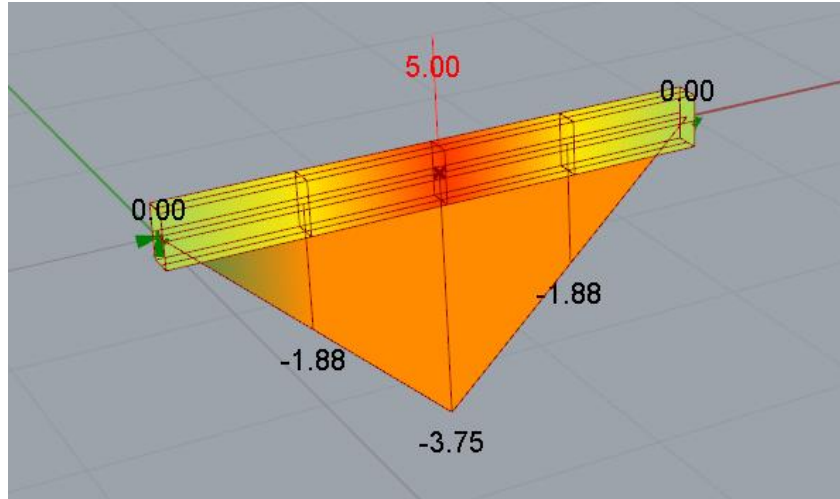
Figure C. 13 Karamba result - Moment Line

If we compare the Karamba displacement result with the analytical one of 0,114 mm, we can see a difference of 2,5% in the two results. This difference is due to the fact that Karamba takes into account also the shear stiffness of the beam. In fact, if we are going to re-calculate the deflection of the beam by taking into account also the shear stiffness of the beam, the result turns to be:

$$w = \frac{1}{48} \cdot \frac{Fl^3}{EI} + \frac{1}{4} \cdot \frac{Fl}{AG}$$

$$w = 0{,}114 \; mm \; + \frac{1}{4} \cdot \frac{5000 \cdot 3000}{150 \cdot 300 \cdot 30000} = 0{,}117 \; mm$$

Which is exactly the same result obtained with Karamba.

The moment line can be seen in the results, with a maximum value in the center of the beam with a value of 3,75 kNm, exactly the same as the one found with analytical calculations.

Internal forces (*N, V* and *M*) of the beam can all be visualized in the same manner as the Moment shown in Figure C. 13. Resultant Forces can be extracted as well by Karamba. If more than one load is applied at the same model, from the command *Model View* the load case can be selected (all loads or a particular load case) and all the results will be dispalyed accordingly to the choice.

Plate Model

The plate model is a glass square plate of dimensions *b = 3m*, with a thickness *t = 300mm*. It is loaded with a surface load *p = 2 kN/m²*. The plate is line supported at two edges.

The plate has been analitically calculated by making few hypothesis: if just a central strip is taken into account, the beam theory can be used. The width of the plate will be taken into consideration in the calculations of the moment of inertia (*I*) of the element.

Where:

b = 3000 mm
t = 300 mm

$$I = \frac{1}{12} \cdot 3000 \cdot 300^3 = 6\ 750\ 000\ 000\ Nmm$$

The deflection of a simply support beam element under a uniformly distributed load *q* is:

$$w = \frac{5}{384} \frac{ql^4}{EI}$$

The line load *q* of the equivalent model can be calculated as the surface load *p* times the width of the plate:

$$q = 0,002\ \frac{kN}{m^2} \cdot 3000\ m = 6\ \frac{N}{m}$$

At this point, the deflection at the center of the plate can be calculated:

$$w = \frac{5}{384} \cdot \frac{6 \cdot 3000^4}{73\ 000 \cdot 6\ 750\ 000\ 000} = 0,0128\ mm$$

Numerical Calculations – Karamba:

The plate analysis is made in order to understand how to interpreter the results related to shell element on Karamba. First, the surface created on Grasshopper has to be meshed. Then, the mesh can be converted to a Shell Element by Karamba. Each support in Karamba is realized by a nodal support, for this reason, if a line support wants to be created, the edge of the plate has to be divided into node elements – which needs to coincide with the mesh node elements – and then each node has to be input in the support command.

The load has to be input as a Mesh Load. Anotehr surface has to be created and meshed, and it will be the surface reference for the load. The value given is already the surface load, which will be converted by the programme into equivalent node-loads. The orientation of the load can be chosen as well, the load can be locally oriented to the element or projected to the element or globally projected, as it is explained in the following picture.
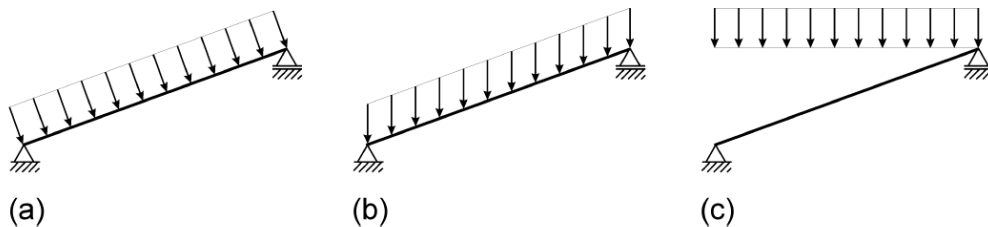
Figure C. 14 Karamba orientation of Load on Mesh: (a) local, (b) global, (c) global projected (Preisinger, 2016)
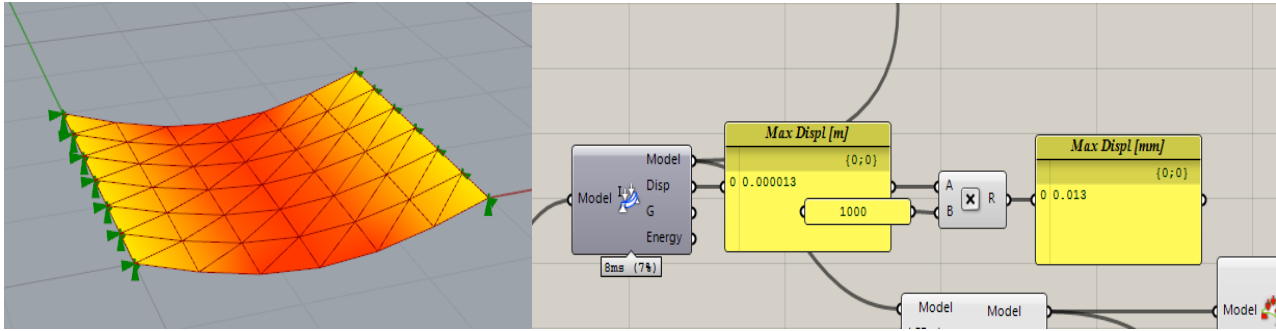
Figure C. 15 Deflection of a two side supported Plate under a surface load

The displacement found in the midde of the plate, results to be 0,013 mm. Which is really close to the 0,0128 mm found analitically.

In order to better understand the post processing visualization of stresses and Shell forces, the same model has also been realized in Femap. The comaprison of the results found in both programes are shown in the following pictures.

Numerical Calculations – Femap:
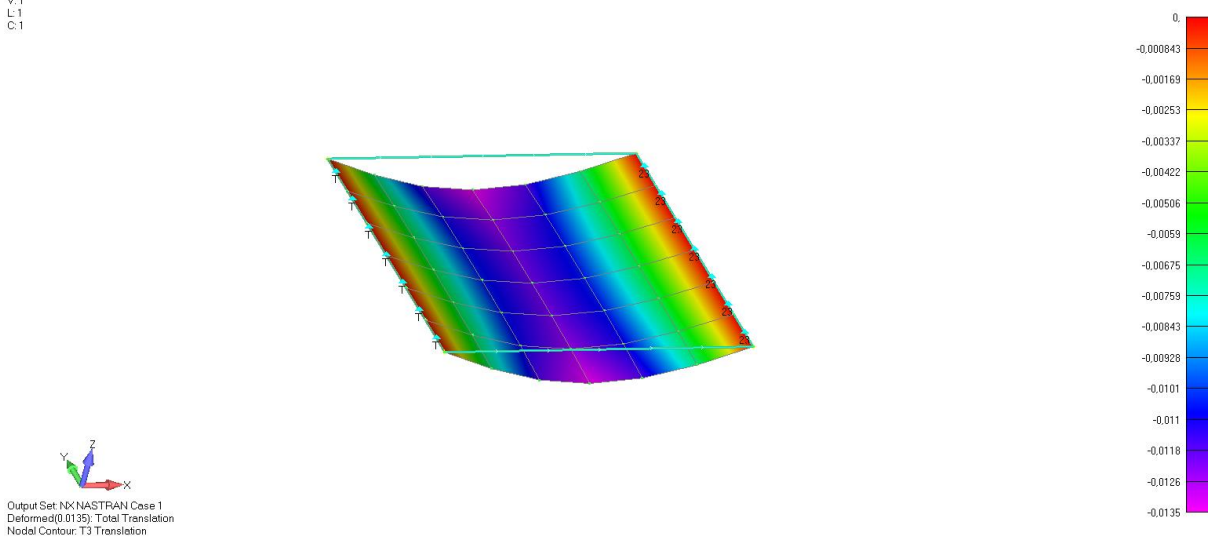
Figure C. 16 Deflection Femap: 0,0135 mm

Principal Stresses are checked. According to the Maximum Principal Stress Theory, failure in the material occurs when the principal stress exceeds the principal stress at which failure occurs in the 1st dimensional loading test. This theory is indeed valid for brittle material, like glass. On the other hand, according to Von Mises Theory, failure occurs when the shear strain energy exceeds the energy per unit volume stored in the material during the 1st dimensional test. Von Mises theory is used for ductile materials, like steel or plastic. For this reason Principal Stresses will be checked.

Principal Stresses Femap: top face

Max: 0,147 N/mm²
Min: -0,0219 N/mm²
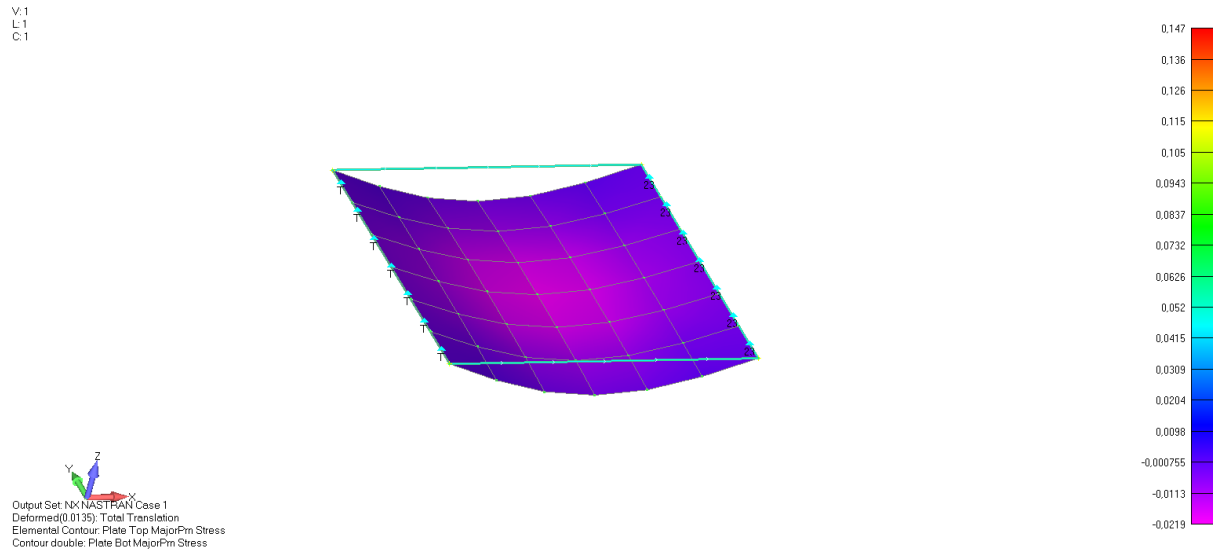
Figure C. 17 Femap - Maximum Principal Stresses Top Face

Principal Stresses Karamba: top face

Max: 0,0146 kN/cm² = 0,146 N/mm²
Min: -0,00217 kN/cm² = -0,0217 N/mm²
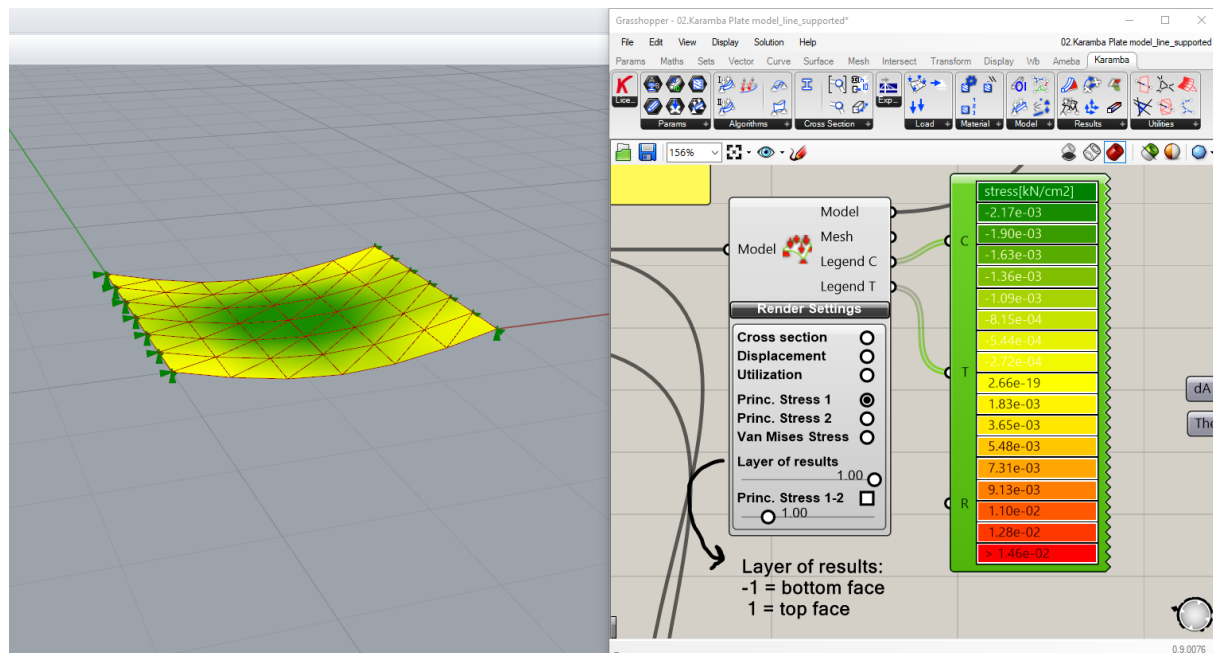
Figure C. 18 Karamba - Maximum Principal Stresses Top Face

Principal Stresses Femap: bottom face

Max: 0,147 N/mm²
Min: 0,0406 N/mm²
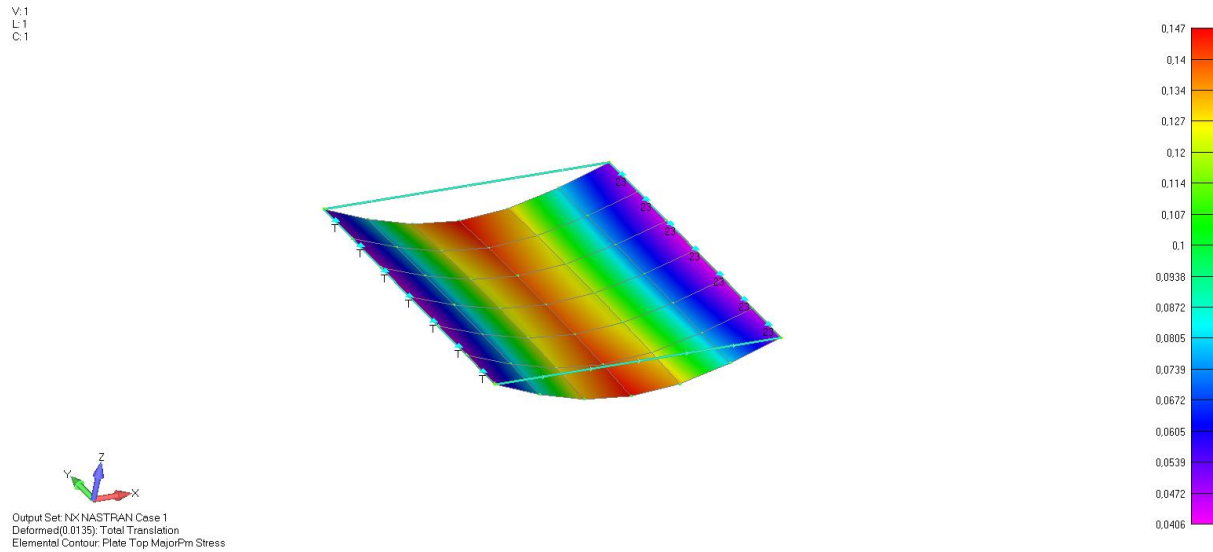
Figure C. 19 Femap - Maximum Principal Stresses Bottom Face

Principal Stresses Karamba: bottom face

Max: 0,0146 kN/cm² = 0,146 N/mm²
Min: -0,00217 kN/cm² = -0,0217 N/mm²
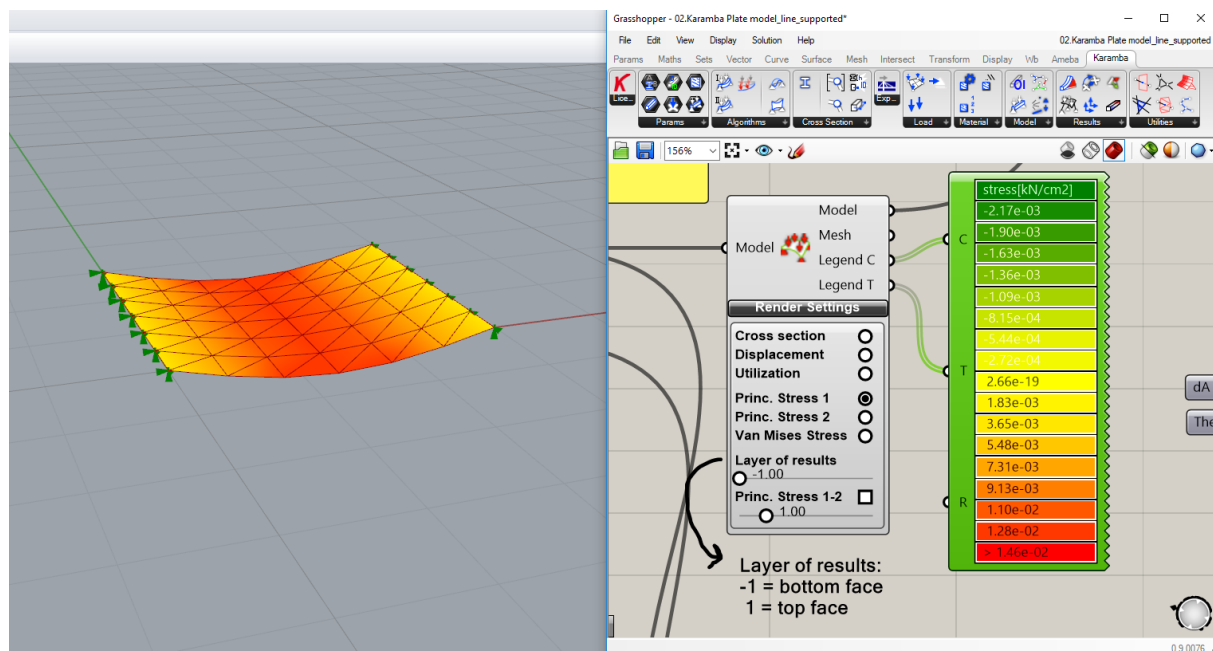
Figure C. 20 12 Karamba - Maximum Principal Stresses Bottom Face

Comments:

The comparison of the result reveals that the two models work accordingly to each other and also to the analytical calculation. Karamba still have the some limits with shell elements: while the deflection and principal stresses are calculated and visualized accordingly, the shear stresses can be seen just as a value and are not given in the shell result visualization. Sometimes it is difficilult to understand which value is related to wich small mesh element.

Sandwich Beam Model – Empty Core

The sandwich beam model has been calculated analytically with two limits situations. The first one, where the core has been schematized as "empty", this means by taking into account just the structural height of the beam, and not the actual material of the core. While, in the second model, a full core had been taken into account, in which the continution of the core is added at the Second Moment of Inertia (I). The first model will result in the a less stiff solution, giving an upper boundary for the deflection of the actual truss beam (maximum deflection experienced). While the second model will give the stiffest result, resulting in the lower boundary for the deflection (minimum deflection experienced).

Empty Core – Upper boundary deflection
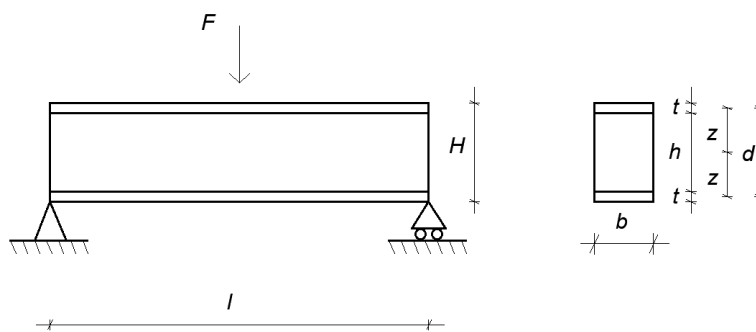
Figure C. 21 Sandwich Beam empty core schematization (left) - Cross Section (right)

The stiffness of the beam has been calculated as a contribution of the stiffness of the two thin glass faces $2 \cdot E_g \cdot \left(\frac{1}{12} bt^3\right)$ plus the contribution given by the stiffness of the two faces about the center of the beam $2 \cdot E_g \cdot (A \cdot z^2)$

$$EI = 2 \cdot \left[E_g \cdot \left(\frac{1}{12} bt^3 + A \cdot z^2 \right) \right]$$

Where:

E_g = 73 000 N/mm²
b = 150 mm
t = 5 mm
h = 290 mm
H = h + 2t = 300 mm
d = H – t = 295 mm
z = d/2 = 147,5mm

$$EI = 2 \cdot \left[73000 \cdot \left(\frac{1}{12} \cdot 150 \cdot 5^3 + (150 \cdot 5) \cdot 147{,}5^2 \right) \right] = 2{,}3825 \times 10^{12} Nmm^2$$

Then, the deflection of a sandwich beam with an ideally empty core, can be defined as:

$$w = \frac{1}{48} \cdot \frac{50 \cdot 3000^3}{2{,}3825 \times 10^{12}} = 0{,}0118 \, mm$$

Karamba

This result will be represented in Karamba by modelling a sandwich beam, with a truss core realized just by hinged connection. Theoretically, a truss element does not have bending stiffness, for this reason the model should not differ from the empty core analytical calculated.

The model is composed by two beams, rectangular cross section *b x t = 150 mm x 5 mm,* which represent the top and bottom chord of the truss model. The truss elements are realized by rods, elements with do not have bending stiffness, hinged at the chords.
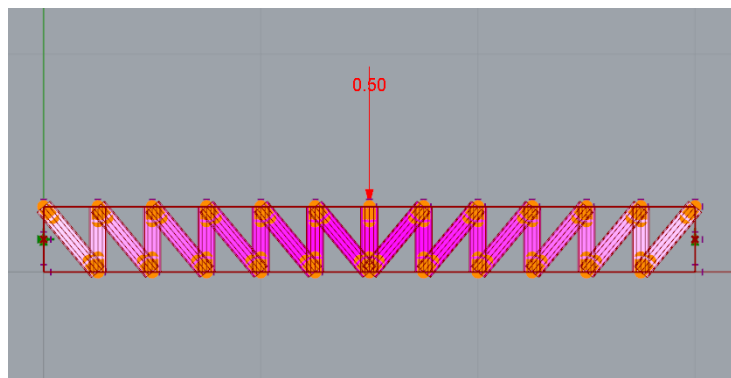
Figure C. 22 Karamba Truss Model

In order to correctly represent the analytical model, the supports have to be located at the center of the height of the beam. In Figure C. 22 they are represented by the green dots, pinned at the left side and roller support at the right side. The yellow dots represent the hinged connection in between the truss elements and the chords.

The point load applied at the center of the span is of 50 N, and the total span is of 3 m.

The deformation at the center results to be 0,01179 mm which can be exaclty approximized at 0,0118 mm found by analytical calculations.
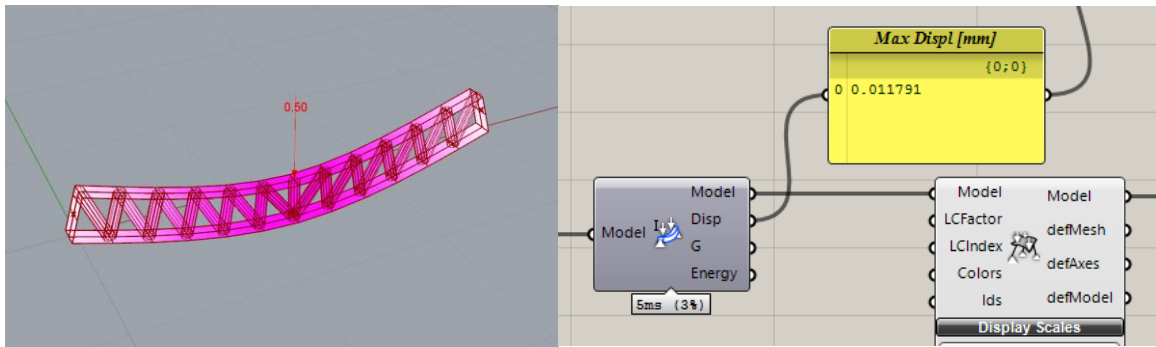
Figure C. 23 Karamba Truss deflection

The nice thing of making this model was the insight that it gave me about parametric design. While the model was still not working, in order to find the reason why it was not close to analytical calculations, a study about the influence of truss element has been performed.

The model has been realized in such a way to be able to shift just one parameter (number of truss element) and the generic sandwich model would have remain the same: same point load at the center of the beam, same support conditions (simply supported).

The initial thought was to obtain a lower deflection, by increasing the number of truss element. I was actually expect the stiffness to increase too. But this didn't happen. The deflection, by increasing the number of truss elements remain the same. This result confirmed the fact that the core is not adding bending stiffness to the system. Moreover, when the truss elements where too many, they started to assume a position that was close to vertical, this cause the samdwich beam to be less stiff compared to a beam with a 45° inclination.

Full Core
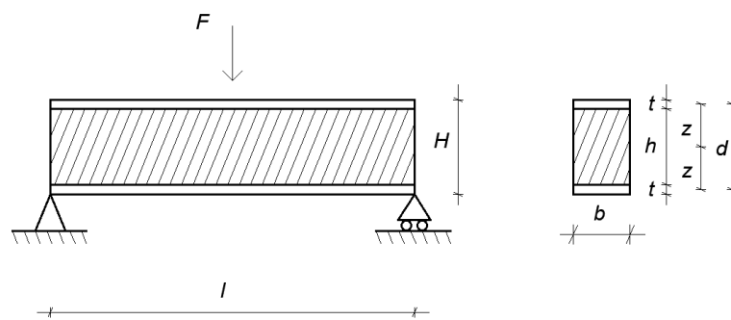
Figure C. 24 Sandwich Beam full core schematization (left) - Cross Section (right)

In order to calculate the stiffness of the sandwich beam with a full core, the stiffness of the core is actually added to the previous term. The stiffness of the beam has been calculated according to Sandwich Beam Theory (Allen, 1969). The Young modulus of glass E_g times the moment of inertia of the glass faces I_g, everything times two since the glass faces are equals and equivalently distant from the center of gravity

of the total panel. The contributions of the polymeric core has to be added with its respective properties $E_c\,I_c$.

$$EI = E_g \cdot \left[2 \cdot \left(\frac{1}{12} bt^3 + A \cdot z^2\right)\right] + E_c \cdot \frac{1}{12} bh^3$$

Where:

E_g = 73 000 N/mm²
E_c = 2 000 N/mm²
b = 150 mm
t = 5 mm
H = 300 mm
h = 290 mm
d = H – t = 295 mm
z = d/2 = 147,5mm

$$EI = 73\,000 \cdot \left[2 \cdot \left(\frac{1}{12} \cdot 150 \cdot 5^3 + (5 \cdot 150) \cdot 147,5^2\right)\right] + 2000 \cdot \frac{1}{12} \cdot 150 \cdot 290^3$$

$$EI = 2,922 \times 10^{12}\ Nmm^2$$

The deflection of the sandwich beam can now be determined as:

$$w = \frac{1}{48} \frac{Fl^3}{EI}$$

Where

F = 50 N
l = 3000 m

$$w = \frac{1}{48} \cdot \frac{50 \cdot 3000^3}{2,922 \times 10^{12}} = 0,00940\ mm$$

The deflection of a sandwich beam with a full core will represent the lower boundary of deflection $w=0,0094\ mm$.

<u>Karamba</u>

In order to realize a full core with Karamba, a shell element has been used. The chords have been realized as before with a beam element, rectangular cross section *b x t = 150 mm x 5 mm.* The core instad, has been created as a surface, converted to a mesh which has been used to create the shell element, with a thickness equivalent to the base of the beam *shell height = 150 mm.*
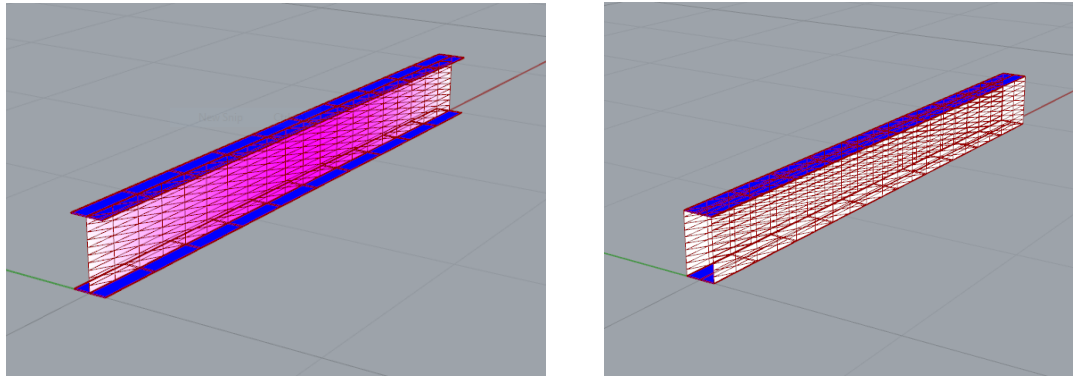
Figure C. 25 Karamba Cross Section Visualization

In Figure C. 25, we can see the same beam element: on the left the thickness of the shell is turned off, and we just see it as a plate element. On the right image, the cross section is visualized with its thickness 150 mm, which corespond at the base of the beam. This is how the full core has been represented.

The mesh size has to be enougth dense to reach an accurate result. Firstly, the result seems not to be accurate and I could not find the problem. Later on I have realized that the more the mesh size is dense, the more accurate result we get.

Load and supports are respectively: 50 N Point Load and simplt supported beam. The supports have to be setted at the center of the height of the beam. As can be seen in Figure C. 26, where the supports are the green dots at the sides od the beam.

The diplacement at the center of the beam results to be 0,00998 mm according to Karamba.
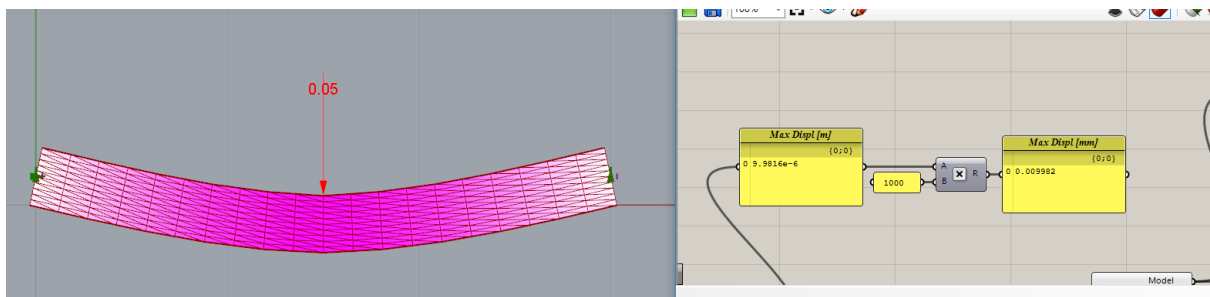
Figure C. 26 Karamba Sandwich Beam full core - Deflection

In this case, the shear stiffness of the beam made such a contribution that could be noticed in the result's comparison with analitical results. We got a displacement of 0,0094 mm considering just bending stiffness. If we add the contribution of shear we get:

$$w = \frac{1}{48} \cdot \frac{Fl^3}{EI} + \frac{1}{4} \cdot \frac{Fl}{AG}$$

Where the first term has been already calculated and:

G_g = 30 000 N/mm²
G_c = 730 N/mm²
b = 150 mm
t = 5 mm
h = 290 mm

$$AG = 2 \cdot (150 \cdot 5) \cdot 30000 + (290 \cdot 150) \cdot 730 = 76\ 755\ 000\ N$$

The total deflection results to be:

$$w = 0{,}0094 + \frac{1}{4} \cdot \frac{50 \cdot 3000}{4 \cdot 76755000} = 0{,}00988\ mm$$

Which is exactly the same result that has been found in Karamba.

Conclusion:

The results found in both Analytical and Numerical calculations are comparable. It can be said that both beam and shell elements can be realized with Karamaba and Femap. While Femap has a better accurancy even if the mesh size of the elements is not so dense, in Karamba this has to be considered carefully: mesh size in Karamba has to be enough dense to assure an accurate results

Appendix C.3 Panel 250 mm x 150 mm

Truss Core – Karamba

The first model that has been realized was the Truss Model on Karamba. The geometry has been previously realized on Rhino + Grasshopper. Now the same geometry will be used to perform the FEA with Karamba and then with Femap.

The top and bottom curved surfaces have been meshed in Karamba. The surface has been divided into 2400 elements, by dividing the short edge into 40 elements and the long edge into 60 elements. By default, Karamba split the mesh from Quad elements into Triangular elements for making the calculations. It is still not possible to use Quad elements in Karamba. If in future the option of Quad Elements willl be available, is highly recommended to use it in order to have more accurate results.

Supports and load conditions are given differently based on the case that will be examined. In general, pinned supports and roller supports have been taken into account. Different loading conditions were also taken into account: a surface load of 1kN/m² has been used to simulate the Wind Load and a Point Load of 50N has been used to compare the numerical model with analytical model. Morover, since the local point load on a node is unlikely to happen in reality, a more distributed point load has been taken into accout. The load of 50 N has been spread into 9 nodes, to have more distribuited stresses in the results and to avoid peak stresses. A line load has been also taken in considerations while comparing the models.

Falcon Glass has been used for experimental tests. Its characteristics has been reproduced also in the computer models. The top and bottom shells have a thickness of 0,5 mm and the properties of Falcon Glass has been attribuited:

E_g = 73 000 N/mm²
G_g = 30 000 N/mm²
Specific Weight = 25 kN/m³

The beam element of the core have a circular hollow section with a radius of 2mm. The thickness of this hollow section is 1mm, since the 3D printed element has not a full cross section. The properties of PETG has been attribuited to the core:

E_c = 2 000 N/mm²
G_c = 730 N/mm²
Specific Weight = 12,7 kN/m³

Since the realized panel will have also 3D printed side elements, as a frame of the core, those elements of 5 mm has been added to the computer model as well, in order to realize a schematization which is as similar as possible to the physical model. PETG side elements have been added.

The model can now be Assembled on Karamba, and analysed. A Static linear analysis has been performed with the assumptions that the whole sandwich panel, which behaves like a monolithic element, will deflect following the theory of small displacement.
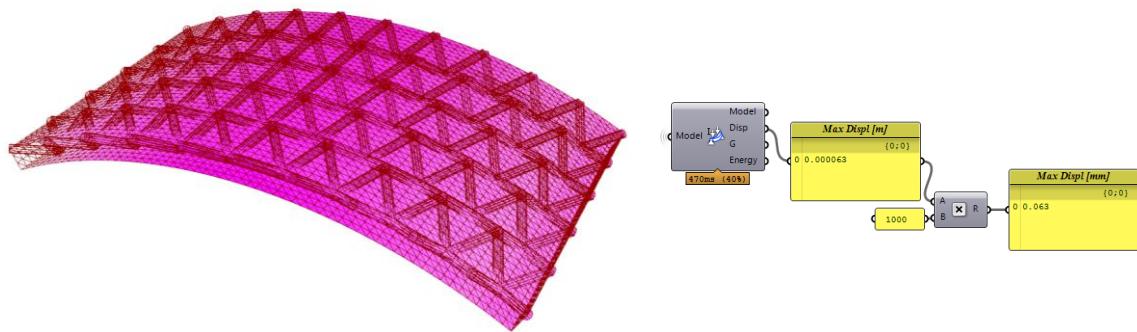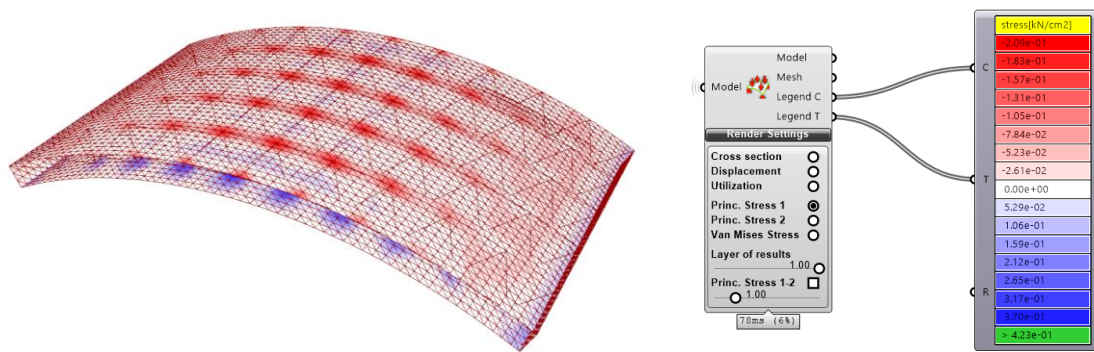
Figure C. 27 Karamba Truss Model – Displacement

Figure C. 28 Karamba Truss Model - Glass Plate Principal Stresses

<u>Femap</u>

To model the same curved sandwich panel in Femap, the geometry has been imported as a dxf file. The 250mm x 150mm curved surfaces have been created and then the edge lines has been divided into 40 and 60 elements respectively, in order to have the same mesh realized in Karamba. The shells have been meshed firstly as a Quad elements, then, the elements have been splitted into Triangular elements. Karamba is using triangular mesh elements, and in order to reduce the deviations between the two models, triangular mesh elements have been used in Femap too.

The Glass Faces have been modeled as a Plate element of 0,5 mm in Femap, while the Truss Element has been modeled as a Beam Element, circular cross section of r = 2mm, with thickness of 1mm. All other inputs has been equally setted and the results given by Femap are shown in the following figures.
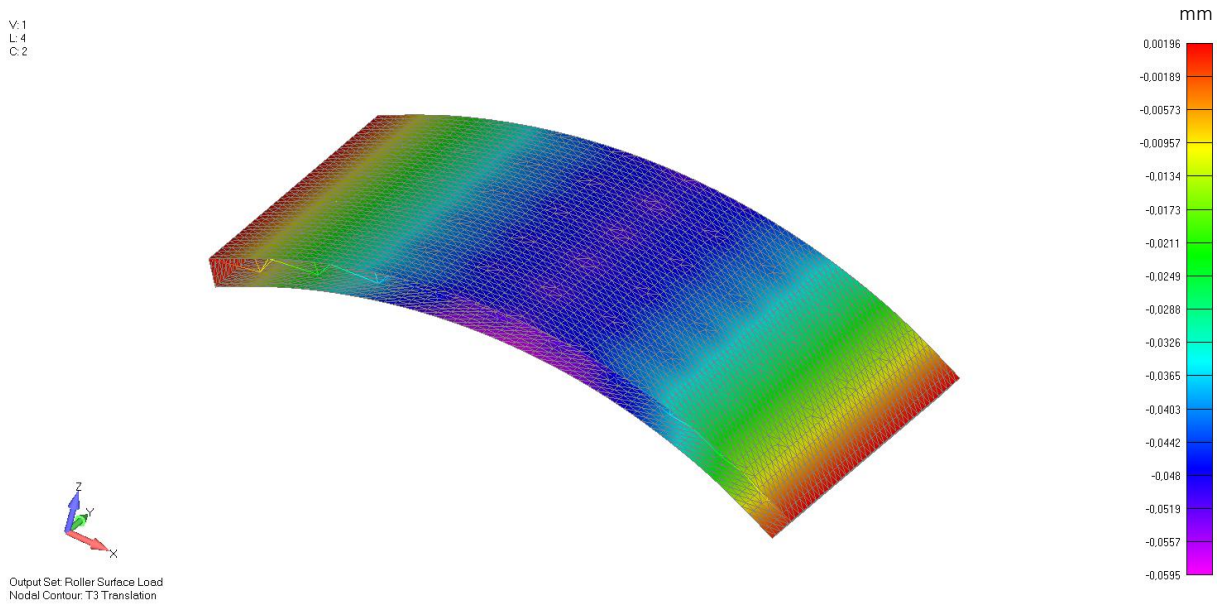
Figure C. 29 Femap Truss Model – Displacement
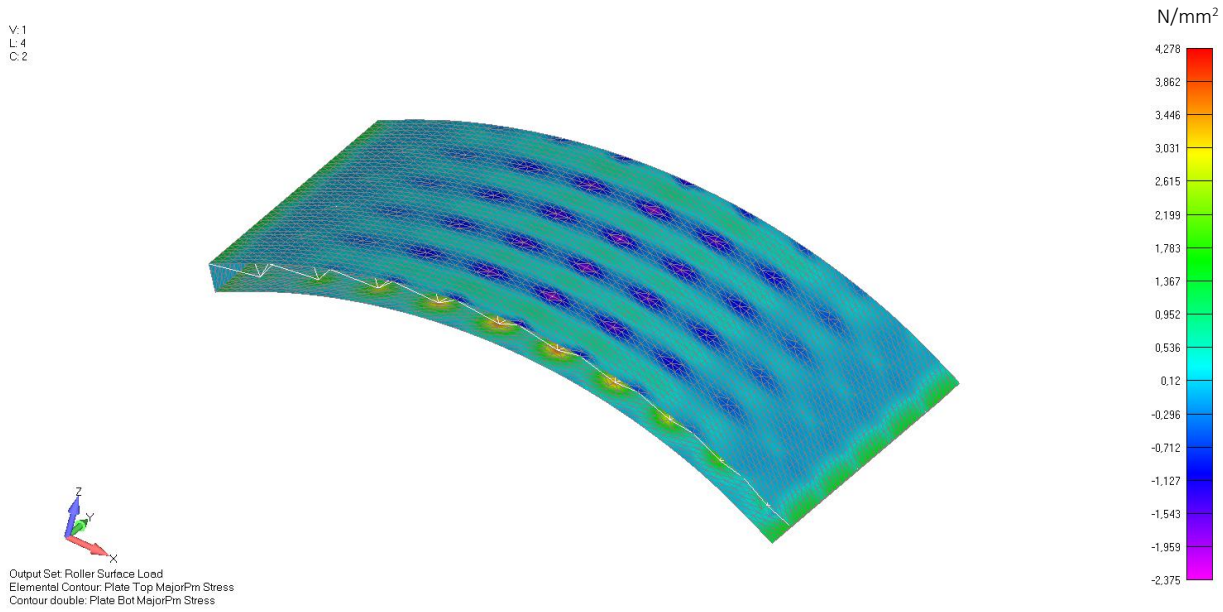
Figure C. 30 Femap Truss Model - Glass Plate Principal Stresses
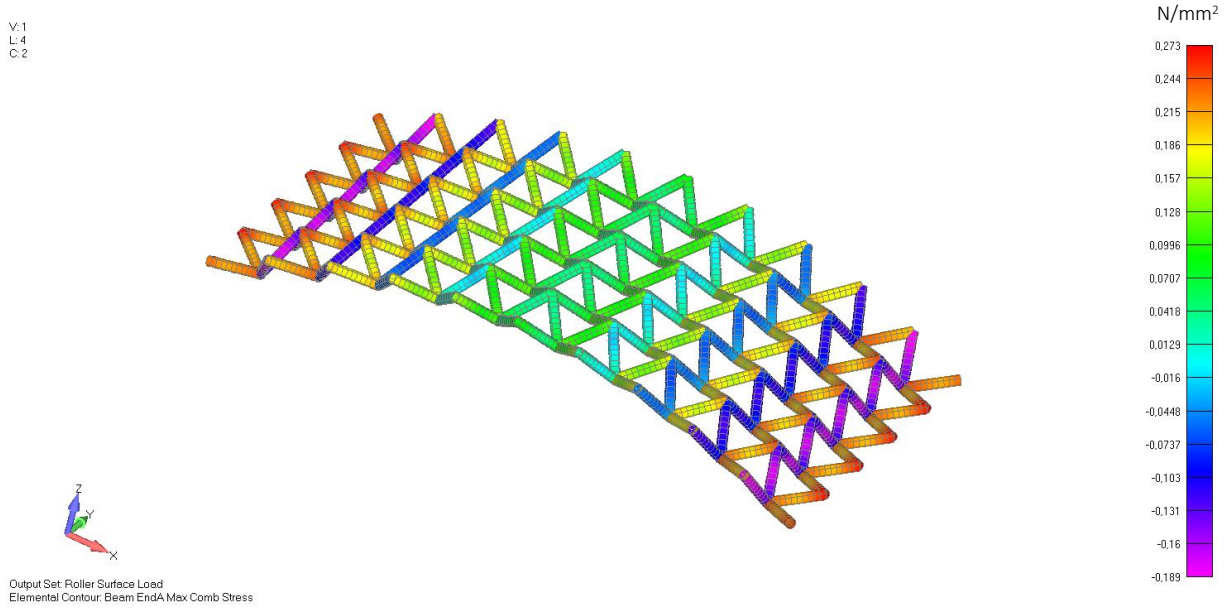
Figure C. 31 Femap Truss Model - Core Combined Stresses
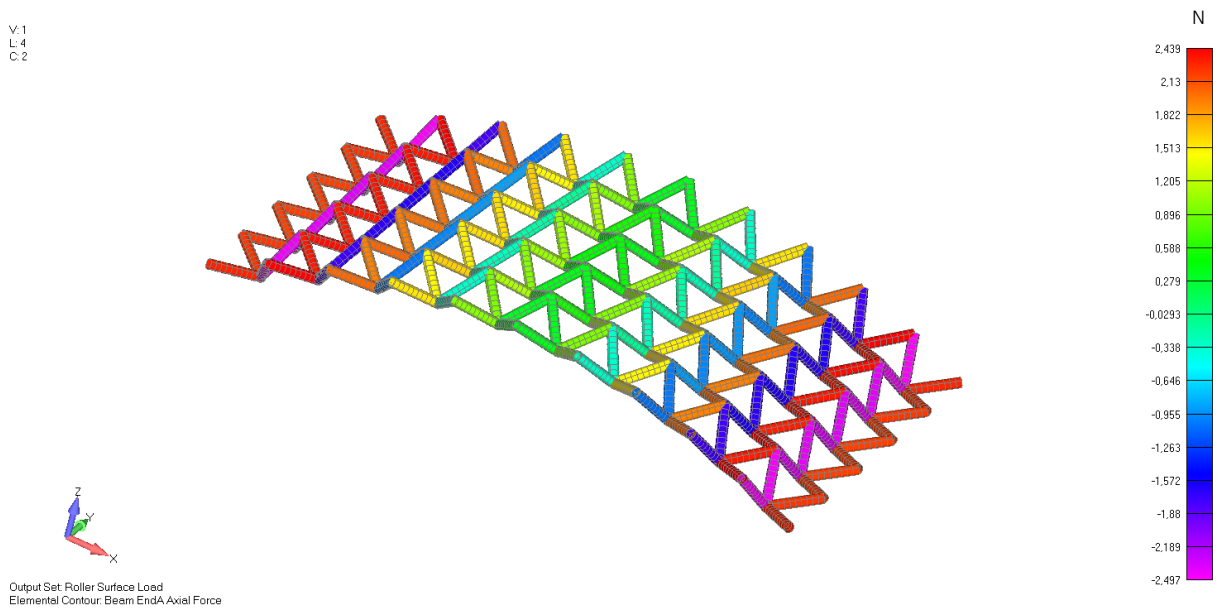
Figure C. 32 Femap Truss Model - Axial Force in the Truss elements
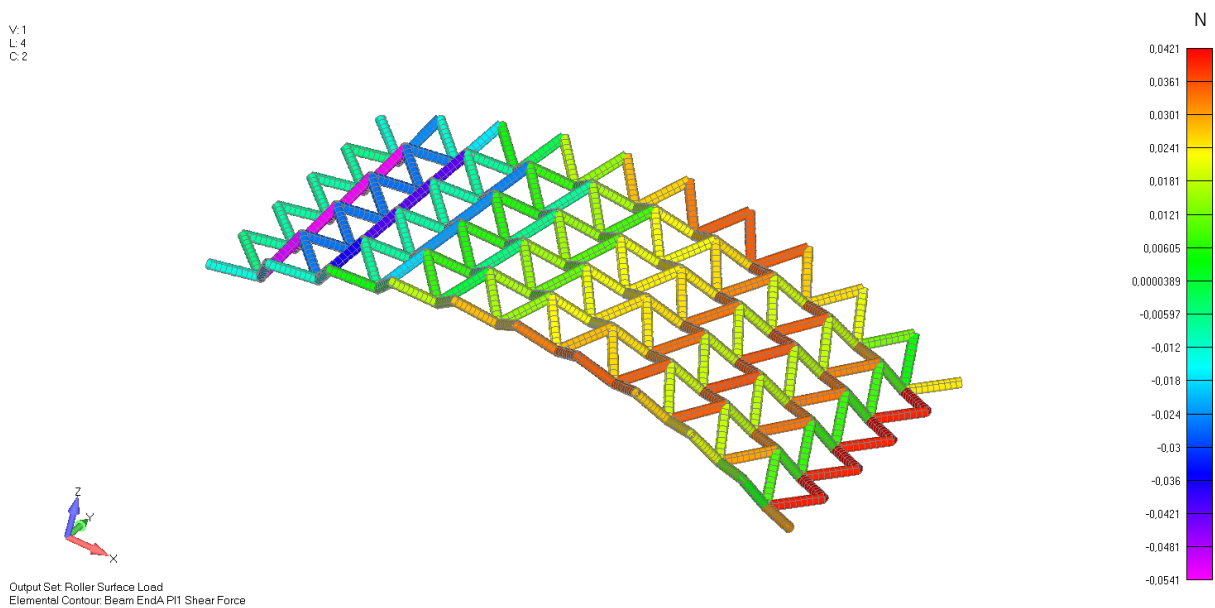
Figure C. 33 Femap Truss Model - Shear Force in the Truss elements

<u>Comparison of Finite Element Models</u>

Once the Finate Element Models were realized both on Karamba and Femap, a comparison of the results was performed. The goal of this analysis was to understand how trustfull are the programmes, and how much will be the deviation between one and another. In Table C.1 the result of the comparison between the two finite element programmes is illustated. As can be seen from the table, the two programmes showed to be consistent. The differences in results are always below 5%.

In order to reach this result, it was important to have an identical mesh in both programmes. Having considered the same type of element was also important. Since Karamba can just solve with Triangular Mesh Elements, the same elements have been used also in Femap. For future researches would be important to check calculations accurancy with Quad4 or Quad8 node elements.

Comparison of Finite Element Models – Truss Model
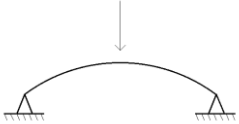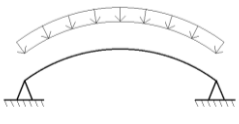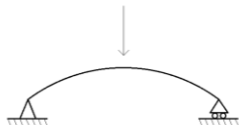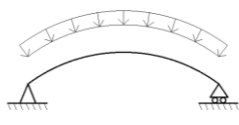
	Boundary Conditions			**Karamba**	**Femap**	**Deviations**
1.	Pinned Supports Point Load 50N	*Deflection*	w [mm]	0,296	0,292	1,35 %
		Principal Stress (Tension)	σ_{max} [N/mm^2]	+123,0	+125,2	1,79 %
2.	Pinned Supports Surface Load 1kN/m^2	*Deflection*	w [mm]	0,004	0,004	0,79 %
		Principal Stress (Tension)	σ_{max} [N/mm^2]	+1,18	+1,17	0,85 %
3.	Simply Supported Point Load 50N	*Deflection*	w [mm]	0,409	0,401	2,00 %
		Principal Stress (Tension)	σ_{max} [N/mm^2]	+120,0	+122,9	2,36 %
4.	Simply Supported Surface Load 1kN/m^2	*Deflection*	w [mm]	0,063	0,060	5,00 %
		Principal Stress (Tension)	σ_{max} [N/mm^2]	+4,23	+4,28	1,17 %

Table C. 1 Truss Model - Numerical Calculations

Waffle Model – Karamba

Same as the truss model, the waffle model has been first drawn as a geometry in Rhino+Grasshopper. The 250mm x 150mm curved surfaces have been meshed in Karamba. The surface has been divided into 1536 elements, 32 division on the short edge and 48 division on the long one. The shell elements have been associated to a cross section of 0,5 mm with the properties of falcon glass, same as the one utilized above. While the ribs of the core have been associated to a shell elements, with a 3 mm cross section, made of PMMA. The core geometry can be seen in Figure C. 34. Support conditions and load conditons are the same as the previous model. Two side supported panel with pinned connections, and in this case a uniformly distribuited load of 1kN/m^2 has been applied. The displacement of the sandwich panel found by the Karamba analysis can be seen in Figure C. 35, while the principal stresses in the glass can be seen in Figure C. 36.
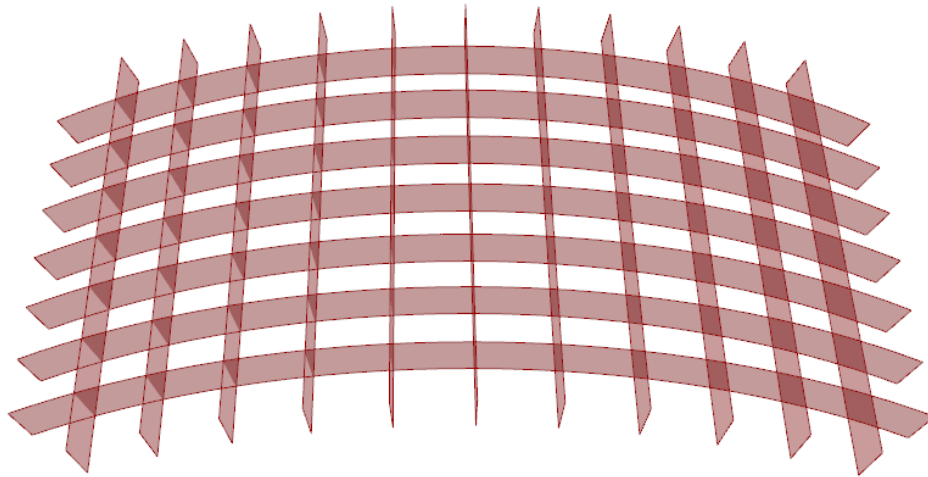
Figure C. 34 Waffle Model - Grasshopper geometry 250mm x 150mm
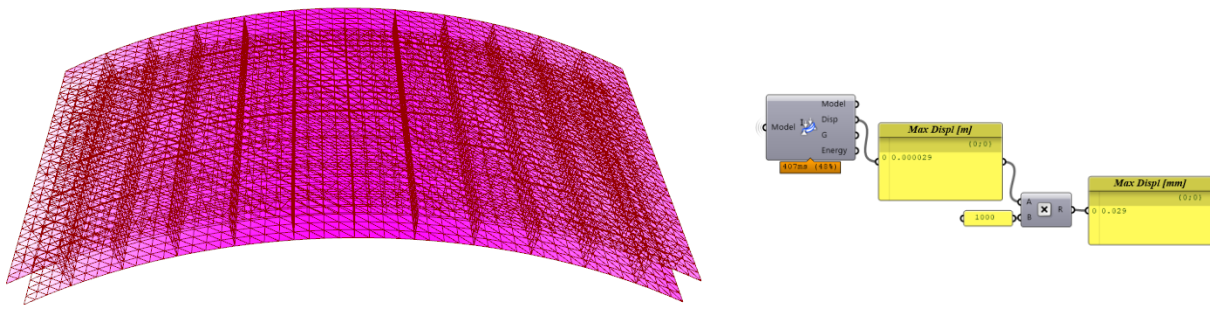
Figure C. 35 Karamba Waffle Model - Displacement
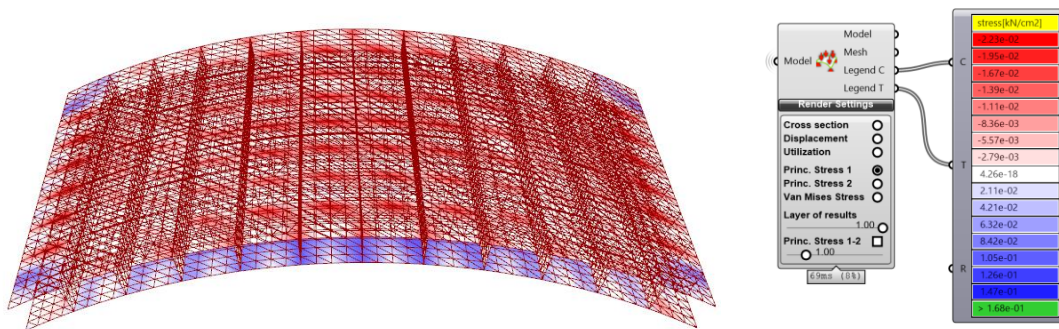
Figure C. 36 Karamba Waffle Model - Principal Stresses

Femap

In order to realize the model in Femap, the waffle geometry has been imported as a dxf file. From the imported lines, boundary surfaces were created. After having realized the correct boundary surfaces, they all have been meshed with the same properties of Karamba. All Quad elements have been splitted into Triangular elements to crate a model as similar as possible as Karamba. A plate element of 0,5 mm thickness, falcon glass material, has been used for the faces of the sandwich panel. While shell elements 3 mm thick, PMMA material, have been used for the core's ribs.

The results obtained from the FEA carried in Femap are shown in the following figures. Moreover, a comparison between Femap and Karamba analyses has been illustrated in Table C.2.

V: 1
L: 1
C: 2

mm

0,0279
0,0261
0,0243
0,0225
0,0207
0,0189
0,0171
0,0153
0,0135
0,0117
0,00987
0,00807
0,00627
0,00446
0,00266
0,000857
-0,000946

Output Set: Roller Surface Load
Nodal Contour: T2 Translation
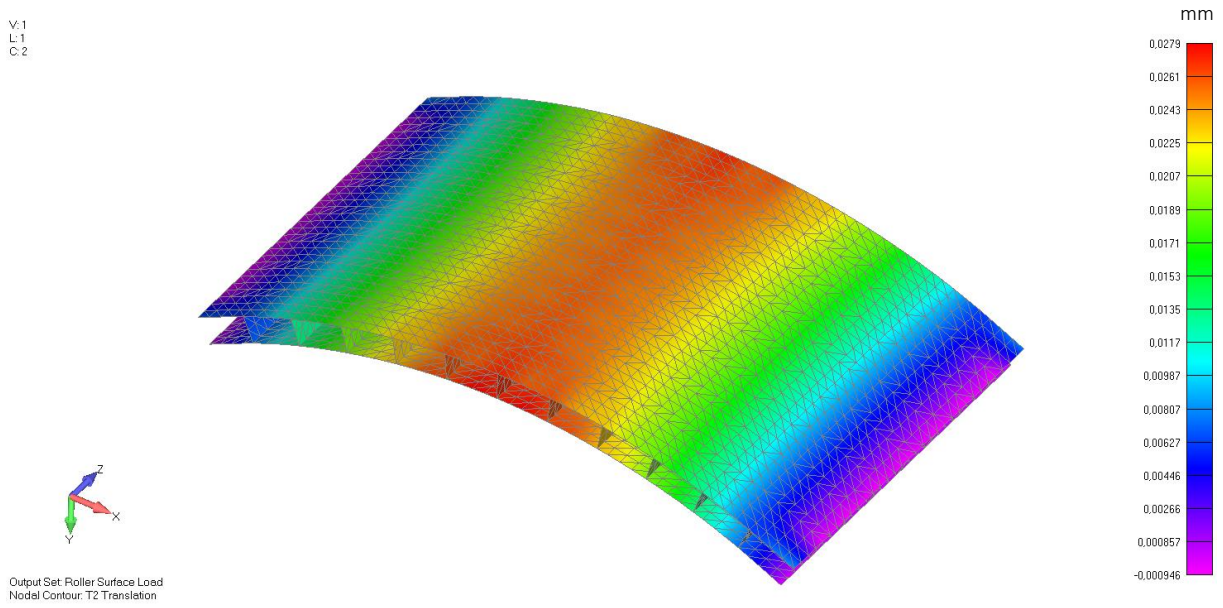
Figure C. 37 Femap Waffle Model – Displacement

V: 1
L: 1
C: 2

N/mm²

1,691
1,567
1,442
1,318
1,193
1,069
0,945
0,82
0,696
0,571
0,447
0,323
0,198
0,0739
-0,0504
-0,175
-0,299

Output Set: Roller Surface Load
Elemental Contour: Plate Top MajorPrn Stress
Contour double: Plate Bot MajorPrn Stress
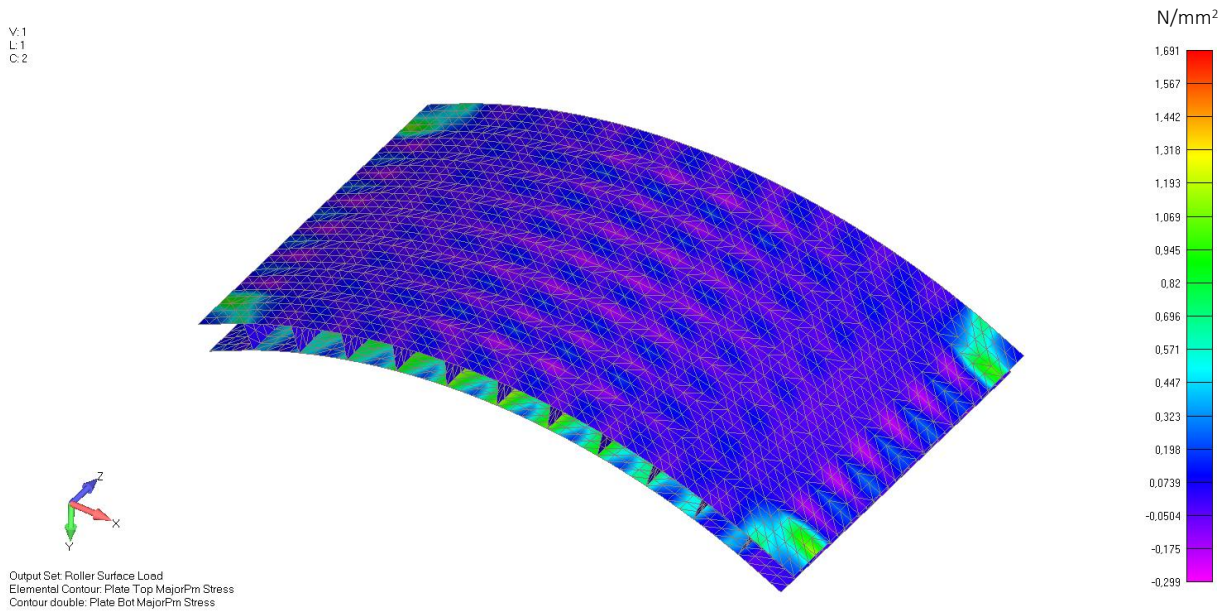
Figure C. 38 Femap Waffle Model - Principal Stresses Top Face
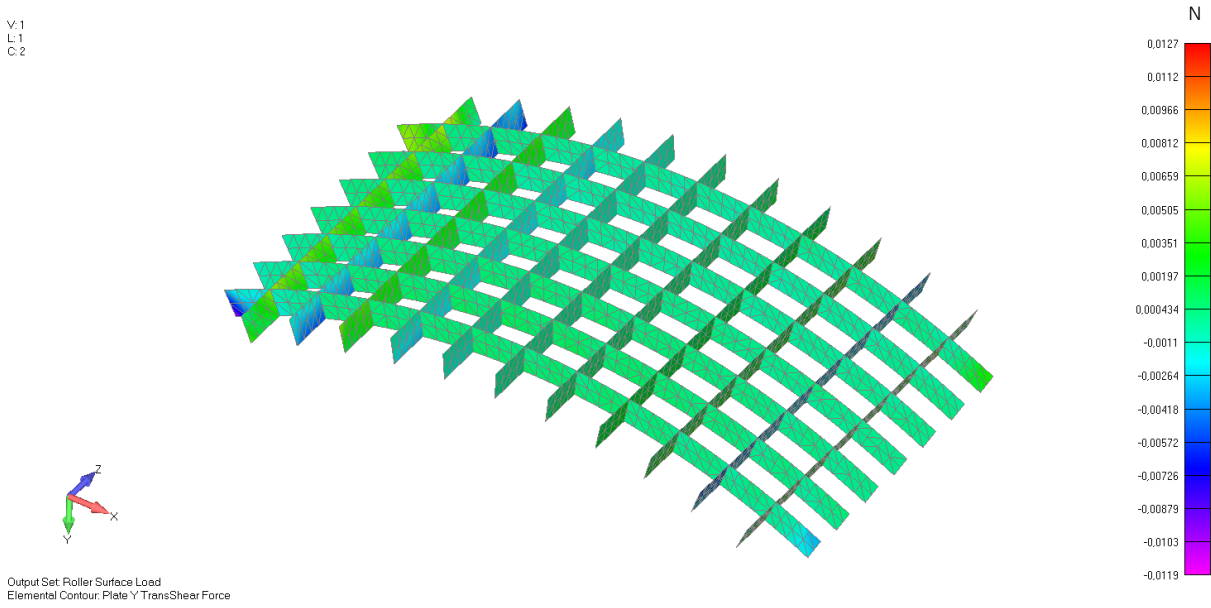
Figure C. 39 Femap Waffle Model - Shear Force in the Core
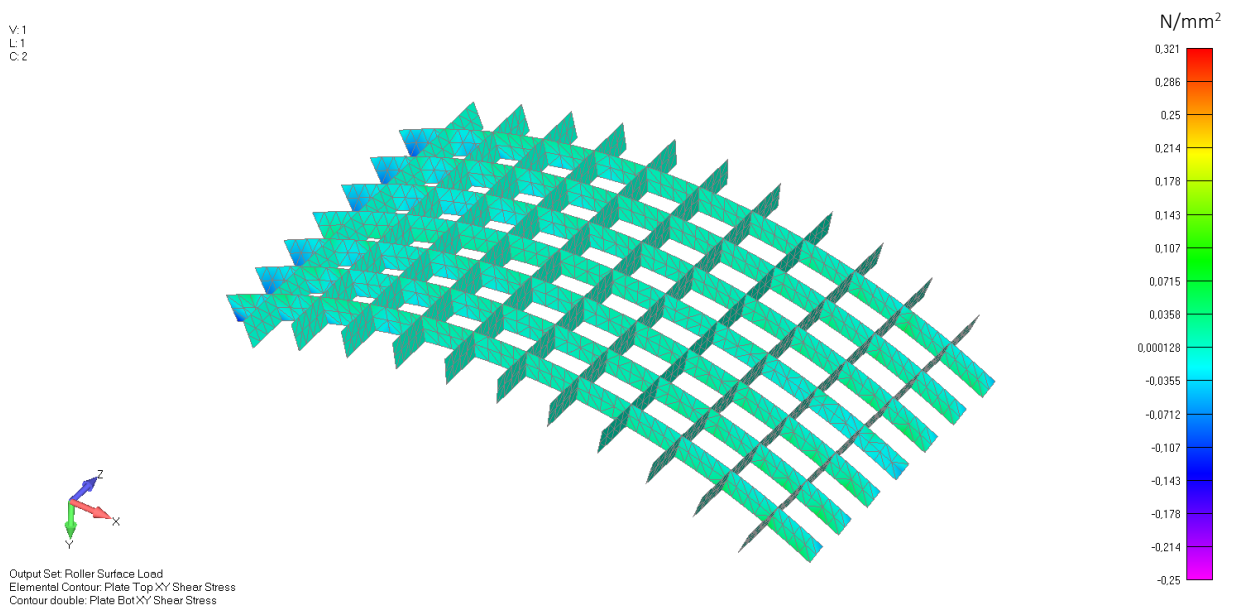
Figure C. 40 Femap Waffle Model - Shear Stresses in the Core

Comparison of Finite Element Models – Waffle Model
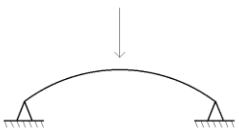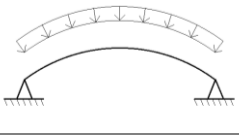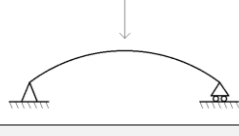
	Boundary Conditions			**Karamba**	**Femap**	**Deviations**
1.	Pinned Supports Point Load 50 N	*Deflection*	w [mm]	0,022	0,023	4,3 %
		Principal Stress (Tension)	σ_{max} [N/mm²]	3,74	4,01	6,7 %
2.	Pinned Supports Surface Load 1kN/m²	*Deflection*	w [mm]	0,008	0,008	0,3 %
		Principal Stress (Tension)	σ_{max} [N/mm²]	1,10	1,17	5,9 %
3.	Simply Supported Point Load 50 N	*Deflection*	w [mm]	0,077	0,075	2,7 %
		Principal Stress (Tension)	σ_{max} [N/mm²]	6,02	6,33	4,9 %
4.	Simply Supported Surface Load 1kN/m²	*Deflection*	w [mm]	0,029	0,028	3,6 %
		Principal Stress (Tension)	σ_{max} [N/mm²]	1,68	1,69	0,6 %

Table C. 2 Waffle Model - Comparison of Karamba and Femap results

Asymmetrical Loading

Since arches behave at their best under compression, testing the panel under a uniformly distributed compression load is not sufficient. For this reason, it has been calculated the deflection of the curved panel under an asymmetric distributed load. The asymmetrical load has been applied as a pressure load of *p = 2kN/m²* just on half of the glass surface, of dimensions 125mm x 150mm. To give a practical estimation of the load, about 6 kg has been applied on the mentioned surface. The mechanical schematization of the panel is shown in the following figure.
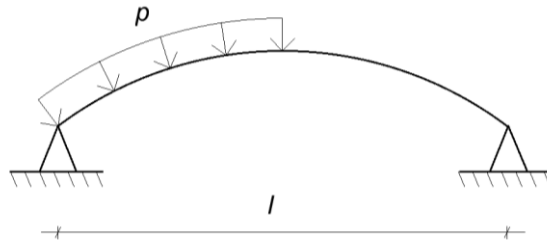
Figure C. 41Asymmetric Load Schematization

Truss Model

The Truss Model has been analysed under a pressure load of 2kN/m² applied on the left side of the panel. The deflection of the panel is shown in Figure C. 42 and in results to be 0,0174 mm.
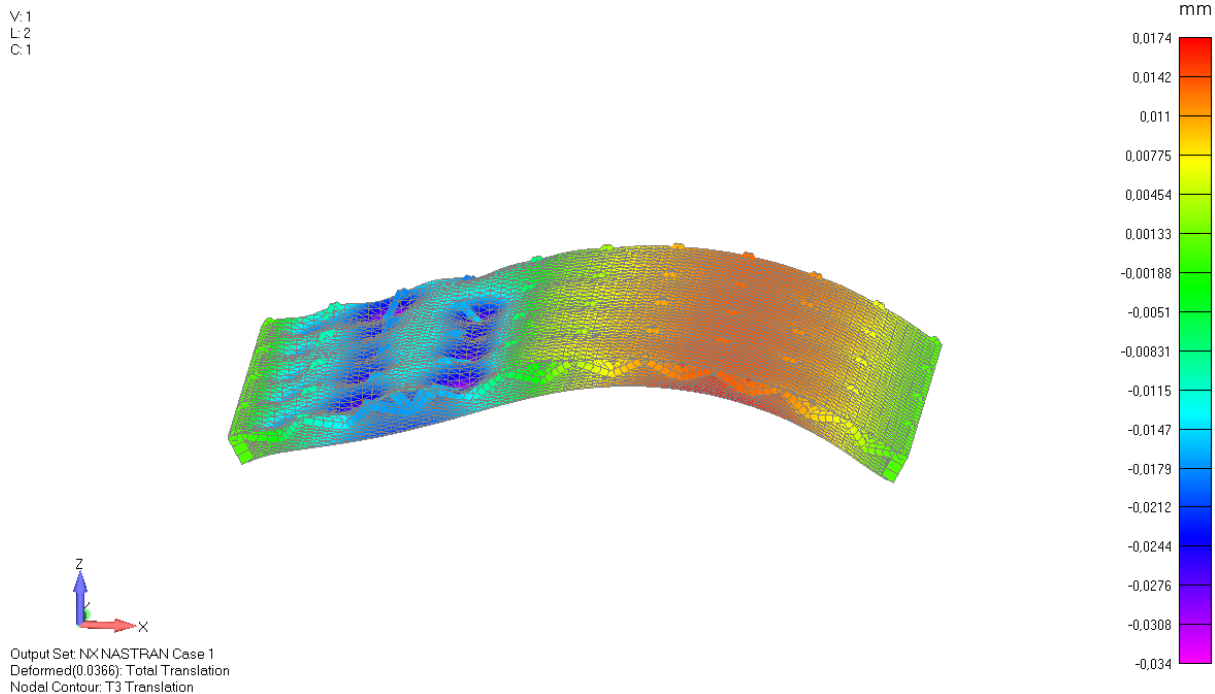

Figure C. 42 Truss Model - Asymmetric Load - Maximum Deflection = 0,0174 mm

The same panel, loaded with a uniformly distributed load of 2kN/m² showed a deflection of 0,00134 mm. Now the panel is loaded by an asymmetric load and the displacement is 0,0174 mm. This result shows that arches behave better with a uniform distributed load, in fact with the asymmetrical load the deflection increase of a factor of about 10. However, the model is still far from the deflection limit w_{lim} of the panel, which is $L_{diag}/65 = 4,49\ mm$.

$$L_{diag} = \sqrt{250^2 + 150^2} = 291,5\ mm$$

$$w_{lim} = \frac{L_{diag}}{65} = \frac{291,5}{65} = 4,49\ mm$$

The Mayor Principal Stresses in the glass are shown in Figure C. 43 (Top Plate) and Figure C. 44 (Bottom Plate).
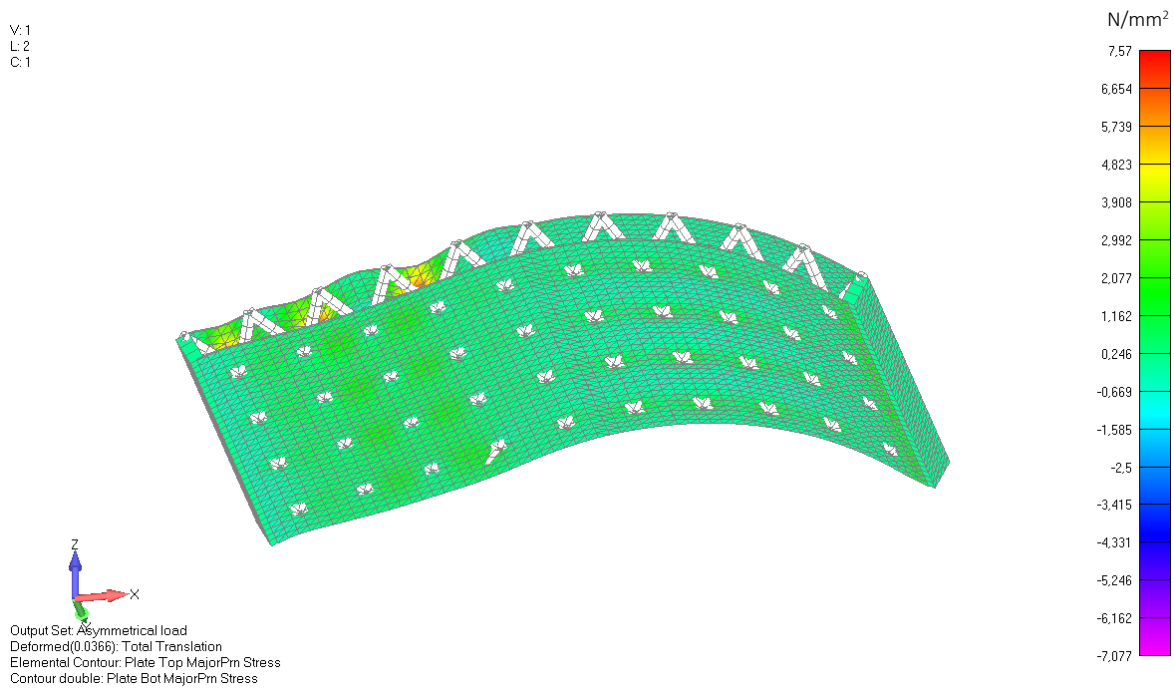

Figure C. 43 Truss Model – Asymmetrical Load – Top Plate Major Principal Stress
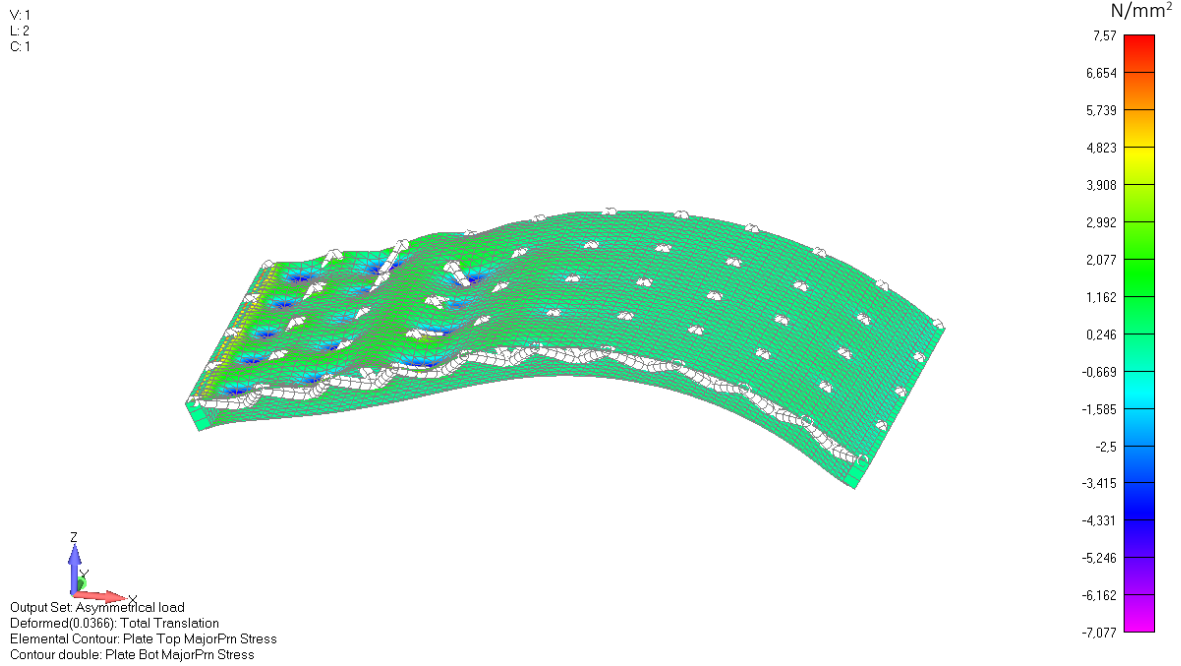
Figure C. 44 Truss Model – Asymmetrical Load – Bottom Plate Major Principal Stresses Tension = 7,57 N/mm²

Waffle Model

The same calculation has been performed on the Waffle Model. The model with a uniformly distributed load of 2kN/m² deflected 0,003 mm. This new model, asymmetrically loaded with 2kN/m² applied just on half of the panel, deflects 0,0046 mm. This result shows that with the asymmetrical load the deflection has increased of 53%. Moreover, by making a comparison with the previous model, we can say that the Waffle pattern is way stiffer and it behaves better also in case of asymmetrical loading conditions.
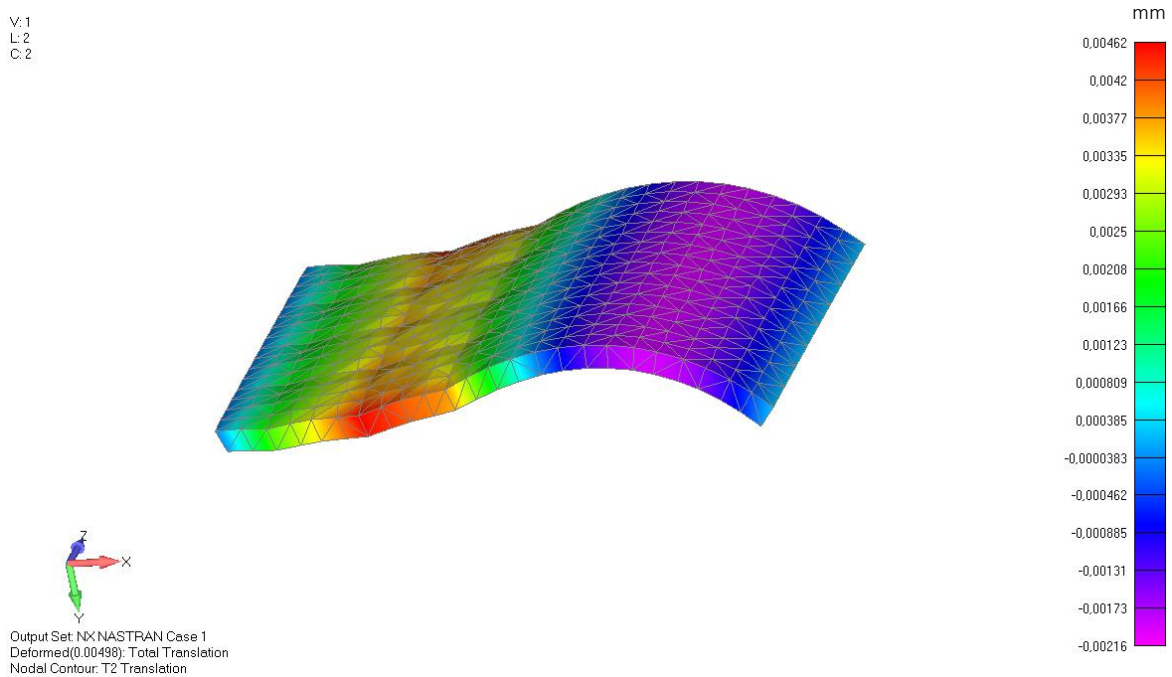

Figure C. 45 Waffle Model – Asymmetrical Load – Maximum Deflection = 0,00462 mm
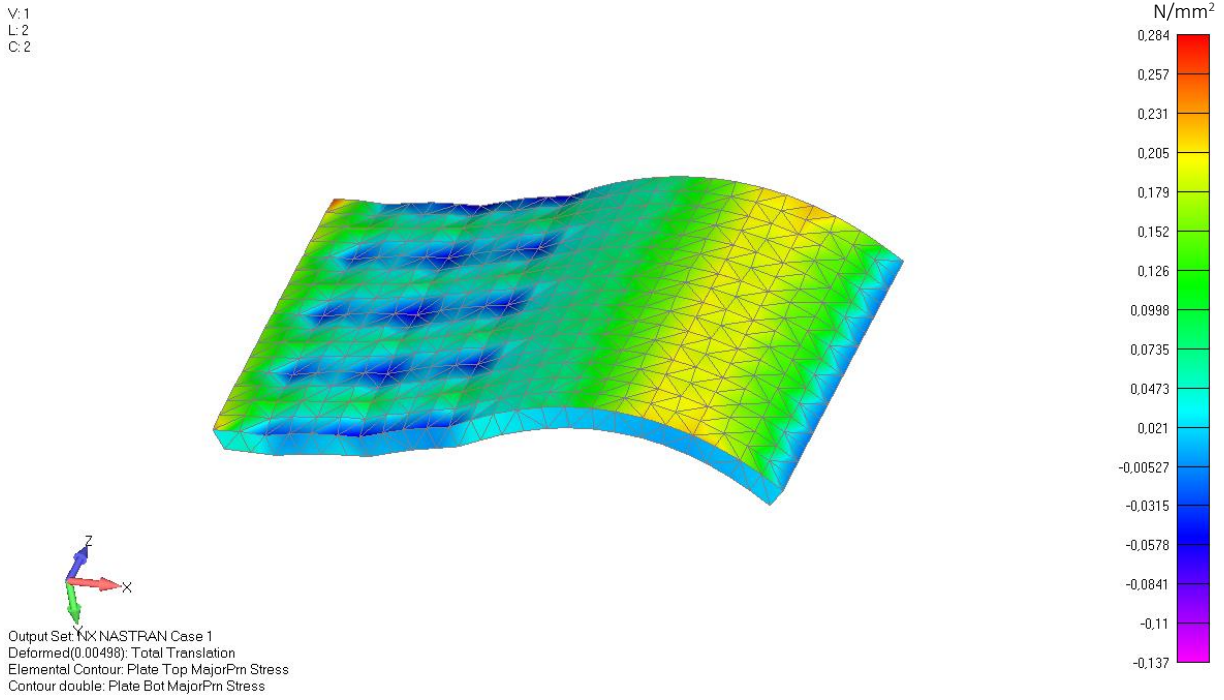
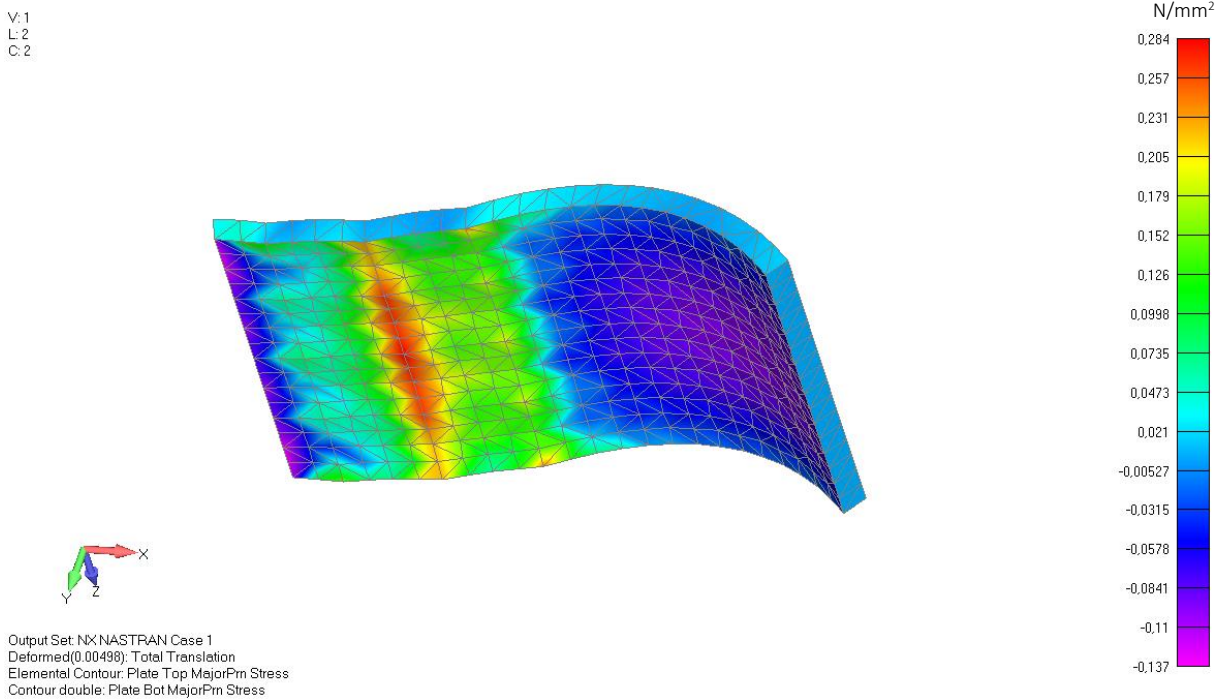Figure C. 46 Waffle Model - Asymmetrical Load - Top Plate Major Principal Stress

Figure C. 47 Waffle Model - Asymmetrical Load - Bottom Plate Major Principal Stress Tension = 0,284 N/mm²

Appendix C.4 Panel 500 mm x 500 mm

A bigger dimensions panel has been also investigated. The dimension of 500mm x 500mm have been chosen as the same as the investigation of Schlösser (Schlösser, 2018), in order to strengthen the research with a final comparison, which can bring to a larger contribution in the conclusions. Naomi Schlosser has investigated the behaviour of a curved thin glass panel, laminated with Sentry Glass and stiffened PVB. The panel has been loaded with a Point Load of 400N, distributed on an area of 50 mm x 50 mm.

In order to realize the numerical model, it was followed the same procedure as the one explained in Paragraph 5.2. Firstly, the thin glass has been cold bent to reach a radius of curvature of R=440mm. The cold bending procedure induces a maximum tensile stress of 64 MPa in top layer of the glass and a compressive stress of 14,4MPa in the bottom layer of glass.

After the glass has been cold bent, the sandwich panel has been investigated under external loading conditions. The panel has been simply supported on two edges and an external point load of 400N has been applied, the load has been distributed on 9 nodes in the FE model. In the worst case scenario, the bottom layer of the glass, the stresses due to loading has to be added to the stresses due to cold bending. This bring the glass to experience a maximum tensile stress of σ = – 14,4 +143,3 = 128,9 MPa.
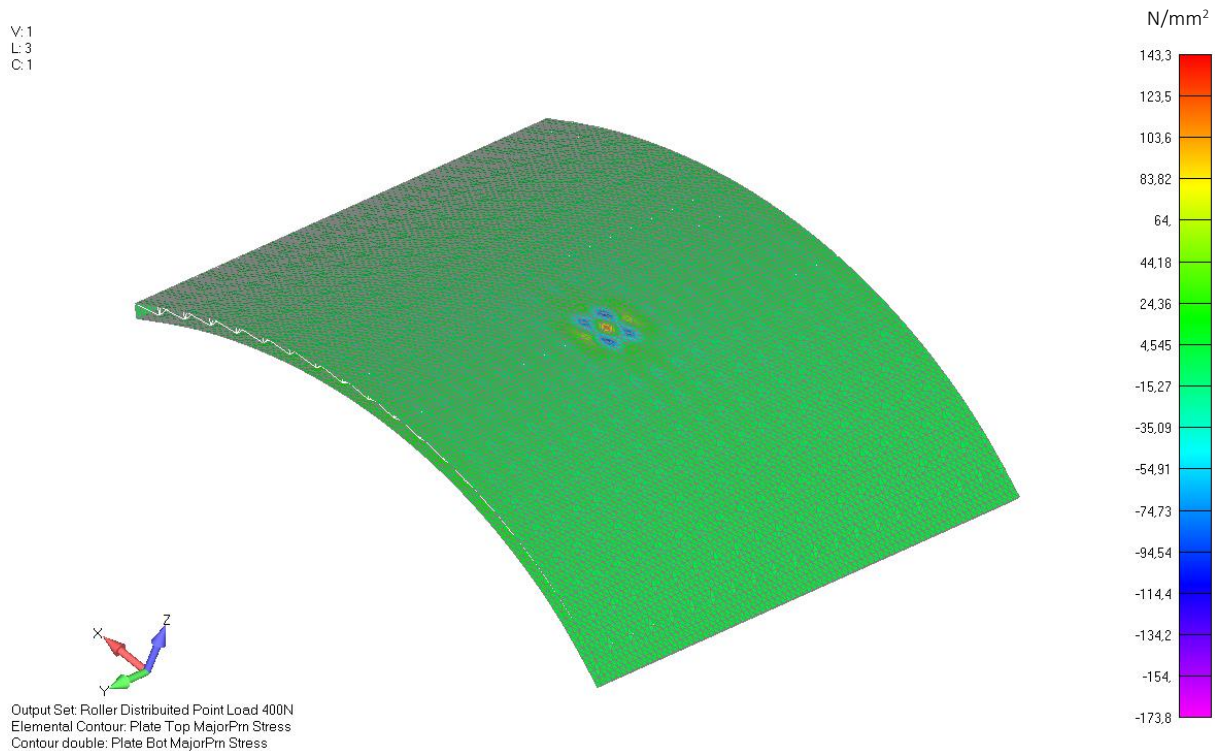

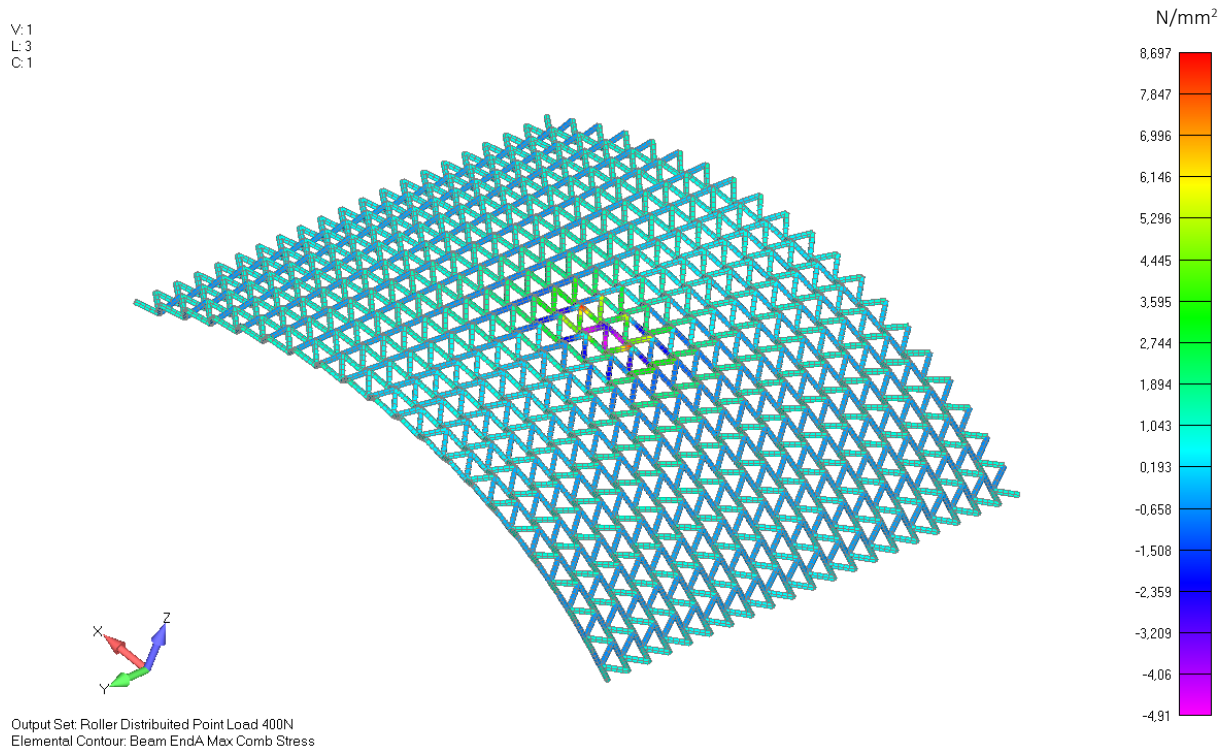Figure C. 48 Glass Face Major Principal Stresses
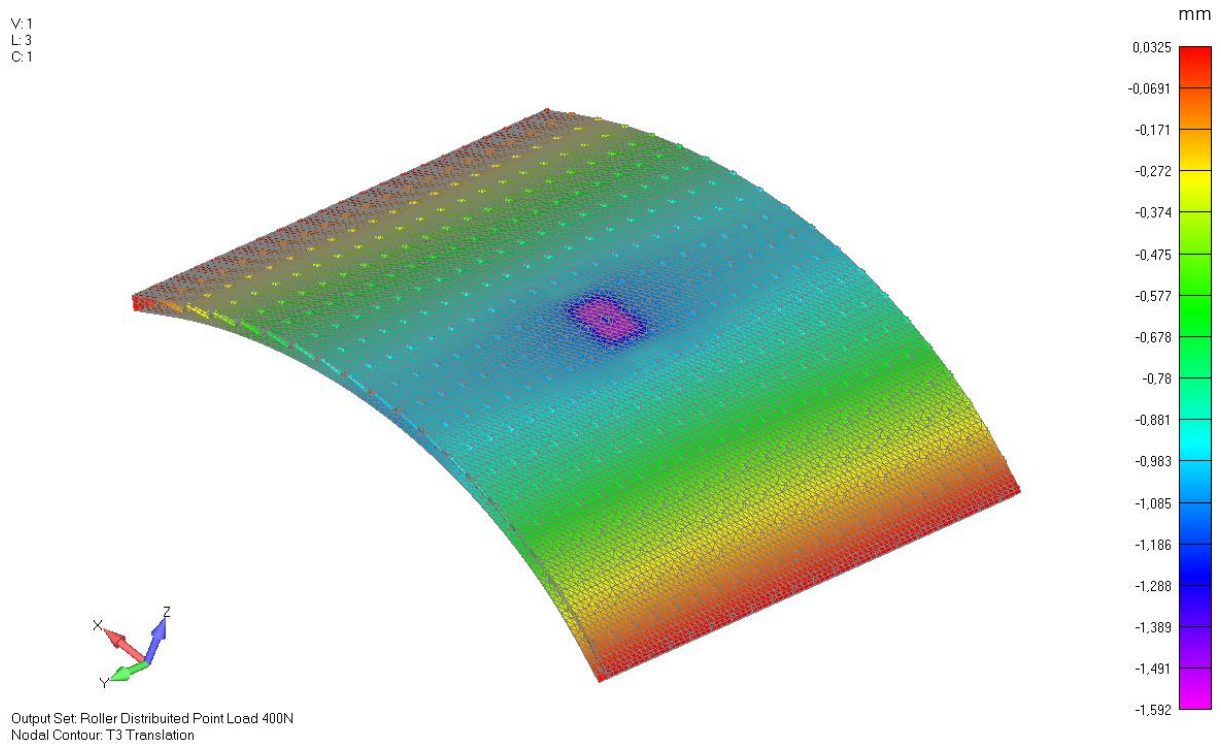
Figure C. 49 Combined Stresses in the Core

Figure C. 50 Truss Model – Deflection = 1,59 mm

The results showed from Figure C. 48 to Figure C. 50 are below summarized.

Simply supported panel
Point Load: 400 N

Deflection: 1,59mm
Major Principal Stress 128,9 MPa

Result's comparison with Schlösser Analysis

Since the testing of this bigger panel will not give the expected results, due to problems during the manufacturing procedure as it is explained in Chapter 6, the comparison with the research of Schlösser is performed within the numerical results.

In the following figure, Schlösser's results are illustrated. In the yellow box, the results of a laminated panel (0,55mm Leoflex Glass + 0,76mm Stiff PVB + 0,55mm Leoflex Glass) is illustrated. While the red box shows a laminated panel made by 0,55mm Leoflex Glass + 0,89mm SentryGlas + 0,55mm Leoflex Glass).

	Relaxation	Loading	Total		Location
REFERENCE SAF					
Deflection DY	-	-70.36	-	mm	Bottom
Principal stresses	-	267.14	267.14	MPa	ply at top
REFERENCE SG					
Deflection DY	-	-43.96	-	mm	Bottom
Principal stresses	-	217.57	217.57	MPa	ply at top
PANEL 1.2					
Deflection DY	-	-72.19	-	mm	Bottom
Principal stresses	0	269.20	269.20	MPa	ply at top
PANEL 1.1/2.1					
Deflection DY	-	-10.38	-	mm	Bottom
Principal stresses	0	156.06	156.06	MPa	ply at top
Deflection DY	-	-12.26	-	mm	Top ply at
Principal stresses	41.21	192.38	233.59	MPa	middle
PANEL 3.1/3.2					
Deflection DY	-	-1.18	-	mm	Bottom
Principal stresses	0	43.75	43.75	MPa	ply at top

Table E.1: Numerical output for deflection and stresses at a load of 400 N

Figure C. 51 Schlosser (2018) numerical results

The comparison in results of the research of Schlösser (2018) and my numerical result (Guidi 2019) is shown in the following table. All the panels have the same dimensions and the same radius of curvature. Schlösser researched a laminated curved thin glass panel, pinned supported at two edges. In my research, a curved sandwich panel is simply supported on two edges. The loading condition is the same, a point load of 400N, distributed on a surface of 50mm x 50mm.

The thickness of the panel of Schlösser research is: 1,86 mm or 1,99 mm depending on the interlayer used. The thickness of my sandwich panel is 0,5mm + 11mm + 0,5mm = 12 mm total.

	Schlösser (2018)		Guidi (2019)
	B.C. Pinned Supports		B.C. Simply Supported
	Panel 1.1	Panel 1.2	Panel
Deflection	10,38 mm	12,26 mm	1,59 mm
Principal Stress (Tension)	156,05 MPa	233,59 MPa	128,9 MPa

Table C. 3 Numerical result's comparison within Schlösser and Guidi research

From the table, it can be seen than the deflection of the panel decreases significantly, from about 10 mm to 1,59 mm. This reduction is due to the higher moment of inertia of the sandwich panel compared to the laminated panel. Moreover, the stresses result to be lower too. Since those value has not be checked with experimental testing, they cannot be validated yet. Further researches on a pinned curved sandwich panel would be of interest to make actual comparison within the research of Schlösser. Additionally, the stiffness of the sandwich panel with pinned supports would also increase. Therefore, it would decrease the value of deflection even more
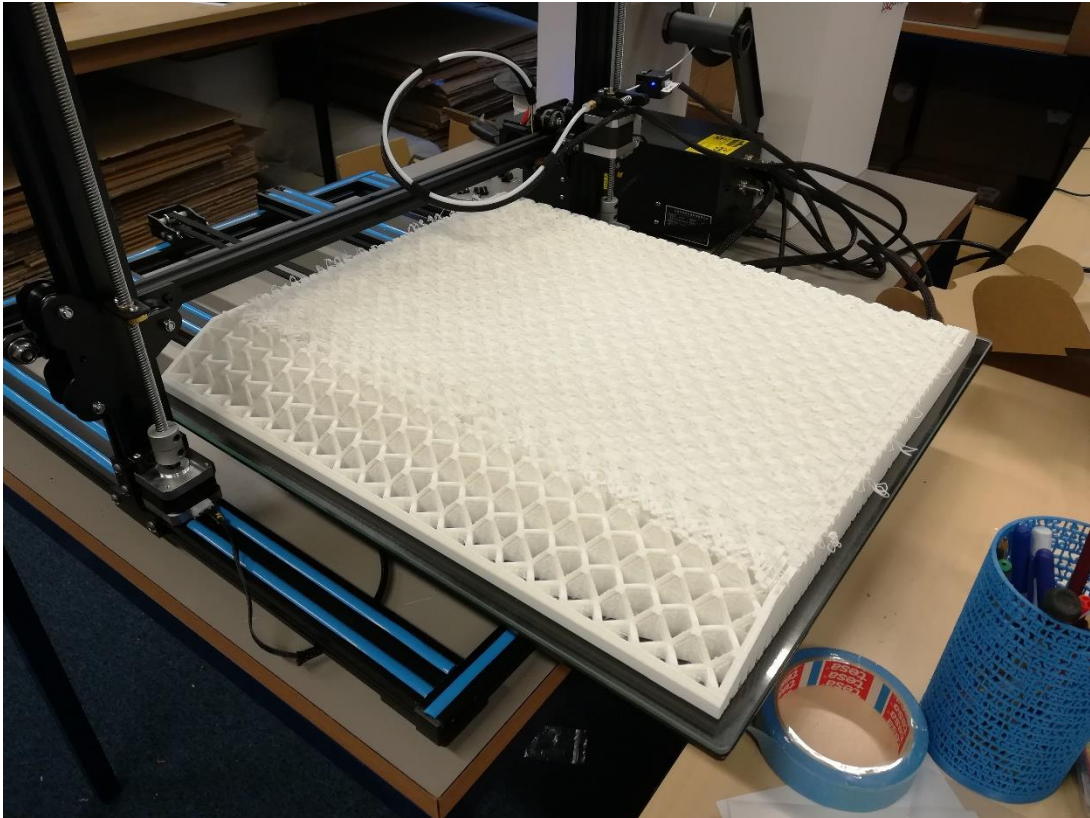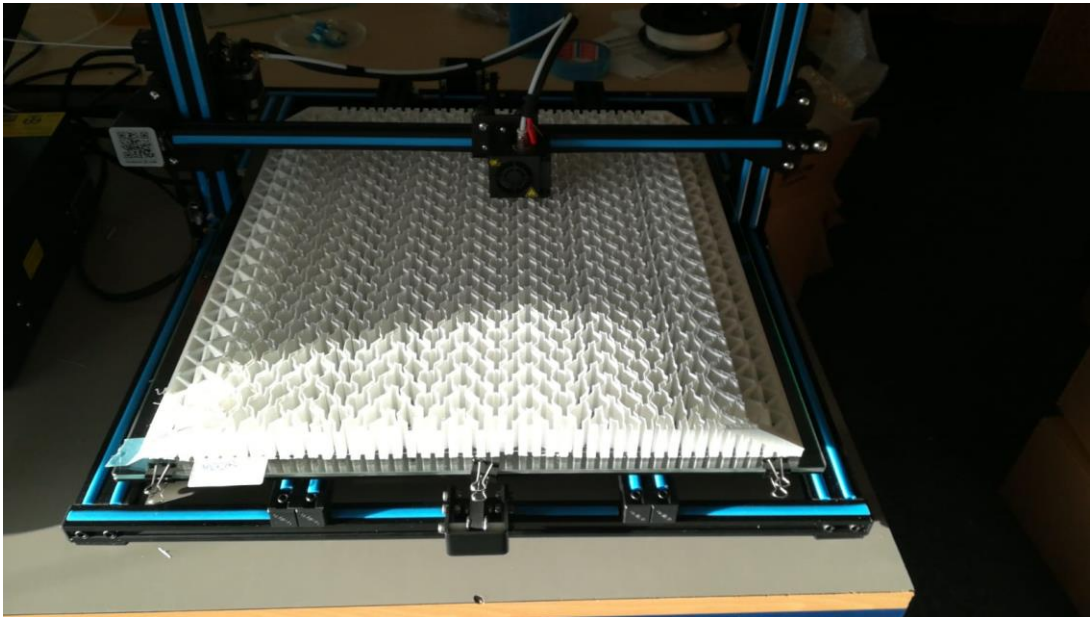
Appendix D – Manufacturing

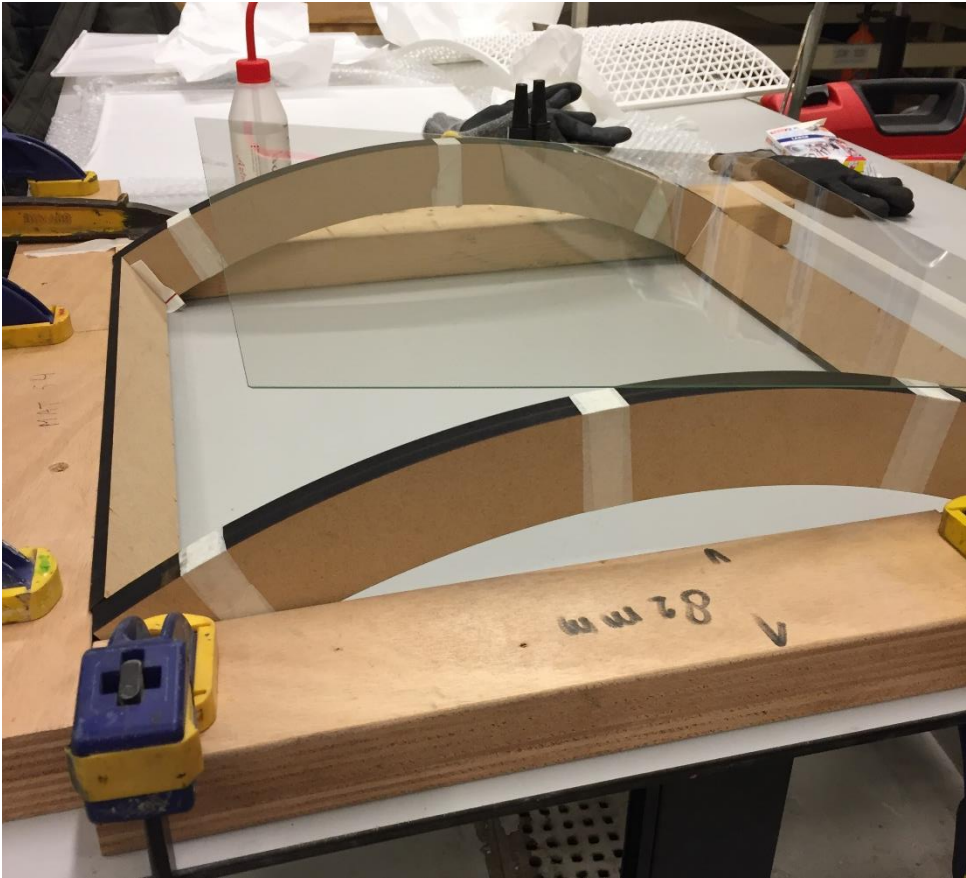Figure D. 1 Truss Model 500mm x 500mm FDM technique

Figure D. 2 Mould to cold bent the glass

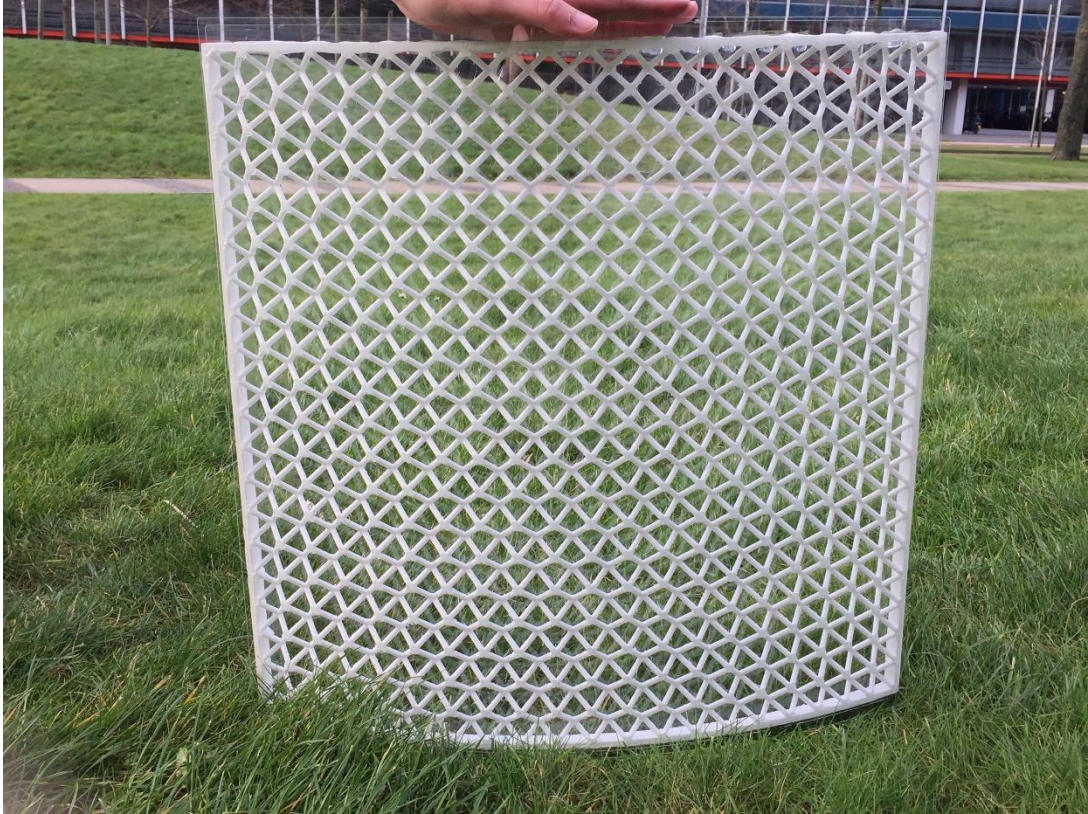Figure D. 3 Tesa Powerstrips: double sided adhesive tape to bond the glass to the mould

Figure D. 4 Panel final resul

Appendix E – Final design Calculations

Wind Load

The value of wind load on a building façade can be calculated according to the code is:

$$F_{wind} = c_s c_d \cdot c_f \cdot q_p(z) \cdot A_{ref}$$

According to coma 6.2 (c) in the Code, the structural factor $c_s c_d$ can be taken equal to 1, for building less than 15m high.

c_f is the force coefficient. The normative does not include curved surface, therefore the top and side view of the building are taken into account as they were flat. According to Figure 7.5 and Table 7.1 in NEN 1991-1-4, the governing values for the force coefficient are $c_f = -1,2$ for wind suction and $c_f = +0,8$ for wind pressure. Wind suction is governing in the corners of the building.

$q_p(z)$ is the peak velocity pressure. According to the code, the Netherlands are divided into wind areas. The building is situated in a built up area of Rotterdam, Wind Zone II, as it can be seen in the following figure.
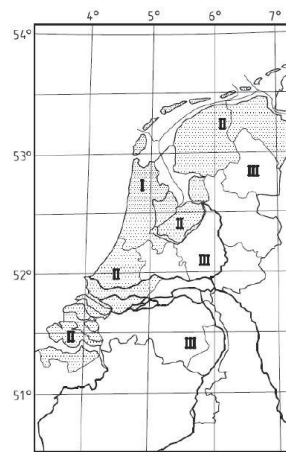
The peak velocity pressure $q_p(z)$ can be calculated ad:

$$q_p(z) = c_e(z) \cdot q_b$$

Where $q_b = \frac{1}{2}\rho v_b^2$

The air density ρ is 1,25 kg/m³, while the basic wind velocity in the Netherlands is 27 m/s, then:

$$q_b = \frac{1}{2} \cdot 1,25 \cdot 27^2 = 455 \frac{N}{m^2} = 0,455 \frac{kN}{m^2}$$

The building is situated in Zone IV terrain category and it has 19m high. Under this condition, the value of $c_e(z)$ is 1,6 according to Figure 4.2 in NEN1991. Thus, the peak velocity pressure has a value of 0,728 kN/m².

Due to the fact that all the loads have been expressed in terms of N/mm², the area of the façade A_{ref} will not be considered at this moment.

The wind load can be now calculated:

$$wind\ pressure = 1\ \cdot\ 0{,}8\ \cdot\ 0{,}727\frac{kN}{m^2} = 0{,}582\ \frac{kN}{m^2} = 0{,}582\ \times 10^{-3}\frac{N}{mm^2}$$

$$wind\ suction = 1\ \cdot(-1{,}2)\cdot\ 0{,}727\frac{kN}{m^2} = -\ 0{,}874\frac{kN}{m^2} = -\ 0{,}874\ \times 10^{-3}\frac{N}{mm^2}$$

Shear strength in the connections

The shear strength of the glue, will be taken as the governing value. Delo Photobond AD494 is used in the final design. The shear strength in between glass and plastic, is 9 MPa. Appendix A can be consulted for the data sheet of the products. To calculate the shear force in the system, the mechanical schematization showed in Paragraph 5.3.3 has been used.

The normal force in the glass needs to be calculated. The mechanical schematization can be simplified as a simply supported beam, loaded in with a uniformly distributed load of q=(1,31kN/m2 + 0,20kN/m2)x 3 m, which is the width of the panel. Thus, q = 4,53 kN/m. The moment in the center of the beam can be calculated as M=ql²/8. And the normal force in the glass is calculated as N = M/d which results in a total normal force N of 67,95kN.
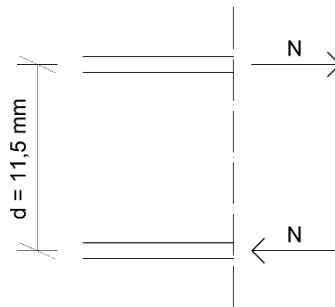
The Normal Force (N) at each connection has to be calculated by taking into account that every time there is a truss element, the force will be transferred both in the glass and in the truss, resulting in a decrease of force on the next connection point.

To simplify the calculation, it is taken as hypothesis that the force N will decrease linearly along the length of the curved beam. It will be maximum under the position of the force (center of the beam) and it will be zero at the support. The cross section taken into account is at a distance dx from the center of the beam. The load N at this point is half of the load, due to the symmetry of the system, since half load will be transferred in the left part of the system and half load in the right part.

To calculate the value of shear stress, it is know that the average value will be at half of the span. At this point, the shear stress is calculated as:

$$\tau = \frac{33\ 975\ N}{42 \cdot 20 \cdot 12{,}57\ mm^2} = 3{,}22\ MPa$$

Where 12,57 mm² is the area of one truss surface of radius 2mm, 42 are the nodes present in the width of the panel and 20 are the truss element on half length of the panel. The shear stress is zero at the end of the beam, and it is 3,22 MPa x 2 = 6,44 MPa, at the cross-section taken into account. The maximum value is still lower than the shear resistance of the glue, which is 9 MPa.